United States
Department
of Agriculture

Forest Service

**Intermountain
Research Station**

Research Paper
INT-RP-484

March 1996

FIRE-BGC—A Mechanistic Ecological Process Model for Simulating Fire Succession on Coniferous Forest Landscapes of the Northern Rocky Mountains

**Robert E. Keane
Penelope Morgan
Steven W. Running**

Authors

Robert E. Keane is a Research Ecologist in the Prescribed Fire and Fire Effects Research Work Unit at the Intermountain Fire Sciences Laboratory, Intermountain Research Station in Missoula, MT. He received his bachelor's degree from University of Maine in 1978 in forest engineering, his master's degree from University of Montana in 1985 in forestry, and has recently complete his Ph.D. degree at the University of Idaho in forest ecology.

Penelope Morgan is an Associate Professor of Fire Ecology at the University of Idaho in Moscow, ID. She received her B.S. and M.S. degrees at Utah State University, Logan, and her Ph.D. degree from the University of Idaho. She conducts research in ecology of disturbance in landscapes of the American West.

Steven W. Running is a Professor of Forestry at the University of Montana in Missoula. He was trained as a Terrestrial Ecologist at Oregon State University (B.S. and M.S. degrees) and Colorado State University (Ph.D. degree, 1979). His primary research interest is the development of global and regional ecology by integration of remote sensing, climatology, and terrestrial ecology using computer simulation. He is a team member for the Earth Observing System Moderate Resolution Imaging Spectrometer (EOS/MODIS) instrument of the National Aeronautics and Space Administration.

Research Summary

A successional model called FIRE-BGC (a FIRE BioGeoChemical succession model) simulates long-term stand dynamics on coniferous forest landscapes of the Northern Rocky Mountains. This model can be used to investigate cumulative fire effects for various fire scenarios, including prescribed burning, fire exclusion, and historical fire regimes. FIRE-BGC is an individual tree model created by merging the gap-phase, process-based model FIRESUM with the mechanistic ecosystem biogeochemical model FOREST-BGC. It has mixed spatial and temporal resolution in the simulation architecture. Ecological processes that act at a landscape level, such as fire and seed dispersal, are simulated annually from stand and topographic information contained in spatial data layers. Stand-level processes such as tree establishment, growth, mortality, organic matter accumulation and decomposition, and undergrowth plant dynamics are simulated both daily and annually on a simulation plot that represents the stand. Tree growth is mechanistically modeled using the ecosystem process approach of FOREST-BGC where carbon compounds are produced daily by forest canopy photosynthesis. Respiration and transpiration are also calculated daily. The net carbon gain allocated to tree stems at the end of the year generates a corresponding diameter and height growth. All model algorithms are discussed and corresponding parameters for several tree species are presented. Included is an application of the model to a whitebark pine landscape in the Bob Marshall Wilderness Complex of Montana. Results of 200 years of simulation on the 20,000-ha landscape for four management scenarios are used to investigate the population dynamics of whitebark pine. A comparison of simulated tree diameter growth predictions with tree growth data collected in the field showed model predictions were within 10 to 30 percent of observed values. FIRE-BGC is continually being tested with field and other model data. It was designed to be applied to different forested landscapes with minimal modification of the computer code.

Acknowledgments

We would like to thank the following individuals who provided critical assistance during model development and testing: Wendel J. Hann, Northern Region, USDA Forest Service, Missoula, MT; Leon F. Neuenschwander, R. Gerald Wright, and John Marshall of the University of Idaho, Moscow; Raymond Hoff, Ronni Korol, and Albert R. Stage of the USDA Forest Service, Intermountain Research Station in Moscow, ID; Joseph White and Peter Thornton of the University of Montana, Missoula; Stephen F. Arno, James K. Brown, Roger G. Hungerford, Mike Jensen, Cameron Johnston, James R. Menakis, Elizabeth D. Reinhardt, and Kevin C. Ryan of the USDA Forest Service, Intermountain Research Station in Missoula, MT; David W. Tippets of the USDA Forest Service, Intermountain Research Station, Ogden, UT; Collin Bevins and Mark Finney, Systems for Environmental Management, Missoula, MT; Kathy Ake, Gordon Ash, Rich Lasko, Maria Mantas, Don Krogstad, Bryan Donner, and Greg Warren of the Flathead National Forest, Kalispell, MT; Seth Diamond of the Lewis and Clark National Forest, Choteau, MT; Carl Key and Dan Fagre, USDI National Biological Service, Glacier Field Station, Glacier National Park, West Glacier, MT; Matthew Arno, Nathan Arno, John Caratti, Thomas Cook, Dynah Geissal, Robert Koss, Brian Parks, John Pierce, and Suzanne Reed of Missoula, MT; D. Kim Wilson of Helena, MT; Rick Kramer and James Gray of Whitefish, MT; and Drew Davol of San Diego, CA.

Intermountain Research Station
324 25th Street
Ogden, UT 84401

Contents

FIRE-BGC—A Mechanistic Ecological Process Model for Simulating Fire Succession on Coniferous Forest Landscapes of the Northern Rocky Mountains

Robert E. Keane
Penelope Morgan
Steven W. Running

Introduction

The simulation of plant succession across forested landscapes is an important tool for evaluating the cumulative effects of management policies in a spatial context over long periods (Dale and others 1985; Urban and Shugart 1992). However, understanding and interpreting ecosystem response to management actions is also becoming an important objective for successional modeling (Botkin 1993; Forman and Godron 1986; Huston and others 1988). Because it is difficult to fully comprehend the complex interactions of ecosystem processes, mechanistic simulation models offer an efficient means to investigate these dynamic relationships and their response to proposed management alternatives (Urban and Shugart 1992). Moreover, the long periods and spatial complexity involved in forest landscape succession preclude the use of field investigations to study and quantify effects of these management actions (Arno and others 1985). Simulation models provide a feasible alternative for comparing the long-term effects of management alternatives on forested landscapes. Also, development of mechanistic models usually identifies areas where future research is critically needed (Barclay and Hall 1986; Bossel 1991).

Historically, forest succession models have been developed at the stand level using empirical and process-based approaches (Dale and others 1985; Shugart and West 1980). Regression models generated temporal plant cover predictions useful in resource management but did not always provide the insight needed to assess why successional pathways differed by disturbance severity (Gay 1989; Keane 1987; Moeur 1985). The family of gap-phase ecological process-based models initially developed by Botkin and others (1972) provided limited explanations for simulated successional response while being somewhat computationally efficient (Aber and others 1978; Botkin 1993; Busing and Clebsch 1987; Dale and Hemstrom 1984; Kienast and Krauchi 1991; Pastor and Post 1986; Shugart and West 1980). However, these models did not account for many ecosystem process interactions across multiple temporal and spatial scales (Leemans and Prentice 1989; Urban and Shugart 1992). These JABOWA-like models operated at a yearly time step so daily ecosystem interactions could not be considered in ecosystem dynamics (Aber and Melillo 1982; Bassow and

others 1990; Kercher and Axelrod 1984; Paster and Post 1985; Reed and Clark 1979; Shugart and Noble 1981).

Mechanistic ecosystem models offer a means to investigate, predict, and explain successional impacts from management actions (Ågren and Axelsson 1980; Blake and others 1990; Bonan 1989; Bossel 1991; Bossel and Schafer 1988; Bossel and others 1991; Burk and others 1990; Huston and others 1988; McMurtrie and Landsberg 1992; Reed 1980). However, many current mechanistic models are not appropriate for management applications because the modeled entities are not useful in management planning (Bonan 1989, 1993b; King 1993; McMurtrie and others 1992; McMurtrie and Wolf 1983; Running and Coughlan 1988; Sievän en 1993; Wang and Jarvis 1990). For example, Running and Coughlan (1988) simulate the change in stand carbon over time, which probably is not directly applicable to many management concerns. In addition, these models are often computationally intensive, requiring large amounts of computer resources for long-term successional simulations. The ideal succession model useful to resource planning would be developed using a mechanistic approach, be computationally efficient, and simulate attributes directly applicable to evaluating management objectives.

This paper presents a mechanistic ecosystem succession model called **FIRE-BGC** (a **FIRE** **B**io**G**eo**C**hemical succession model). This model simulates important ecological processes across coniferous forest landscapes for use in natural resource management. FIRE-BGC models the interaction of disturbance processes such as fire with stand development processes such as tree regeneration, growth, and mortality. All algorithms and parameters used in FIRE-BGC along with related modeling assumptions are documented in the first portion of this paper.

The second portion of this paper details the application of FIRE-BGC to a whitebark pine (*Pinus albicaulis*) forest in the Bob Marshall Wilderness Complex (BMWC) of Montana. This simulation is referred to in this paper as the "BMWC project." The objective was to investigate the consequences of management policies on the whitebark pine ecosystem dynamics in a spatial domain. Several management scenarios were simulated on a 20,000 ha upper subalpine landscape in the southwestern part of the Swan Range of the BMWC to determine the response of whitebark pine to various management actions. Many FIRE-BGC parameters presented in this paper were quantified specifically for this study area using field data collected by Keane and Morgan (1994) and Keane and others (1994). Examples of these parameters are provided throughout model documentation.

Model Description and Development

FIRE-BGC is a mechanistic, individual tree succession model containing stochastic properties implemented in a spatial domain. Tree growth, organic matter decomposition, litterfall, and other ecological processes are simulated using detailed physical relationships. Tree establishment and mortality are modeled using probability functions with ecologically derived parameters. A FIRE-BGC application also includes a spatial simulation of fire behavior and fire effects on ecosystem components across the landscape. Insect and disease interactions are also included in the model.

FIRE-BGC has a mixed time and space resolution built into the simulation design. Primary canopy processes of interception, evaporation, transpiration, photosynthesis, and respiration are simulated at a daily time step at the stand level. Driving variables for these processes are taken from daily weather data. The annual carbon and nitrogen gains computed daily for each stand are allocated to each tree in the stand at the end of the year. These secondary canopy processes of carbon and nitrogen allocation are accomplished at a yearly time step and are done at a tree level. The carbon and nitrogen allocated to each tree are then portioned to the stem, roots, and leaves. Allocation of carbon to the stem of a tree is used to calculate a corresponding diameter and height growth.

Model Creation

FIRE-BGC is the union of two ecosystem models that were developed using different approaches. The process-based, gap-replacement model FIRESUM (Keane and others 1989, 1990a,b) was merged with the mechanistic biogeochemical simulation model FOREST-BGC (Running and Coughlan 1988; Running and Gower 1991) to predict changes in species composition in response to various ecosystem processes over long periods. The mechanistic approach of FOREST-BGC improved the level of detail needed to understand those ecosystem processes that govern successional dynamics. FIRESUM's comprehensive simulation of forest dynamics in multispecies stands, and its integration of fire interactions with ecosystem components, allow FIRE-BGC to simulate changes in species composition and abundance as a consequence of multiple disturbances over long periods.

FIRESUM is derived from the JABOWA (Botkin and others 1972; Kercher and Axelrod 1984; Shugart and West 1980; Urban 1990) family of models where individual trees are grown deterministically using an annual time-step difference equation. Tree growth is affected by several site factors including available light, water stress, and growing season warmth. These environmental factors are represented in FIRESUM as scalars (values between 0 and 1) that reduce an optimal tree diameter annual growth increment. Tree establishment and mortality are modeled stochastically using Monte Carlo techniques. Fuel accumulation and decomposition are empirically calculated yearly. Fires are simulated at stochastic or fixed intervals and effects of each fire are simulated by reduction of litter, duff, and down woody fuels; and by tree mortality and by post-fire tree regeneration and growth.

FOREST-BGC (a FOREST BioGeoChemical process model) is a process-level ecosystem simulation model that calculates the cycling of carbon, water, and nitrogen

through forest ecosystems (Running and Coughlan 1988). It dynamically calculates the flow of energy between ecosystem components at a daily time step using fundamental physical and ecophysiological relationships. The model simulates these fluxes on a forest stand usually 0.1 ha in area. FOREST-BGC has mixed time resolution with carbon and nitrogen allocation and flow simulated at a yearly time step, and key forest canopy processes such as transpiration, photosynthesis, and respiration simulated at a daily time step. The ecosystem is represented by a set of compartments called state variables and the flow of carbon, water, and nitrogen to and from these compartments is simulated through the quantification of process relationships.

FOREST-BGC does not identify individual trees in its simulation approach (Running and Coughlan 1988). Rather, it treats the whole forest as one "large tree" with one "big" leaf whose thickness is proportional to leaf area index. This "tree" is defined in terms of the carbon and nitrogen within the stems, leaves, and roots representing all trees that make up the stand. FOREST-BGC assumes horizontal homogeneity (uniform stand conditions) and models most ecosystem fluxes in the vertical dimension (Running and Coughlan 1988; Friend and others 1993). Korol and others (1991) successfully used FOREST-BGC to create an individual tree model of stand dynamics called TREE-BGC. However, TREE-BGC only recognized one tree species (Douglas-fir) and does not simulate landscape interactions.

Creation of FIRE-BGC used the mechanistic design of FOREST-BGC as the framework and engine for ecosystem simulation. Then important FIRESUM algorithms were added to the framework to simulate multispecies forest succession over long periods. These FIRESUM routines were then refined to utilize the detailed information generated by the mechanistic FOREST-BGC routines. Finally, this modeling framework was implemented in a landscape context by recognizing the spatial distribution of these processes across a simulation area (Busing 1991; Shugart and Seagle 1985; Urban and others 1991). This allowed detailed simulation of ecosystem processes that act across several spatial scales (Bonan and Shugart 1989). Kimmins (1993) used a similar approach in the development of his FORCYTE-11 succession model.

Model Design

FIRE-BGC models the flow of carbon, nitrogen, and water across various ecosystem components to calculate tree growth. The major compartments and processes simulated by the model are diagrammed in figure 1 and illustrated in figure 2. Carbon is fixed by tree leaves (needles) via photosynthesis using solar radiation, temperature, and precipitation, and this carbon is then distributed to leaves, stems, and roots. A portion of the leaves, stems, and roots are lost each year and accumulate on the forest floor in the litter, duff, and soil (fig. 1). These forest floor compartments lose carbon through decomposition. Nitrogen is cycled through the system from the available nitrogen pool.

Spatial Scales—Two spatial scales are explicitly implemented in FIRE-BGC. Ecosystem processes that occur at the landscape level, such as seed dispersal and fire, are modeled in a spatial domain using raster data layers (Hunsaker and others 1993). Stand-level processes, such as

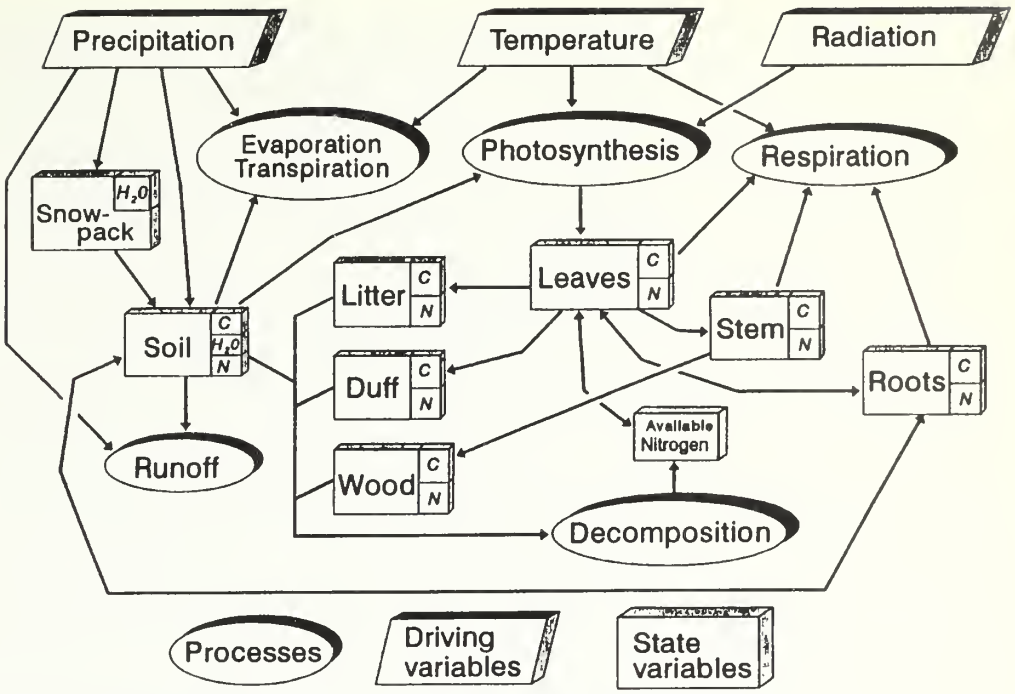

Figure 1—Model diagram of the mechanistic process model FIRE-BGC.

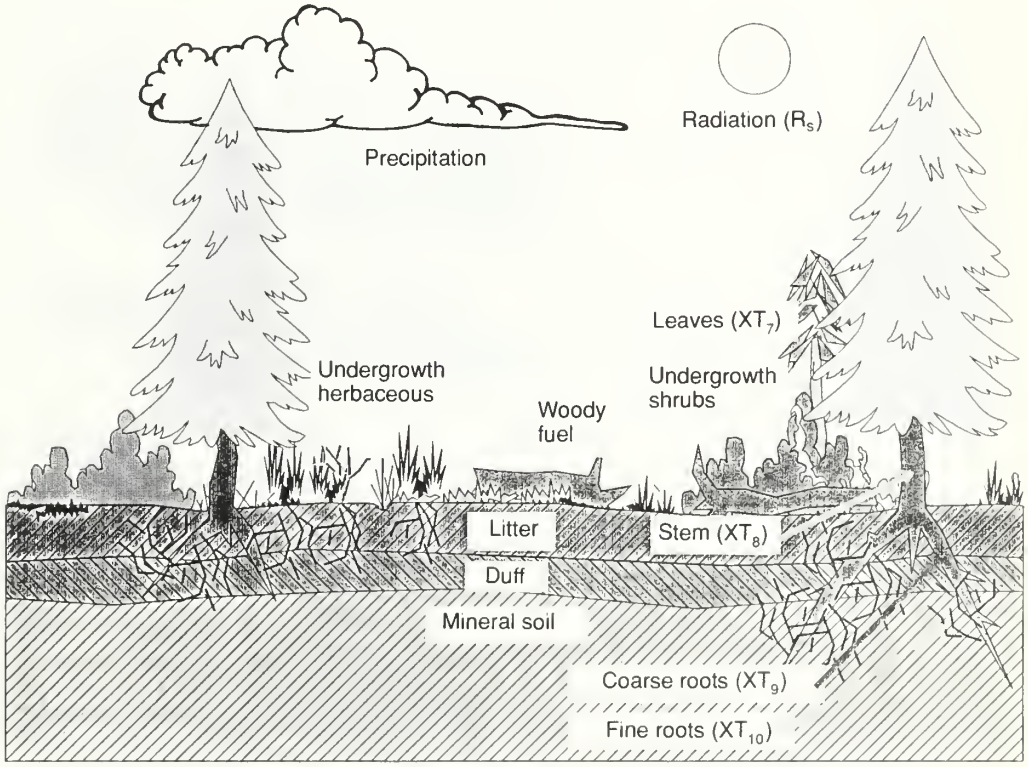

Figure 2—Illustration of important driving and state variables in the model FIRE-BGC.

tree growth and regeneration, are modeled independent of the spatial environment. Dynamic data bases provide the linkage between the spatial simulation and the stand-level process simulation. Information recorded in these data bases is always summarized by stand. For instance, fire behavior is predicted for each pixel in the landscape then the behavior estimates are averaged across all pixels within the stand boundaries for use in predicting tree mortality and fuel consumption.

Organizational Scales—Five levels of organization are explicitly recognized in FIRE-BGC (fig. 3). The organization levels are hierarchically nested in FIRE-BGC design (Turner and others 1989). The coarsest level is the simulation **landscape** which is defined as a large expanse of land (greater than 10,000 ha) delineated by the natural boundaries that control the major properties of that ecosystem. These properties include climate, vegetation, and disturbance. This landscape is divided into units of land called **sites** that have similar topography, soils, weather, and potential vegetation. The boundaries of each site are static and do not change in a FIRE-BGC simulation. The physical locations of these sites are mapped into a spatial data layer raster file called the Site Map.

The third level of organization is the **stand**. Each site comprises a number of stands that are delineated by successional stage differentiated by vegetation composition and structure. Each stand has homogeneous vegetation and disturbance conditions. By definition, stand boundaries cannot extend past site boundaries. Stand boundaries are not stationary in

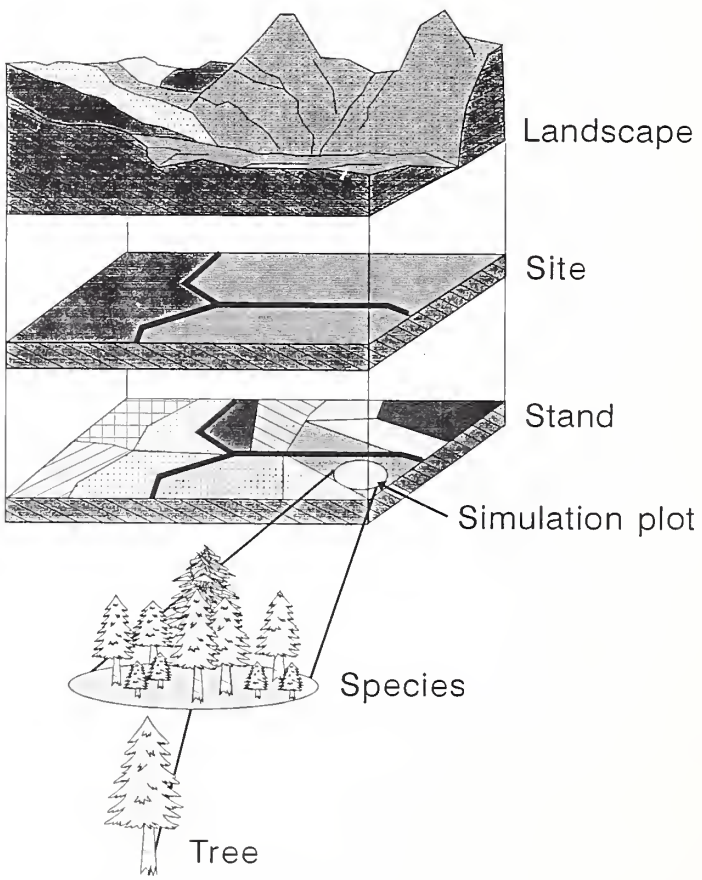

Figure 3—The five levels of organization represented in FIRE-BGC architecture.

FIRE-BGC. Instead, the processes of succession, fire, and pathogens serve to alter stand boundaries within a site. Stand boundaries are updated after major disturbances such as fire or every 20 years to account for successional changes. Initial stand boundaries are mapped into a raster file called the Stand Map.

FIRE-BGC does not explicitly model all entities across the spatial extent of an entire simulation stand because of computational limitations. Instead, the model simulates ecosystem processes in a small portion or "vignette" of the stand called the **simulation plot**. The size and characteristics of the simulation plot are input to FIRE-BGC and can be adjusted to improve computation time and better approximate ecological conditions. Conditions within the simulation plot are assumed to be representative of conditions across the entire **stand.**

The fourth organization level is the **species** level. Any number of species can inhabit a stand. Many modeled processes, such as canopy dynamics, are performed at the species level. The fifth and finest level of organization is the **tree** level. Each tree within a simulation plot is explicitly modeled in the FIRE-BGC architecture. Many structural and ecophysiological attributes of each tree, such as leaf carbon, diameter and height, are simulated in FIRE-BGC. However, these trees are not spatially defined. Discussion of FIRE-BGC simulation methods are stratified by these organizational levels.

Scale Interactions—FIRE-BGC links many across-scale interactions in the simulation of ecosystem processes (Hunsaker and others 1993). The treatment of weather in the model is a good example of scale linkages that progress downward in organizational scale. The weather year is selected for the entire landscape, then that year is used to access weather for a site. Each site is assigned a separate daily weather file. Photosynthesis and respiration are computed from the daily weather data at the stand level for that site. Important weather events such as frost and drought are computed at the stand level for the simulation of species dynamics. Carbon fixed through photosynthesis at the stand level is allocated to the trees based on the distribution of radiation in forest canopy, which is computed from the site weather file and the stand's canopy structure.

FIRE-BGC also accounts for interactions that occur upward in organizational scale. At the end of the simulation year, FIRE-BGC sums all carbon and nitrogen tree compartments for a new estimate of stand carbon and nitrogen components. The abundance of a stand's seed crop trees by species is written to dynamic data files for use in the landscape application of the seed dispersal model. Simulated fires burn a stand's forest floor compartments (fuels) but use site level weather files and landscape topography for computation of fire spread and intensity.

The FIRE-BGC Program

FIRE-BGC was written in the C programming language using a modular approach where organizational levels implemented in model design were used to develop in separate modular components (Levine and others 1993). Relationships and parameters are shared across modules as objects or functions (Kernighan and Ritchie 1988). The program was implemented on a SUN Sparc Model 10 workstation and accesses several software packages during execution (fig. 4).

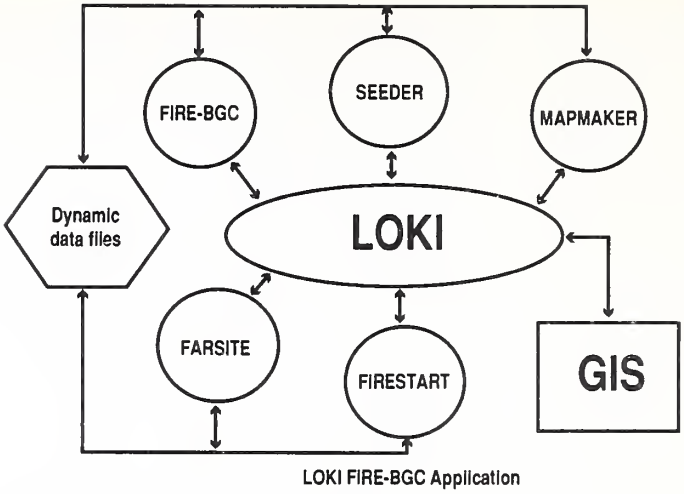

Figure 4—Diagram of the FIRE-BGC application using the LOKI modeling platform to link computer programs.

Loki Modeling Platform—The Loki modeling architecture is used to link and schedule the execution of FIRE-BGC and its submodels SEEDER (seed dispersal model), MAPMAKER (an ecological mapping routine), FIRESTART (a fire occurrence simulator) and FARSITE (fire behavior model) at the appropriate time intervals (Bevins and Andrews 1994; Bevins and others 1994) (fig. 4). These submodels are detailed later in this paper. Loki routines also provide FIRE-BGC and the submodels a means to query, modify, and create digital landscape maps during simulation. The GRASS spatial GIS package is used for organizing, displaying, and analyzing the geo-referenced boundaries of sites and stands stored as raster files (USA CERL 1990).

Dynamic Data Bases—The FIRE-BGC application in Loki shares values across programs (spatial scales) through the use of dynamic data bases. Each year FIRE-BGC updates a "Stand Attribute" file (called FIRE-BGC.STAND) with new values for important parameters used by the other submodels integrated in Loki. The SEEDER program accesses this Stand Attribute file to obtain number of seed-producing trees for each stand. FIRESTART and FARSITE acquires fuel loadings and stand characteristics from this file. In turn, these submodels update other dynamic data files for use in FIRE-BGC. SEEDER creates a "Seed Dispersal" file (called FIRE-BGC.SEED) that contains average seed dispersal probability for each stand.

FIRE-BGC Program Flow—A generalized FIRE-BGC program flowchart is shown in figure 5. The program reads all initial values and parameters from a collection of input data files specified by the user. Then all state variables in the model are initialized with that input information. Simulation starts with the spatial simulation of cone abundance and seed dispersal. Then the daily simulation of stand-level processes is accomplished using the FOREST-BGC routines in the following procedure. First, weather is estimated by site from data in a weather file. Daily photosynthesis, respiration, and water budgets are then calculated to obtain yearly carbon gains. At the end of the simulation year, stand carbon

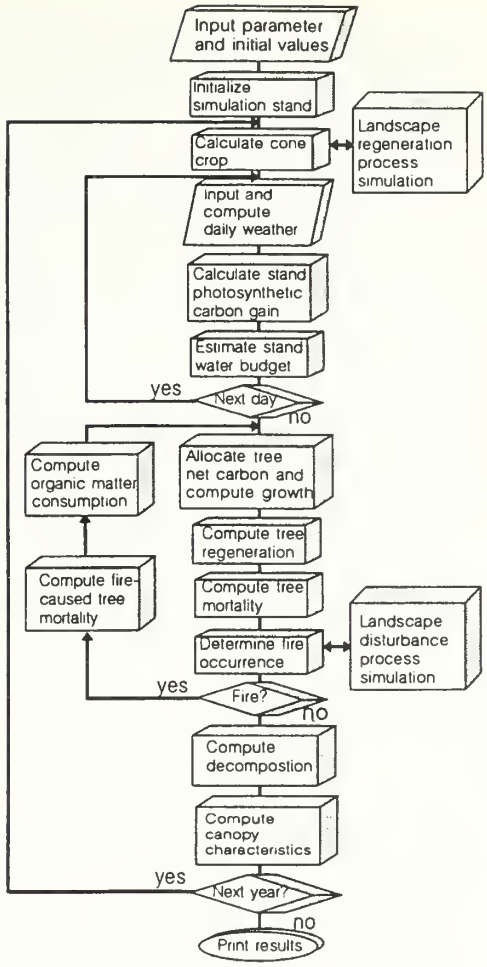

Figure 5—Model flow chart of the FIRE-BGC model.

and nitrogen are allocated to each tree in the stand and then to the leaf, stem, and root components of each tree. The carbon allocated to the tree's stem is converted to a diameter increment growth. Establishment of new trees is then assessed by species in the regeneration routine. The possibility of tree death is evaluated in the mortality algorithm. Then fire occurrence and subsequent fire behavior and effects are dynamically modeled on the landscape. Forest floor decomposition is simulated daily, and the forest canopy characteristics are recomputed at year's end, and the process is repeated for the next year.

Documentation Format

Documentation of FIRE-BGC algorithms and parameters is presented in the following sections. The first section describes the methods used to quantify algorithm parameters and to initialize program variables. The next five sections detail the procedures that simulate the processes that occur at the various organizational levels (landscape, site, stand, species, and tree levels). The next two sections discuss the simulation of disturbance effects at stand and tree levels. The last section deals with the forms of output generated by FIRE-BGC.

A unique convention is used to name variables that appear in the model documentation. This convention follows that described by Swartzman (1979) where state variables start with the letter **X**, intermediate variables start with **G**, and parameters start with **B**. The next letter in the variable name refers to the level of organization represented by that variable. The letter **P** refers to simulation plot and concerns stand level data, **T** refers to tree-level information, and **S** refers to species-level values. For instance, species parameters are stored in the **BS** variables, tree state variables in the **XT** variables, and **GP** variables are used to store intermediate plot or stand level results. Subscripts denote the identity of the elements that compose the variables. For example, $\mathbf{BS}_0$ represents a tree species' specific leaf area. Subscripts start with zero to provide consistency of variable naming between the FIRE-BGC **C** program and this document. General variables that do not fit with the above convention are given a descriptive name. Appendix A details the name and units given each variable used in this document and the FIRE-BGC program. Elements of the intermediate variables **GP** and **GT** are identical so only the **GP** variables are given in appendix A.

Parameterization and Initialization

Model Parameterization

FIRE-BGC requires the quantification of many algorithm parameters, as is the case with most multi-species mechanistic models (Bossel 1991; Burk and others 1990; Sollings and others 1979). However, it was difficult, and sometimes impossible, to gather all information needed to parameterize every relationship included in the model. Critical ecophysiological research needed for model parameterization was lacking for most forest species. Therefore, a scheme was devised to assign parameter values taken from well-studied tree species to the less-studied tree species. This scheme involved grouping tree species into similar ecological groups. Then, if data were not available to quantify a FIRE-BGC species parameter, the parameter for the species group was used (Kellomäki and Väisänen 1991).

Tree species were grouped according to their role in the successional process (table 1) using the Minore (1979) classifications. Tree species with similar successional roles seemed to display similar ecological, morphological, and physiological qualities (Bazzaz 1979, 1990; Drury and Nisbet 1973; Grime 1966, 1974; Grime and Hunt 1975; Marks 1975; Wallace 1991). For instance, early seral species tend to have high photosynthetic rates, low tolerance for shade, rapid height and diameter growth, frequent cone crops, long lifespans, and short crown lengths (Bazzaz 1990; Grime

Table 1—Tree species ecological groupings by successional stage.

Early seral	Mid seral	Late seral
Ponderosa pine	Douglas-fir	Western red cedar
Lodgepole pine	Whitebark pine	Western hemlock
Western larch	Western white pine	Subalpine fir
Alpine larch	Engelmann spruce	Grand fir

1979; Horn 1974; van Hulst 1978). Late seral species appear to show opposite qualities (Drake 1991; Finegan 1984). Parameter values assigned to each species are shown in table 2. Descriptions and units of these parameters are given in the variable list presented in appendix A.

Quantification of site and stand initial values and algorithm parameters is time consuming and sometimes costly to accomplish from landscape inventory. A similar scheme was devised to assign information from a sampled stand to a similar unsampled stand. Site and stand parameter values were quantified using a potential vegetation approach where sites were classified to a "fire group" from topographical information provided by the GIS DEM (Digital Elevation Model) layers (Davis and others 1980; Fischer and Bradley 1987). The list of fire groups and the corresponding topographical criteria used to key these fire groups on the BMWC landscape are presented in table 3. Stand and site parameters that were not directly measured for this study (Keane and Morgan 1994; Keane and others 1994) were quantified in the input file based on data taken from other studies for the fire group.

Most parameters and initial values for FIRE-BGC are stored in a suite of ASCII data files that are immediately scanned at the start of simulation (fig. 5). These files are stratified based upon the overall organizational architecture of the model (landscape, site, stand, species, and tree) with examples depicted in appendix B. The names of these input files are furnished in a "Driver" file (DRIVER.DAT in appendix B) that is specified as an argument in the program execution command line. General simulation parameters such as simulation plot size (PAREA) and simulation time span (NSPAN) are stored in the "Simulation" file (SIM.DAT). Parameters and initial values pertaining to sites are entered in the "Site" file (SITE.DAT). Stand-specific data including initial loadings (weights per unit area) of the forest floor compartments are taken from the "Stand" file (STAND.DAT). Parameters that describe characteristics of the fuels (fuel models) are defined in the "Fuel" file (FUEL.DAT), and undergrowth plant parameters are taken from the "Plant" file (PLANT.DAT). Information needed to model the whitebark pine regeneration process is specified in the "Whitebark" file (PIAL.DAT) (Keane and others 1990b). Tree species parameters are contained in the "Species" file (SPECIES.DAT). And lastly, individual tree data for each simulation stand are contained in the "Tree" file (TREE.DAT).

FIRE-BGC Initialization

Most input information needed to initialize and parameterize the simulation comes from the input files mentioned above. Many other values are calculated from these input data for use mostly as starting values for the simulation run. The procedure of reading the input files and calculating these starting values is called "primary initialization." FIRE-BGC also contains a second level of initialization ("Annual Initialization") where stand and tree values are recalculated at the start of each year of simulation to account for any changes incurred on the landscape.

Tree Compartment Primary Initialization—FIRE-BGC uses generalized tree input data taken from the Tree file to compute tree attributes needed in the simulation. Tree data are input to the model by stand from tables of tree density and age by species and diameter class (for example, TREE.DAT in appendix B). The size of the diameter class (cm) and number

Table 2—Values for tree species parameters as implemented in FIRE-BGC.

Species parameters	Species code[1]												References[2]
	PIPO	ABGR	PSME	PICO	LAOC	ABLA	PIEN	PIAL	LALY	PIMO	THPL	TSHE	
tolerance	1	4	3	1	1	4	4	2	1	2	5	5	
bs(0)	20.0	40.0	22.8	21.9	14.0	35.0	30.0	22.0	14.0	25.0	20.0	30.0	2,3,33,43,58,69,78,80
bs(1)	–0.65	–0.40	–0.40	–0.60	–0.612	–0.40	–0.40	–0.60	–0.612	–0.40	–0.30	–0.30	2,4,11,31,44,59,79
bs(2)	0.0005	0.0005	0.0005	0.0005	0.0005	0.0005	0.0005	0.0005	0.0005	0.0005	0.0005	0.0005	5,65
bs(3)	0.1	0.12	0.10	0.10	0.10	0.14	0.10	0.10	0.10	0.10	0.14	0.12	6,44,45
bs(4)	0.5	0.5	0.5	0.5	0.5	0.5	0.5	0.5	0.5	0.5	0.5	0.5	5,7
bs(5)	4000.0	3000.0	3000.0	3000.0	5000.0	4000.0	4000.0	4000.0	5000.0	3000.0	3000.0	3000.0	5,66
bs(6)	0.0025	0.003	0.0016	0.0020	0.0020	0.0030	0.0025	0.0020	0.0020	0.0025	0.0022	0.0022	5,34,66,73,85
bs(7)	1.65	1.4	1.90	1.46	1.50	1.30	1.60	1.65	1.00	1.50	1.40	1.30	7,9,28,58,84,85
bs(8)	0.05	0.05	0.05	0.05	0.05	0.05	0.05	0.05	0.05	0.05	0.05	0.05	5,7,60
bs(9)	560.0	370.0	300.0	550.0	550.0	400.0	400.0	440.0	600.0	450.0	300.0	300.0	2,9,28,39,50,60,72
bs(10)	11000.0	8208.0	9700.0	10000.0	9730.0	8200.0	7128.0	9000.0	10000.0	9740.0	9000.0	5400.0	2,5,9,42,50,72
bs(11)	0.0008	0.0008	0.0008	0.0008	0.0008	0.0008	0.0008	0.0008	0.0008	0.0008	0.0008	0.0008	5
bs(12)	–1.0	–1.0	–2.0	–5.0	–3.0	–7.0	–4.0	–9.0	–10.0	–1.0	0.0	0.0	2,9,20,28,61,72,73
bs(13)	45.0	41.0	41.0	40.0	38.0	38.0	37.0	37.0	35.0	40.0	40.0	40.0	9,28,60,61,72,73
bs(14)	0.00015	0.00015	0.00015	0.00015	0.00015	0.00015	0.00015	0.00015	0.00015	0.00015	0.00015	0.00015	2,5,6
bs(15)	0.00200	0.00200	0.00200	0.00200	0.00200	0.00200	0.00200	0.00200	0.00200	0.00200	0.00200	0.00200	2,5,6
bs(16)	0.00020	0.00020	0.00020	0.00020	0.00020	0.00020	0.00020	0.00020	0.00020	0.00020	0.00020	0.00020	2,5,6
bs(17)	4.0	4.0	4.0	4.0	4.0	4.0	4.0	4.0	4.0	4.0	4.0	4.0	2,5,6
bs(18)	0.085	0.085	0.085	0.085	0.085	0.085	0.085	0.085	0.085	0.085	0.085	0.085	5,32
bs(19)	0.045	0.0480	0.0440	0.0460	0.0390	0.0220	0.0220	0.0420	0.0370	0.0450	0.040	0.040	8,35,36,50,75,76
bs(20)	0.01	0.0150	0.0132	0.0120	0.0100	0.0110	0.0110	0.0120	0.0100	0.0100	0.0100	0.0100	8,35,36,50,75,76
bs(21)	0.50	0.50	0.50	0.50	0.90	0.50	0.40	0.50	0.90	0.50	0.50	0.50	5,6,11,59,89
bs(22)	8.00	12.00	10.00	7.00	6.00	12.00	12.00	6.00	5.00	8.00	13.00	15.00	1,10,12,27,31,61,68
bs(23)	3.0	6.0	5.0	3.0	1.0	6.0	6.0	6.0	1.0	3.0	6.0	4.0	1,2,10,14,15,33,42,47,58,61
bs(24)	0.25	0.28	0.28	0.23	0.20	0.28	0.22	0.22	0.20	0.22	0.21	0.206	5,35,36,74
bs(25)	1.0	1.0	1.0	1.0	1.0	1.0	1.0	1.0	1.0	1.0	1.0	1.0	5
bs(26)	120.0	110.0	120.0	180.0	115.0	140.0	140.0	150.0	150.0	120.0	150.0	150.0	1,10,26
bs(27)	200.0	280.0	280.0	280.0	280.0	280.0	250.0	250.0	210.0	250.0	250.0	250.0	1,10,26
bs(28)	0.04	0.09	0.01	0.05	0.05	0.10	0.10	0.05	0.05	0.10	0.10	0.10	2,4,5,6,11,51
bs(29)	0.08	0.01	0.03	0.05	0.10	0.10	0.10	0.10	0.10	0.10	0.10	0.10	2,6,35,51,
bs(30)	0.35	0.40	0.30	0.35	0.40	0.40	0.40	0.35	0.40	0.35	0.35	0.35	2,4,5,6,8,33,41,72,78
bs(31)	0.30	0.30	0.30	0.30	0.30	0.30	0.30	0.30	0.30	0.30	0.30	0.30	2,4,5,6,8,33,41,72,78
bs(32)	0.30	0.35	0.30	0.35	0.35	0.35	0.35	0.35	0.35	0.30	0.35	0.35	2,4,5,6,8,33,41,72,78
bs(33)	0.80	0.80	0.80	0.80	0.80	0.80	0.70	0.80	0.80	0.80	0.80	0.80	5,11,35,51,63
bs(34)	650.000	350.000	400.000	220.000	450.000	230.000	350.000	1000.000	800.000	600.000	750.000	500.000	1,10,12,30,37,46,61,86,90
bs(35)	21.0	20.0	15.0	22.0	30.0	18.0	23.0	17.0	15.0	25.0	22.0	21.0	1,10,12,61,81,86
bs(36)	0.5	0.3330	0.1700	0.3180	0.3680	0.3330	0.1670	0.4000	0.3680	0.3180	0.2500	0.2500	10,13,14,53,54,56,57,61
bs(37)	2	2	2	2	2	2	2	1	2	2	2	2	1,10,14,53,54,55,56,57,61
bs(38)	20.0	15.0	20.0	15.0	15.0	25.0	25.0	60.0	50.0	15.0	20.0	20.0	1,10,38,56,61,68
bs(39)	0.01	0.020	0.050	0.005	0.016	0.008	0.008	0.006	0.007	0.016	0.006	0.006	1,10,12,15,60,61,68
bs(40)	10.5900	40.0100	38.6900	14.1200	20.1700	40.0100	40.0100	40.0100	40.0100	40.0100	40.0100	40.01	17
bs(41)	2.7400	5.1150	4.2400	2.2800	5.5900	6.1150	6.1150	6.1150	6.1150	6.1150	6.1150	6.1150	17
bs(42)	13.1251	13.4099	14.1251	12.6760	14.3257	13.4099	12.7470	12.7470	12.7470	12.7470	12.7470	12.7470	16
bs(43)	0.0255	0.0183	0.0222	0.0376	0.0148	0.0183	0.0251	0.0251	0.0251	0.0251	0.0251	0.0251	16
bs(44)	3.54	2.35	2.85	3.54	2.25	2.04	2.80	3.54	2.25	3.50	2.80	2.80	1,20,21,27,32,33
bs(45)	0.070	0.033	0.065	0.014	0.071	0.015	0.022	0.022	0.022	0.014	0.050	0.033	1,17,18,22,25
bs(46)	0.02	0.0400	0.0400	0.0300	0.0300	0.0500	0.0500	0.0300	0.0300	0.0500	0.0500	0.0500	35,51,61,67,68,77,83
bs(47)	0.01	0.030	0.0200	0.0100	0.0100	0.0300	0.0300	0.0100	0.0100	0.0300	0.0300	0.0300	35,51,61,67,68,77,83
bs(48)	0.01	0.0200	0.0200	0.0100	0.0100	0.0200	0.0200	0.0100	0.0100	0.0200	0.0200	0.0200	35,51,61,67,68,77,83
bs(49)	400.460	320.367	480.550	410.070	512.588	320.367	349.200	410.070	518.995	379.635	320.367	320.367	19,26

(con.)

Table 2—(Con.)

Species parameters	Species code[1]												References[2]
	PIPO	ABGR	PSME	PICO	LAOC	ABLA	PIEN	PIAL	LALY	PIMO	THPL	TSHE	
tolerance	1	4	3	1	1	4	4	2	1	2	5	5	
bs(50)	349.200	599.087	438.903	424.487	389.246	438.903	490.162	424.487	389.246	419.681	599.870	599.870	19,26
bs(51)	0.4	0.8	0.8	0.5	0.4	0.8	0.8	0.4	0.4	0.5	0.8	0.8	1,10,12,68,87
bs(52)	26.0	21.0	20.0	21.0	20.0	17.0	18.0	13.0	17.0	20.0	18.0	18.0	2,9,28,29,33,61,70,72,73
bs(53)	0.10	0.30	0.20	0.20	0.20	0.30	0.30	0.20	0.20	0.30	0.3	0.3	10,68
bs(54)	15.0	10.0	15.0	10.0	7.0	25.0	25.0	30.0	27.0	15.0	30.0	30.0	10,12,68,86
bs(55)	0.50	0.80	0.60	0.50	0.40	0.80	0.60	0.40	0.40	0.40	0.80	0.80	10,12,68,87
bs(56)	1.4	1.5	1.4	1.4	1.8	1.5	1.5	1.5	1.4	1.8	1.5	1.5	10,12,68
bs(57)	0.0	0.0	0.0	0.0	0.0	0.0	0.0	0.0	0.0	0.0	0.0	0.0	
bs(58)	0.0	0.0	0.0	0.0	0.0	0.0	0.0	0.0	0.0	0.0	0.0	0.0	
bs(59)	0.95	1.00	0.95	0.90	1.00	1.00	1.00	1.00	1.00	1.00	1.00	1.00	82
bs(60)	0.90	0.90	0.90	0.80	0.90	0.90	0.90	0.90	0.90	0.90	0.90	0.90	82,87
bs(61)	0.80	0.80	0.80	0.10	0.80	0.80	0.80	0.80	0.80	0.80	0.80	0.80	82,87
bs(62)	0.10	0.20	0.10	0.10	0.20	0.20	0.20	0.20	0.20	0.20	0.20	0.20	82
bs(63)	0.0	0.0	0.0	0.0	0.0	0.0	0.0	0.0	0.0	0.0	0.0	0.0	82
bs(64)	120.00	90.00	90.00	90.00	90.00	90.00	90.00	90.00	90.00	90.00	90.00	90.00	10,26
bs(65)	280.00	280.00	280.00	280.00	280.00	280.00	280.00	280.00	280.00	280.00	280.00	280.00	10,26
bs(66)	120.0	110.0	180.0	200.0	150.0	210.0	210.0	220.0	220.0	110.0	110.0	110.0	10,26,88
bs(67)	260.00	260.00	260.00	260.00	260.00	260.00	260.00	240.00	240.00	280.00	280.00	280.00	10,26,88

[1]PIPO-*Pinus ponderosa*, ABGR-*Abies grandis*, PSME-*Pseudotsuga menziesii*, PICO-*Pinus contorta*, LAOC-*Larix occidentalis*, ABLA-*Abies lasiocarpa*, PIEN-*Picea engelmannii*, PIAL-*Pinus albicaulis*, LALY-*Larix lyallii*, PIMO-*Pinus monticola*, THPL-*Thuja plicata*, TSHE-*Tsuga heterophylla*.

[2]Reference number corresponds to the following citations:

1- Keane and others (1989)
2- Mohren and Bartelink (1989)
3- Mohren and others (1984)
4- Van Gerwen and others (1987)
5- Running and Coughlan (1988)
6- Sollings and others (1979)
7- Lopushinsky (1969)
8- Korol and others (1991)
9- Larcher (1969)
10- Burns and Honkala (1990)
11- Sievanen (1993)
12- Keane and Morgan (1994)
13- McDonald (1992)
14- Kercher and Axelrod (1984)
15- Reed and Clark (1979)
16- McCaughey and others (1985)
17- Boyce (1985)
18- Faurot (1977)
19- Simpson (1993)
20- Kaufmann and others (1982)
21- Smith (1972)
22- Lange (1971)
23- Lynch (1959)
24- Myers and Alexander (1972)
25- Ryan and Reinhardt (1988)
26- Wenger (1984)
27- Dale and others (1986)
28- Bassman (1988)
29- Hellmers and others (1970)
30- Dale and Hemstrom (1984)
31- Dalla-tea and Jokela (1991)
32- Ryan and Waring (1992)
33- Friend and others (1993)
34- Massman and Kaufmann (1991)
35- Weinstein and others (1982)
36- Pastor and Post (1986)
37- Weishampel and others (1992)
38- Lotan and Perry (1983)
39- Leemans (1989)
40- Pinty and others (1992)
41- Sprugel (1990)
42- Fry and Phillips (1977)
43- Klinka and others (1992)
44- Kaifez-Bogataj (1990)
45- Eck and Deering (1992)
46- Burton and Urban (1990)
47- Fowells (1965)
48- Gottfried and Ffolliot (1983)
49- Harlow and Harrar (1969)
50- Matysseck (1986)
51- Makela and Hari (1986)
52- Minore (1979)
53- Boe (1954)
54- Eis and Craigdallie (1983)
55- Lotan and Perry (1983)
56- Shearer (1985)
57- Shearer and Schmidt (1970)
58- Gower and others (1992)
59- Bolstad and Gower (1990)
60- Benecke and others (1981)
61- Arno (1970)
62- Kajimoto (1990)
63- Marshall and Waring (1985)
64- Arno and Hoff (1989)
65- Arp and Yin (1992)
66- Neilson (1992)
67- Jeske and Bevins (1976)
68- Data collected by authors
69- Brown and Higginbotham (1986)
70- Yue and Margolis (1993)
71- Trost (1990)
72- Bossel and Schafer (1989)
73- Matthes-Sears and Larson (1990)
74- Aber and others (1990)
75- Nambiar and Fife (1991)
76- Sheriff and others (1986)
77- Versfeld and Donald (1991)
78- McMurtrie and others (1992)
79- Whitehead and Kelliher (1991)
80- Raison and others (1992)
81- Pfister and others (1977)
82- Brown and others (1985)
83- Bevins (1977)
84- Brix (1979)
85- Cui and Smith (1991)
86- Alexander and others (1984)
87- Gary (1976)
88- Hellmers and others (1970)
89- Hellmisaari (1992)
90- Hunt (1986)

Table 3—Topographic description of fire groups used in the BMWC project.

Fire group	General description	Elevation		Slope		Aspect[1]
		Min	Max	Min	Max	
		- - - - feet - - - -		- percent -		
0	Scree, meadow, grassy bald	3,000	14,000	0	100	All
6	Moist Douglas-fir	5,000	6,000	0	10	All
7	Cool types, dominated by lodgepole	5,500	7,500	0	50	SW, SE
8	Dry, lower subalpine	5,000	7,000	10	100	SW, SE
9	Moist, lower subalpine	5,000	6,500	10	100	NW, NE
10	Cold, moist upper subalpine	6,000	8,500	0	100	NW, NE

[1]SW-Southwest, SE-Southeast, NW-Northwest, NE-Northeast.

of diameter classes are specified in the Tree file for all stands. FIRE-BGC reads this tree input table and creates a list of all trees in a stand from the tree density information and assigns the appropriate age to the trees. Then, FIRE-BGC computes those attributes explicitly utilized by the model for each tree.

The tree's structural characteristics are computed first (see "Structural Characteristics" in the Tree Processes section). Tree diameter at breast height or 1.37 m aboveground (DBH cm) is randomly estimated between the lower and upper limit of its associated diameter class (Keane and others 1989). Tree age (AGE years) is explicitly defined in the input file. Tree height (HT m) is tentatively estimated from the Milner (1992) equations, and the height to bottom of the tree's crown (HBC m) is initially calculated from the default live crown ratio (BS_{51} m^{-1}) and tree height (HT m). These two tree height attributes are recalculated after canopy leaf area distribution is computed to adjust for existing light conditions.

The tree's ecophysiological compartment (XT_i) values are initialized next because most of these compartments are quantified from allometric equations that use the structural characteristics as independent variables. Leaf carbon (XT_7 kg C) is approximated from the Brown (1976, 1978) equations that estimate foliar biomass from DBH and species. This biomass estimate is then multiplied by the fraction of leaf biomass that is carbon (BP_6 kg C kg C^{-1}). Leaf area is estimated from the product of the specific leaf area (BS_0 m^2 kg C^{-1}) and leaf carbon (XT_7 kg C). Stem carbon (XT_8 kg C) is estimated from the stem and bark volume equations of Faurot (1977) and crown volume equations of Brown (1978). Stem and bark volume, computed from DBH and HT, are multiplied by their respective densities (BS_{49} and BS_{50}, kg m^{-3}) and added together to obtain stem biomass. This biomass is then multiplied by the fraction that is carbon (BP_{21} kg C kg biomass^{-1}) to estimate stem carbon (XT_8 kg C). Coarse and fine root carbon (XT_9 and XT_{10}, kg C) are estimated from the empirical biomass equations (see "Structural Characteristics" in the Tree Processes section). The biomass estimates are multiplied by the fraction of that biomass that is carbon (BP_{23} kg C kg biomass^{-1}) to obtain carbon in the coarse and fine roots (XT_9 and XT_{10}, kg C).

Tree nitrogen compartments are initially computed as proportions of the tree's corresponding carbon pools. Leaf nitrogen (XT_{11} kg N) is a proportion (BP_{51} kg N kg C^{-1}) of leaf carbon (XT_7 kg C). Stem, coarse root, and fine root nitrogen (XT_{12}, XT_{13}, XT_{14}, kg N) is the fraction (BP_{52}, BS_{53}, BS_{54}, kg N kg C^{-1}) of stem and root carbon (XT_8, XT_9, XT_{10}, kg C).

Finally, the model initializes compartments that define the amount of resources available to the tree (Sharpe and others 1986). A resource allocation factor (XT_{16} dimensionless) is computed as the fraction of stand leaf area contributed by the tree. The tree's "effective stand area" (XT_4 m^2) is defined as the amount of the simulation plot occupied by the tree. It is computed as the maximum between the projected crown area and root area. Crown area is estimated from the empirical Moeur (1981) crown width equations. If the stand is open (leaf area index <1), then the crown area estimate is multiplied by 1.5 (Korol and others 1991). Root area is approximated as a fraction of total stand leaf area taken by the tree's leaf area. Soil water available to the tree (XT_1 m^3 H_2O) is estimated as the product of the resource allocation factor and available soil water (XP_1 m^3 H_2O). The tree's portion of the snowpack (XT_2 m^3 H_2O) is estimated in the same manner. The annual gross photosynthesis compartment (XT_5 kg C) is initialized at 1 percent of the leaf carbon (XT_7 kg C). The maintenance respiration compartment (XT_6 kg C) and last year's stem carbon compartment (XT_3 kg C) are initialized at zero.

Stand Compartment Primary Initialization—Most stand compartments are initialized from the sum of the corresponding tree compartments. Stand leaf area (LA m^2) is the sum of leaf area for all trees (XT_0 m^2). Leaf, stem, fine root, and coarse root carbon (XP_7, XP_8, XP_9, XP_{10}, kg C), and nitrogen (XP_{15}, XP_{16}, XP_{17}, XP_{18}, kg N) is the sum of the corresponding tree components. Photosynthesis for the stand (XP_5 kg C) is also a sum of the tree photosynthesis compartment XT_5 (kg C).

Some initial stand attributes are quantified from the stand input file. Stand available nitrogen (XP_{13} kg N) is specified in the stand file, as are estimates of the Leaf/Root Litter carbon (XP_{20} kg C) and nitrogen (XP_{21} kg N), and Soil carbon and nitrogen (XP_{12} kg C, XP_{18} kg N). Snowpack (XP_0 m^3 H_2O) and Soil water (XP_1 m^3 H_2O) also receive initial values from the stand file. Starting values for all compartments that make up the forest floor (see "Forest Floor Dynamics" in the Stand Processes section) and undergrowth (see "Undergrowth Dynamics" in the Stand Processes section) are obtained from the stand file (see appendix B for examples).

Annual Initialization—Many stand and tree compartments are recalculated at the start of the daily biogeochemical simulation to provide for consistency across the tree and stand scales and to account for any changes that have occurred in the simulation across levels. First, all intermediate variables (GP_i and GT_i) are initialized to zero. Then, stand leaf area is recalculated from the sum of leaf area across all trees and from the leaf area contained in the undergrowth. Stand leaf, stem, coarse root, and fine root compartments (XP_7, XP_8, XP_9, XP_{10}, kg C) are reassessed from the sum of the corresponding tree compartments (XT_7, XT_8, XT_9, XT_{10}, kg C) across all trees in the stand. Contributions of the undergrowth to stand compartments are assumed to be negligible. Stand nitrogen compartments (XP_{14}, XP_{15}, XP_{16}, XP_{17}, kg N) are taken from the sum of tree nitrogen compartments (XT_{11}, XT_{12}, XT_{13}, XT_{14}, kg N). Snowpack (XP_0 m^3 H_2O) and Soil Water (XP_1 m^3 H_2O) compartments are not modified in this annual initialization. The remaining compartments are set to zero (XP_2, XP_3, XP_4, XP_6, XP_{11}, XP_{19}) except for those FOREST-BGC compartments that represent the forest floor. These compartments (XP_{12} kg C, XP_{13} kg N, XP_{18} kg N, XP_{20} kg C, XP_{21} kg N) are recalculated from the FIRE-BGC

forest floor compartments (LITTER, SOIL and DUFF). Available nitrogen (XP_{13} kg N) is assigned a value from the forest floor compartment AVAILN (see "Forest Floor Dynamics" in the Stand Processes section).

New estimates of some tree compartments are also computed at simulation year's end. A new tree leaf area is estimated from leaf carbon. Effective tree area and the resource allocation factor is recomputed from the new stand and tree leaf area estimates. Photosynthesis is initialized for the year at 10 percent of last year's net carbon gain to simulate the effect of carbon storage on the growth process (Running and Hunt 1993).

All data files that link the spatial landscape simulation to stand simulations are updated each year. The "Seed Output" file created by FIRE-BGC contains the number of seed-producing trees by species for each stand and is used to compute a spatial distribution of seed dispersal by the submodel SEEDER. The number of seed-producing trees is calculated as the number of trees of each species greater than 10 cm diameter (DBH) and above a minimum cone-bearing age (BS_{38} years) (Keane and others 1989).

Landscape Processes

Fire

Fire Occurrence—Occurrence and points of origin of simulated fires are stochastically predicted yearly on the simulation landscape using the submodel FIRESTART (fig. 4). FIRESTART uses site-level fire frequency inputs (average fire-free interval) to compute a probability of fire occurrence for that site (Keane and others 1989). The origin of fires is computed by pixel using fire frequency probabilities and average fire size estimates.

FIRESTART simulates fire occurrence by cycling through Site and Stand Map spatial data layers that describe the simulation landscape. These data layers are made up of cells called pixels that have assigned identification (ID) numbers. FIRESTART gathers the site and stand ID numbers from these layers starting in the northwest corner of the simulation landscape. It then computes a probability of fire occurrence (P_f) for a pixel from the following three parameter Weibull probability density distribution:

$$P_f = \frac{C_i}{FFREQ_i}\left[\frac{(X_j - FREBURN_i)}{FFREQ_i}\right]^{(C_i-1)} e^{\left[-\left(\frac{X_j - FREBURN_i}{FFREQ_i}\right)^{C_i}\right]} \quad (1)$$

where C_i is the Weibull shape constant for site i, $FREBURN_i$ is the time before reburn (years), $FFREQ_i$ is the expected recurrence time or average fire frequency (years) for site i, and X_j is the time since last fire disturbance (years) for stand j. This algorithm is based on the equations and algorithms presented in Baker (1989), Clark (1990), Fox (1989), Johnson (1979), Johnson and Van Wagner (1985), and Van Wagner (1978). This probability P_f is then adjusted to account for fire size using the following relation:

$$P_{fp} = P_f\left[\frac{PIXEL^2}{FSIZE_i}\right] \quad (2)$$

where P_{fp} is the probability of fire start at a pixel, PIXEL is width of a landscape cell (m), and $FSIZE_j$ is average fire size (m^2) (Marsden 1983;

Reed 1994). The pixel's fire probability (P_{fp}) is then compared to a generated random number (RNUM). A fire start is simulated for the pixel in question if RNUM is less than P_f. The random number generators used in FIRE-BGC, FIRESTART, and other submodels are taken from Press and others (1992) and L'Ecuyer (1988).

Fire-free intervals for the BMWC project were taken from fire history data collected by Keane and others (1994) and Gabriel (1976) where this landscape was estimated to have a major fire every 144 years with a minimum of 50 years and a maximum of over 500 years. Average fire sizes and other Weibull parameters were estimated from Baker (1989), Clark (1990), Johnson (1979), Johnson and Van Wagner (1985), and also from fire atlases compiled by various National Forests. These values are entered into the FIRE-BGC Site file, which is accessed by FIRESTART.

Pixels with low fine fuel loadings limiting the ignition and spread of fire (loadings of twigs, needles, and herbaceous biomass <0.2 kg m^{-2}), such as stands primarily comprising rock and bare soil and areas recently burned (<10 years), cannot have a fire start in the simulation. These attributes are taken from the "Stand Attribute" dynamic data file created by FIRE-BGC and referenced using the stand ID number from the Stand Map. Future versions of FIRESTART will include detailed modeling of the factors that determine fire ignition including lightning strikes, fuel moistures, and topography. Once fire locations have been simulated, the FARSITE model is then called by the LOKI routines to simulate fire behavior and spread (fig. 4).

Fire Behavior—Fire is dynamically modeled on the simulation landscape using the FARSITE spatial fire model (Finney 1994). This model predicts the fire intensity and rate of spread of a fire as it moves across a landscape (Albini 1976a; Rothermel 1972). It uses the spatial data layers of topography, vegetation, weather, and fuels to predict fire dynamics.

FARSITE obtains fuel and stand attributes from the Stand Attribute dynamic file generated by FIRE-BGC. Fuel loadings are computed from carbon pools in the forest floor compartments (see "Forest Floor Dynamics" in the Stand Processes section). Stand descriptive values required by FARSITE are computed from stand attributes (see Stand Processes section). Fuel models are taken from site input files.

Currently FIRE-BGC does not simulate some input parameters to the level of detail implemented in FARSITE. For instance, daily fuel moistures and wind are not available from the FIRE-BGC simulation. Instead, a static set of weather and fuel conditions is used in FARSITE to simulate fire behavior. These values for the BMWC project were taken from typical conditions measured during upper subalpine fires in north-central Montana. These data were supplied by the Flathead National Forest.

FARSITE creates a spatial data layer of fire intensity (kW m^{-2}) and flame length (m) from the spatial predictions of fire spread. FIRE-BGC then averages the fire intensity of all pixels within a stand and uses that intensity to calculate subsequent fire effects.

Seed Abundance and Dispersal

Two aspects of the tree regeneration process are spatially simulated at a landscape level during a FIRE-BGC simulation. The occurrence of an

abundant cone crop is stochastically determined for each tree species in the simulation. Then, the spatial distribution of tree seed dispersal by species is computed across the landscape. Again, these spatial processes are linked with stand-level processes through dynamic data bases.

Seed Abundance Simulation—Each year a tree species can have a "good" or "poor" cone crop. Tree regeneration occurs only in good cone crop years. Species' cone crop abundances are modeled at the landscape level rather than the stand level because the processes that govern cone production, such as climate and topography, work at the coarser spatial scale (Boe 1954; Eis and Craigdallie 1983). Cone crops are simulated by comparing a generated random number (RNUM) to the probability of a good crop for a species (BS_{36} table 2) and, if RNUM is less than BS_{36}, a good cone crop is initiated. This Monte Carlo method is based on the approach used by Kercher and Axelrod (1984) and Keane and others (1989). The chance of having a good cone crop in subsequent years is blocked for BS_{37} years based on the assumption that trees must store sufficient energy reserves before generating another good cone crop. Future versions of FIRE-BGC will mechanistically simulate cone crops based on carbon budgets.

Seed Dispersal Simulation—The probability of a seed falling onto a stand is computed by the submodel SEEDER (figs. 4, 5) for all tree species from the spatial distribution of stand composition and structure (Anderson 1991; Greene and Johnson 1989; Kellomäki and others 1987; Ribbens and others 1994). First, the number of cone-producing trees ($TREE_{seed}$) by species in each simulation plot is obtained from the dynamic Stand Attribute data file. Then, the probability of seed dispersal to every pixel in the landscape is then computed using this form of the equations of McCaughey and others (1985):

$$P_d = \frac{e^{[BS_{42} + BS_{43} DIST]}}{e^{[BS_{42}]}} \tag{3}$$

where P_d is the probability of a seed landing on a pixel, DIST (m) is the distance between the seed source pixel and target pixel, and BS_{42} and BS_{43} are equation coefficients by species as shown in table 2. The above equation is only for species whose seeds are wind dispersed (Kellomäki and others 1987). The probability of seed dispersal of the bird-disseminated whitebark pine seed is calculated from the equation of Tomback and others (1990):

$$P_d = \frac{10^{[-0.8062 - (0.000454 DIST)]}}{0.1563} \tag{4}$$

Calculating the spatial distribution of P_d for each tree species across the landscape involves selecting a "source" pixel (starting in the northwest corner of the landscape) and obtaining the stand ID number for this pixel from the stand data layers using LOKI routines (Bevins and Andrews 1994). The number of seed-producing trees for the stand describing the pixel is gathered from the Stand Attribute file. A dispersal reduction factor for seed tree density (r_{st}) is computed from the simple relationship presented in Keane and others (1989):

$$r_{st} = MIN\left(\frac{TREE_{seed}}{5}, 1.0\right) \tag{5}$$

where $TREE_{seed}$ is the number of seed-producing trees of a species (trees ha^{-1}), and MIN denotes the minimal value of the two arguments. Then, the distance from this source pixel to all other "target" pixels on the simulation landscape is calculated using the Euclidean distance formula ($X^2 + Y^2 = Z^2$). This distance, DIST (m), is used in the dispersal probability equations presented above to obtain a P_d for the pixel. This P_d is then multiplied by r_{st} to adjust for limited seed source production. Then, another source pixel is selected, and the procedure is repeated for all landscape pixels as targets. This process is reiterated for all pixels as sources with the calculated P_d's summed for each pixel. The sum of all computed P_d's is divided by the number of iterations to obtain a final P_d as shown in this equation:

$$P_d = \frac{\sum P_d}{(n_{pixel})^2} \tag{6}$$

where n_{pixel} is the number of pixels that make up the landscape. Then an average P_d for each stand is computed by averaging the P_d across all pixels within stand boundaries.

The final step in this landscape simulation of seed dispersal is to write simulation results to a file used in the stand-level regeneration process simulation of FIRE-BGC ("Seed Dispersal" file). The success of cone crop (0 = no cone crop, 1 = cone crop) and probability of seed dispersal (P_d) are written to the "Seed Dispersal" file (SEED.DAT) by species for each stand in the simulation (see dynamic data bases in fig. 4).

Currently, topographic and wind effects on seed dispersal are not included in the simulation. Future versions of FIRE-BGC will implement these interactions into the dispersal process.

Site Processes

Weather

A daily weather data file is specified for each site modeled in FIRE-BGC and represented in the Site Map spatial data layer. This file contains many years of daily weather data computed for that site using the Mountain Climate Model MT-CLIM (Hungerford and others 1989; Running and others 1987). MT-CLIM takes daily temperature (minimum and maximum, °C) and precipitation (m) values recorded at a valley base station and extrapolates these and other attributes to mountainous terrain. Values computed by MT-CLIM and used by FIRE-BGC include minimum air temperature (T_{min} °C), maximum air temperature (T_{max} °C), dew point temperature (T_{dew} °C), shortwave radiation (R_s kJ m^{-2} day^{-1}), and precipitation (PPT m). These values are computed for every day across all years in the base station weather data file and then stored in a binary file for FIRE-BGC input (fig. 5). The weather data computed for all sites in the BMWC project were taken from the Seeley Lake National Weather Service Station for 1954 to 1991.

At the beginning of each simulation year FIRE-BGC randomly selects a weather year to use for all sites. Then the daily weather data for that year is sequentially input into the model from the site's weather file and used to simulate ecosystem processes for all stands within that site. Many

weather-related parameters are computed from these stored MT-CLIM generated values and they are discussed in the following subsections.

Temperatures—Average daily air temperature (T_{ave} °C) is computed from an arithmetic average of T_{min} and T_{max} (°C). Soil temperature is computed as a 14-day running average of T_{ave} and is initialized at 0 °C. Average daytime air temperature (T_{day} °C) is computed from the following empirical equation (Running and Coughlan 1988):

$$T_{day}=T_{ave}+[0.212(T_{\max}-T_{ave})] \tag{7}$$

and average nighttime air temperature (T_{night} °C) is computed from:

$$T_{night}=\frac{(T_{day}+T_{\min})}{2} \tag{8}$$

Humidity—A daily average relative humidity (H_r %) is computed from the following relationship detailed in Campbell (1977):

$$H_r=100[\frac{6.1078e^{[\frac{(17.269T_{dew})}{(237.3+T_{dew})}]}}{6.1078e^{[\frac{(17.269T_{ave})}{(237.3+T_{ave})}]}}] \tag{9}$$

The vapor pressure deficit (VPD mbar) is computed from the slope of the saturation vapor pressure deficit curve using the following relationship shown in Campbell (1977):

$$VPD=SVP-(\frac{H_r}{100}SVP) \tag{10}$$

where the saturation vapor pressure (SVP mbar) is calculated from the Campbell (1977) equation:

$$SVP=6.1078e^{[\frac{(17.269T_{day})}{(237.3+T_{day})}]} \tag{11}$$

Radiation—Net radiation to the site (R_n kJ m^{-2} day^{-1}) is estimated as the unreflected proportion of daily shortwave radiation (R_s kJ m^{-2} day^{-1}) using site albedo (1-BP_7) (Gay and Knoerr 1975):

$$R_n=R_s(BP_7) \tag{12}$$

Daylength for a flat surface is computed from the equation:

$$D_l=3060(\alpha\sin(0.01721(YD-79)+12) \tag{13}$$

where YD is yearday (Julian date), and α is the amplitude of the diurnal day length sine function estimated from:

$$\alpha=\frac{e^{[7.42+0.45LAT]}}{3600} \tag{14}$$

where LAT is the latitude of the site in decimal degrees as specified in the Simulation file (SIM.DAT in appendix B).

Frost—Some ecological weather attributes are also estimated from the raw weather data. FIRE-BGC estimates the latest spring frost as the last day before the middle of the growing season (GS_{mid} yearday) with a minimum air temperature (T_{min}) below –3 °C. The middle of the growing season is computed as an average of beginning (BP_{35} yearday) and end (BP_{36} yearday) of the site's growing season. The earliest fall frost is computed in a similar manner where the earliest autumnal frost after the middle of growing season is recorded. These parameters are used in the Tree Regeneration algorithms.

Fuel Models

A fuel model is a set of parameters that quantitatively describes the fuelbed for the prediction of fire behavior (Albini 1976a; Anderson 1982; Rothermel 1972). The fuelbed comprises a number of live and dead fuel components. Each component has a list of attributes that are used in the calculation of fire intensity and fire effects. The number of live and dead fuel components is specified at the start of simulation in the Simulation file (SIM.DAT in appendix B). Currently, FIRE-BGC recognizes a maximum of eight dead and two live fuel components, but these parameters can be easily changed for future applications. Fuel models are defined in the Fuel file (FUEL.DAT in appendix B) and given a unique identification number (ID number). Each site is assigned a fuel model in the Site file (SITE.DAT in appendix B) by referencing the ID number in the Fuel file.

The set of parameters that describe each fuel component is shown in table 4 for all sites in the BMWC project. Some of these values are used as input to the SPREAD fire behavior model (Rothermel 1972) as implemented by Finney (1994) in the FARSITE model to compute fire intensity, flame length, and scorch height. The ovendry particle density (RHOP), surface area to volume ratio (SVR) and heat content (LHV) values are taken from Albini (1976a), Anderson (1969), Brown (1970). Other fuel model component values are used to predict fuel consumption by fire (consumption fraction CF) (see Fire Effects section). These CF values are taken from Brown and others (1985).

Table 4—Fuel model components and parameters as implemented in FIRE-BGC.

Fuel model components	Fuel model parameters				
	RHOP[1]	LHV[2]	SVR[3]	MOIST[4]	CF[5]
Duff	0.550	18586.7	111.000	0.60	0.90
Litter	0.510	18586.7	57.410	0.08	0.90
1-hour	0.390	18586.7	11.760	0.06	0.89
10-hour	0.390	18586.7	2.880	0.08	0.84
100-hour	0.390	18586.7	0.980	0.10	0.84
1,000-hour	0.390	18586.7	3.156	0.20	0.79
Shrub dead	0.510	18586.7	91.856	0.10	0.90
Herb dead	0.510	18586.7	3.000	0.05	0.99
Shrub live	0.513	18595.7	49.200	0.90	0.50
Herb live	0.513	18595.7	91.860	0.75	0.90

[1]RHOP = ovendry particle density.
[2]LHV = heat content.
[3]SVR = surface area to volume ratio.
[4]MOIST = moisture content.
[5]CF = consumption fraction.

Some fuel model parameters are not stratified by fuel component. Values for duff and litter bulk densities (BULK) and surface area to volume ratios (SVR) are taken from Brown (1970, 1981) (appendix B) and are used to calculate duff and litter depth (see discussion on regeneration in Species Processes section). Moisture of extinction (MEXT) values used in FARSITE are from Rothermel (1972) and Frandsen and Andrews (1979). Values for fuel moisture contents (MOIST) and windspeed (WIND) are specified in the Fuel file and are usually taken from a typical fire prescription (see Fire Effects section). Values for these parameters used in the BMWC project were estimated from weather data gathered by Flathead National Forest personnel. Future applications of FIRE-BGC will include a submodel that mechanistically simulates fuel moistures using site weather data. Examples of these parameters are given in the Fuel file in appendix B (FUEL.DAT).

All fuel model parameters remain constant throughout the simulation except for the fuel loadings. Loadings (LOAD, kg biomass m^{-2}) for the six dead fuel components are computed from the forest floor carbon pools by dividing the carbon mass by the fraction carbon (BP_{21} kg C kg biomass^{-1}) and the simulation plot area (PAREA m^2) (see "Forest Floor Dynamics" in the Stand Processes section). Dead shrub and herb component loadings are summed from the simulation plot's intolerant and tolerant shrub ($SHRUB_i$ and $SHRUB_t$) and herb ($HERB_i$ and $HERB_t$) biomass compartments (see "Undergrowth Dynamics" in the Stand Processes section) using the following relationships:

$$SHRUB_{dead} = \frac{[(SHRUB_i)(FDEAD_i) + (SHRUB_t)(FDEAD_t)]}{PAREA} \quad (15)$$

$$HERB_{dead} = \frac{[(HERB_i)(FDEAD_i) + (HERB_t)(FDEAD_t)]}{PAREA} \quad (16)$$

where $SHRUB_{dead}$ and $HERB_{dead}$ (kg m^{-2}) are the dead shrub and herb fuel component loadings, PAREA (m^2) is the area of the simulation plot, and FDEAD is the fraction of the appropriate shrub or herb compartment that is dead at the time of the fire. Values of FDEAD were taken mostly from Brown and Bevins (1986) and are shown in table 5 with other undergrowth parameters. The remaining shrub and herb biomasses are considered live (fraction not dead, or 1-FDEAD) and are assigned to the live shrub and herb fuel components.

Table 5—Undergrowth (shrub and herb) parameter values implemented in FIRE-BGC.

Variable names	General description	Intolerant shrub	Tolerant shrub	Intolerant herb	Tolerant herb
USLA	Specific leaf area (m^2)	10.000	10.000	3.000	4.000
UHGT	Average height (m)	2.000	1.000	0.100	0.100
$MASS_{max}$	Max biomass (kg m^{-1})	0.142	0.101	0.017	0.020
FLEAF	Proportion biomass leaf	0.800	0.850	1.000	1.000
TURNW	Wood turnover proportion	0.200	0.200	0.000	0.000
TURNB	Leaf turnover proportion	0.200	0.200	0.950	0.950
CFRAC	Leaf fraction carbon	0.550	0.550	0.550	0.550
NFRAC	Leaf fraction nitrogen	0.008	0.008	0.015	0.015
FLIG	Leaf lignin proportion	0.258	0.250	0.250	0.250
FDEAD	Proportion dead at fire	0.250	0.250	1.000	1.000

The moisture contents of the fuel components are constant throughout a simulation run and represent average fuel moisture conditions that occurred over the duration of a fire. Windspeed is another dynamic variable that is treated as static in FIRE-BGC. Future versions of FIRE-BGC will incorporate mechanistic simulations of these critical fire behavior inputs.

Stand Processes

Canopy Dynamics

A major limitation of the FOREST-BGC model is that species are not explicitly recognized in the model (Running and Coughlan 1988; Friend and others 1993). Stand canopy dynamics are greatly influenced by the changes in species composition through succession (Bonan 1993a,b; Shugart and West 1980). FIRE-BGC improves the simulation of canopy dynamics over FIRESUM and FOREST-BGC by recognizing the size, leaf area distribution, and species of each tree on the simulation plot. This allows a more accurate characterization of the forest canopy above the simulation plot.

Canopy Leaf Area Distribution—All canopy-related parameters used in FOREST-BGC routines are computed from a weighted average of leaf area by species. Stand leaf area (LA m^2) is summed by species and then used as a weight to compute canopy and stand parameters (BP_j) from the species parameters (BS_i) as depicted in this equation:

$$BP_j = \frac{[\sum (BS_i)(LA_i)]}{LA} \qquad (17)$$

where LA_i is the leaf area of species i (m^2) and LA is stand leaf area (m^2). This algorithm is used for all BP_j parameters except for BP_5, BP_{21}, BP_{28}, BP_{38}, BP_{39}, $BP_{45\text{-}54}$ because these variables do not relate to species characteristics.

The distribution of light within the forest canopy is primarily dependent on the vertical arrangement of leaf area (Grime and Jeffrey 1965) (fig. 6a). This vertical leaf area profile is influenced by tree species, height, and

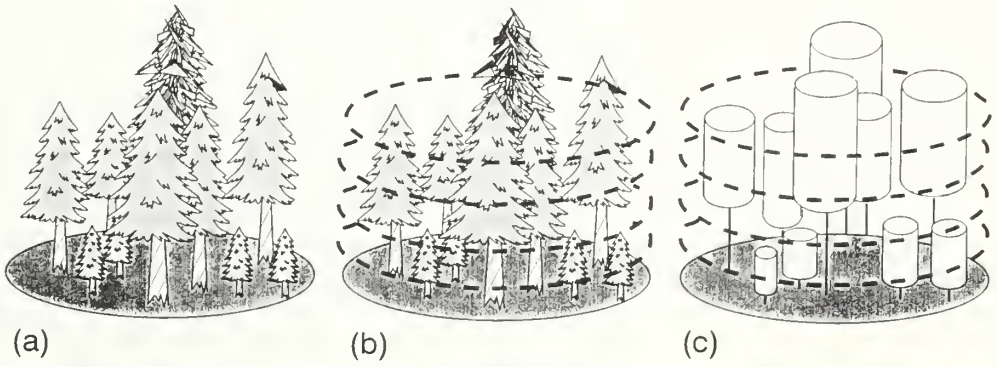

Figure 6—Vertical canopy distribution on a FIRE-BGC simulation plot: (a) representation of trees on the simulation plot, (b) "slicing" the forest canopy into canopy layers, (c) modeling tree foliage in each canopy layer with cylindrical crown shapes.

crown dimensions. FIRE-BGC computes the amount of light attenuated to various parts of the forest canopy by "slicing" the area above the simulation plot into vertically arranged canopy layers (fig. 6b) (Friend and others 1993). The thickness of each canopy layer (HSIZE m) and the number of layers (MXHGT) is input to the model from the Simulation file (SIM.DAT appendix B). Canopy layer leaf area is then computed by multiplying the proportion of the tree crown within a canopy layer (that is, canopy layer width, HSIZE in meters, divided by the crown length, CL in meters) by the total leaf area of the tree. This assumes that leaf area is evenly distributed throughout the crown and each tree crown is cylindrical (fig. 6c) (Keane and others 1989; Friend and others 1993). Crown length (CL m) is obtained by subtracting the height to base of crown (HBC m) from the tree height (HT m). This procedure is repeated for every canopy layer and every tree in the stand.

The contribution of shrub and herb foliage to canopy layer leaf area is also computed in FIRE-BGC. The leaf areas of tolerant and intolerant shrubs ($SHRUB_{la}$ m^2) and herbs ($HERB_{la}$ m^2) are calculated from the following:

$$SHRUB_{la}=[CFRAC_i SHRUB_i FLEAF_i USLA_i]+[CFRAC_t SHRUB_t FLEAF_t USLA_t] \quad (18)$$

$$HERB_{la}=[CFRAC_i HERB_i FLEAF_i USLA_i]+[CFRAC_i HERB_t FLEAF_t USLA_t] \quad (19)$$

where $SHRUB_i$, $SHRUB_t$, $HERB_i$, and $HERB_t$ are the total biomass of the intolerant and tolerant shrub and herb components (kg biomass), CFRAC is the portion of biomass that is carbon (kg C kg biomass^{-1}), FLEAF is the proportion of intolerant and tolerant shrub or herb biomass that is foliar biomass (Means and others 1994), and USLA is the specific leaf area for the intolerant and tolerant shrubs and herbs (table 5). Some FLEAF and USLA values were computed using the BIOPAK program developed by Means and others (1994) and were input to the model from the Plant file (see PLANT.DAT file in appendix B).

Shrub and herb leaf area distribution by canopy layer is computed by multiplying the proportion of the shrub or herb height (UHGT m) in a canopy layer ($HSIZE/UHGT_j$) by the respective leaf areas. If the canopy layer width (HSIZE m) is greater than an undergrowth compartment height ($UHGT_i$ in table 5) then all leaf area is allocated to the bottom canopy layer. Shrub and herb crown shape is again assumed to be cylindrical, and it is also assumed that the crown encompasses the entire height of the undergrowth compartment (Keane and others 1989). Shrub and herb average heights are input to the model from the Plant file and their values for the BMWC project were taken from field data (Keane and Morgan 1994; Keane and others 1994).

Vertical Light Distribution—Canopy light dispersion is calculated by first computing the cumulative leaf area index for each canopy layer summing from the highest layer progressing to the bottom (ground) layer. The proportion of available light in each layer is then estimated from this cumulative leaf area profile using the Beers-Lambert equation:

$$AL_i=e^{[(-BP_1)(\frac{PLA_i}{PAREA})]} \quad (20)$$

where AL_i is the proportion of available light at canopy layer i, PLA_i is the cumulative projected leaf area (m^2) at canopy layer i, PAREA (m^2) is the area of the simulation plot, and BP_1 is the extinction coefficient of the canopy. The parameter BP_1 is computed as a weighted average of all species' extinction coefficients (BS_1 dimensionless) in the canopy (see previous discussion). Values of BS_1 are shown in table 2 and are taken from the literature. These BP_1 extinction coefficient values assume average annual solar zenith angles and vegetation foliar tilt angles. Projected leaf area by canopy layer is computed by dividing leaf area by a weighted leaf projection factor (BP_{49} m^2 m^{-2}) calculated from BS_{44} and the species leaf area.

Mechanistic Modeling of Daily Stand Processes

A shortcoming of most JABOWA models is the lack of detail in the method used to estimate tree growth. The optimal annual diameter increment is reduced using a set of scalars (values from 0-1) (Botkin and others 1972). These scalars abstractly represent the effects of important ecosystem processes, such as light attenuation, on diameter growth (Urban and others 1990). Some scalars remain constant throughout the simulation run. Although this approach is computationally efficient, it lacks the detail to fully understand the dynamic and complex process of tree growth. An improvement of FIRE-BGC over JABOWA gap models is the integration of a mechanistic treatment of forest growth into the succession model architecture. This was accomplished by replacing the scalar-based tree growth algorithm in FIRESUM with the mechanistic ecosystem simulation model FOREST-BGC (Running and Coughlan 1988). A similar model was developed by Friend and others (1993) but lacked the ability to simulate mixed species stands and did not incorporate fire processes into the simulation architecture.

The following sections describe the portions of the FOREST-BGC model that were included in FIRE-BGC. The original FOREST-BGC model was reprogrammed in the C computer language. Some algorithms in FOREST-BGC were refined and these refinements are presented in detail here. For a more detailed treatment of FOREST-BGC documentation refer to Running (1984), Running and Coughlan (1988), Running and Gower (1991), and Running and Hunt (1993). A general matrix describing the flow of water, energy, carbon, or nitrogen is provided in figure 7 for reference.

Water Processes—The flow of water across ecosystem compartments in a stand is explicitly modeled in FOREST-BGC from daily temperature and precipitation (fig. 1). Precipitation (PPT m) will fall as snow if nighttime temperature (see "Weather" in Site Processes section) is below freezing (0 °C). This amount of water (GP_1 m^3 H_2O) is multiplied by the simulation plot area (PAREA m^2) and added to the Snowpack Compartment (XP_0 m^3 H_2O) (fig. 1). Snowmelt (GP_2 m^3 H_2O) is estimated from the product of average daytime temperature (°C) and a snowmelt coefficient (BP_5 m^3 H_2O $°C^{-1}$ day^{-1}) (Allen and Walsh 1993). The melted water (GP_2 m^3 H_2O) is added directly to the soil water compartment (XP_1 m^3 H_2O) and removed from Snowpack (XP_0 m^3 H_2O) (see fig. 7).

If nighttime air temperature (T_{night}) is above freezing the precipitation falls as rain. The amount of rain reaching the forest floor is estimated from the following equation:

$$GP_0 = PAREA[PPT - (LAI)(BP_3)] \quad (21)$$

From this ↓ to this →	Snowpack	Soil water	Water loss	Transpire	Evaporate	Photosyn	Respirate	Leaf C	Stem C	C. Root C	F. Root C	Leaf N	Stem N	C. Root C	F. Root N	Litter C	Duff C	Soil C	Wood C	Litter N	Duff N	Soil N	Wood N	Decomp	Loss N	Avail N
Snowpack (XP_0)	G_1	G_2			G_5																					
Soil water (XP_1)		G_0	G_{17}	G_{16}	G_5																					
Water loss (XP_2)																										
Photosynthesis (XP_5)						G_{25}	G_{24}	G_{69} G_{62}	G_{70} G_{63}	G_{71} G_{64}	G_{71} G_{64}															
Leaf carbon (XP_7)																G_{44}	G_{45}									
Stem carbon (XP_8)																			G_{31}- G_{33}							
Coarse root C (XP_9)																		G_{47}								
Fine root C (XP_{10})																		G_{46}								
Leaf N (XP_{14})																				G_{36}	G_{36}					G_{72}
Stem N (XP_{15})																							G_{76}- G_{78}			
Coarse root N (XP_{16})																						G_{37}				
Fine root N (XP_{17})																						G_{38}				G_{38}
Litter																								G_{112}		
Duff carbon																								G_{115}		
Soil carbon																								G_{118}		
Wood carbon																								G_{121}- G_{127}		
Litter nitrogen																										G_{85}
Duff nitrogen																										G_{86}
Soil nitrogen																										G_{87}
Wood nitrogen																										G_{130}- G_{133}
Available nitrogen											G_{69}	G_{70}	G_{70}	G_{77} G_{38}											B_{37}	B_{38} B_{39}

Figure 7—Flow matrix of important FOREST-BGC and FIRE-BGC intermediate calculations. Flow of these computations (that is, GP_j) is FROM the vertical compartments TO the horizontal compartments.

where PAREA is the simulation plot area (m^2), GP_0 is the water that reaches the forest floor (m^3 H_2O), LAI is the stand's projected leaf area index (m^2 m^{-2}), and BP_3 is a canopy interception coefficient (m^3 H_2O LAI^{-1} day^{-1}) estimated from a weighted average with leaf area across all species in the stand (see "Canopy Dynamics" in the Stand Processes section). The remainder of rainfall is intercepted by the forest canopy and may be lost through evaporation from the stand. The potential evaporation of precipitation (GP_3 m^3 H_2O) is calculated as the difference between total rainfall and GP_0 (m^3 H_2O). Then a radiation-limited estimate of potential evaporation (GP_4 m^3 H_2O day^{-1}) is calculated from:

$$GP_4 = 2.5x10^6(R_n) \tag{22}$$

where R_n is the net radiation to the canopy (kJ m^{-2} day^{-1}) (see "Weather" in the Site Processes section). The final estimate of evaporation (GP_5 m^3 H_2O day^{-1}) is estimated as the difference between GP_3 and GP_4. Site water balance is then computed from flows depicted in figure 1 and figure 7.

Predawn leaf water potential is assumed to be the soil water potential (GP_9 –MPa), and it is computed from the Running and Coughlan (1988) reciprocal function:

$$GP_9 = \frac{0.2}{(XP_1/BP_2)} \qquad IF \quad GP_9 < BP_8 \tag{23}$$

$$GP_9 = BP_8 \qquad IF \quad GP_9 \geq BP_8 \tag{24}$$

where BP_2 (m^3 H_2O) is the soil water holding capacity, XP_1 (m^3 H_2O) is the soil water, and BP_8 (–MPa) is the maximum springtime leaf water potential (Webb 1975). Soil water holding capacity was estimated for the BMWC simulation study using data collected by Keane and Morgan (1994) and Keane and others (1994). The value of GP_9 is set equal to 1.5 –MPa if the soil temperature (T_{soil} in Weather section, °C) is less than freezing (0 °C) or if snowpack (XP_0) greater than 0.1 m thick to account for the decrease in soil water potential when soil water is frozen (Running and Coughlan 1988). The denominator in this relationship (XP_1/BP_2) is termed the soil water fraction (GP_6 m^3 H_2O m^{-3} H_2O). A portion of the soil water is lost to overland flow and ground water (GP_7 m^3 H_2O day^{-1}) (fig. 7) and is computed by reducing the amount of soil water (XP_1 m^3 H_2O) by the fraction BP_{28}.

Energy Processes—Canopy radiation is estimated from solar radiation values (R_s kJ m^{-2} day^{-1}) in the input weather file for the site. Net radiation (R_n kJ m^{-2} day^{-1}) is estimated by multiplying input solar radiation (R_s) by stand surface albedo difference or the portion of light that is not reflected (1-BP_7) (see "Weather" in the Site Processes section). Then the average canopy radiation (R_c kJ m^{-2} day^{-1}) is estimated from the following formula:

$$R_c = R_n \frac{(1 - e^{[-BP_1(LAI)]})}{-BP_1(LAI)} \tag{25}$$

where BP_1 is the extinction coefficient estimated for the canopy (see "Canopy Dynamics" in this section) and LAI is the stand projected leaf area index.

Transpirational Processes—Canopy transpiration (GP_{16} m^3 H_2O day^{-1}) is estimated from leaf area index (LAI m^2 m^{-2}) and canopy conductance (GP_{14} m sec^{-1}) using the Penmon-Monteith algorithm detailed in Campbell (1977), Running (1984), Running and Coughlan (1988). This equation assumes a well-ventilated canopy with an aerodynamic resistance (r_a sec m^{-1}) of 5.0 and conifer needle geometry:

$$GP_{16}=\frac{[\Delta R_n+\frac{(c_p p_a)VPD}{r_a}]}{[\Delta+\gamma(1+\frac{r_c}{r_a})](1000\lambda)}(LAI)(D_l) \quad (26)$$

where GP_{16} is canopy transpiration (m^3 H_2O day^{-1}), R_n is average canopy net radiation (W m^{-2}), c_p is specific heat of air (J kg^{-1} $°C^{-1}$), p_a is air density (kg m^{-3}), VPD is the vapor pressure deficit from canopy to air (mbar) (see "Weather" in the Site Processes section), r_c is canopy resistance (sec m^{-1}) which is the inverse of canopy conductance ($1/GP_{15}$), γ is the psychometric constant (mbar $°C^{-1}$), λ is the latent heat of water vaporization (J kg^{-1}), and D_l is daylength in seconds (Arp and Yin 1992). Δ is the slope of the saturation vapor pressure curve (mbar $°C^{-1}$) computed from:

$$\Delta=6.1078e^{[\frac{17.269T_a}{237.3+T_a}]} \quad (27)$$

where T_a is average daytime temperature (°C). Transpiration is subtracted from the soil water compartment (X_1) daily.

Canopy leaf conductance (GP_{14} m sec^{-1}) is computed by reducing a maximum leaf conductance (GP_{10} m sec^{-1}) possible for the current predawn leaf water potential (GP_9 –MPa) by functions that account for temperature, humidity, and radiation effects on canopy conductance. The predawn maximum conductance is:

$$GP_{10}=BP_{10}-[\frac{BP_{10}}{(BP_{11}-BP_8)}][GP_9-BP_8] \quad (28)$$

where BP_{10} is the maximum canopy conductance (m sec^{-1}), BP_{11} is leaf water potential at stomatal closure (–MPa), and BP_8 is the minimum springtime leaf water potential (–MPa). The relationship of predawn water potential with leaf conductance in frozen and unfrozen soil is illustrated in figure 8a. If the day's minimum temperature (T_{min} °C) is less than freezing, then GP_{10} is decreased by ($0.0002T_{min}$). If T_{min} is above freezing, GP_{10} is adjusted using the following relationship detailed in Running and Coughlan (1988):

$$GP_{10}=GP_{10}+[0.00003GP_{10}(T_{day}-10)] \quad (29)$$

where T_{day} is the average daily temperature (°C in "Weather" in Site Processes section) (Running and Coughlan 1988). The influence of absolute humidity on canopy conductance is approximated into a new estimate of conductance (GP_{11} m sec^{-1}) using this relationship:

$$GP_{11}=GP_{10}-[GP_{10}BP_{12}(0.000006H_a-4.0)] \quad (30)$$

where BP_{12} is the slope of the canopy conductance vs. absolute humidity relationship (m sec^{-1} μg^{-1} m^{-3}), and H_a is the absolute humidity deficit (μg

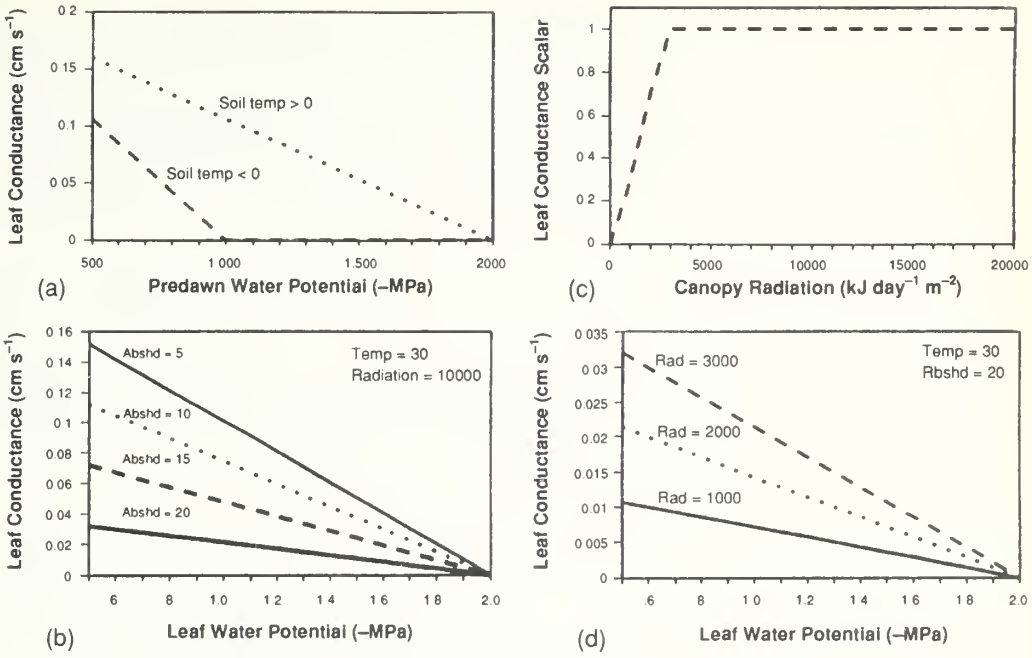

Figure 8—Leaf conductance relationships to environment: (a) predawn leaf water potential influences on leaf conductance in frozen and unfrozen soil, (b) predawn leaf water potential, and absolute humidity interactions with conductance, (c) radiation effects scalar, (d) radiation and leaf water potential effects on conductance.

m^{-3}) (fig. 8b) (Sandford and Jarvis 1986; Webb 1975). This quantity (GP_{11}) is then reduced by multiplying it with the scalar GP_{13} (fig. 8c), which approximates the effect of light on conductance:

$$GP_{13}=MIN[(\frac{R_c}{BP_9}),1] \tag{31}$$

where R_c is average canopy radiation (kW m^{-2} day^{-1}), BP_9 is radiation threshold for maximum canopy conductance (kJ m^{-2} day^{-1}), and MIN signifies the minimum value between the two arguments. The relationship of radiation to predawn leaf water potential with constant temperatures and humidities is presented in figure 8d. Final canopy conductance (GP_{14} m sec^{-1}) is estimated as the product of GP_{11} and GP_{13}.

Mesophyll conductance, conductance of CO_2 across the leaf mesophyll, is calculated as a reduction from a maximum mesophyll conductance (BP_{15} m sec^{-1}) using scalars that represent the environmental effects of nitrogen, light, temperature, and humidity on CO_2 conductance across the mesophyll cells. The leaf nitrogen scalar (GP_{18} dimensionless) is computed from:

$$GP_{18}=0.5+18.2L_n \tag{32}$$

where L_n is the leaf nitrogen concentration (kg N kg dry $weight^{-1}$). L_n is computed from the following relationship:

$$L_n=[\frac{XP_{14}}{BP_{30}BP_{25}}](BP_{25}-BP_{26})+BP_{26} \tag{33}$$

where XP_{14} is leaf nitrogen (kg N), BP_{30} is the maximum possible leaf area index for the stand ($m^2\ m^{-2}$), BP_{25} is the maximum and BP_{26} is the minimum average canopy leaf nitrogen concentration (kg N kg dry weight^{-1}). This modeled relationship between leaf nitrogen concentration and mesophyll conductance is illustrated in figure 9a. The mesophyll conductance radiation scalar (GP_{19} dimensionless) is computed from this equation:

$$GP_{19} = \frac{(R_c - BP_{13})}{(R_c + BP_{14})} \tag{34}$$

where R_c is average canopy radiation, BP_{13} is the amount of radiation at the light compensation point (kJ m^{-2} day^{-1}), and BP_{14} is the radiation level (kJ m^{-2} day^{-1}) where the photosynthetic rate is 0.5 of maximum (fig. 9b). The temperature scalar for mesophyll conductance (GP_{20}), illustrated in figure 9c, is calculated from:

$$GP_{20} = \frac{[(BP_{17} - T_{day})(T_{day} - BP_{16})]^v}{[(BP_4 - BP_{16})(BP_{17} - BP_4)]^v} \tag{35}$$

where BP_{17} and BP_{16} are the maximum and minimum temperature thresholds for photosynthesis (°C), BP_4 is the optimum temperature for photosynthesis (°C), and T_{day} is the average daytime temperature (°C) (Kajfez-Bogataj 1988; Keane and others 1989; Reed and Clark 1979). The parameter v (dimensionless) is calculated from the equation:

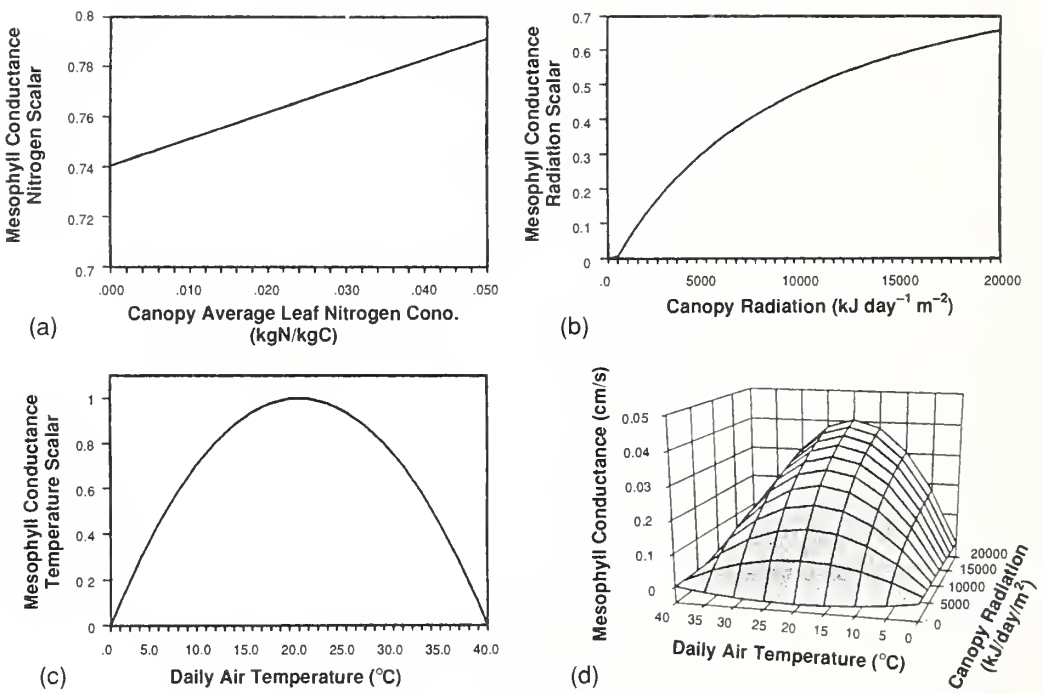

Figure 9—Mesophyll conductance relationships to environment: (a) influence of leaf nitrogen concentration, (b) influence of canopy radiation, (c) influence of temperature, and (d) interaction of temperature and radiation, on mesophyll conductance.

$$v=\frac{(BP_{17}-BP_4)}{(BP_4-BP_{16})} \tag{36}$$

The final mesophyll conductance (GP_{21} m sec^{-1}) is calculated from the product of all scalars:

$$GP_{21}=BP_{15}(GP_{18})(GP_{19})(GP_{20}) \tag{37}$$

where BP_{15} is the maximum mesophyll conductance (m sec^{-1}). The interaction of two scalars on mesophyll conductance is shown in figure 9d.

Photosynthetic Processes—Gross canopy photosynthesis (GP_{23} kg CO_2 day^{-1}) is computed from the Lohammar and others (1980) equation:

$$GP_{23}=[\frac{(1.6dCO_2GP_{14}GP_{21})}{(1.6GP_{14}+GP_{21})}](LAI)(D_l) \tag{38}$$

where dCO_2 is the carbon dioxide diffusion gradient from canopy to air (kg m^{-2}, computed as a constant 0.0006-0.00007), GP_{14} is the canopy conductance (m sec^{-1}), GP_{21} is mesophyll conductance (m sec^{-1}), and D_l is daylength (sec). This gross estimate (GP_{23}) is then multiplied by 0.3 to convert to kg C day^{-1}. A daily net carbon gain for the leaves (GP_{25} kg C day^{-1}) is estimated from the difference of GP_{23} (gross daily photosynthesis, kg C day^{-1}) and GP_{24} (night respiration, kg C day^{-1}). Net photosynthesis (GP_{25} kg C day^{-1}) is summed daily over the entire year in the stand compartment XP_5 (kg C), and stem and root respiration is summed daily over the year in XP_6 (kg C).

Respirational Processes—Night respiration of the leaves (GP_{24} kg C day^{-1}) is computed from the following equation:

$$GP_{24}=XP_7BP_{18}e^{[BP_{24}T_{night}(24-\frac{D_l}{3600})]} \tag{39}$$

where BP_{18} is the leaf respiration coefficient (kg C kg C^{-1}), BP_{24} is the Q_{10} scaling factor for respirational surfaces (dimensionless), T_{night} is the average nighttime air temperature (°C), and XP_7 is the leaf carbon of the simulation plot (kg C). Maintenance respiration of stems (GP_{29} kg C day^{-1}) and roots (GP_{30} kg C day^{-1}) are computed from the following equations taken from Running and Coughlan (1988):

$$GP_{29}=BP_{19}e^{[BP_{24}T_{ave}]}e^{[0.67\ln(XP_8)]} \tag{40}$$

$$GP_{30}=BP_{20}e^{[BP_{24}T_{soil}]}(XP_9)(XP_{10}) \tag{41}$$

where BP_{24} is the Q_{10} scaling factor, BP_{19} and BP_{20} are the stem and root respiration coefficients (kg C kg C^{-1}), T_{ave} and T_{soil} are the average daily air temperature and soil temperature (°C), XP^8 is stem carbon (kg C), and XP_9 and XP_{10} are the coarse and fine root carbon compartments (kg C).

Undergrowth Dynamics

The undergrowth plant component of the simulation stands is defined as the biomass of all non-tree vascular plant species. This undergrowth biomass (kg) is stratified by two lifeform groups (shrubs and herbs) and

then stratified again by life-form shade tolerance class (intolerant and tolerant). This yields four undergrowth compartments: shade intolerant shrubs ($SHRUB_i$), shade tolerant shrubs ($SHRUB_t$), shade intolerant herbaceous plants (grasses and forbs) ($HERB_i$), and shade tolerant herbs ($HERB_t$) (Keane and others 1989). FIRE-BGC will allow a finer stratification of undergrowth life forms such as species guilds.

FOREST-BGC does not explicitly simulate undergrowth growth interactions with other ecosystem processes. However, forest undergrowth dynamics are important in FIRE-BGC. These plants are considered part of the fuel bed and are therefore included as fuel in generating fire behavior predictions. Their influence on tree regeneration (see "Regeneration" in Tree Processes section) and light distribution (see "Canopy Dynamics" in this section) is also accounted for in the model. Annual shrub and herb carbon and nitrogen contributions to the forest floor compartments are also explicitly modeled in FIRE-BGC (see "Forest Floor Dynamics" in this section).

Input parameters for the four compartments are specified by site in FIRE-BGC from the Plant file (PLANT.DAT, appendix B) to account for differences in undergrowth species composition across a landscape. The undergrowth input parameters for a BMWC project site are shown in table 5 in "Fuel Models" in the Site Processes section. These values were mostly taken from field data (Keane and others 1994; Keane and Morgan 1994). A generalized diagram describing the flow of undergrowth carbon and nitrogen is provided in figure 10 for reference.

Growth in biomass of the undergrowth compartments is computed using the deterministic method detailed in Keane and others (1990a) and Kercher and Axelrod (1985) that estimates the growth in biomass (kg) of undergrowth compartment i ($GROWTH_i$) from the following equation:

$$GROWTH_i = r_{al} n_i (MASS_i)[1 - (\frac{MASS_i}{MASS_{\max,i}})] \quad (42)$$

where $MASS_i$ is the current biomass of undergrowth compartment i (kg biomass m^{-2}), n_i is a growth constant for compartment i ($year^{-1}$), and $MASS_{max,i}$ is the maximum attainable biomass for compartment i (kg m^{-2}). Values for n_i (table 5) were taken as 1.44 yr^{-1} for shrubs (Sampson 1944) and 10.842 yr^{-1} for herbaceous fuel (from unpublished data collected by the authors). $MASS_{max,i}$ values (table 5) are from Brown and Bevins (1986) and Irwin and Peek (1979) and field data collected for the BMWC project. The light reduction scalar r_{al} (dimensionless) is calculated from the same equation presented in "Growth" of the Tree Processes section, with the shade tolerant undergrowth ($SHRUB_t$, $HERB_t$) having a shade tolerance class of 4 and shade intolerant undergrowth ($SHRUB_i$, $HERB_i$) having a class of 1 (Arno and others 1985).

Forest Floor Dynamics

The method used to calculate decomposition dynamics in FIRE-BGC is based on the Running and Gower (1991) FOREST-BGC approach where forest floor respiration is influenced by atmospheric and vegetation inputs. However, the FOREST-BGC decomposition routine did not provide the detail needed to simulate fire process interactions because compartments representing the forest floor were not stratified by fuel size class.

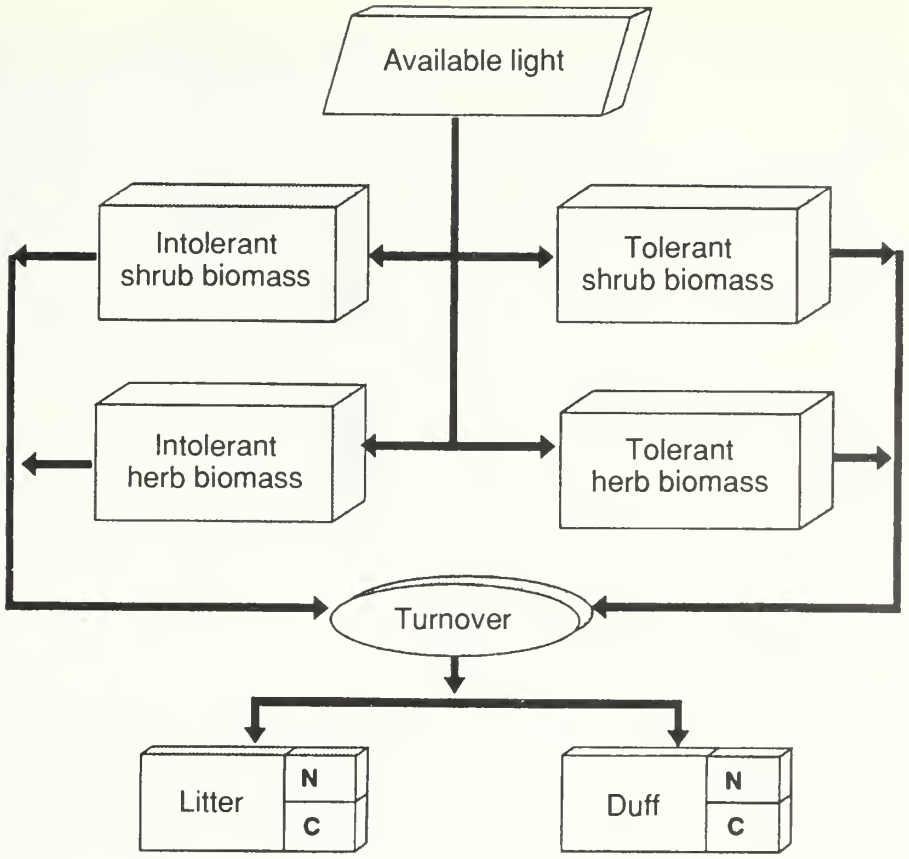

Figure 10—Model diagram of the undergrowth compartments in FIRE-BGC.

The FOREST-BGC decomposition module only recognizes Leaf/Root Litter and Soil compartments (Running and Gower 1991). Therefore, the FOREST-BGC approach was refined to stratify the forest floor into seven compartments so they can be used to predict fire behavior and effects. The FOREST-BGC decomposition routine is also included in the FIRE-BGC program for comparison purposes and to provide consistency between simulation approaches.

Organic matter on the forest floor is represented in FIRE-BGC as carbon and nitrogen pools contained within seven compartments (fig. 11). These compartments are quantified by the loading or biomass of the fuel classes on the forest floor (fig. 12). The Mineral Soil (SOIL) and Duff (DUFF) carbon and nitrogen compartments are typically composed of mostly lignin-based, partially decomposed material from leaf turnover. The Litter (LITTER) compartment contains the carbon and nitrogen of freshly deposited leaf material that is not lignin. The four Woody compartments ($_i$WOOD) are defined by the average diameter or size of woody particle. The first Woody compartment ($_1$WOOD) is for twigs of 0-1 cm diameter. Branches of 1 to 3 cm diameter compose the second woody size class compartment ($_2$WOOD). Large branchwood of 3 to 7 cm diameter is the third compartment ($_3$WOOD). Logs of 7+ cm diameter are contained in the last woody compartment ($_4$WOOD). These particle size classes correspond to standard woody fuel size classes used to predict fire behavior

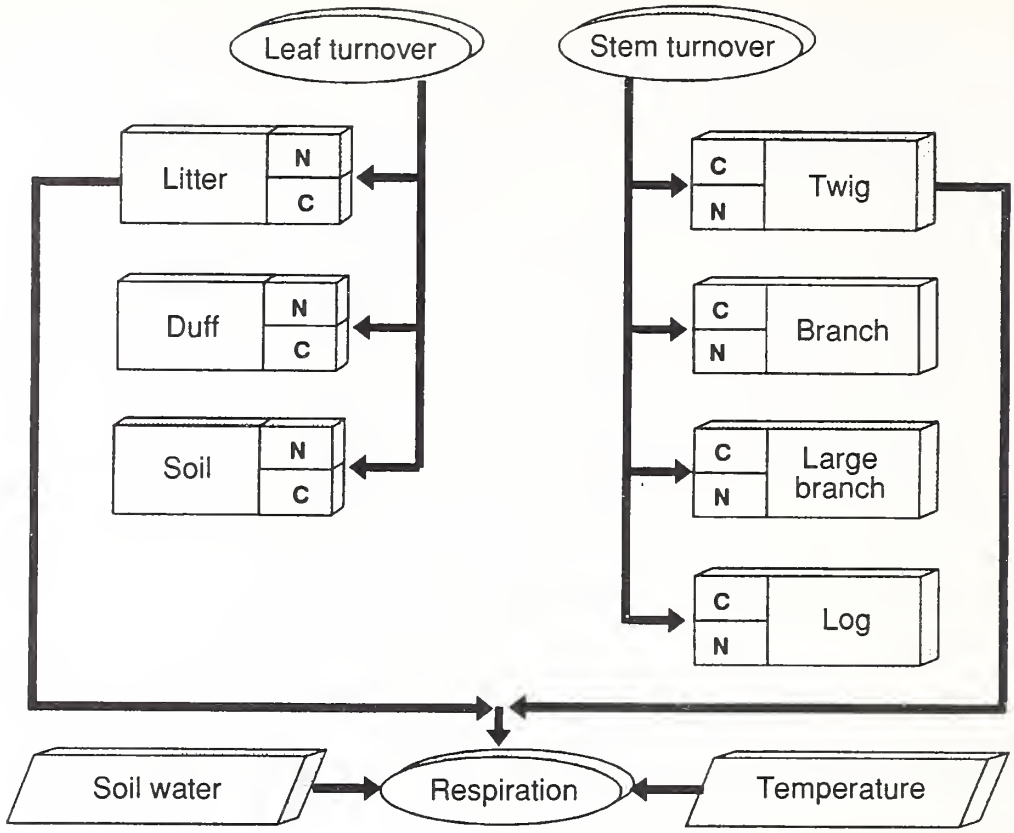

Figure 11—Model diagram of the forest floor compartments in FIRE-BGC.

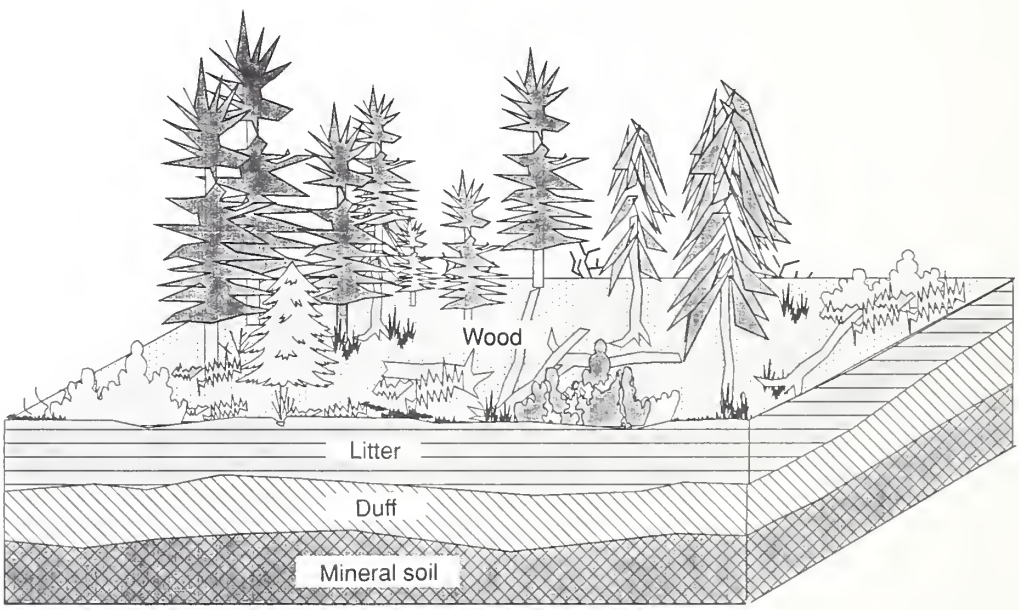

Figure 12—Illustration of forest floor compartments in a stand.

(1-, 10-, 100-, and 1000-hour timelag woody fuel components) (Albini 1976b; Fosberg 1970).

Organic Matter Accumulation—Accumulation of organic material on the forest floor is annually computed from stem, leaf, and root turnover of simulated trees and undergrowth (fig. 11) (Turner and Long 1975). Carbon and nitrogen inputs to the forest floor compartments from trees are computed as proportions of the tree's stem, leaf, and root compartments that are lost each year. Carbon deposited into the $LITTER_c$ compartment (GP_{44} kg C) is that portion of the leaffall that is not lignin (Meetenmeyer 1978; Piene and Van Cleve 1978) and is calculated from:

$$GP_{44} = \frac{XT_7(1 - BS_{24})}{BS_{23}} \tag{43}$$

where BS_{23} is the tree species' leaf retention time (years), BS_{24} is the leaf lignin fraction (kg lignin kg C^{-1}) of that species, and XT_7 is the tree's leaf carbon (kg C). Needle carbon contribution to the $DUFF_c$ compartment (GP_{45} kg C) is that portion of the leaffall that is lignin:

$$GP_{45} = \frac{XT_7 BS_{24}}{BS_{23}} \tag{44}$$

Carbon additions to the $SOIL_c$ compartment from roots (GP_{46} kg C) are derived mostly from fine root turnover that is the product of fine root carbon (XT_{10} kg C), and fine root turnover coefficient (BS_{33} kg C kg C^{-1}) (Nadelhoffer and Raich 1992). Coarse root turnover (GP_{47} kg C) is a minor contribution to $SOIL_c$ carbon pool and is computed as the product of coarse root carbon (XT_9 kg C) and the coarse root turnover coefficient (BS_{29} kg C kg C^{-1}). Woody material ($GP_{31\text{-}33}$ kg C) is added to three smallest woody components ($_iWOOD_c$) using a similar relationship where woody fuel accumulation for size class i is computed from:

$$GP_{30+i} = (CM_i)(BP_{21})(BS_{45+i}) \tag{45}$$

where CM_i is amount of tree biomass in woody size class i as calculated from the Brown (1978) equations, BP_{21} is the fraction of wood that is carbon, and BS_{45+i} is the turnover fraction for woody size class i (Mathews 1972). The index i corresponds to the Twig, Branchwood, Large Branchwood woody size class compartments ($_1WOOD_c$ to $_3WOOD_c$ in kg C). It is assumed that no material greater than 7.5 cm (that is, logs) are contributed to the forest floor annually. Instead, logs are only added to the forest floor in the event of tree death (Keane and others 1989) (see Tree Processes section).

Nitrogen additions to the $LITTER_n$ compartment (GP_{35} kg N) are computed in the same manner as carbon accumulation except that the translocation of nitrogen from the leaf to the available nitrogen pool ($AVAIL_n$ kg N) is accounted for using the following equation:

$$GP_{35} = \frac{XT_{11}}{BS_{23}}(1 - BS_{21})(1 - BS_{24}) \tag{46}$$

where XT_{11} is the tree's leaf nitrogen (kg N), BS_{23} is the tree species leaf retention time (years), BS_{24} is the tree species leaf lignin fraction, and BS_{21} is the fraction of leaf nitrogen that was translocated from the leaffall to the available nitrogen pool (scalar). Nitrogen contribution to the $DUFF_n$

compartment (GP_{36} kg N) is computed by replacing the (1-BS_{24}) term in the previous equation with BS_{24} which is the amount of needle nitrogen contained in lignin. The root nitrogen contribution to the $SOIL_n$ (GP_{37} kg N) is computed by multiplying the fine root turnover coefficient BS_{29} (kg C kg C^{-1}) by fine root nitrogen (XT_{14} kg N) and adding it to the product of BS_{29} and the tree's coarse root nitrogen (XT_{13} kg N). Root nitrogen translocation is thought to be zero (Nambiar 1987), and the release of nitrogen from root decomposition and subsequent reabsorption is so rapid at a yearly time step that the model returns all nitrogen in root turnover to the available nitrogen pool ($AVAIL_n$), (Hellmisaari 1992; Nadelhoffer and others 1985; Running and Gower 1991). The nitrogen inputs to the ${}_iWOOD_n$ compartments are obtained by multiplying the carbon additions to these compartments ($GP_{31\text{-}34}$ kg N) by the fraction of that carbon turnover that is nitrogen (BP_{52} kg N kg C^{-1}).

Undergrowth plant contributions to the $LITTER_c$ and $DUFF_c$ compartments are computed from SHRUB and HERB biomass turnover, estimated as fraction (TURNB) of total biomass carbon. This fraction is partitioned into the $LITTER_c$ and $DUFF_c$ by the fraction that is lignin (FLIG) (table 5). Some twigwood is added to the ${}_1WOOD_c$ compartment, and this amount is computed from the product of intolerant and tolerant shrub biomass and the fraction of that biomass that is wood (TURNW). This lost biomass is not subtracted from the component biomass loadings because it is assumed that all lost biomass will be replaced the next year. Undergrowth nitrogen contributions to $LITTER_n$ and $DUFF_n$ are estimated by multiplying the carbon turnover by the nitrogen fraction (NFRAC) (table 5). The amount of nitrogen contributed to the forest floor is subtracted from the available nitrogen pool (AVAILN kg N). It is assumed that undergrowth inputs to the SOIL carbon and nitrogen pools are minimal. Biological fixation of nitrogen by the biota are calculated as a constant input as described later in this section.

Decomposition—Decomposition from forest floor compartment carbon pools is calculated as a function of the average daily water fraction and a daily soil temperature degree-day summation (Running and Gower 1991). The amounts of carbon respired each day from the $LITTER_c$ (GP_{111} kg C day^{-1}), $DUFF_c$ (GP_{114} kg C day^{-1}), $SOIL_c$ (GP_{117} kg C day^{-1}), and $WOOD_c$ ($GP_{120,\ 122,\ 124,\ 126}$ kg C day^{-1}) compartments are computed from the following equations:

$$GP_{111} = \frac{LITTER_c BP_{47}\left(GP_6 + \frac{T_{ave}}{BP_{45}}\right)}{365} \tag{47}$$

$$GP_{114} = \frac{DUFF_c BP_{46}\left(GP_6 + \frac{T_{soil}}{BP_{45}}\right)}{365} \tag{48}$$

$$GP_{117} = \frac{SOIL_c BP_{46}\left(GP_6 + \frac{T_{soil}}{BP_{45}}\right)}{365} \tag{49}$$

$$GP_{120,122,124,126} = \frac{{}_iWOOD_c BP_{46}\left(GP_6 + \frac{T_{ave}}{BP_{45}}\right)}{365} \tag{50}$$

where GP_6 is the daily soil water fraction (m^3 H_2O m^{-3} H_2O), i indicates the size class of woody fuel compartment ($_iWOOD_c$), BP_{45} is the optimal temperature for decomposition (°C), BP_{47} is a scalar (dimensionless) for litter decomposition, and T_{ave} and T_{soil} are average daily air and soil temperatures (°C) (Chertov 1990; Fogel and Cromack 1977; Kellomäki and Kolström 1992). The parameter BP_{46} is a fraction that expresses the amount of decomposition of a forest floor compartment relative to the amount of litter decomposition (Ågren and others 1991; Allison and Klein 1961; Chertov 1990; Maclean and Wien 1978; Running and Gower 1991). If either T_{ave} or T_{soil} is less than 0 °C then that temperature is set to zero. Decomposition estimates for each compartment are summed over the year in the intermediate variables GP_{112}, GP_{115}, GP_{118} for the $LITTER_c$, $DUFF_c$, and $SOIL_c$ compartments respectively, and $GP_{121, 123, 125, 127}$ for the four $WOOD_c$ compartments. At year's end these sums are subtracted from the appropriate compartments (fig. 7).

Nitrogen Cycling—Nitrogen is released from the forest floor compartments as a function of the fraction of carbon decomposed and a decomposition release factor (Running and Gower 1991). The amount of nitrogen lost from the $LITTER_n$ compartment is calculated by multiplying the litter nitrogen ($LITTER_n$) by fraction of $LITTER_c$ decomposed ($GP_{112}/LITTER_c$) and the fraction of nitrogen release relative to carbon release (BP_{29}) (Edmonds 1979). This method is used for all forest floor compartments (Aber and McClaugherty 1990; Aber and others 1991; Prescott and others 1993).

The nitrogen released by the decomposition process goes directly into the available nitrogen pool ($AVAIL_n$) except for a portion ($1/BP_{37}$) that is lost from the simulation plot (Fahey 1983). The parameter BP_{37} (years) is the mobile nitrogen retention time that represents the rate of leaching, volatilization or some other loss of nitrogen from the system (Aber and Melillo 1978; Aber and others 1991; Berg and Ekbohm 1993). Volatilization from fire is the only other means where nitrogen can be lost from the stand (see Fire Effects section). The only external sources of nitrogen input are atmospheric deposition (BP_{38} kg N $year^{-1}$) and biological fixation by plants or microbes (BP_{39} kg N $year^{-1}$). Both of these parameters are assumed to be constants across simulation time. Values for BP_{38} are taken from Aber and others (1991), Johnson and others (1993), Lovett (1994), Lovett and Lindberg (1993), and Weinstein and others (1982). Values for BP_{39} are taken from Chertov (1990) and Running and Coughlan (1988). Nitrogen inputs from soil weathering are considered minor.

Species Processes

Regeneration

Establishment of new trees on the simulation plot is accomplished at the species level. Climate and stand conditions are evaluated each year at both landscape and stand levels to compute establishment success of a tree species. First, information in the Seed Dispersal file (FIRE-BGC.SEED as described in the Landscape Processes section) is used to obtain cone crop and dispersal information. Only species currently having a good cone crop will contribute to new tree regeneration. Then, seed dispersal probabilities (P_d, see Landscape Processes section) by species are used as scalars

($r_{disp} = P_d$) expressing the effect of seed source distribution on stand tree regeneration.

New trees of a species are established on the simulation plot if several environmental criteria were met. First, the latest acceptable spring frost date for the species (BS_{66} Julian date) is compared with the latest frost that occurred during that simulation year (Hänninen 1990). The earliest acceptable fall frost for the species (BS_{67}) is also compared with the earliest autumnal frost for that simulation year (Hänninen 1990). If there is a late spring frost or an early fall frost for a species, then no tree regeneration is simulated that year for that species. The latest and earliest frost is evaluated relative to the midpoint of the species' growing season (GS_{mid} yearday) as computed from:

$$GS_{mid} = \frac{(BS_{64} + BS_{65})}{2} \tag{51}$$

where BS_{64} and BS_{65} are the start and end of the species' growing season (yearday). The latest spring frost is the last frost occurring before GS_{mid}, and the earliest autumnal frost is the first to occur after GS_{mid}.

Next the species must pass the water stress criteria. If annual average predawn leaf water potential (GP_9 averaged across the growing season, –MPa) is greater than the leaf water potential at stomatal closure (BS_7 –MPa), it is assumed the year was too dry for species establishment and no trees are added.

Lastly, no tree species can become established if there has not been adequate time elapsed after a major disturbance. Stand-replacement fires often render the site inhospitable to seedling establishment (Agee and Smith 1984; Alexander 1984; Arno and others 1985; Bossel and Krieger 1991; Canham and Marks 1985). The subsequent mitigation of site conditions for tree ecesis is a complex process and difficult to model. This process is indirectly modeled in FIRE-BGC through the use of a waiting period. This waiting period, called the regeneration lag time, is represented in FIRE-BGC by the variable LAG (years) specified in the Site file (SITE.DAT in appendix B). Trees will not be established in the simulation plot until LAG number of years have elapsed after a stand-replacement fire (98 percent fire-caused tree mortality) (Agee and Smith 1984; Little and others 1994). Regeneration lag times often exceed 30 years in some upper subalpine ecosystems (Little and others 1994).

The number of trees actually established on the simulation plot for any species is calculated as a reduction of maximum seedling establishment using four scalars that indirectly represent environmental effects on tree species ecesis (Keane and others 1989; Kercher and Axelrod 1984; Urban 1990). The maximum seedling density ($SEED_{max}$ seedlings m^{-2}) is specified by site in the Site file (SITE.DAT in appendix B) and includes new trees from all species. Values for this parameter were taken from Alexander (1984), Arno and others (1985), Knapp and Smith (1982), Pfister and Shearer (1977), Schimdt and others (1976), and Shearer (1975, 1985).

The first regeneration scalar evaluates the effect of duff and litter depth on seedling survival for a species. This scalar (r_{sur}) is calculated from a modification of Boyce's (1985) empirical seedling survival equations of the form:

$$r_{sur} = \frac{(BS_{40} - \frac{BS_{41} DEPTH_{d,l}}{2.54})}{BS_{40}} \tag{52}$$

where BS_{40} and BS_{41} are regression coefficients stratified by species (table 2) (Keane and others 1989). $DEPTH_{d,l}$ is the depth of the duff and litter layer (cm) and is computed from the following formula:

$$DEPTH_{d,l} = \frac{1}{100(PAREA)(BP_{21})}\left[\frac{LITTER_c}{BULK_l} + \frac{DUFF_c}{BULK_d}\right] \quad (53)$$

where PAREA is the area of simulation plot (m^2) input in the Simulation file, BP_{21} is the fraction of the duff and litter biomass that is carbon, $LITTER_c$ and $DUFF_c$ are the amounts of carbon in the litter and duff forest floor compartments (kg C), and $BULK_l$ and $BULK_d$ are the bulk density (kg m^{-3}) of the litter and duff forest floor layers, respectively. Bulk densities are specified in the fuel model for the site (see "Fuel Models" in the Site Processes section) and are taken from Brown (1981).

The effect of shade on species establishment is represented in the second regeneration scalar (r_{shade}) taken from FIRESUM (Keane and others 1989). This scalar uses the shade tolerance of a species to key to one of these equations:

$$r_{shade} = e^{[-0.8LAI]} \qquad \textit{Shade Intolerant} \quad (54)$$

$$r_{shade} = e^{[0.25(LAI+1)]} \qquad \textit{Moderately Tolerant} \quad (55)$$

$$r_{shade} = 1 - e^{[-0.25(LAI+0.2)]} \qquad \textit{Shade Tolerant} \quad (56)$$

where LAI is stand projected leaf area index (m^2 m^{-2}) for all trees and undergrowth, and Shade Intolerant indicates species of shade tolerance class 1 or 2, Moderately Tolerant is shade class 3, and Shade Tolerant is shade class 4 and 5. Graphical representations of these equations (fig. 13) show

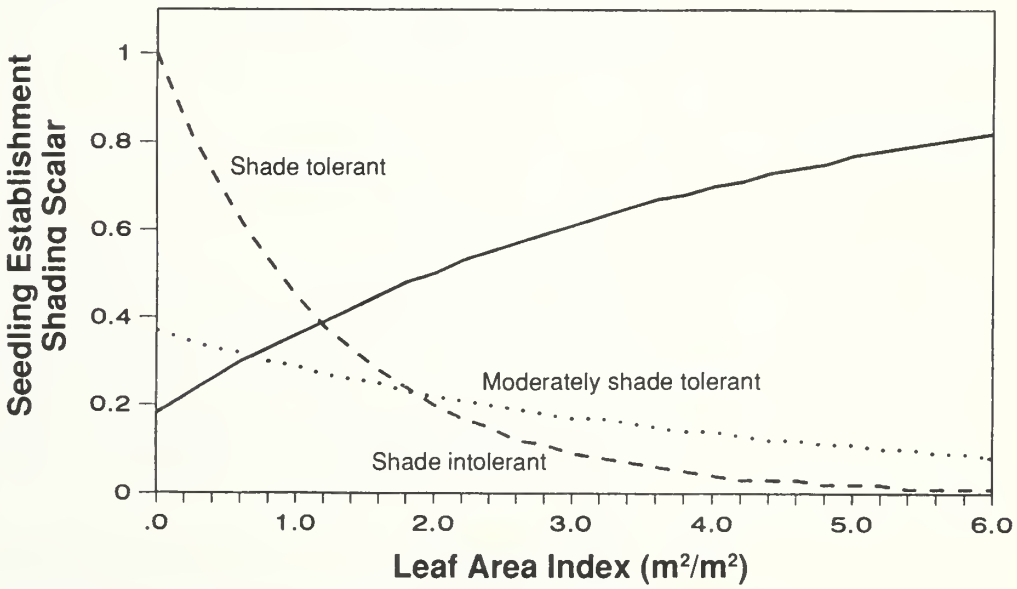

Figure 13—Relationship of the seedling shading scalar to leaf area index for reducing the number of trees established on the simulation plot.

shade tolerant species have the best chance of establishing under a dense canopy (Bossel and Krieger 1991; Grime and Jeffery 1965).

The third scalar (r_{dens}) adjusts seedling establishment based on an index of crowding in the stand. The scalar is computed from the minimum of two indexes that indirectly assess crowding using leaf area and stand density. The algorithm is as follows:

$$r_{dens}=MIN[(\frac{LAI}{BP_{30}}),(\frac{BA}{BP_{55}})] \quad (57)$$

where BP_{30} is the maximum leaf area index for the stand ($m^2\ m^{-2}$), BA is the stand basal area ($m^2\ ha^{-1}$), and BP_{55} is the maximum stand basal area ($m^2\ ha^{-1}$). Values for BP_{30} and BP_{55} were estimated for the BMWC project from Pfister and others (1977) and Shearer (1974) and data collected by the authors (Keane and Morgan 1994; Keane and others 1994).

The last scalar, r_{disp}, represents the chance of tree species' seed falling within the stand (P_d). This parameter is discussed in detail in "Seed Abundance and Dispersal" in the Landscape Process section.

The final estimate of seedlings established is the product of all regeneration scalars and maximum seedling density:

$$SEED=SEED_{\max}(r_{sur})(r_{shade})(r_{dens})(r_{disp}) \quad (58)$$

where SEED is the number of seedlings established on the simulation plot for that tree species (trees $PAREA^{-1}$) (Pukkala 1987). The model ensures that the number of trees established across all species does not exceed $SEED_{max}$ by keeping a running sum of the number of trees established.

Whitebark pine regeneration is computed differently from other tree species because, instead of being wind-dispersed, the seeds of whitebark pine are disseminated by a bird, the Clark's nutcracker. The whitebark pine regeneration module in FIRE-BGC simulates the effects of seed crop, nutcrackers, and light on whitebark pine tree seedling establishment (Keane and others 1990b). A complete discussion of the whitebark pine regeneration algorithm is presented in Keane and others (1990b). Parameters that quantify these algorithms are contained in the Whitebark file (PIAL.DAT in appendix B).

Species Growth Potential

Carbon fixed via photosynthesis at the stand level is allocated to each tree using algorithms described in "Stand-to-Tree Carbon Allocation" of the Tree Processes section. However, a method is used in FIRE-BGC to evaluate the efficiency of carbon gain across tree species. Species carbon allocation factors ($rPSN_i$, where i is species index, dimensionless) are calculated by assuming the stand's canopy is composed of a single species and then computing potential photosynthetic gain for that species keeping all other stand conditions constant, such as soil water potential (Waring 1989). These allocation factors are used as weights when allocating stand photosynthetic carbon gain to individual trees (Waring and Schlesinger 1985).

The species carbon allocation method involves calculating leaf and mesophyll conductances using the equations described in "Mechanistic Modeling of Daily Stand Processes" in the Stand Processes section. But instead of using the stand parameters (BP_i), the corresponding species

parameters (BS_i) are used. For example, BP_{10} (maximum canopy conductance, m sec^{-1}) is replaced with the BS_6 for the species under consideration. Then, a net daily photosynthetic gain is computed for that species using the two conductances (Waring 1989; Webb 1975). This process is repeated for each species present on the simulation plot. The net gain is summed across the entire year in variable $SPPPSN_i$ (kg C) where i denotes the species.

The species carbon allocation factors ($rPSN_i$) are computed by determining the maximum annual net photosynthetic gain across all tree species present on the simulation plot. This value (PSN_{max}, kg C) is then used as the denominator in the following equation:

$$rPSN_i = \frac{SPPPSN_i}{PSN_{max}} \tag{59}$$

where $rPSN_i$ is a scalar with values between 0 and 1, and i is the species index. The species having the highest potential photosynthetic gain ($PSN_{max} = SPPPSN_i$) will receive the highest weighting, while the species with the lowest $SPPPSN_i$ will have the lowest weighting. This algorithm allows the species best adapted to grow in the stand to receive proportionately more carbon (for details see "Tree Compartment Allocation" in the Tree Processes section).

Tree Processes

Each tree simulated in FIRE-BGC is defined by a set of structural characteristics in addition to the carbon and nitrogen compartments (XT_i). These characteristics are used to describe the physical aspects of the stand and are important in assessing vertical structure and its influences on ecosystem processes. The primary structural characteristics of diameter, height, age, and height to crown bottom are dynamically modeled in FIRE-BGC. Secondary structural characteristics of crown width, stem bole and bark biomass, coarse and fine root biomass and crown biomass, are computed from these primary structural variables using allometric equations. These secondary characteristics are used throughout the simulation for resource allocation, initialization, and ancillary data computation. They are not stored for each tree, but rather calculated from empirical relationships whenever needed. Many of the dimensional attributes described in this section are illustrated in figure 14.

Primary Structural Characteristics

Diameter (DBH cm)—Each tree specified in the input file is assigned a stem diameter measured at breast height (1.37 m above the ground) or DBH. Tree diameter is used in most empirical equations that compute secondary structural characteristics of trees. Each year the diameter of a tree is increased in geometric proportion to the amount of carbon allocated to the stem as computed from the ecosystem process simulation (see "Mechanistic Modeling of Daily Stand Processes" in the Stand Processes section).

Age (AGE years)—The age of the tree is simply the number of years a tree remains alive and is incremented by one each simulation year. Initial tree ages are taken from the Tree file (appendix B) at the start of simulation.

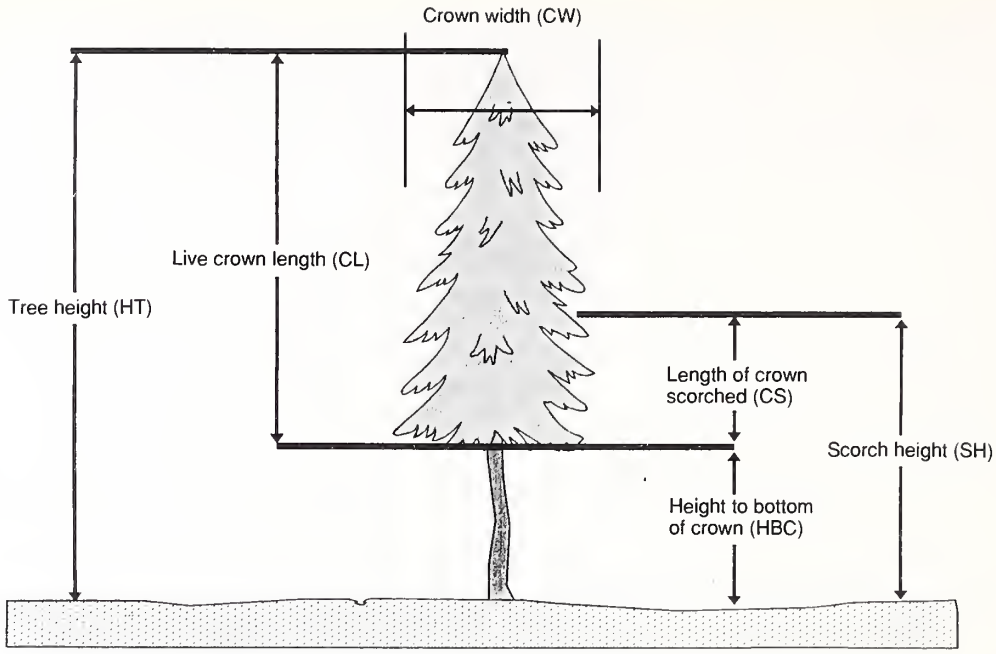

Figure 14—Tree structural characteristics explicitly simulated in FIRE-BGC. Also shown are dimensions used to model the effect of fire's scorch height on tree mortality.

Tree age is an important variable used to estimate tree height and mortality.

Height (HT m)—Tree height is computed as a reduction in the maximum height for a tree species based on the amount of available light. Maximum height is computed from the Milner (1992) empirical equations of the form:

$$HT_{\max} = a + b[1 - e^{(c(AGE))}]^d + f[1 - e^{(g(AGE)}]^h [BS_{35} - i] \quad (60)$$

where a, b, c, d, f, g, h, and i are regression coefficients (table 6), HT_{max} is maximum height (m), AGE is age of tree (years), and BS_{35} is the site index of the tree's species at age 50 (m). Site index is the maximum height of a tree at year 50. Site index values for the tree species in the BMWC project (see table 2) are taken from tree age and height data measured in the field (Keane and others 1994; Keane and Morgan 1994) and Fowells (1965). The maximum height growth increment ($HINC_{max}$ m) is the difference between the solution of the Milner (1992) equation for the current and next year's tree height. The estimated maximum height growth increment ($HINC_{max}$) is then reduced using available light reduction scalars computed from equations based on Klinka and others (1992). These equations compute a relative height growth (r_{ht} dimensionless) scalar based on the amount of light available to the tree crown:

$$\ln(r_{ht}) = a - be^{[-100c(AL)]} \quad (61)$$

where a, b, and c are regression coefficients (table 7), and AL is the proportion of light available to the tree canopy computed for each tree as an

Table 6—Regression coefficients for Milner (1992) tree height equation by tree species.

Species[1] code	Regresssion coefficients							
	a	b	c	d	f	g	h	i
PIPO	4.5	121.40	–0.01736	1.483	1.189	–0.05799	2.630	59.6
ABGR	4.5	114.60	–.01462	1.179	1.703	–.02214	1.321	57.3
PSME	4.5	114.60	–.01462	1.179	1.703	–.02214	1.321	57.3
PICO	4.5	96.93	–.01955	1.216	1.410	–.02656	1.297	59.6
LAOC	4.5	127.80	–.01655	1.196	1.289	–.03211	1.047	69.0
ABLA	4.5	114.60	–.01462	1.179	1.703	–.02214	1.321	57.3
PIEN	4.5	121.40	–.01736	1.483	1.189	–.05799	2.630	59.6
PIAL	4.5	96.93	–.01955	1.216	1.410	–.02656	1.297	59.6
LALY	4.5	127.80	–.01655	1.196	1.289	–.03211	1.047	69.0
PIMO	4.5	96.93	–.01955	1.216	1.410	–.02656	1.297	59.6
THPL	4.5	114.60	–.01462	1.179	1.703	–.02214	1.321	57.3
TSHE	4.5	114.60	–.01462	1.179	1.703	–.02214	1.321	57.3

[1]PIPO-*Pinus ponderosa*, ABGR-*Abies grandis*, PSME-*Pseudotsuga menziesii*, PICO-*Pinus contorta*, LAOC-*Larix occidentalis*, ABLA-*Abies lasiocarpa*, PIEN-*Picea engelmannii*, PIAL-*Pinus albicaulis*, LALY-*Larix lyallii*, PIMO-*Pinus monticola*, THPL-*Thuja plicata*, TSHE-*Tsuga heterophylla*.

Table 7—Height growth light reduction scalar equation coefficients by shade tolerance classes.

Shade tolerance classes	Regression coefficients		
	a	b	c
1	4.70	4.00	0.040
2	4.60	3.50	.040
3	4.50	3.00	.039
4	4.40	2.63	.035
5	4.40	2.33	.030

integrated average of the available light at the top and bottom of the crown (dimensionless). The values for available light are taken from the vertical light distribution computed for the forest canopy (see "Canopy Dynamics" in the Stand Processes section).

Actual height growth is then computed by multiplying the maximum height growth ($HINC_{max}$ m) by the available light growth reduction factor (r_{ht}). This growth is then added to the tree's height (HT) to obtain a new tree height. The r_{ht} scalar function by shade tolerance category (see table 2) is graphically shown in figure 15.

Initial tree heights (HT and HBC, m) are estimated directly from the Milner (1992) equations without any adjustment for light conditions. This is because these heights are used to compute the vertical distribution of leaf area with the forest canopy that is in turn used to compute canopy light distribution (see "Canopy Dynamics" in the Stand Processes section). Once initial heights are assessed, then the vertical distribution of available light is computed and the tree heights are recomputed taking into account the effect of limited light on tree height.

Height to Bottom of Crown (HBC m)—The height from the ground to the bottom of the crown for all trees in the initial input stand is computed from a default live crown ratio (BS_{51}, m m^{-1}). This live crown ratio

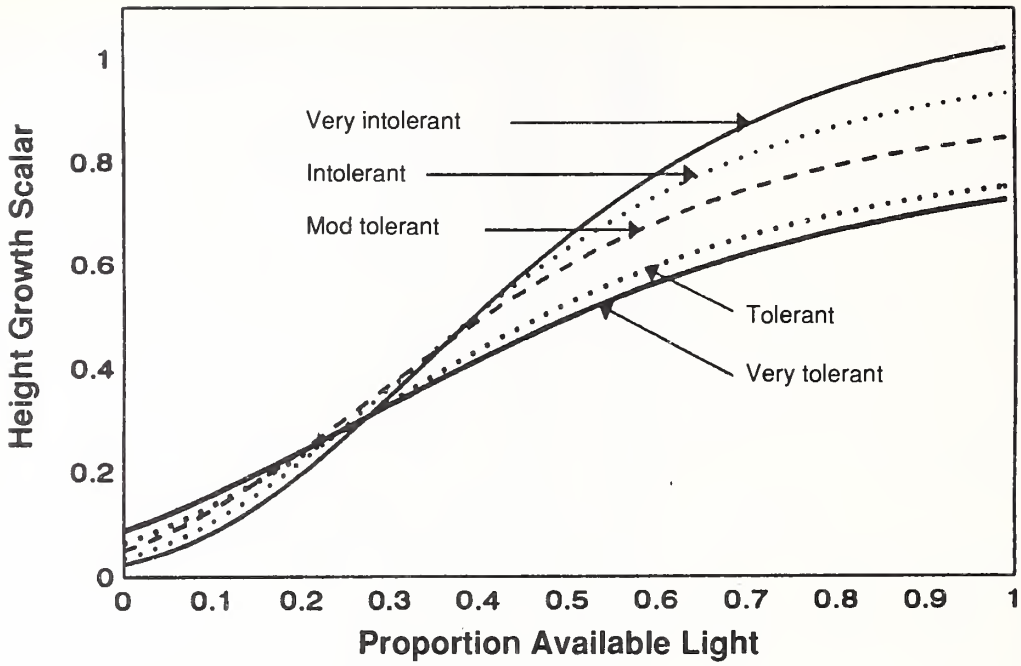

Figure 15—Relationship of available light to the scalar that reduces optimal tree height growth.

is the proportion of tree height that is tree crown. It is multiplied by tree height to get crown length (CL m), and then crown length is subtracted from tree height to obtain height to bottom of crown (HBC m). After initialization, the crown height is calculated dynamically by first computing the average daily radiation to the stand during the growing season. The amount of radiation to the bottom of the tree crown is then estimated by multiplying the available light at the canopy layer encompassing the bottom of the crown by the average growing season radiation. Height to bottom of crown is adjusted upward one canopy height increment (HSIZE m) if the growing season radiation is less than the radiation at light compensation point for that species (BS_9 kJ m^{-2} day^{-1}). This characteristic is used to calculate the vertical distribution of light in the canopy of the stand. It is also used to compute fire-caused tree mortality and crown weights.

Secondary Structural Characteristics

Crown Biomass (CM_i kg)—Crown biomass is composed of twigs (0 to 2.5 cm diameter), branches (2.5 to 7.5 cm diameter), and live foliage components computed separately from the empirical crown weight equations of Brown (1978) and Gary (1976). These equations are used to estimate the proportion of total crown biomass for each crown component. Since Brown's (1978) equations apply to mostly dominant and codominant trees, a correction factor of 0.4 was multiplied by crown biomass estimates to adjust for trees grown in a closed canopy. Twig and branch biomass are used to estimate the contribution of twig and branchwood to the respective woody fuel compartments on the forest floor for live and dead trees.

Crown Width (CW m)—The width of a tree crown is computed from the diameter (DBH cm), height (HT m), basal area (BA m^2 ha^{-1}) and crown length (CL m) using the equations of Moeur (1981). Crown width is used to compute resource allocation and leaf area index for individual trees and for the entire forest stand. Crown width estimates were multiplied by a correction factor of 1.5 in open canopy conditions (Korol and others 1991).

Stem Biomass ($STEM_m$ kg)—Bole and bark biomass estimates for each tree stem are calculated using the equations of Faurot (1977) where bark and stem volume are estimated from tree diameter and height. This volume is then converted to biomass using wood and bark density estimates (BS_{49} and BS_{50}) from Brown and others (1977) and Simpson (1993) (table 2). Initial stem carbon (XT_8 kg C) is calculated from the sum of wood and bark biomass multiplied by the fraction of stem biomass that is carbon (BS_{21}). This empirically derived stem carbon estimate is only used to initialize the stem carbon component (XT_8 kg C). Once initialized, it is dynamically simulated from estimates of carbon allocation to the stem (see "Tree Compartment Allocation" in the Tree Processes section).

Root Biomass ($ROOT_m$ kg)—Coarse and fine root biomass is also empirically estimated for tree carbon compartment initialization (XT_9 and XT_{10}, kg C). Root biomass estimates are computed from the empirical biomass equations of Evert (1985), Foster (1985), Gower and others (1991), Gower and others (1987), Grier and others (1981), Feller (1992), Means and others (1994), Pearson and others (1984), Stanek and State (1978), and Standish and others (1985). This biomass is converted to fine and coarse root carbon by multiplying by the carbon root fraction (BP_{23}). The results are stored in the XT_9 (coarse root, kg C) and XT_{10} (fine root, kg C) compartments. Again, these values are only computed during simulation initialization. After that, root biomass is simulated dynamically from estimates of carbon allocation to roots (see "Tree Compartment Allocation" in this section).

Regeneration

The FIRE-BGC tree regeneration routine uses data gathered at two spatial resolutions to predict the number of new trees to add to the simulation plot. Cone crop occurrence and seed dispersal probabilities are estimated across the landscape from data summarized at the stand level (see "Seed Abundance and Dispersal" in the Landscape Processes section). Seedling establishment and survival are evaluated at the stand level for each tree species (see "Regeneration Processes" in the Species Processes section). Data computed at these two levels are used to compute the number of new trees to add to the simulation plot by species as detailed in the Species Processes section.

Each new tree established on the simulation plot is randomly assigned a diameter (DBH cm) between 1 and 2 cm using a uniform probability distribution. Tree age (BS_{54} years), height (BS_{56} m), and height to bottom of crown (as computed from the difference of tree height and live crown ratio BS_{55}, m) are taken from parameters in the input Species file (table 2). The initial ecophysiological characteristics (XT_i) of established seedlings are then calculated from these structural characteristics using empirical equations as detailed in the Parameterization and Initialization section.

Stand-to-Tree Carbon Allocation—The first step in FIRE-BGC tree growth modeling is the allocation of stand net photosynthetic carbon gain (XP_5 kg C) and stem/root respiration carbon loss (XP_6 kg C) to each tree in the stand. This is accomplished annually using an iterative method that weights tree carbon allocation by leaf area, the species growth allocation factor (see "Species Growth Potential" in the Species Processes section) and the tree's use of available light as presented in the following equations:

$$XT_5 = XP_5[\frac{XT_0}{LA}](rPSN_i)(r_{al}) \tag{62}$$

$$XT_6 = XP_6[\frac{(XT_8 + XT_9 + XT_{10})}{(XP_8 + XP_9 + XP_{10})}] \tag{63}$$

For each tree in the stand, the stand photosynthetic carbon gain (XP_5 kg C) is multiplied by the tree's (XT_0, m^2) fraction of stand leaf area (LA m^2), the species carbon allocation factor ($rPSN_i$, i is species index) and the shade tolerance available light scalar (r_{al}) computed for the tree's species (Sievänen and others 1988). Korol and Zuuring (1990) developed a similar algorithm for allocation but used height and basal area as weights. The scalar r_{al} is computed from the following exponential function taken from Friend and others (1993) with different coefficients for each class of shade tolerance:

$$r_{al} = a_i(1 - e^{[-b_i(AL - c_i)]}) \tag{64}$$

where AL is the proportion of available light in the canopy layer containing the top part of the tree crown, and a_i, b_i, and c_i are equation constants for shade class i (five shade tolerance classes as assigned by species in table 2). Values of these constants are shown in table 8, and the equation curve forms are depicted in figure 16. These equations are solved for each tree in the stand. Then the entire procedure is repeated until there is no more stand carbon ($XP_5 = 0$).

Allocation of respiration to the trees (XT_6 kg C) is solved directly using the tree's proportion of stem (XT_8 kg C) and coarse and fine root carbon

Table 8—Available light carbon allocation reduction scalar equation coefficients by shade tolerance classes.

Shade tolerance classes	Regression coefficients		
	a	b	c
1	1.49	1.23	6.09
2	1.24	1.28	6.08
3	1.11	2.52	0.07
4	1.04	3.44	0.06
5	1.01	4.62	0.05

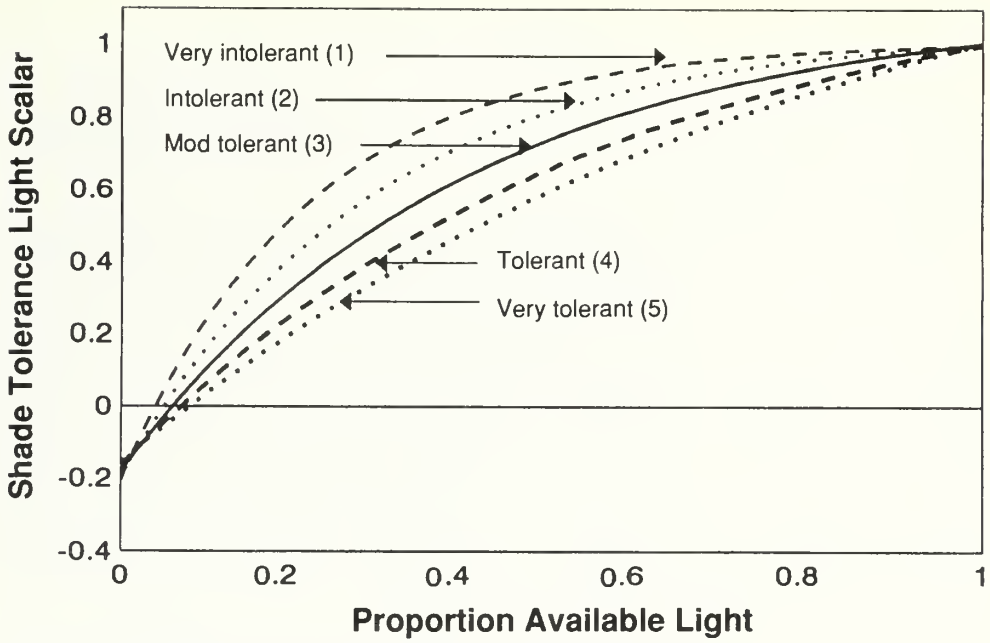

Figure 16—Relationship of available light to the shade tolerance reduction scalar used to allocate stand carbon to individual trees.

(XT_9 and XT_{10}, kg C) to the stand's corresponding stem and root compartments (XP_8, XP_9, XP_{10}, kg C) (McMurtrie and Wolf 1983; Waring and Schlesinger 1985).

Tree Compartment Allocation—Stand carbon and nitrogen allocated to each tree is then partitioned to the appropriate tree compartments (XT_i) using dynamic allocation algorithms detailed by Running and Gower (1991). This method emphasizes leaf area index as a key structural attribute controlling ecosystem process rates. The first step is to calculate the net carbon gain available for tree growth. This is simply the difference between gross photosynthetic gain (minus night respiration) (XT_5 kg C) and stem-root maintenance respiration (XT_6 kg C). If this amount (PSN kg C) is above zero (net carbon gain), then 10 percent of PSN is returned back into the XT_5 compartment to simulate carbon storage in a tree. Otherwise, no carbon is allocated to storage (Hari and others 1991).

Structural Carbon Allocation—The model computes three estimates of the proportion of PSN carbon (kg C) to allocate to leaf growth. The first estimate (GT_{52} kg C) is the amount of leaf carbon to allocate if carbon was limiting, as calculated from the following equation:

$$GT_{52} = PSN(GT_{51})(1 - BS_{30}) \tag{65}$$

where BS_{30} is the leaf growth respiration coefficient (kg C kg C^{-1}), and GT_{51} is the leaf:root ratio with a maximum value of 0.5 (dimensionless). The variables GT_i are defined the same as GP_i except that they pertain to individual trees rather than the simulation plot. This leaf:root allocation ratio is computed from:

$$GT_{51}=[\frac{(GT_{49}+\frac{XT_{15}BS_{25}}{LAI_{max}BS_{19}})}{4}] \quad (66)$$

where GT_{49} is the average daily soil water fraction (that is, XP_1/BP_2 averaged over a year), XT_{15} is the nitrogen available to the tree (kg N), LAI_{max} is the maximum possible leaf area index for the tree species ($m^2\ m^{-2}$), BS_{19} is the maximum leaf nitrogen concentration (kg N kg C^{-1}) for the species, and BS_{25} is the available nitrogen allocation factor (dimensionless) (Running and Gower 1991). This equation integrates the effect of water and nitrogen availability on leaf and root carbon allocation.

The second estimate of leaf growth carbon allocation (GT_{53} kg C) assesses the effect of nitrogen availability on leaf carbon allocation (Andrews 1986). This equation also uses the leaf:root ratio (GT_{51}):

$$GT_{53}=\frac{XT_{15}GT_{51}}{GT_{41}} \quad (67)$$

where GT_{41} (kg N kg C^{-1}) is leaf nitrogen concentration as estimated from:

$$GT_{41}=[\frac{2XT_{15}GT_{51}}{LAI_{max}BS_{19}}](BS_{19}-BS_{20})+BS_{20} \quad (68)$$

where BS_{19} and BS_{20} are maximum and minimum leaf nitrogen concentrations (kg N kg C^{-1}).

The last leaf carbon allocation estimate (GT_{54} kg C) accounts for water stress interactions. The following formula is used to estimate this relationship:

$$GT_{54}=(\frac{BS_7}{LWP_{max}})(\frac{XT_7}{BS_{23}})[1+\frac{BS_{30}}{1-BS_{30}}] \quad (69)$$

where BS_7 is the leaf water potential at stomatal closure for the species (–MPa), LWP_{max} is the maximum leaf water potential experienced by the tree in the year (–MPa), XT_7 is current year's leaf carbon (kg C), BS_{23} is the leaf retention time (years), and BS_{30} is the leaf growth respiration coefficient (kg C kg C^{-1}).

The model then takes the minimum of the three carbon estimates and computes a proportion of PSN to allocate to leaf, stem, and root growth (GT_{56}) as follows:

$$GT_{56}=MIN[GP_{52},GP_{53},GP_{54}] \quad (70)$$

where MIN selects the minimum of the arguments and GT_{55} is the leaf allocation factor (Dickson 1989; Dickson and others 1990; Johnson 1985). The proportion of PSN to allocate to root growth is calculated as:

$$GT_{57}=MIN[(\frac{GT_{56}}{GT_{51}}),(1-GT_{56})] \quad (71)$$

where MIN is the function that takes the minimum of the two terms. The proportion allocated to stem growth is computed from subtraction:

$$GT_{58} = 1 - GT_{57} - GT_{56} \quad (72)$$

These proportions are then multiplied by PSN to obtain gross carbon growth for leaves (GP_{59}, kg C), stem (GP_{60}, kg C), and roots (GT_{61}, kg C). Growth respiration is then computed for each of the three compartments by multiplying gross carbon growth by the appropriate growth respiration coefficients (BS_{30}, BS_{31}, BS_{32}, kg C kg C^{-1}). Net carbon growth is then computed for leaves (GT_{66} kg C), stem (GT_{67} kg C), and roots (GT_{68} kg C) from the subtraction of growth respiration from gross carbon allocation. These net carbon gains for leaves and stems are added to each tree compartment (XT_7 and XT_8, kg C). The net carbon growth to the roots is divided into coarse and fine roots using an allocation proportion (GT_{75}). The proportion GT_{75} is multiplied by root carbon growth and added to the fine root compartment (XT_{10} kg C). The remaining carbon is added to the coarse roots (XT_9, kg C). This proportion is currently a constant (0.8) in FIRE-BGC (Johnson 1985; Marshall and Waring 1985; Persson 1979; Santautonio and Hermann 1985), but will be modified as new research becomes available.

The amount of nitrogen needed to sustain this growth is added to the appropriate tree compartments based on the leaf nitrogen concentration (GT_{41}). Leaf growth nitrogen allocation is the product of net carbon growth (GT_{66} kg C) and leaf nitrogen concentration (GT_{41} kg N kg C^{-1}). Stem nitrogen growth allocation is the product of GT_{41}, net stem carbon growth (GT_{67} kg C) and stem nitrogen fraction (BP_{52}). Root nitrogen growth allocation is the product of GT_{41}, GT_{68}, and BP_{53}. This nitrogen is taken from the available nitrogen pool. The last parameter estimated is the amount of leaf nitrogen that was translocated to the available nitrogen pool during leaf fall (GT_{72} kg N). This is estimated from the equation:

$$GT_{72} = \frac{XT_{11}}{BS_{23}} BS_{21} \quad (73)$$

where XT_{11} is the current leaf nitrogen (kg N), BS_{23} is leaf longevity (years), and BS_{21} is the fraction of nitrogen translocated from the leaf for that species. Then the growth nitrogen estimates are added to appropriate compartments, and translocation is added to available nitrogen pool (see figs. 1 and 7).

Dimensional Growth—Tree diameter (DBH cm) and height (HT m) growth increments are computed at year's end from the estimates of carbon growth proportioned to the tree stem carbon compartment (XT_8 kg C) (Gordon and Larson 1968). First, tree age is incremented by 1 year. Then a new tree height (HT_t m) for this simulation year (year t) is computed from the Tree Height algorithm (detailed in the structural characteristics discussions in the Tree Processes section) using the new age. The minimum possible diameter (DBH_{min} cm) for this year is first computed from the following equation:

$$DBH_{\min} = DBH_{t-1} + BS_{39} \quad (74)$$

where BS_{39} is the minimum threshold diameter increment for the tree species (cm) (Keane and others 1989) and DBH_{t-1} is last year's diameter

(cm). Next, the branchwood carbon is subtracted from last and this year's stem carbon ($XT_{8,t-1}$ and $XT_{8,t}$, kg C) using the equations of Brown (1978) to yield stem carbon estimates ($STEMC_{t-1}$ and $STEMC_t$ kg C). These estimates are used to solve for this year's diameter (DBH_t) using the following equation:

$$DBH_t = \sqrt{\frac{(STEMC_t)(HT_{t-1})(DBH_{t-1})^2}{(STEMC_{t-1})(HT_t)}} \quad (75)$$

where DBH_{t-1} is last year's tree diameter (cm), HT_{t-1} is last year's tree height (m), and HT_t is this year's tree height (m). This approach assumes a truncated frustrum stem geometry and uniform diameter growth over the entire stem.

If this new diameter growth is less than the minimum diameter increment ($DBH_t < DBH_{min}$) then that tree is marked as experiencing growth-related stress, and the diameter and height estimates are modified according to shade tolerance class. If the species is shade intolerant (Tolerance class 1 and 2), then stem carbon growth is allocated to height growth not diameter growth. This involves setting the new diameter (DBH_t cm) to DBH_{min} and solving the following form of the above equation for the new height estimate (HT_t m):

$$HT_t = \frac{(DBH_{t-1})^2(HT_{t-1})(STEMC_t)}{(DBH_t)^2(STEMC_{t-1})} \quad (76)$$

However, if the species is shade tolerant (Tolerance class 3, 4, or 5), then new diameter (DBH_t cm) and height (HT_t m) estimates are simultaneously solved so equal proportions of carbon can be allocated to height and diameter growth. Again, assuming a truncated frustrum, the following equation is used to iteratively solve for diameter (DBH_t cm) and height (HT_t m):

$$STEMC = \frac{\pi BP_{21} BS_{49} (0.01 DBH_t)^2 HT_t}{8} \quad (77)$$

where STEMC is an intermediate estimate of stem carbon (kg C), BP_{21} is the fraction of stemwood that is carbon (kg C kg biomass^{-1}), and BS_{49} is the density of stemwood (kg biomass m^{-3}). DBH_t is set to DBH_{t-1} and HT_t is set to HT_{t-1} at the start of the procedure and incremented 1 percent of their value at each step in the iterative process. This method also assumes the stem shape approximates a truncated frustrum. The iterative process ends when STEMC converges to within 0.01 percent of $STEMC_t$.

The last computation in the dimensional growth analysis is the modification of tree crown height (HBC_{t-1} m). The model calculates the light conditions at the bottom of the canopy by multiplying the available light for the canopy layer containing the bottom of the crown by the average daily solar radiation (kJ m^{-2} day^{-1}) that occurred during the tree's growing season. If this amount was less than the photosynthetic light compensation point for the tree species (BS_9 kJ m^{-2} day^{-1}) then the bottom of the crown is pruned to the top of that canopy layer. Only one canopy layer is evaluated each year.

Mortality

Four causes of tree mortality are stochastically simulated in FIRE-BGC—random, stress, fire, and pathogens (Keane and others 1989). "Random mortality" is the chance of death from random events such as endemic insect attack, windthrow, or other local perturbations that a tree experiences throughout its lifetime (Botkin and others 1972; Keane and others 1989; Kercher and Axelrod 1984). The probability of random mortality (P_{random}) is calculated by the equation:

$$P_{random} = \frac{\epsilon}{BS_{34}} \tag{78}$$

where BS_{34} is the maximum age attained by the tree species and ϵ is an empirically fitted coefficient (years). This coefficient is estimated based on the assumption that 2 percent of the trees (98th percentile) survive to the maximum attainable age for a species (BS_{34}). Analysis of stand data from Montana, Idaho, and eastern Oregon (Arno and others 1985; Keen 1940; Seidel 1975) suggests that 2 percent is reasonable for most western conifers. The value of ϵ was assumed to be 4.0 for most species to approximate the 2 percent estimate. However, stand data collected by Keane and others (1994) found ϵ closer to a value of 3.0 for whitebark pine.

"Stress mortality" is tree death resulting from severe stress over long periods. Stress mortality can be caused by water scarcity, insufficient light or tree crowding (Keane and others 1989; Kercher and Axelrod 1984; Shugart and Noble 1981). The amount of carbon allocated to the stem is used to evaluate tree stress (see "Dimensional Growth" in this section). A stress counter (Y_{stress} years) is incremented by 1 year if the tree cannot produce enough stem carbon to exceed a minimal diameter growth. This counter (Y_{stress}) is used in the following two-parameter Weibull probability function (Reed and Clark 1979):

$$P_{stress} = a[1 - e^{[-bY_{stress}]}] \tag{79}$$

where P_{stress} is the probability of mortality resulting from stress, and a and b are coefficients by shade tolerance class (table 9). The shade tolerance category for each tree species is presented in table 2. These coefficients were approximated from data gathered in the BMWC field study (Keane and Morgan 1994; Keane and others 1994). The cumulative probability of

Table 9—Stress mortality Weibull function parameters by shade tolerance classes as used to calculate tree death from stress-related causes in FIRE-BGC.

Shade tolerance classes	Equation parameters		
	a	b	c
1	10.00	2.00	3.00
2	20.00	2.00	3.00
3	30.00	2.00	5.00
4	40.00	2.00	10.00
5	50.00	2.00	10.00

stress mortality (P_{stress}) over 100 years of continued stress is depicted in figure 17. Stressed trees become healthy after experiencing 3 consecutive years of diameter growth above the minimum allowable growth (BS_{39} cm).

The last two causes of mortality, fire, and pathogens, are presented in the Fire Effects and Pathogens sections. Pathogens include both insects and disease in this modeling effort. The probability of mortality from these factors is represented by P_{fire} for fire-caused mortality and P_{path} for pathogen-caused mortality.

Tree death is evaluated separately for each mortality agent. First, a random number (RNUM) is compared to P_{random} and, if RNUM is less than P_{random}, the tree dies. If the tree lives, another random number is compared to P_{stress} and if less, death is the result. This process is also repeated for P_{fire} and P_{path}. The tree must pass all four comparisons to continue to live.

Each tree that dies, regardless of the cause of mortality, contributes its carbon to the forest floor compartments (fig. 11). Needle carbon, computed from the Brown (1978) and Brown and others (1985) empirical equations, is allocated to the $LITTER_c$ and $DUFF_c$ forest floor compartments based on the species needle lignin fraction as detailed in "Decomposition" in the Stand Processes section. Woody branchwood carbon is added to the ${}_iWOOD_c$ forest floor compartments by size class using Brown (1978) equations. The remaining stem carbon is added to the log woody compartment (${}_4WOOD_c$). Methods used to calculate nitrogen additions to the forest floor compartments from the dead tree components are identical to those used for component turnover as detailed in "Decomposition" of the Stand Processes section.

An additional set of computations detailed in the Fire Effects section is performed if the tree is killed by fire. It is assumed scorched foliage is not

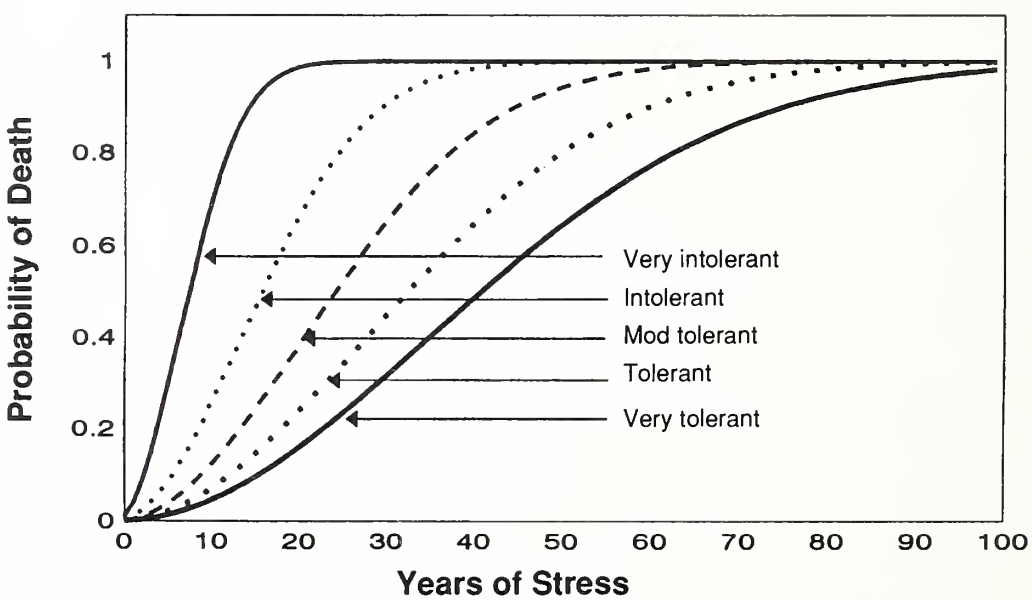

Figure 17—Probability of death of stressed trees by species shade tolerance category.

consumed by the fire and is added to the fuel bed, unless the fire was a crown fire in which case the carbon is lost from the simulation plot. This mortality algorithm assumes that a tree falls to the ground immediately after death. Future versions of FIRE-BGC will account for the temporal distribution of fuel accumulation from dead trees or snags.

Fire Effects

Direct effects of wildfire on ecosystem components and processes are computed in FIRE-BGC as a general cycling of carbon and nitrogen. Carbon and nitrogen losses are directly computed from the amount of forest floor biomass oxidized by the fire (fuel consumption). Most fuels will not be completely consumed by a fire. Forest floor carbon that is consumed by a fire from any fuel compartment is assumed to be lost to the simulation plot. Tree mortality from fire is computed from the amount of crown scorched and size of the tree. Dead tree carbon and nitrogen not consumed by the fire are added to the forest floor compartments.

Fuel Consumption

The reduction of the forest floor compartments by fire is computed using modifications of the empirical approaches of Brown and others (1985). In FIRE-BGC, forest floor compartments are reduced by a consumption fraction (CF_i where i is the fuel component) taken from the fuel model for that site using the following relationships:

$$_iWOOD_c = {}_iWOOD_c(CF_i) \tag{80}$$

$$LITTER_c = LITTER_c(CF_i) \tag{81}$$

These fractions (CF_i) apply to the appropriate components of the specified fuel model (table 4) and are taken from Brown and others (1985), Keane and others (1994), Reinhardt and others (1991), Sandberg (1980), and Norum (1974). Under model assumptions, no soil carbon ($SOIL_c$ kg C) is consumed. Litter and woody fuel consumption is modeled independently of fire intensity (Brown and others 1985). Moisture content influences fuel consumption in FIRE-BGC, but fuel moistures are static in FIRE-BGC. Therefore, organic matter consumption is modeled using a static consumption fraction (CF_i) (Brown and others 1985). However, duff ($DUFF_c$) reduction is simulated from preburn duff loading and moisture content (DMOIST, percent dry weight). The equation for duff reduction is taken from Brown and others (1985) and is used for all fuel models:

$$DUFF_c = DUFF_c\left[\frac{(83.7 - 0.426(DMOIST)}{100}\right] \tag{82}$$

where $DUFF_c$ is the preburn and postburn duff carbon (kg C). DMOIST (percent dry weight) is specified in the fuel model (see "Fuel Models" in the Site Processes section) but will be dynamically modeled in future versions of FIRE-BGC.

Shrub biomass ($SHRUB_i$ and $SHRUB_t$) and herbaceous biomass ($HERB_i$ and $HERB_t$) are also consumed by the fire. Live and dead shrub and herb

biomass consumption fractions (CF_j) specified in the site's fuel model are used in the following equation:

$$CONSUME_{live} = CF_{ls}[SHRUB_i(1-FDEAD_i)+SHRUB_t(1-FDEAD_t)] + CF_{lh}[HERB_i(1-FDEAD_i)+HERB_t(1-FDEAD_t)] \quad (83)$$

$$CONSUME_{dead} = CF_{ds}[SHRUB_i FDEAD_i + SHRUB_t FDEAD_t] + CF_{dh}[HERB_i FDEAD_i + HERB_t FDEAD_t] \quad (84)$$

where $CONSUME_{live}$ and $CONSUME_{dead}$ are the consumptions of live and dead shrub and herbaceous fuels (kg C). These fractions apply to both intolerant and tolerant SHRUB (CF_{ls} and CF_{ds}) and HERB (CF_{lh} and CF_{dh}) compartments (table 4). The proportion of shrub and herb compartments that are dead ($FDEAD_j$ proportion) at the time of the fire are specified in the Plant file for each site (table 5). These values are taken from Martin (1982) and data collected by the authors for the BMWC project.

The cycling of nitrogen after fire is simulated in the same manner as carbon cycling except some nitrogen from the consumed nitrogen pools goes to the available nitrogen pool (Grier 1975; Pehl and others 1986; Schoch and Binkley 1986). Fuel consumption fractions (CF_j) are multiplied by the nitrogen loadings for the $LITTER_n$ (kg N) and $_iWOOD_n$ (kg N) forest floor compartments to obtain the amount of nitrogen lost from those compartments. The calculated duff consumption estimate is multiplied by duff nitrogen ($DUFF_n$ kg N). These estimates of nitrogen loss from the forest floor compartments are then multiplied by a volitalization fraction (BP_{50} kg N kg C^{-1}) to obtain the actual loss of nitrogen from the site. The nitrogen not volatilized becomes available for plant growth and is added to the available nitrogen pool ($AVAIL_n$ kg N) using the equation:

$$AVAIL_n = DUFF_n CF_i(1-BP_{50}) + LITTER_n CF_i(1-BP_{50}) + \sum [\ {}_iWOOD_n CF_i(1-BP_{50})] \quad (85)$$

This volitalization fraction (BP_{50}) is specified by site in the Site file (SITE.DAT), and its values for this study were taken from Ryan and Covington (1986), Little and Ohmann (1988), Kutiel and Shaviv (1992), Klemmedson and others (1962), Groeschl and others (1993), and Covington and Sackett (1984). The shrub and herb nitrogen losses and contributions to the available nitrogen pool are computed using the equations:

$$AVAIL_n = CF_j(1-BP_{50})[(SHRUB_i)(NFRAC_i)+(NFRAC_t)(SHRUB_t)] \quad (86)$$

$$AVAIL_n = CF_j(1-BP_{50})[(HERB_i)(NFRAC_i)+(NFRAC_t)(HERB_t)] \quad (87)$$

where $NFRAC_i$ is the nitrogen fraction of shrub or herb biomass component, and CF_j is the consumption fraction for the jth fuel model component that corresponds to dead shrub and herbs.

Fire-Caused Tree Mortality

Tree mortality from fire is modeled as a function of scorch height, which is dependent on fire intensity and wind. When a fire spreads through an

area it kills trees by scorching foliage and killing stem cambium. The scorching of crown foliage involves killing the needles from heat exposure without consuming them. Sometimes the fire is so intense that tree crowns are entirely consumed by fire and tree death is an immediate result in most conifers. Live crown consumption by fire is assumed to occur if the fire's flame length (FL m) is greater than the height to the bottom of the crown (HBC m). If the flame length is lower than the crown, indirect mortality from crown scorch and cambial kill is evaluated.

The degree of crown scorch and cambial kill depends on fire intensity and duration. Ryan and Reinhardt (1988) developed an empirical mortality equation that implicitly accounts for both causes of fire death. The equation was implemented in FIRE-BGC as:

$$P_{fire} = \frac{1}{1 + e^{[-1.941 + 6.32(1 - e^{(-BS_{45}DBH)}) - 0.000535CK^2]}} \quad (88)$$

where P_{fire} is the probability of mortality from fire after 1 year, BS_{45} is the factor that converts DBH to bark thickness (cm bark cm DBH^{-1}), DBH is tree diameter (cm), and CK is the percent of scorched crown volume for the tree (%). Values for BS_{45} are taken from Faurot (1977), Lange (1971), Lynch (1959), Myers and Alexander (1972), Ryan and others (1987), and Ryan and Reinhardt (1988) and are presented in table 2. Predictions of the probability of fire-caused mortality for ponderosa pine at various scorch heights from this equation are presented in figure 18. The decision of whether or not the tree dies is detailed in "Mortality" in the Tree Processes section.

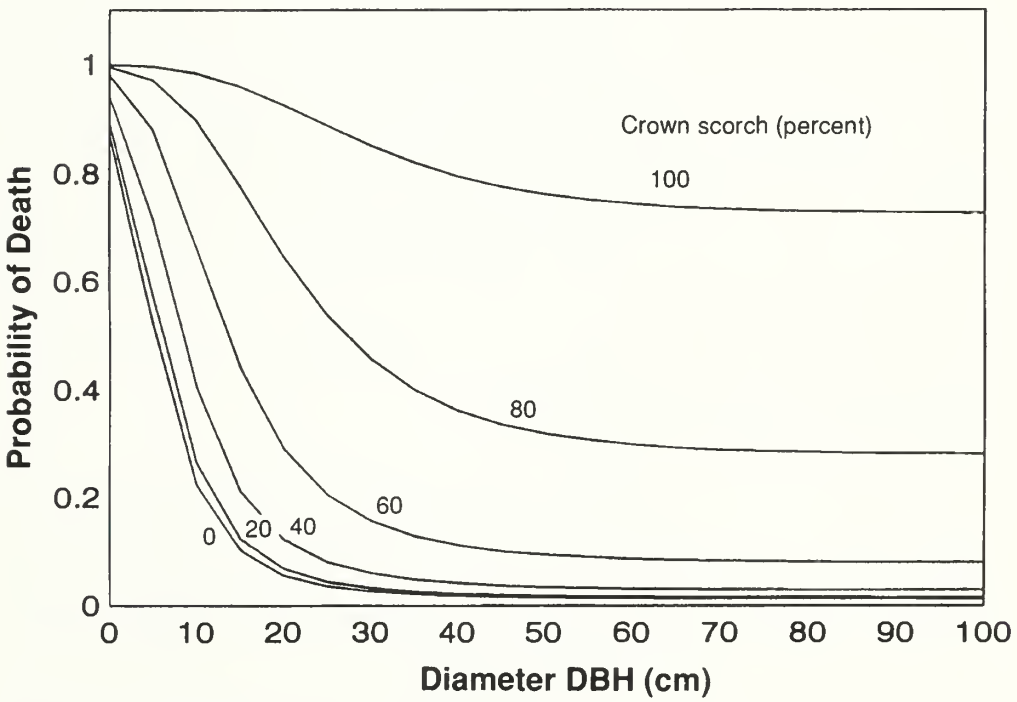

Figure 18—Probability of death 1 year after a fire for various diameter ponderosa pine trees experiencing different levels of crown scorch.

Scorched crown volume percent (CK %) is estimated using the following formula:

$$CK=100[\frac{CS(2CL-CS)}{CL^2}] \quad (89)$$

where CS is the length of crown that is scorched (m) and CL is crown length (m) (as shown in fig. 13 and described in the discussion on structural characteristics in the Tree Processes section). This relationship assumes the crown shape approximates a paraboloid (Peterson 1985; Ryan and others 1986). The dimension CS is solved by the equation:

$$CS=SH-[HT-CL] \quad (90)$$

where HT is tree height (m), and SH is scorch height (m). Scorch height is calculated from an empirical expression developed by Van Wagner (1973):

$$SH=\frac{a(FI)^{1.667}}{[b(FI)+c(WIND)^3]^{0.5}(T_{kill}-T_{ave})} \quad (91)$$

where FI is fire intensity (kW m^{-1}), WIND is wind speed (km hr^{-1}) at mid-flame height, T_{ave} is ambient air temperature (°C), and T_{kill} is the lethal temperature for tree foliage (assumed as 60 °C). The constants a, b, and c were derived empirically and are 0.74183 m $°C^{-1}$, 0.025574 (kW $m^{-1})^{4/3}$, and 0.021433 km^{-1} hr (kW $m^{-1})^{7/9}$, respectively. Fire intensity (FI) is taken from the landscape map of fire intensity produced by FARSITE and averaged across all pixels within the stand in question. Ambient air temperature was taken for the day in which the fire occurred and specified as a constant in the Site file (appendix B).

Although the fire mortality equation is robust and allows for a wide range of diameters and species, data for small diameter (<10 cm) tree mortality are lacking. Because the majority of simulated trees are less than 10 cm DBH, additional refinement of this equation to account for small diameter tree mortality is needed.

A stand-replacement fire is assumed to happen if more than 98 percent of the living trees on the plot die as a result of fire. A stand-replacement fire results in a lack of tree regeneration for a number of years (LAG years) because of the severe postfire site conditions that might limit tree establishment (see Species Processes section).

Tree Compartment Consumption

Once a tree dies from fire damage (see "Mortality" in the Tree Processes section), its foliage, branchwood and stemwood carbon are added to the appropriate forest floor compartments. However, some crown material from dead trees may get consumed by the wildfire. FIRE-BGC computes this amount consumed by fire using the flame length (FL m) as computed by the FARSITE model (Finney 1994). If the flame length is greater than the height to bottom of the crown (HBC m) (that is, FLAME >HBC) then it is assumed that fire ignited and burned the tree crown and killed the tree. This means a proportion of the foliage (BS_{59}), twigs (BS_{60}), branchwood (BS_{61}), and large branchwood (BS_{62}) was consumed. These proportions

are specified by species and are presented in table 2. The unconsumed portions of the crown compartments are added to the appropriate forest floor carbon and nitrogen compartments (see "Organic Matter Accumulation" in the Stand Processes section). All crown carbon and nitrogen is assumed to be lost from the simulation plot. If flame length is below the crown bottom (FLAME <HBC), then no crown parts are consumed and all crown material from the dead tree is added to the appropriate carbon and nitrogen compartments using the methods detailed in "Mortality" in the Tree Processes section.

Trees may continue to live with some crown scorch, in which case the scorched foliage dies and its carbon and nitrogen are added to the forest floor compartments. The proportion of crown scorched (that is, CK/100) is multiplied by the tree's leaf carbon (XT_7 kg C) and nitrogen (XT_{11} kg N) to obtain the amount of killed foliage to add to the LITTER and DUFF carbon and nitrogen compartments. No branchwood is added to the forest floor. The height to the bottom of crown (HBC m) is then adjusted upward proportional to the percent crown kill (CK/100).

Pathogens

Insect- and disease-caused mortality is the fourth type of tree mortality simulated in FIRE-BGC. Currently, FIRE-BGC only simulates tree mortality caused by white pine blister rust (*Cronartium ribicola*) and mountain pine beetle (*Dendroctonus ponderosae*) in high elevation ecosystems. Details of these mortality algorithms can be found in Keane and others (1990b). The initial year of blister rust (YRUST) or pine beetle (YBEETLE) epidemic is entered in the Simulation file (SIM.DAT appendix B). The probablity of tree mortality is assessed for each pathogen during the epidemic and tree death is simulated using the methods detailed in "Mortality" of the Tree Processes section.

This submodel of FIRE-BGC was designed so any new pathogen algorithm can be added with minimal program modification. Most insect and disease mortality algorithms were developed from empirical data using regression analysis. However, future versions of FIRE-BGC will be linked with mechanistic simulation of pathogen dynamics to fully understand the interaction of these disturbance processes on ecosystem function.

White Pine Blister Rust Mortality

The spread of blister rust is modeled at the stand level for each western haplopaxon (five-needle) pine (whitebark pine, limber pine, or western white pine) using a probability of infection (P_{infec}) as specified in the Simulation file (SIM.DAT in appendix B). A random number (RNUM) is generated each year after the start of the infestation. If RNUM is less than P_{infec} and the tree is an uninfected five-needle pine, then the tree is infected by rust. Once infected, a tree remains infected for the remainder of its life and its cone crop is reduced by 90 percent. The probability of death from blister rust (P_{rust}) is computed from the following equation:

$$P_{rust} = e^{[-0.15(DBH)]} \quad (92)$$

where DBH is tree diameter (cm). Resistance to the disease is simulated in the model by randomly assigning a portion (XRUST) of the five-needle pine trees as being rust resistant. Blister rust kills only nonrust-resistant five-needle pines. There is no cone crop reduction for rust-resistant five-needle pine. The parameter XRUST is entered in the Simulation file.

Mountain Pine Beetle Mortality

The probability of mortality from mountain pine beetles (P_{beetle}) is calculated each year of a beetle attack using the empirical equations:

$$P_{beetle}=0.007664(DBH)-0.00222 \qquad \textit{Whitebark Pine} \qquad (93)$$

$$P_{beetle}=0.00555(DBH) \qquad \textit{Lodgepole Pine} \qquad (94)$$

where DBH is tree diameter (cm). These regression equations were developed by the authors from unpublished data provided by the USDA Forest Service Northern Region, and Gene Amman, Intermountain Research Station. A pine beetle attack ends when the number of surviving pines divided by the number of pines prior to attack is less than a minimum infestation level (BINFES proportion) as entered in the Simulation file.

Output

The LOKI application of FIRE-BGC contains many ways to generate simulation output. The FIRE-BGC submodel produces a variety of daily and annual stand and tree table files. FIRE-BGC also allows the user to specify a variety of stand characteristics to print in the dynamic Stand Attribute file. The MAPMAKER submodel then reads this Stand Attribute file every year and creates and displays spatial data layers of those characteristics that can then be input into a Geographic Information System such as GRASS (USA CERL 1990) (fig. 4). Stand characteristics printed to the Stand Attribute file are selected by the user in the Driver file. These characteristics include net primary productivity (NPP), water use efficiency (WUE), standing crop (SC), and dominance type based on species basal area (DT).

FIRE-BGC provides many avenues for the printing of intermediate, nonspatial results during program execution. Model calculations can be printed to a variety of ASCII files depending on the temporal and organization scale (see appendix C for examples). These ASCII files can then be imported into statistical and graphics software packages for analysis and display. The model was programmed to allow the printout of additional variables with little or no modification of the program. All output file names are specified in the Driver file (appendix B). Also specified in the Driver file are the state and intermediate variables whose values are to be printed at the appropriate time step.

Any ecophysiological component at the stand (XP_i) and tree (XT_i) levels, and any intermediate variable at the stand (GP_i) and tree (GT_i) levels, can be printed to the appropriate files. This is done by specifying the index (i) of the compartment or intermediate variable in the Driver file (DRIVER.DAT in appendix B). A seasonal window is also available to limit the printing these daily values to only a portion of the year. Only output data calculated for

days between a specified starting and ending yearday as entered in the Driver file will be printed in the appropriate file. No data will be printed to any of the following output files if the starting yearday for the seasonal window is entered as zero.

The first file created by FIRE-BGC is the Echo file containing all input data and initialization data as computed by the model (ECHO.OUT in appendix C). This file is used to verify input file structure and data values are correct. The remaining output files are stratified by the time step at which they are updated (year or day) and the organizational scale described by the data (tree or stand).

Daily Output

Stand-level predictions for specified stand compartment (XP_i) and intermediate (GP_i) variables as specified in the Driver file are printed each simulation day for every stand in the simulation into the Stand Day file (STAND.DAY in appendix C). No tree level predictions are printed at a daily time step.

Annual Output

Each year FIRE-BGC writes a number of computed values to the FIRE-BGC file (FIRE-BGC.OUT file in appendix C). Currently, FIRE-BGC writes site ID number, stand ID number, basal area by tree species (m^2 ha^{-1}), leaf area by species (m^2), litter carbon (kg C), duff carbon (kg C), and woody carbon (kg C). This list of variables is static and can only be changed by modifying the program. A second annual stand output file, the Stand Year file (STAND.YR in appendix C), contains the simulated yearend values for the XP_i and GP_i variables as specified in the Driver file.

Yearly tree output data are written to two files by FIRE-BGC. The Tree List file (TREE.LIST in appendix C) contains a list of trees by simulation year, site, and stand. Each tree is described by tree ID number, species acronym, diameter (DBH cm), height (HT m), and age (AGE years). This variable list is also static and cannot be changed without FIRE-BGC program modification. The yearend values of the XT_i and GT_i variables for a selected tree are written to the second tree output file, Tree Year file (TREE.YR in appendix C). The target tree is specified by number in the Driver file (DRIVER.DAT in appendix B). These yearly values are written for that same tree number across every stand in the simulation. No predictions are written for that tree once it dies.

Bob Marshall Wilderness Complex Whitebark Pine Simulation Project

Whitebark pine (*Pinus albicaulis*) is an important component of Northern Rocky Mountain high elevation forests. Although it has limited use as a commercial timber species, whitebark pine produces seeds that are highly valued by many species of wildlife as an important source of food. Clark's nutcrackers (*Nucifraga columbiana*) play a mutualistic role in the whitebark pine regeneration process because they are essentially the only dispersal vector for the heavy, wingless whitebark pine seed (Tomback 1982). Whitebark pine also protects snowpack in high elevation watersheds and delays snowmelt (Arno and Hoff 1989; Hann 1990).

Whitebark pine is rapidly decreasing in some subalpine landscapes of the northern and western part of its geographical range (Arno 1986; Ciesla and Furniss 1986; Keane and Arno 1993; Kendall and Arno 1990). This decline is a result of three factors acting separately or in concert: (1) successional replacement by more shade tolerant conifers, (2) white pine blister rust, and (3) mountain pine beetle. Successional replacement of whitebark pine by subalpine fir (*Abies lasiocarpa*) and Engelmann spruce (*Picea engelmannii*) is a process that is usually retarded by naturally occurring fires. However, 60 years of fire exclusion combined with mountain pine beetle and blister rust attacks have allowed fir and spruce to become dominant in forests historically dominated by whitebark pine (Arno 1986). Blister rust, an exotic disease from Europe introduced in the Western United States in 1910, is probably the major agent causing mortality in the mesic portions of the species range (Keane and Arno 1993; Kendall and Arno 1990). Mountain pine beetle epidemics killed many mature whitebark pine trees during the 1940's (Baker and others 1971).

Consequences of this apparent decline of whitebark pine has never been assessed at a landscape level (Keane and others 1994). This simulation study was initiated to investigate the fate of whitebark pine forests under various simulation scenarios. Results of this simulation effort can be used to develop management strategies for maintaining whitebark pine ecosystems on the upper subalpine landscape.

Simulation Study Area

The Bob Marshall Wilderness Complex (BMWC) is a remote 600,000 ha preserve in northwestern Montana consisting of the Great Bear, Bob Marshall, and Scapegoat Wilderness Areas (fig. 19). This area consists of mountainous terrain dissected by major river drainages. Two periods of glaciation shaped the rugged cirque and peak landscape and filled valley bottoms with loosely consolidated glacial outwash alluvium (Alt 1985; Deiss 1958). The simulation area used in this study is a large (7,700 ha), contiguous, upper subalpine expanse in the Swan Front Range in the southwestern portion of the BMWC at the headwaters of Monture Creek and Young's Creek (fig. 19). This area, called the Monture Simulation Study Area (MSSA), was historically and is currently dominated by whitebark pine (Gabriel 1976; Keane and Morgan 1994; Keane and others 1994). However, recent infections of blister rust and the lack of fires in the MSSA are rapidly advancing the successional replacement of whitebark pine with subalpine fir. Parent material is mostly quartzite and argillite (Alt 1985). The climate is modified maritime with cool wet winters and short, warm-dry summers. Average annual precipitation ranges from 200 to over 275 cm $year^{-1}$ (Soil Conservation Service 1981).

Fires were common on this landscape during the last four centuries. Large, stand-replacement fires are typical in the study area, especially in the whitebark pine zone (Losensky 1990; Steele 1960). The great dispersal distances of the Clark's nutcracker allow whitebark pine a competitive advantage in colonizing large burns; also, Clark's nutcrackers prefer open, burned areas to cache whitebark pine seeds (Tomback and others 1990). Some fires in the higher and drier areas of the BMWC contain evidence of less severe, more frequent surface fires (Gabriel 1976). These fires tend to kill mostly subalpine fir, which favors the somewhat fire-resistant

Figure 19—The Bob Marshall Wilderness Complex with the Monture Simulation Study Area shown in the lower left.

whitebark pine (Arno 1986). As a result, these fires maintain whitebark pine dominance and eliminate the subalpine fir understory (Arno and Hoff 1989).

Simulation Methods

The FIRE-BGC model was used to investigate the effects of fire, insects, and pathogens on landscape dynamics in the MSSA whitebark pine forest. The following simulation scenarios were simulated with FIRE-BGC for the Monture Simulation Study Area:

1. No Fires (NOFIRE)—A fire exclusion alternative where all fires are suppressed within the study area.
2. Historical Fire Occurrence (HIST-FIRE)—Fires are stochastically simulated on the study area at approximately the same frequency as they occurred prior to European/American settlement.
3. Blister Rust/No Fire (RUST-NOFIRE)—A blister rust epidemic is simulated while all fires are excluded from the landscape.
4. Blister Rust/Fire (RUST-FIRE)—A blister rust epidemic is simulated while the landscape is experiencing fires at the historical frequency.

Each scenario was modeled for 200 years and used the same initial conditions at the beginning of model execution. Blister rust epidemics were started at simulation year 50.

The above scenarios were simulated at two spatial resolutions. They were applied to both a typical whitebark pine stand and the MSSA landscape. The representative whitebark pine stand chosen to be simulated was sampled by Keane and others (1994) and located in the northern portion of the MSSA near Pyramid Peak. The sampled data were used for the initial conditions in the stand FIRE-BGC application to generate stand-level predictions for the four scenarios without the use of the LOKI system (see fig. 4). The MSSA landscape-level application of FIRE-BGC involved the creation of various thematic spatial data layers in a GIS environment for input to the LOKI implementation of FIRE-BGC. These data layers were initialized from sample data collected by Keane and others (1994) used to classify satellite imagery to create data layers. Details of the creation and parameterization of the spatial data layers are discussed next.

Site-Level Input Spatial Data Layers—Sites within the simulation study area were delineated from a topographic raster map layer called a Digital Elevation Model (DEM) (color plate 1, p. 86) using the GRASS GIS software (USA CERL 1990). This DEM layer was queried to divide the landscape into sites based on topographic constraints. Fire group descriptions (table 3) were used to create 16 topographic classes (sites) from combinations of the elevation, aspect and slope classes presented in table 10 (4 elevation classes x 2 aspect classes x 2 slope classes = 16 topographic classes) (Band and others 1991). These site types are shown in color plate 2. Soils and climate are somewhat homogeneous throughout the simulation area (Soil Conservation Service 1981) so they were not used as delineation criteria.

Stand-Level Input Spatial Data Layers—A cover type map layer showing the spatial delineation of dominant vegetation was created from a spectral classification of a Thematic Mapper (TM) scene (color plate 3)

Table 10—Topographic classes used to delineate sites on the Monture Simulation Study Area.

Elevation	Aspect	Slope
m	*Azimuth*	*Percent*
1,525 to 1,830	270 to 90 (north)	0 to 20 (flat)
1,831 to 2,135	90 to 270 (south)	Above 21 (steep)
2,136 to 2,440		
Above 2,441		

(Keane and others 1994). This cover type layer was overlaid with the site layer to produce a map of stands that are hierarchically nested within the Site spatial data layer (color plate 4). A tabular list of stands by site and cover type was generated using GRASS GIS to produce the input files required by FIRE-BGC.

Input File Creation—Field data collected by Keane and others (1994) were summarized by classified cover type to quantify initial stand and tree conditions for input to FIRE-BGC. Tree age and size structure data measured on field plots representative of each cover type were entered into a FIRE-BGC tree input table (Tree file, for example, TREE.DAT in appendix B). Field plots at or near the MSSA were used if they existed for a cover type. The tree table for a stand was taken from tree data collected for the cover type of the stand (Keane and others 1994). Stand and site level input data (for example, fuel models, organic matter loadings, and understory biomass) were also taken from the cover type summaries of field data, and GIS queries of the topographic layer. Forty years of weather data from the nearby Seeley Lake National Weather Service Station were extrapolated to all 16 delineated sites using the MTCLIM climate model (Hungerford and others 1989), and these extrapolated data were then stored in binary files. Names of all input files (appendix B) were entered in a Driver file. Examples of input parameters used in this simulation exercise are presented in appendix B.

Predictions of landscape dynamics using FIRE-BGC can be presented in many forms. Programs that summarize FIRE-BGC intermediate calculations were included in the LOKI implementation. Other programs can be written to summarize simulation data into thematic layers. Such a program called MAPMAKER was written to map the major dominance types on the MSSA simulation landscape from FIRE-BGC predictions at 50 year intervals. Only three dominance types were delineated by this program based on the preponderance of basal area for the overstory tree species. The three dominance types are whitebark pine, subalpine fir, and shrub/herbaceous/rock/soil. The initial MSSA landscape classified to these three types is presented in color plate 5. FIRE-BGC predictions of landscape composition classified to the dominance types can be directly compared to this initial landscape.

Tree Growth Predictions Validation—Little data were available to compare predictions of the model with actual conditions observed on upper subalpine landscapes over long periods. However, Keane and others (1994) collected tree chronologies from a variety of tree species and sample sites across the BMWC. These tree ring width data records provide a means to assess the validity of FIRE-BGC estimates of tree growth.

Predicted diameter increments were contrasted with the measured ring widths to evaluate FIRE-BGC behavior.

Stand conditions of about 40 years ago (circa 1954) were reconstructed from the tree structure and age data using sampled diameter and growth estimates. This reconstructed stand then served to quantify initial conditions for a FIRE-BGC simulation starting at the year 1950, which is the start of the weather record. This simulation was continued for 40 years to the year 1990. The simulated ring width increments and diameters of two trees were compared to the actual sampled growth record taken from the sampled tree representing the modeled tree (Keane and others 1994). The predicted ring widths were compared to observed ring widths to estimate model accuracy.

Stand Compartment Predictions Validation—Keane and Morgan (1994) also sampled adjacent burned-over (disturbed) and mature (undisturbed) whitebark pine stands. Two of these sample sites, Tilison and Cliff Mountain, were used as a test of FIRE-BGC predictions. These test sites are generally described in table 11. Stand data sampled for the mature stands were used as initial conditions for the model. Then a fire was simulated in FIRE-BGC at simulation year 10, and succession was modeled to the simulation year corresponding age of the disturbed stand. Subsequent predictions of basal area, leaf area, litter/duff depth, and fuel loadings were compared to observed conditions sampled on the burned-over stand.

Results

Many types of simulation results can be generated by FIRE-BGC (see Output section). Intermediate computations may be output daily and yearly at the stand, tree, and landscape level. For example, canopy leaf and mesophyll conductance can be plotted across the entire year or against each other. Presented below are some simulation results predicted by FIRE-BGC at the stand, tree, and landscape level at various time steps. Stand and tree level results were generated using the Pyramid sample stand data as initial conditions. The landscape application is for the entire Monture Simulation Study Area.

Stand Level Results—The daily carbon balance simulation predictions for the Pyramid stand over a year are presented in figure 20. Daily net photosynthesis (gross photosynthesis minus night respiration) is contrasted with the daily respirational requirements of the stems and roots in the stand. The cumulative photosynthesis and respiration predictions

Table 11—General description of the sample sites used in the test of FIRE-BGC.

Sample sites	Elevation	Aspect	Slope	Age	Basal area	Leaf area index
	m	*az*	*percent*	*yrs*	$m^2\ ha^{-1}$	
Tilison						
Mature	7,350	350	70	312	115	2.3
Disturbed	7,355	10	65	81	33	0.6
Cliff						
Mature	6,950	90	20	285	280	5.6
Disturbed	6,890	100	18	81	66	3.0

are depicted in figure 21 showing an annual net carbon gain of approximately 400 kg carbon. Daily soil water contents predicted throughout the same year are graphed in figure 22. Other daily predictions are given in appendix C in the Stand.day file (STAND.DAY).

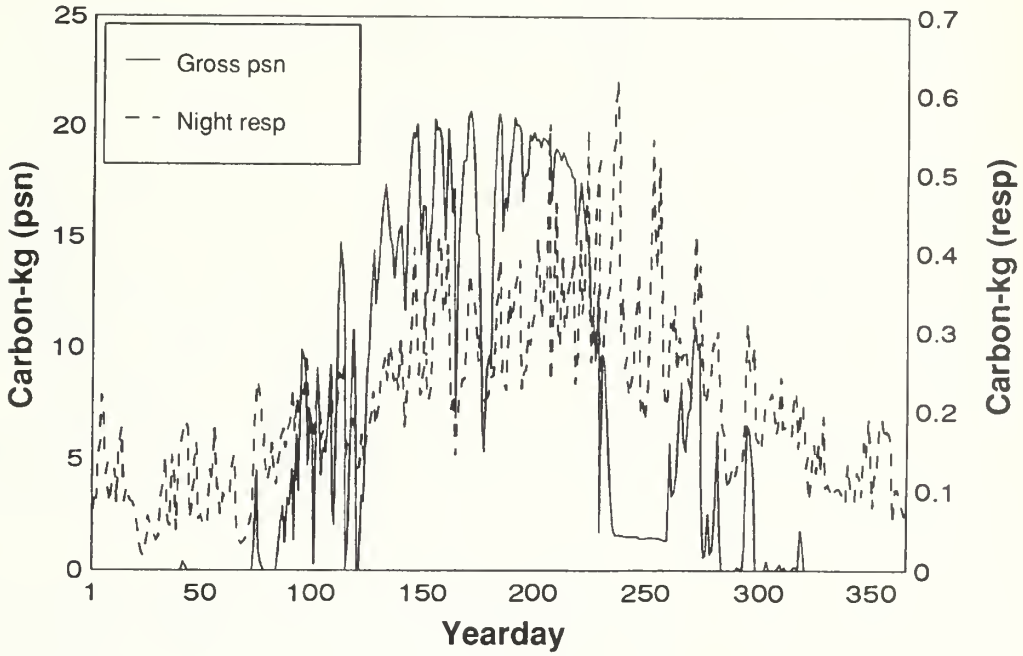

Figure 20—Daily photosynthesis and respiration FIRE-BGC predictions for the Pyramid simulation stand for the 1990 weather year.

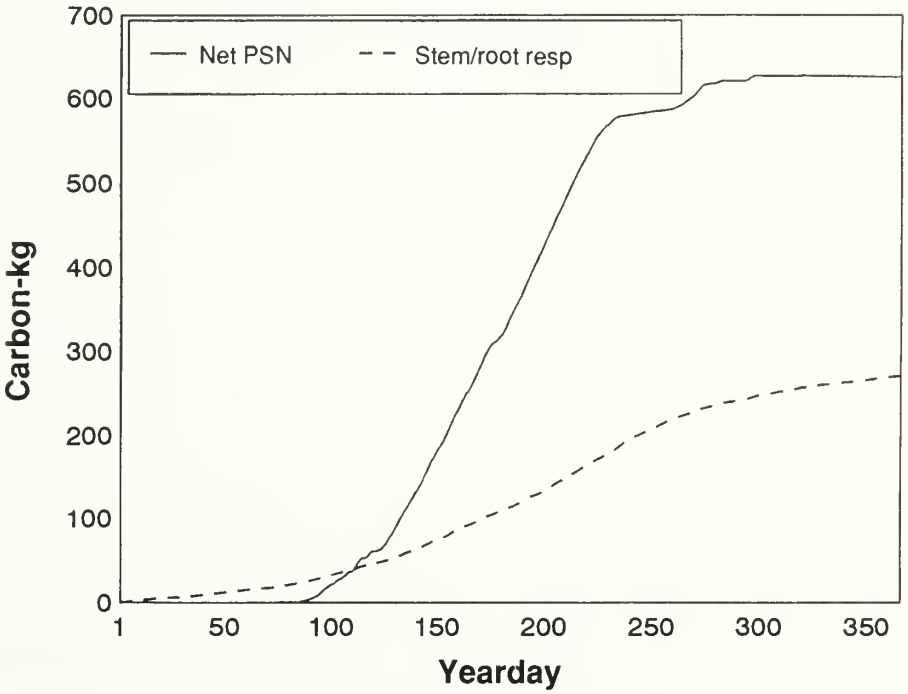

Figure 21—Cumulative daily carbon fixed via photosynthesis and lost through respiration for the Pyramid simulation stand.

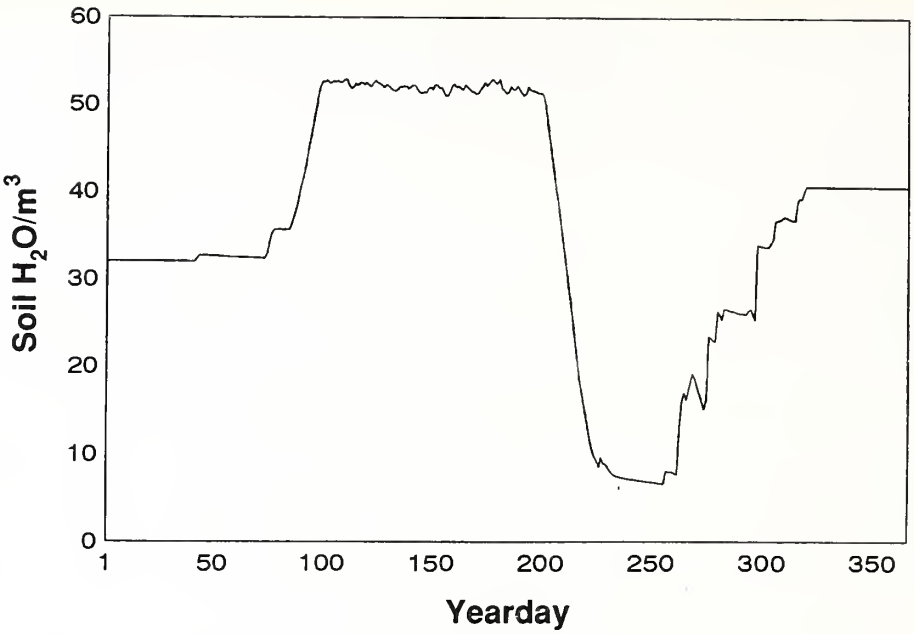

Figure 22—Daily soil water predictions for weather year 1990 for the Pyramid simulation stand.

Annual FIRE-BGC basal area predictions by tree species for each of the four simulation scenarios are depicted in figures 23 through 26 for the Pyramid sample stand. The NOFIRE scenario shows a significant decline of whitebark pine over the course of two centuries with a subsequent increase in subalpine fir (fig. 23). Results of the HIST-FIRE scenario as shown in figure 24 demonstrate the consequences of a stand-replacement fire in year 51 with subsequent whitebark pine regeneration and its continued dominance in the stand. The RUST-NOFIRE scenario depicts the immediate future of the Pyramid stand under fire exclusion policies (fig. 25). The consequence of an exotic rust infection and complete exclusion of all fires is the accelerated decline in whitebark pine with a corresponding increase in subalpine fir. Whitebark pine is virtually eliminated from the stand by the end of simulation. Results of the RUST-FIRE simulation scenario seem to indicate that even with fire, maintenance of whitebark pine in the stand would be at low levels (fig. 26). The sharp decline of whitebark pine after the simulated fire at year 51 indicates the fire was quite severe and killed many whitebark pine trees.

Examples of annual FIRE-BGC predictions other than basal area are depicted for the NOFIRE scenario in figures 27 through 29. Fire exclusion in the Pyramid stand seems to result in a general increase in litter/duff depth (fig. 27), woody fuel loadings (fig. 28), and leaf area index (fig. 29).

Landscape Level Results—Simulation results for the NOFIRE scenario on the Monture Simulation Study Area landscape are presented in color plates 6 through 9. A slow trend of subalpine fir domination from year 50 (color plate 6) to year 200 (color plate 9) is evident in the maps created from this simulation. A majority of the landscape has been converted to subalpine fir by year 150 (color plate 8). Results of the remaining scenarios are contrasted with the NOFIRE scenario in table 12 for

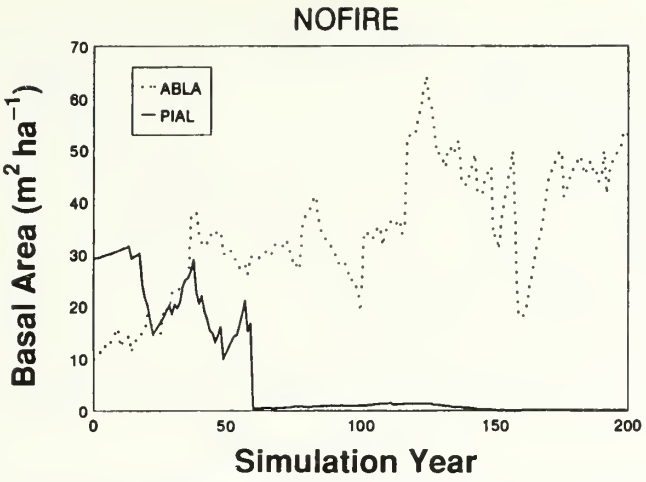

Figure 23—FIRE-BGC basal area predictions for the NOFIRE scenario over 200 years of simulation.

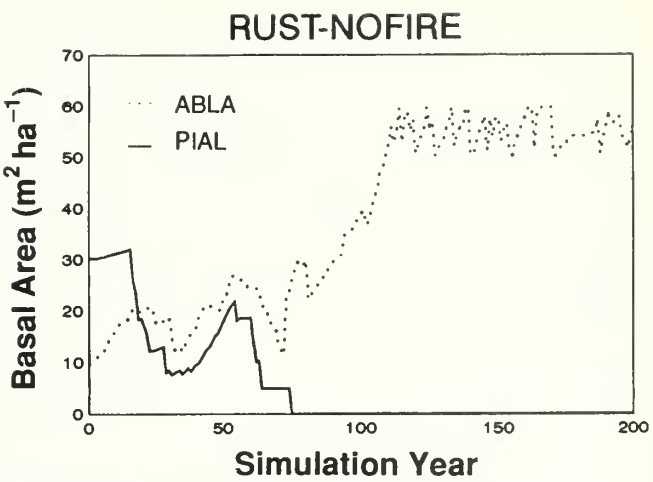

Figure 25—FIRE-BGC basal area predictions for the RUST-NOFIRE scenario for 200 years of simulation.

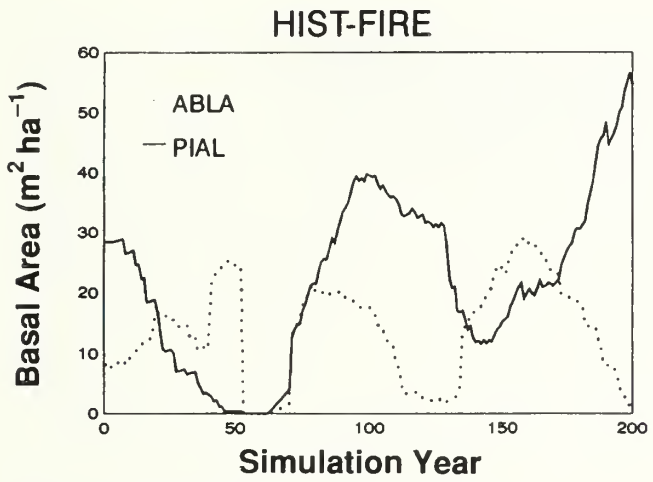

Figure 24—FIRE-BGC basal area predictions for the HIST-FIRE scenario over 200 years of simulation.

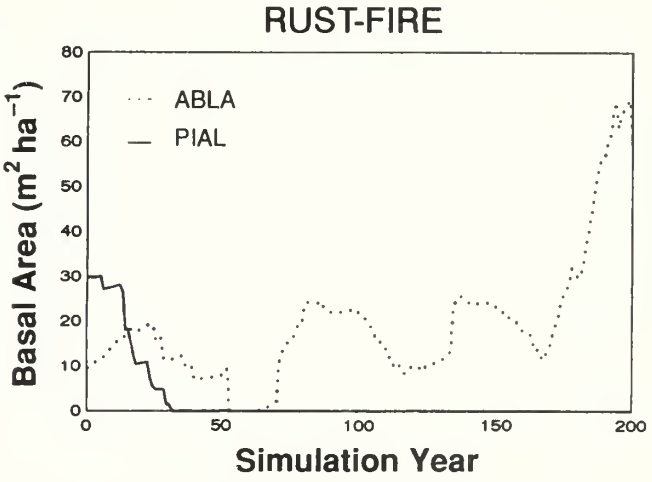

Figure 26—FIRE-BGC basal area predictions for the RUST-FIRE scenario over 200 years of simulation.

brevity. These scenario results show that fire tends to maintain whitebark pine on the MSSA landscape while the interaction of rust infection with fire exclusion seems to cause an accelerated landscape conversion to subalpine fir. This rapid decline seems to take place within the first century (table 12).

FIRE-BGC Tree Validation Results—Comparisons of predicted FIRE-BGC tree diameter increments with measure values for a subalpine fir and a whitebark pine tree on the Pyramid plot are shown in figures 30 and 31. Predictions seem to match closely at the beginning of simulation but disagree by simulation year 40. Projected diameters for the subalpine fir (fig. 32) and whitebark pine (fig. 33) seem to compare well, especially early in the simulation. The disagreement between predicted and observed diameter values during the last part of the simulation originates

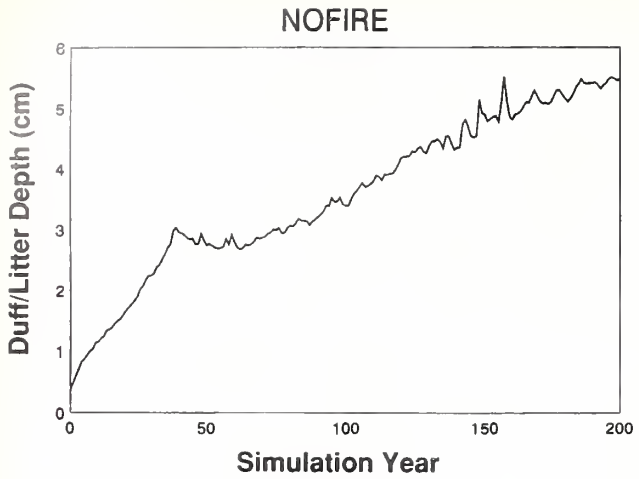

Figure 27—Predicted duff and litter depths (cm) for the NOFIRE simulation scenario using FIRE-BGC.

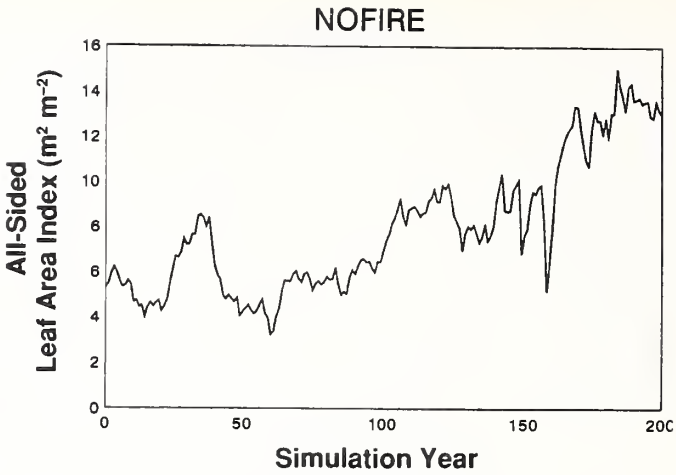

Figure 29—Predicted all-sided leaf area index for the NOFIRE scenario using FIRE-BGC.

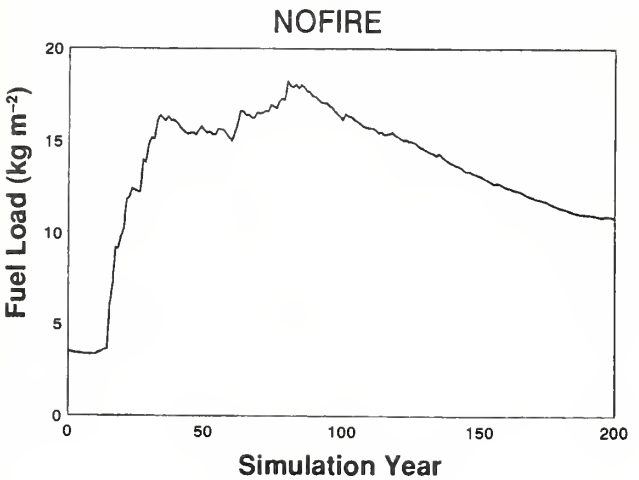

Figure 28—Predicted woody fuel loadings for the NOFIRE scenario using FIRE-BGC. Loadings are for all size classes of woody fuels (1, 10, 100, 1,000 hour fuel classes).

Table 12—Landscape simulation results for the four scenarios on the Monture Simulation Study Area. Numbers shown indicate percent of the landscape occupied by each forest cover type.

Simulation scenario	Simulation year				
	0	50	100	150	200
	Landscape dominated by whitebark pine (percent)				
NOFIRE	86.2	78.1	75.8	5.1	5.1
HIST-FIRE	86.2	78.1	79.4	81.8	88.4
RUST-NOFIRE	86.2	78.1	6.6	0.0	0.0
RUST-FIRE	86.2	78.1	4.1	0.2	0.0
	Landscape dominated by subalpine fir (percent)				
NOFIRE	8.1	16.2	19.3	90.2	90.2
HIST-FIRE	8.1	16.2	15.4	12.8	8.4
RUST-NOFIRE	8.1	16.2	89.1	94.5	94.5
RUST-FIRE	8.1	16.2	69.3	76.2	88.2

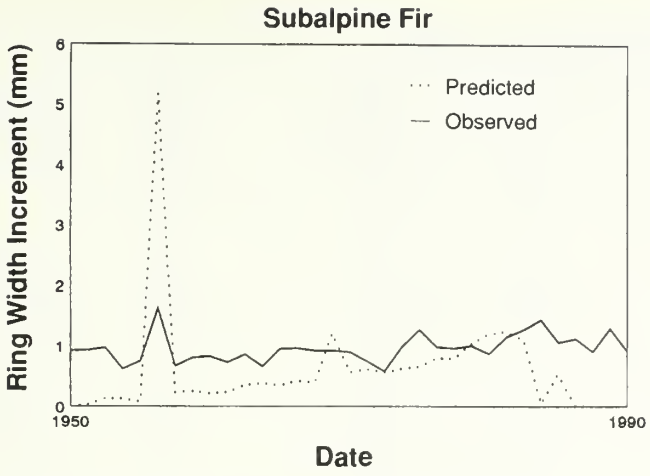

Figure 30—Predicted and observed diameter increments for a subalpine fir tree on the Pyramid simulation plot.

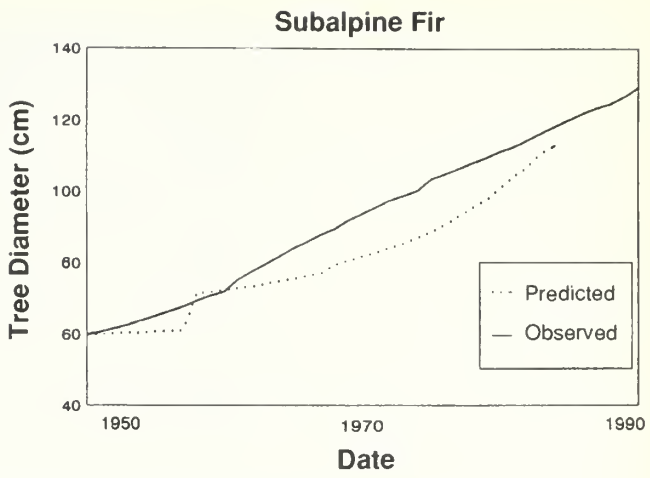

Figure 32—Predicted and observed diameters (DBH) for a subalpine fir tree.

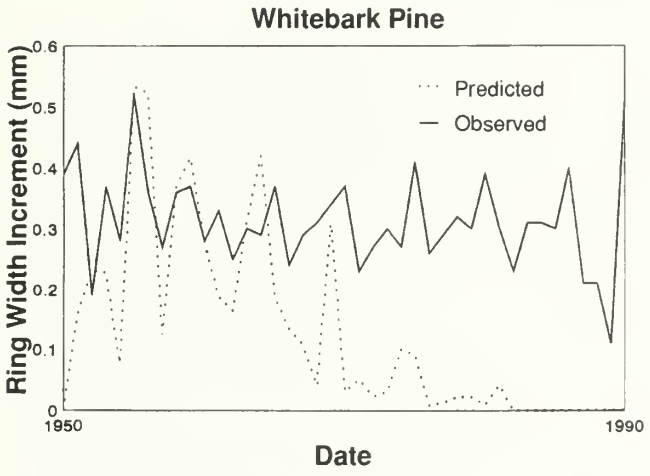

Figure 31—Predicted and observed diameter increments for a whitebark pine tree on the Pyramid simulation plot.

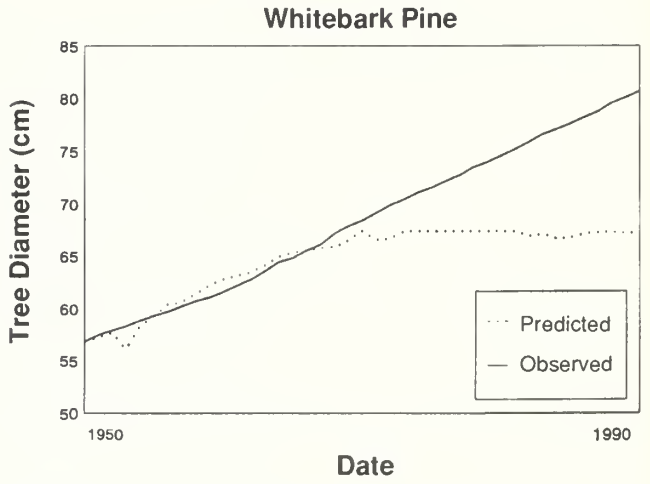

Figure 33—Predicted and observed diameters (DBH) for a whitebark pine tree.

from the tree carbon allocation to stem, roots, and leaves. Additional refinement is needed in this algorithm to improve model behavior. The overprediction of diameter increment at year 1957 in figure 30 is probably due to inaccurate weather conditions generated by the MT-CLIM climate model (Hungerford and others 1989).

FIRE-BGC Stand Validation Results—Results of the Tilison and Cliff Mountain tests of FIRE-BGC are shown in table 13. Model predictions generally seem to be greater than measured values. Basal area predictions are underpredicted for Cliff and overpredicted for Tilison test sites. Fuel loading and litter/duff depth predicted values seem to be somewhat closely aligned with simulated estimates, especially considering the high measurement errors involved in sampling these compartments (Brown 1970) and the complexity of the decomposition routine. Predicted

Table 13—Test results of long-term FIRE-BGC predictions of successional dynamics on Tilison and Cliff Mountain disturbed test sites.

Observed vs. predicted	Whitebark pine basal area	Subalpine fir basal area	Duff/ litter depth	Total fuel load	Leaf area index
	$m^2\ ha^{-1}$	$m^2\ ha^{-1}$	*cm*	$kg\ m^{-2}$	
Tilison Test Site					
Observed	7.0	0.7	0.4	5.0	0.6
Predicted	11.6	6.2	1.5	11.5	1.8
Percent error	65.7	785.7	275.0	130.0	200.0
Cliff Test Site					
Observed	10.1	5.8	2.0	8.3	1.0
Predicted	6.9	2.3	5.2	8.5	2.8
Percent error	–31.6	–60.3	160.0	2.9	180.0

and observed leaf area index values are off quite a bit, mostly as a result of the carbon allocation to tree leaves. These algorithms will be refined as future testing is scheduled for FIRE-BGC.

Discussion and Conclusions

Whitebark Pine Simulations—Whitebark pine populations in the Monture Simulation Study Area are predicted to decrease at an alarming rate. Most stands will probably be converted to dense subalpine fir and spruce with minor components of whitebark pine within the next few decades (figs. 23-26, table 12). Blister rust is predicted to kill the majority of whitebark pine, even with the reintroduction of fire on the landscape. However, wildfires seem to retain some whitebark pine on the landscape (fig. 26), presumably because of the creation of superior caching sites for the nutcrackers (burn, open areas). An estimated 3 to 8 percent of whitebark pine populations may be genetically resistant to blister rust (Arno and Hoff 1989; Bingham 1972; Hoff and others 1980). Caching in burned areas may increase the level of rust resistance in whitebark pine populations because the seeds that are cached will probably come from trees that survive rust infection. This might allow whitebark pine to remain on the landscape at low levels. However, the combined effects of blister rust and successional replacement due to fire exclusion will make it impossible to maintain current whitebark pine population levels even with high rust resistance. Also, if these populations become small, nutcracker seed consumption during the summer could destroy most of the seed crop (Tomback 1982). Breeding rust-resistant populations will be important for maintaining whitebark pine in the critical portions of its range, especially where it is currently a major food for the grizzly bear. Encouraging nutcracker caching by opening dense stands with fire may also promote whitebark pine populations (Tomback and others 1990).

Results of this study could be extrapolated to other parts of whitebark pine's range that experience similar weather patterns. Whitebark pine population levels in and around Glacier National Park and portions of the Bitterroot range in Montana and Idaho have decreased drastically since the mid 1970's (Arno 1986; Keane and Arno 1993; Kendall and Arno 1980) due mainly to blister rust. Blister rust has been documented in the southern portions of whitebark pine's range, but the mortality has not been as

extensive, presumably due to drier weather conditions (Keane and Arno 1993). However, given suitable weather conditions, blister rust may infect many more trees in the drier portions of its range.

Reduction of whitebark pine cone crops could affect many species of wildlife. Shifts in vegetation composition and wildlife migration brought about by rust mortality can invoke major changes in diversity and structure on the landscape. In turn, this may affect the pattern of fire processes in whitebark pine forests.

FIRE-BGC Model Performance—The ecophysiological process model FIRE-BGC shows great promise in predicting stand and landscape dynamics of coniferous forest ecosystems. The investigative power of FIRE-BGC seems immense. Effects of various natural and human-caused disturbance processes on the many ecosystem components can be assessed at any number of temporal and spatial scales. Although FIRE-BGC predictions are not precise (table 12), the temporal trends simulated by the model provide insight into successional processes. In addition to predicting successional changes in species composition and structure, FIRE-BGC can be used to investigate changes in an ecosystem's physical components such as soil water, snow pack, and available nitrogen.

FIRE-BGC does have a great number of limitations. First, it is computationally intensive with a simulation of 200 years taking 15 to 60 minutes for a stand and over 20 hours for an entire landscape (100-120 stands). Future sensitivity tests of the model will reveal algorithms that can be modified to reduce computation time.

Second, the model is parameter intensive. There are over 1,200 parameters that must be accurately quantified for successful simulation. Model behavior is only acceptable when all parameters reflect realistic conditions. For instance, some parameters, such as maximum leaf conductance, are so sensitive that their minor modification could result in an entirely different set of model predictions.

Third, many additional programs must be written and included into the LOKI system to display, tabulate, and understand FIRE-BGC predictions. This represents a significant programming effort.

Fourth, some FIRE-BGC runs may not be repeatible across similar simulations. The stochastic elements in FIRE-BGC require the model be executed several times, perhaps at least eight (Keane and others 1989; Kercher and Axelrod 1984). However, long execution times, spatial data recognition and complex data output severely limit the number of times FIRE-BGC can be executed to obtain between-run variability.

Fifth, the complexity inherent in FIRE-BGC often prevents a comprehensive interpretation of results.

The FIRE-BGC initialization process often creates incompatible conditions within the model. The great amounts and specificity of input data needed to initialize model compartments precludes the use of field data to quantify all starting conditions. Regression equations provide efficient and economical estimates of initial tree components, but often do not account for biophysical influences on tree and stand characteristics. As a result, ecosystem compartments are in conflict with simulated ecosystem processes. Two solutions to this enigma are possible. Time and effort can be spent to field-measure states of all ecosystem components in the simulation area. However, this seems almost intractable considering the money and effort required to complete such a task for an entire landscape.

A more reasonable solution might be to run the model using computed initial values until ecosystem states have stabilized, then output the simulated ecosystem component values to a file to be used as input on subsequent runs.

FIRE-BGC does not simulate undergrowth ecosystem processes at the detail provided for tree species. Consequently, processes such as net primary productivity and evapotranspiration are often underpredicted for early seral forest stands and perennial shrub lands and herb lands because of the lack of trees in the stand. Undergrowth contributions to the forest floor are also overpredicted because there is no feedback to regulate growth based on environmental conditions. Future modifications of FIRE-BGC will include the detailed treatment of undergrowth physiological processes intricately linked to tree processes as in Running and Hunt's (1993) BIOME-BGC.

FIRE-BGC does not adequately rectify life cycle characteristics of trees with ecophysiological dynamics of the stand. The link between tree regeneration, mortality, and growth with stand carbon, nitrogen, and water cycling needs a more comprehensive and mechanistic treatment in FIRE-BGC. There needs to be a closer relationship to net primary productivity and tree growth cycles, and tree regeneration and mortality must be connected to net primary productivity and other stand-level processes.

Carbon allocation from the stand-level to individual trees needs improvement. Contributions of stand photosynthate production by trees of different species and sizes present a complex computation in the model. FIRE-BGC calculates a species-specific allocation factor from daily ecosystem process calculations assuming stand leaf area was wholly comprised by the species in question. The species with the greatest photosynthetic production would receive the highest allocation factor. Then, another allocation factor is computed to represent a tree's position in the forest canopy. This factor is based on available light and the species' shade tolerance. The last factor is based on the proportion of stand leaf area comprised by the tree in question. Currently, these allocation factors cause greater amounts of carbon to be allocated to shade-tolerant trees and to understory trees. Modification of this procedure should take into account the efficiency and rate of photosynthate production relative to the amount of leaf area by species and tree size.

Weather data used for simulating climatic processes are probably not appropriate for long-term successional modeling. First, the length of weather record (often less than 40 years) is too short for multicentury simulations. Important ecosystem states respond closely to weather cycles, and repeating short, 40-year weather cycles is not representative of the climate pattern that influenced ecosystem formation. Second, the raw weather data used in the simulation came from one weather station just outside Monture Simulation Study Area boundaries. Extrapolation of these data to the complex mountain terrain may not fully represent the true range of weather conditions that controlled vegetation development. Many local weather events such as cold air drainage, frost pockets, and wind-funneling are not predicted by the MTCLIM weather model (Hungerford and others 1989). Long-term weather records from many weather stations are needed for future long-term successional modeling in FIRE-BGC.

The FIRE-BGC model will be used in many projects. Landscape structural and compositional changes as a result of disturbance regime modification will

be investigated using the LOKI implementation of FIRE-BGC. The effect of fire regime on ecosystem functions such as net primary productivity, water yield, and nutrient cycling will be simulated on a ponderosa pine/ Douglas-fir landscape. Consequences of global climate warming on plant species migration and landscape composition will also be simulated for a portion of Glacier National Park in Montana, U.S.A. Another project is simulating mountain pine beetle epidemic effects on landscape function.

References

Aber, J.D.; Botkin, D.B.; Melillo, J.M. 1978. Predicting the effects of different harvesting regimes on forest floor dynamics in northern hardwoods. Can. J. For. Res. 8:306-315.

Aber, J.D.; Melillo, J.M.; McClaugherty, C.A. 1990. Predicting long-term patterns of mass loss, nitrogen dynamics, and soil organic matter formation from initial fine litter chemistry in temperate forest ecosystems. Can. J. Bot. 68:2201-2208.

Aber, John D.; Melillo, Jerry M. 1982. FORTNITE: A computer model of organic matter and nitrogen dynamics in forest ecosystems. R3130 Research Bulletin, V.P.I. & S.U. Library, Blacksburg, Virginia. 49 p.

Aber, John D.; Melillo, Jerry M.; Nadelhoffer, Knute J.; Pastor, John; Boone, Richard D. 1991. Factors controlling nitrogen cycling and nitrogen saturation in Northern temperate forest ecosystems. Ecological Applications. 1:303-315.

Agee, James, K.; Smith, L. 1984. Subalpine tree establishment after fire in the Olympic Mountains, Washington. Ecology. 65:810-819.

Ågren, G.I.; Axelsson B. 1980. PT-A tree growth model. Ecol. Bull. (Stockholm) 32:525-536.

Ågren, G.I.; McMurtrie, R.E.; Parton, W.J. 1991. State-of-the-art of models of production-decompostion linkages in conifer and grassland ecosystems. Ecological Applications. 1(2), pp.118-138.

Albini, Frank A. 1976a. Computer-based models of wildland fire behavior: a user's manual. Ogden, UT: U.S. Department of Agriculture, Forest Service, Intermountain Forest and Range Experiment Station. 68 p.

Albini, Frank A. 1976b. Estimating wildfire behavior and effects. Gen. Tech. Rep. INT-30. Ogden, UT: U.S. Department of Agriculture, Forest Service, Intermountain Forest and Range Experiment Station. 92 p.

Alexander, Robert R. 1984. Natural regeneration of Engelmann spruce after clear-cutting in the central Rocky Mountains in relation to environmental factors. Res. Pap. RM-254. Fort Collins, CO: U.S. Department of Agriculture, Forest Service, Rocky Mountain Forest and Range Experiment Station. 17 p.

Alexander, Robert R.; Shearer, Raymond C.; Shepperd, W.D. 1984. Silvical characteristics of subalpine fir. Gen. Tech. Rep. RM-115. Fort Collins, CO: U.S. Department of Agriculture, Forest Service, Rocky Mountain Forest and Range Experiment Station. 29 p.

Allison, F.E.; Klein, C.J. 1961. Comparitive rates of decomposition in soil of wood and bark particles of several softwood species. Soil Society Science Proceedings. 25:193-196.

Alt, D. 1985. Geology of the Bob Marshall. In: Montana's Bob Marshall Country by R. Craetz. Montana Magazine, Inc., Helena, Montana: 9-19.

Andersen, Mark. 1991. Mechanistic models for the seed shadows of wind-dispersed plants. The American Naturalist. 137(4):476-497.

Anderson, Hal E. 1982. Aids to determining fuel models for estimating fire behavior. Gen. Tech. Rep. INT-122. Ogden, UT: U.S. Department of Agriculture, Forest Service, Intermountain Forestry and Range Experimental Station. 22 p.

Anderson, Hal E. 1969. Heat transfer and fire spread. Res. Pap. INT-69. Ogden, UT: U.S. Department of Agriculture, Forest Service, Intermountain Forest and Range Experiment Station. 20 p.

Andrews, M. 1986. The partioning of nitrate assimilation between root and shoot of higher plants. Plant, Cell and Environment. 9:511-519.

Angell, Raymond .F.; Richard F. Miller. 1994. Simulation of leaf conductance and transpiration in *Juniperus occidentalis*. Forest Science. 40(1):5-17.

Arno, S.F.; Hoff, R.J. 1989. Silvics of whitebark pine (*Pinus albicaulis*). USDA Forest Service Gen. Tech. Rep. INT-253.

Arno, Stephen F. 1986. Whitebark pine cone crops: a diminishing source of wildlife food? W. J. Appl. For. 1(3):92-94.

Arno, Stephen F. 1970. Ecology of aline larch (*Larix lyallii*) in the Pacific Northwest. Missoula, MT: University of Montana. 264 p. Dissertation.

Arno, Stephen F.; Simmerman, Dennis G.; Keane, Robert E. 1985. Forest succession on four habitat types in western Montana. Gen. Tech. Rep. INT-177. Ogden, UT: U.S. Department of Agriculture, Forest Service, Intermountain Forest and Range Experiment Station. 74 p.

Arp, P.A.; Yin, X. 1992. Predicting water fluxes through forests from monthly precipitation and mean monthly air temperature records. Can. J. For. Res. 22:864-877.

Baker, B. H.; Amman, G.D.; Trostle G.C. 1971. Does the mountain pine beetle change hosts in mixed lodgepole and whitebark pine stands? USDA For. Serv. Res. Note INT-151. 7 p.

Baker, William L. 1989. Effect of scale and spatial heterogeneity on fire-interval distributions. Can. J. For. Res. 19:700-706.

Band, L.E.; Peterson, D.L.; Running, S.W.; Coughlan, Joseph; Lanners, Richard; Dungan, Jennifer; Nemani, Ramakrishna. 1991. Forest ecosystem processes at the watershed scale: basis for distributed simulation. Ecological Modeling. 56:171-196.

Barclay, H.J.; Hall, T.H. 1986. Shawn: a model of Douglas-fir ecosystem response to nitrogen fertilization and thinning: a preliminary approach. Information Report BC-X-280. Canadian Forestry Service, Pacific Forestry Centre. Victoria, B.C. 30 p.

Bassman, John H. 1988. Photosynthesis and water relations of Ponderosa pine. SD-397. In: D.M. Baumgartner and J.E. Lotan, eds., Ponderosa Pine: the species and its management symposium proceedings. Washington State University Cooperative Extension, Pullman, Washington. pp 66-77.

Bassow, Susan L.; Ford, E.D.; Kiester, A.R. 1990. A critique of carbon-based tree growth models. In: Dixon, R.K.; Meldahl, R.S.; Ruark, G.A.; Warren, W.G., eds. Process modeling of forest growth responses to environmental stress, Portland, OR: Timber Press: 50-57.

Bazzaz, F.A. 1990. Plant-plant interactions in successional environments. In: Grace, James B. and Tilman, D. eds. Perspectives on Plant Competition. Academic Press, Inc.: 239-263.

Bazzaz, F.A. 1979. The physiological ecology of plant succession. Ann. Rev. Ecol. Syst. 10:351-371.

Benecke, U.; Schulze, E.D.; Matyssek, R.; Havranek, W.M. 1981. Environmental control of CO_2-assimilation and leaf conductance in *Larix decidua* Mill. Oecologia. 50:54-61.

Berg, Björn; Ekbohm, Gunnar. 1993. Decomposing needle litter in *Pinus contorta* (Lodgepole Pine) and *Pinus sylvestris* (Scots Pine) Monocultural systems—is there a maximum mass loss? Scand. J. For. Res. 8:457-465.

Bevins, Collin D. 1977. Natural fuels accumulations in lodgepole pine. Final Report. Ogden, UT: Intermountain Forest and Range Experiment Station. 31 p.

Bevins, C.D.; Andrews, P.L.; Keane, R.E. 1995. Forest succession modelling using the Loki software architecture. Lesnictvi-Forestry. 41(4):158-162.

Bevins, C.D.; Andrews, P.L. 1994. The Loki software architecture for fire and ecosystem modeling: A tinker toy approach. In: 12th Conference on Fire and Forest Meteorology, October 26-28, Jekyll Island, Georgia. Society of American Foresters, Washington D.C. pp. 252-260.

Bingham, R. T. 1972. Taxonomy, crossability, and relative blister rust resistance of 5-needled white pines. In: Biology of rust resistance in forest trees. Misc. Pub. No. 1221. USDA: 271-280.

Blake, John I.; Somers, Greg L.; Ruark, Gregory A. 1990. Perspectives on process modeling of forest growth responses to environmental stress. In: Dixon, R.K.; Meldahl, R.S.; Ruark, G.A.; Warren, W.G., eds. Process modeling of forest growth responses to environmental stress, Portland, OR: Timber Press: 9-17.

Boe, K.N. 1954. Periodicity of cone crops for five Montana conifers. Proceedings of the Montana Academy of Sciences. 14:5-9.

Bolstad, Paul V.; Gower, Stith T. 1990. Estimation of leaf area index in fourteen southern Wisconsin forest stands using a portable radiometer. Tree Physiology. 7:115-124.

Bonan, G.B. 1989. A computer model of the solar radiation, soil moisture, and soil thermal regimes in boreal forests. Ecological Modeling 45:275-306.

Bonan, Gordon B. 1993. Importance of leaf area index and forest type when estimating photosynthesis in boreal forests. Remote Sens. Environ. 43:303-314.

Bonan, Gordon B.; Shugart, Herman H. 1989. Environmental factors and ecological processes in boreal forests. Annu. Rev. Ecol. Syst. 20:1-28.
Bossel, Hartmut. 1991. Modeling forest dynamics: moving from description to explanation. For. Ecol. Manage. 42: 129-142.
Bossel, Hartmut; Krieger, Holger. 1991. Simulation model of natural tropical forest dynamics. Ecological Modeling. 59:37-71.
Bossel, Hartmut; Schäfer, Heiner. 1988. Eco-physiological dynamic simulation model of tree growth, carbon, and nitrogen dynamics. In: Wensel, Lee C.; Biging, Greg S., tech. eds. 1990. Forest simulation systems: proceedings of the IUFRO conference; 1988 November 2-5, Berkeley, CA. Bull. 1927. Berkeley, CA: University of California, Division of Agriculture and Natural Resources. 420 p.
Bossel, H.; Krieger, H.; Schäfer, H.; Trost, N. 1991. Simulation of forest stand dynamics, using real-structure process models. For. Ecol. Manage. 42:3-21.
Bossel, H.; Schäfer, H. 1989. Generic simulation model of forest growth, carbon and nitrogen dynamics, and application to tropical acacia and European spruce. Ecological Modeling. 48:221-265.
Botkin, Daniel B. 1993. Forest Dynamics: An Ecological Model. New York: Oxford University Press. 309 p.
Botkin, D.B.; Janak, J.F.; Wallis, J.R. 1972. Some ecological consequences of a computer model of forest growth. Journal of Ecology. 60:849-872.
Boyce, R.B. 1985. Conifer germination and seedling establishment on burned and unburned seedbeds. Moscow, ID: University of Idaho. Thesis. 71 p.
Brix, H. 1979. Effects of plant water stress on photosynthesis and survival of four conifers. Canadian Journal of Forest Research. 9:160-165.
Brown, James K. 1970. Ratios of surface area to volume for common fire fuels. Forest Science. 16:101-105.
Brown, James K. 1981. Bulk densities of nonuniform surface fuels and their application to fire modeling. Forest Science. 27: 667-683.
Brown, James K. 1976. Predicting crown weights for eleven Rocky Mountain conifers. Oslo Biomass Studies IUFRO Congress: 103-115.
Brown, James K. 1978. Weight and density of crowns of Rocky Mountain conifers. Res. Pap. INT-197. Ogden, UT: U.S. Department of Agriculture, Forest Service, Intermountain Forest and Range Experiment Station. 56 p.
Brown, James K.; Bevins, Collin D. 1986. Surface fuel loadings and predicted fire behavior for vegetation types in the Northern Rocky Mountains. Res. Note INT-358. Ogden, UT: U.S. Department of Agriculture, Forest Service, Intermountain Forest and Range Experiment Station. 9 p.
Brown, James K.; Marsden, Michael A.; Ryan, Kevin C.; Reinhardt, Elizabeth D. 1985. Predicting duff and woody fuel consumed by prescribed fire in the Northern Rocky Mountains. Res. Pap. INT-337. Ogden, UT: U.S. Department of Agriculture, Forest Service, Intermountain Forest and Range Experiment Station. 23 p.
Brown, James K.; See, Thomas E. 1981. Downed dead woody fuel and biomass in the Northern Rocky Mountians. Gen. Tech. Rep. INT-117. Ogden, UT: U.S. Department of Agriculture, Forest Service, Intermountain Forest and Range Experiment Station. 48 p.
Brown, James K.; Snell, J.A. Kendall; Bunnell, David L. 1977. Handbook for predicting slash weight of western conifers. Gen. Tech. Rep. INT-37. Ogden, UT: U.S. Department of Agriculture, Forest Service, Intermountain Forest and Range Experiment Station. 35 p.
Brown, Kevin; Higginbotham, K.O. 1986. Effects of carbon dioxide enrichment and nitrogen supply on growth of boreal tree seedlings. Tree Physiology. 2:223-232.
Bunce, J.A.; Chabot, B.F.; Miller, L.N. 1979. Role of annual leaf carbon balance in the distribution of plant species along an elevational gradient. Bot. Gaz. 140:288-294.
Burk, Thomas E.; Sievänen, Risto; Ek, Alan R. 1990. Construction of forest growth models based on physiological principles. In: Proceedings of a symposium, Aspen symposium '89, 1989 July 25 -27, Duluth, MN. Gen. Tech. Report NC-140. 348 p.
Burns, Russell M.; Honkala, Barbara H., tech. coords. 1990. Silvics of North America: Volume 1, Conifers. Agriculture Handbook 654. U.S. Department of Agriculture, Forest Service, Washington, DC. vol. 1. 675 p.
Burton, Philip J.; Urban, Dean L. 1990. An overview of ZELIG, a family of individual-based gap models simulating forest succession. In: Evelyn Hamilton (compiler), Symposia Proceedings Vegetation Management: An integrated approach, 14-16 November, 1989, Victoria, B.C. Forestry Canada Pacific Forestry Centre FRDA Report 109. pp. 92-96.

Busing, R.T. 1991. A spatial model of forest dynamics. Vegetation Science. 92:167-179.
Busing, R.T.; Clebsch, E.E.C. 1987. Application of a spruce-fir forest canopy gap model. For. Ecol. Manage. 20:151-169.
Campbell, Gaylon S. 1977. An Introduction to Environmental Biophysics. New York: Springer-Verlag. 159 p.
Canham, Charles D.; Marks, P.L. 1985. The response of woody plants to disturbance: patterns of establishment and growth. In: The Ecology of Natural Disturbance and Patch Dynamics, San Diego, CA: Academic Press: 197-216.
Chertov, O.G. 1990. SPECOM –a single tree model of pine stand/raw humus soil ecosystem. Ecological Modeling. 50:107-132.
Ciesla, W. M.; Furniss, M. M. 1986. Idaho's haunted forests. Am. For. 81(8):32-35.
Clark, James S. 1990. Fire and climate change during the last 750 years in northwestern Minnesota. Ecological Monographs. 60(2):135-159.
Covington, W. W.; Sackett, Stephen S. 1984. The effect of a prescribed burn in Southwestern ponderosa pine on organic matter and nutrients in woody debris and forest floor. Forest Sci. 30(1): 183-192.
Cui, Muyi; Smith, William K. 1991. Photosynthesis, water relations and mortality in *Abies lasiocarpa* seedlings during natural establishment. Tree Physiology. 8:37-46.
Dale, V.H.; Doyle, T.W.; Shugart, H.H. 1985. A comparison of tree growth models. Ecological Modeling. 29:145-169.
Dale, Virginia H.; Hemstrom, Miles. 1984. CLIMACS: a computer model of forest stand developement for western Oregon and Washington. USDA Forest Service Research Paper PNW-327. Portland, OR: U.S. Department of Agriculture, Forest Service, Pacific Northwest Forest and Range Experiment Station. 60 p.
Dale, V.H.; Hemstrom, M.; Franklin, J. 1986. Modeling the long-term effects of disturbances on forest succession, Olympic Peninsula, Washington. Can. J. For. Res. 16:56-67.
Dalla-Tea, F.; Jokela, E.J. 1991. Needlefall, canopy light interception, and productivity of young intensively managed slash and Loblolly pine stands. Forest Science. 37(5): 1298-1313.
Davis, Kathleen M.; Clayton, Bruce D.; Fischer, William C. 1980. Fire ecology of Lolo National Forest habitat types. Gen. Tech. Rep. INT-79. Ogden, UT: U.S. Department of Agriculture, Forest Service, Intermountain Forest and Range Experiment Station. 77 p.
Deiss, C. 1958. Geology of the Bob Marshall Wilderness. In: Guide to the Bob Marshall Wilderness. USDA For. Serv. Northern Region Rep., Missoula, Montana. 36 p.
Dickson, R.E. 1989. Carbon and nitrogen allocation in trees. Ann. Sci. For. 46:631-647.
Dickson, Richard E.; Isebrands, J.G.; Tomlinson, Patricia T. 1990. Distribution and metabolism of current photosynthate by single-flush northern red oak seedlings. Tree Physiology. 7:65-77.
Drake, James A. 1991. Community-assembly mechanics and the structure of an experimental species ensemble. The American Naturalist. 137:1-26.
Drury, William H.; Nisbet, Ian C.T. 1973. Succession. The Arnold Arbor. J. 54(3):331-368.
Eck, T.F.; Deering, D.W. 1992. Canopy albedo and transmittance in a spruce-hemlock forest in mid-September. Agric. For. Meteorol. 59:237-248.
Edmonds, R. L. 1979. Decomposition and nutrient release in Douglas-fir needle litter in relation to stand developement. Canadian Journal of Forest Research. 9:132-140.
Eis, S.; Craigdallie, D. 1983. Reproduction of conifers. A handbook for cone crop assessment. For. Tech. Rep. No. 31. Canadian Forest Service: 12-27.
Evert, F. 1985. Systems of equations for estimating ovendry mass of 18 Canadian tree species. Information Report PI-X-59. Canadian Forestry Service, Petawawa National Forestry Institute. 49 p.
Fahey, T. 1983. Nutrient dynamics of aboveground detritus in lodgepole pine (*Pinus contorta* var. *latifolia*) ecosystems in southeastern Wyoming. Ecological Monographs. 53:51-72.
Faurot, James L. 1977. Estimating merchantable volume and stem residue in four timber species. Res. Pap. INT-196. Ogden, UT: U.S. Department of Agriculture, Forest Service, Intermountain Forest and Range Experiment Station. 55 p.
Feller, M.C. 1992. Generalized versus site-specific biomass regression equations for *Pseudotsuga menziesii* var. *menziesii* and *Thuja plicata* in Coastal British Columbia. Bioresource Technology. 39:9-16.
Finegan, Bryan. 1984. Forest succession. Nature. 312:109-114.

Finney, Mark A. 1994. Modeling the spread and behavior of prescribed natural fires. In: 12th Conference on Fire and Forest Meteorology, October 26-28, Jekyll Island, Georgia. Society of American Foresters, Washington D.C. 6 p. (In Press)

Fischer, Christine; Höll, Wolfgang. 1992. Food reserves of scots pine (*Pinus sylvestris* L.). Trees. 6:147-155.

Fischer, William C.; Bradley, Anne F. 1987. Fire ecology of western Montana forest habitat types. General Technical Report INT-223. Intermountain Research Station. U.S. Department of Agriculture, Forest Service. 95 p.

Fogel, R.; Cromack, K., Jr. 1977. Effect of habitat and substrate quality on Douglas-fir litter decomposition in western Oregon. Canadian Journal of Botany. 55:1632-1640.

Forman, Richard T.T.; Godron, M. 1986. Landscape Ecology. New York: John Wiley and Sons. 619 p.

Fosberg, M.A. 1970. Drying rates of heartwood below fiber saturation. Forest Science. 16:57-63.

Foster, Jeffrey R. 1985. Coarse root biomass in subalpine balsam fir forests. Forest Science. Vol. 31, No. 4, pp. 952-956.

Fowells, H. A. 1965. Silvics of the forest trees of the United States. Agric. Hdbk. No. 271. Washington, DC: U.S. Department of Agriculture, Forest Service. 762 p.

Fox, John F. 1989. Bias in estimating forest disturbance rates and tree lifetimes. Ecology. 70(5):1267-1272.

Frandsen, William H., Andrews, Patricia L. 1979. Fire behavior in nonuniform fuels. Res. Pap. INT-232. Ogden, UT: U.S. Department of Agriculture, Forest Service, Intermountain Forest and Range Experiment Station. 34 p.

Friend, A.D.; Schugart, H.H.; Running, S.W. 1993. A physiology-based gap model of forest dynamics. Ecology. 74(3):792-797.

Fry, D.J.; Phillips, I.D.J. 1977. Photosynthesis of conifers in relation to annual growth cycles and dry matter production. Physiol. Plant. 40:300-306.

Gabriel, H.W. 1976. Wilderness ecology: The Danaher Creek drainage, Bob Marshall Wilderness, Montana. Master's Thesis, University of Montana, Missoula. 224 p.

Gary, Howard L. 1976. Crown structure and distribution of biomass in a lodgepole pine stand. Research Paper RM-165. Fort Collins, CO: U.S. Department of Agriculture, Forest Service, Rocky Mountain Forest and Range Experiment Station. 20 p.

Gay, Cheryl A. 1989. Modeling tree level processes. Air pollution effects on vegetation including forest ecosystems; proceedings of the second US-USSR Symposium. Noble, Reginald D., and others Broomall, PA: Northeastern Forest Experiment Station. 311 p.

Gay, Lloyd Wesley; Knoerr, Kenneth R. 1975. The forest radiation budget. Bulletin 19. Durham, North Carolina: Duke University School of Forestry and Environmental Studies. 165 p.

Gordon, John C.; Larson, Philip R. 1968. Seasonal course of photosynthesis, respiration, and distribution of carbon in young *Pinus resinosa* trees as related to wood formation. Plant Physiol. 43:1617-1624.

Gottfried, Gerald J.; Ffolliot, P. F. 1983. Annual needle and leaf fall in an Arizona mixed conifer stand. Res. Note RM-428. Fort Collins, CO: U.S. Department of Agriculture, Forest Service, Rocky Mountain Forest and Range Experiment Station. 4 p.

Gower, S.T.; Grier, C.C.; Vogt, D.J.; Vogt, K.A. 1987. Allometric relations of deciduous (*Larix occidentalis*) and evergreen conifers (*Pinus contorta* and *Pseudotsuga menziesii*) of the Cascade mountains in central Washington. Can. J. For. Res. 17:630-634.

Gower, Stith T.; Reich, Peter B.; Yowhan, Son. 1991. Canopy dynamics and aboveground production of five tree species with different leaf longevities. Tree Physiology. 12: 327-345.

Gower, Stith T.; Vogt, Kristiina A.; Grier, Charles C. 1992. Carbon dynamics of Rocky Mountain Douglas-fir: influence of water and nutrient availability. Ecological Monographs. 62(1): 43-65.

Greene, D.F.; Johnson, E.A. 1989. A model of wind dispersal of winged or plumed seeds. Ecology. 70:339-347.

Grier, C.C. 1975. Wildfire effects on nutrients distribution and leaching in a coniferous ecosystem. Can. J. For. Res. 5:599-607.

Grier, C.C.; Vogt, K.A.; Keyes, M.R.; Edmonds, R.L. 1981. Biomass distribution and above–and below-ground production in young and mature *Abies amabilis* zone ecosystems of the Washington Cascades. Can. J. For. Res. 11:155-167.

Grime, J.P. 1966. Shade avoidance and shade tolerance in flowering plants. In: Light as an Ecological Factor (R. Bainbridge, G.C. Evans, and O. Rackham, eds.), Symp. Br. Ecol. Soc. 6:187-207.

Grime, J.P. 1979. Plant strategies and vegetation processes. Wiley, New York. 321 p.

Grime, J.P. 1974. Vegetation classification by reference to strategies. Nature. 250:26-31.

Grime, J.P.; Hunt, R. 1975. Relative growth rate: its range and adaptive significance in a local flora. J. Ecol. 63:393-422.

Grime, J.P.; Jeffery, D.W. 1965. Seedling establishment in verticle gradients of sunlight. Journal of Ecology. 53:621-642.

Groeschl, David A.; Johnson, James E; Smith, David W. 1993. Wildfire effects on forest floor and surface soil in a table mountain pine-pitch pine forest. Int. J. Wildland Fire. 3(3):149-154

Hänninen, Heikki. 1990. Modeling dormancy release in trees from cool and temperate regions. In: Dixon, R.K.; Meldahl, R.S.; Ruark, G.A.; Warren, W.G., eds. Process modeling of forest growth responses to environmental stress. Portland, OR: Timber Press: 159-164.

Hann, W. J. 1990. Landscape ecology and vegetation management in whitebark pine ecosystems. In Proceedings of Whitebark pine ecosystems: Ecology and management of a high mountain resource. March 29-31, 1989, Bozeman, Montana. USDA For. Serv. Gen. Tech. Rep. INT-270.

Hari, P.; Nygren, P.; Korpilahti, E. 1991. Internal circulation of carbon within a tree. Can. J. For. Res. 21:514-515.

Harlow, W. M.; Harrar, E. S. 1969. Textbook of dendrology. Fifth edition. New York: McGraw-Hill. 432 p.

Hellmers, H.; Genthe, M. K.; Ronco, F. 1970. Temperature affects growth and development of Engelmann spruce. Forest Science. 16:447-452.

Hellmisaari, Heljä-Sisko. 1992. Nutrient retranslocation in three *Pinus sylvestris* stands. Forest Ecology and Management. 51: 347-367.

Hoff, R.; Bingham, R.; Macdonald, G.J. 1980. Relative blister rust resistance of white pines. European J. For. Pathology. 10:307-316.

Horn, Henry S. 1974. The ecology of secondary succession. Annual Reviews of Ecology and Systematics. 5:25-37.

Hungerford, R.D.; Nemani, R.R.; Running S.W.; Coughlan, J.C. 1989. MTCLIM: A mountain microclimate simulation model. Research Paper INT-414. Ogden, UT: U.S. Department of Agriculture, Forest Service, Intermountain Research Station. 52 p.

Hunsaker, Carolyn T.; Nisbet, Robert A.; Lam, David C.; Brower, Joan A.; Baker, William L.; Turner, Monica G.; Botkin, Daniel B. 1993. Spatial models of ecological systems and processes: The role of GIS. In: Goodchild, Michael F.; Parks, Bradley O.; and Steyaert, Loius T. Environmental modeling with GIS. Oxford University Press, New York: 248-264.

Hunt, F.A. 1986. National register of big trees. American Forests. 94(4):21-52.

Huston, M.; DeAngelis, D; Post, W. 1988. New computer models unify ecological theory. BioScience. 38(10):682-691.

Irwin, L.L.; Peek, James M. 1979. Shrub production and biomass trends following five logging treatments within the cedar-hemlock zone of Northern Idaho. Forest Science. 25:415-426.

Jeske, B.W.; Bevins, Collin D. 1976. Spatial and temporal distribution of natural fuels in Glacier National Park. In: First Conference on Scientific Research in the National Parks, November 9-13, New Orleans, LA:1-21.

Johnson, D.W.; Lindberg, S.E.; Van Miergroet, H.; Lovett, G.W.; Cole, D.W.; Mitchell, M.J.; Binkley, D. 1993. Atmospheric deposition, forest nutrient status, and forest decline: Implications of the integrated forest study. In: R.F. Huettl and D. Mueller-Dombois (editors) Forest decline in the Atlantic and Pacific region. Springer Verlag, New York. pp. 66-81.

Johnson, E.A. 1979. Fire reoccurrence in the subartic and its implications for vegetation composition. Can. J. Bot. 57:1374-1379.

Johnson, E.A.; Van Wagner, C.E. 1985. The theory and use of two fire history models. Can. J. For. Res. 15:214-220.

Johnson, I.R. 1985. A model of the partitioning of growth between the shoots and roots of vegetative plants. Annals of Botany. 55:421-431.

Kaifez-Bogataj, Lucka. 1988. Dynamic photosynthetical model of CO_2 exchange in forest stands. Forest simulation systems: Proceedings of the IUFRO Conference, Berkeley, California:235-245.

Kajimoto, T. 1990. Photosynthesis and respiration of *Pinus pumila* needles in relation to needle age and season. Ecol. Res. 5:333-340.

Kaufmann, Merrill R.; Edminster, Carleton B.; Troendle, Charles A. 1982. Leaf area determinations for subalpine tree species in the central Rocky Mountains. Res. Pap. RM-238. Fort Collins, CO: U.S. Department of Agriculture, Forest Service, Rocky Mountain Forest and Range Experiment Station. 7 p.

Keane, Robert E. 1987. Forest succession in western Montana—a computer model designed for resource. Research Note INT-376. U.S. Department of Agriculture, Forest Service, Intermountain Research Station. 8 p.

Keane, R.E.; Arno, S.F. 1993. Rapid decline of whitebark pine in western Montana; Evidence from 20-year remeasurements. Western Journal of Applied Forestry. 8(2):44-47.

Keane, R.E.; Morgan, Penelope. 1994. Decline of whitebark pine in the Bob Marshall Wilderness Complex of Montana, USA. In: Proceedings of subalpine stone pines and their environment: The status of our knowledge, W. Schmidt ed. Sept 5-11, 1992. USDA Forest Service General Technical Report INT. pp 342-356.

Keane, R.E.; Morgan, Penelope; Menakis, James. 1994. Landscape assessment of the decline of whitebark pine (*Pinus albicaulis*) in the Bob Marshall Wilderness Complex, Montana, USA. Northwest Science. 68(3):213-229.

Keane, Robert E.; Arno, Stephen F.; Brown, James K. 1989. FIRESUM -An ecological process model for fire succession in Western conifer forests. Gen. Tech. Rep. INT-266. Ogden, UT: U.S. Department of Agriculture, Forest Service, Intermountain Research Station. 76 p.

Keane, Robert E.; Arno, Stephen F.; Brown, James K. 1990a. Simulating cumulative fire effects in ponderosa pine/Douglas-fir forests. Ecology. 71(1):189-203.

Keane, Robert E.; Arno, Stephen F.; Brown, James K.; Tomback, Diana F. 1990b. Modeling stand dynamics in whitebark pine (*Pinus albicaulis*) forests. Ecological Modeling. 51:73-95.

Keen, F.P. 1940. Longevity of ponderosa pine. Journal of Forestry. 38:597-598.

Kellomäki, S.; Kolström, M. 1992. Simulation of tree species compostion and organic matter accumulation in Finnish boreal forest under changing climatic conditions. Vegetatio. 102:47-68.

Kellomäki, Seppo; Hänninen, Heikki; Kolström, T.; Kotisaari, Ahti; Pukkala, Timo. 1987. A tentative model for describing the effects of some regenerative processes on the properties of natural seedling stands. Silva Fennica. 21(1):1-10.

Kellomäki, Seppo; Väisänen, Hannu. 1991. Application of a gap model for the simulation of forest ground vegetation in boreal conditions. Forest Ecology and Management. 42:35-47.

Kendall, K.C.; Arno, S.F. 1990. Whitebark pine—an important but endangered wildlife resource. In: Proceedings of the symposium: Whitebark pine ecosystems: Ecology and management of a high mountain resource, March 29-31, 1989. Bozeman, Montana, USA. USDA Forest Service. Gen. Tech. Rep. INT-270:264-274.

Kercher, James R.; Axelrod, M.C. 1984. A process model of fire ecology and succession in a mixed-conifer forest. Ecology. 65(6):1725-1742.

Kernighan, Brian W.; Ritchie, Dennis M. 1988. The C programming language, Second Edition. Prentice Hall, Englewood Cliffs, New Jersey. 272 p.

Kienast, Felix; Kräuchi, Norbert. 1991. Simulated successional characteristics of managed and unmanaged low-elevation forests in central Europe. For. Ecol. Manage., 42:49-61.

Kimmins, J.P. 1993. Scientific foundations for the simulation of ecosystem function and management in FORCYTE-11. Inf. Report NOR-X-328. Edmonton, Alberta: Forestry Canada, Morthwest Region, Northern Forestry Centre. 88 p.

King, David A. 1993. A model analysis of the influence of root and foliage allocation on forest production and competition between trees. Tree Physiology. 12:119-135.

Klemmedson, J.O.; Schultz, A.M.; Biswell, H.H. 1962. Effect of prescribed burning of forest litter on total soil nitrogen. Soil Science Society Proceedings:200-202.

Klemmendson, J.O.; Meier, C.E.; Campbell, R.E. 1985. Needle decomposition and nutrient release in ponderosa pine ecosystems. Forest Science. 31(3):647-660.

Klinka, K.; Wang, Q.; Kayahara, G.J.; Carter, R.E.; Blackwell, B.A. 1992. Light-growth response relationships in Pacific silver fir (*Abies amabilis*) and subalpine fir (*Abies lasiocarpa*). Can. J. Bot. 70:1919-1930.

Knapp, A.K.; Smith, W.K. 1982. Factors influencing understory seedling establishment of Engelmann spruce (*Picea engelmannii*) and subalpine fir (*Abies lasiocarpa*) in southwest Wyoming. Canadian Journal of Botany. 60:2753-2761.

Korol, R.L.; Running, S.W.; Milner, K.S.; Hunt, E.R. Jr. 1991. Testing a mechanistic carbon balance model against observed tree growth. Can. J. For. Res. 21:1098-1105.

Korol, R.L.; Zuuring, H.R. 1990. Development of a mechanistic stand growth model for uneven-aged Douglas-fir in South-Central British Columbia. In: Wengel, L.C.; Biging, G.S., eds. IUFRO Forest Simulation Systems Conference; 1988 November 2-5; Berkeley, California: UC Div. of Agriculture and Natural Resource Bulletin 1927:31-38.

Kutiel, P.; Shaviv, A. 1992. Effects of soil type, plant composition and leaching on soil nutrients following a simulated forest fire. For. Ecol. Manage. 53:329-343.

Lange, Robert W. 1971. Bark thickness, k, factors for four Montana coniferous tree species. Res. Note. No. 9. Missoula, MT: Montana Forest and Conservation Experiment Station, School of Forestry, University of Montana. 2 p.

Larcher W. 1969. The effect of environmental and physiological variables on the carbon dioxide gas exchange of trees. Photosynthetica. 3(2):167-198.

L'Ecuyer, Pierre. 1988. Efficient and portable combined random number generators. Communications of the ACM. 31(6):742-758.

Leemans, R. 1989. Description and simulation of stand structure and dynamics in some Swedish forests. Uppsala, Sweden: Uppsala University. 149 p.

Leemans, R.; Prentice, I. 1989. FORSKA, a general forest succession model. Uppsala, Sweden: Institute of Ecological Botany. 45 p.

Levine, E.R.; Ranson, K.J.; Smith, J.A.; Williams, D.L.; Knox, R.G.; Shugart, H.H.; Urban D.L.; Lawrence, W.T. 1993. Forest ecosystem dynamics; linking forest succession, soil process and radiation models. Ecological Modeling. 75:199-219.

Little, Ronda, L.; Peterson, David L.; Conquest, Loveday, L. 1994. Regeneration of subalpine fire (*Abies lasiocarpa*) following fire: effects of climate and other factors. Can. J. For. Res. 24:934-944.

Little, Susan N.; Ohmann, Janet L. 1988. Estimating nitrogen lost from forest floor during prescribed fires in Douglas-fir/western hemlock clearcuts. Forest Science. 34(1):152-164.

Lohammar, T.; Larsson, S.; Linder, S.; Falk, S.O. 1980. FAST-Simulation models of gaseous exchange in Scots pine. In: T. Persson (editor). Structure and function of northern coniferous forests—an ecosystem study. Ecol. Bull. 32:505-523.

Lopushinsky W. 1969. Stomatal closure in conifer seedlings in response to leaf moisture stress. Bot. Gaz. 130:258-263.

Losensky, J. 1990. A comparison of the 1988 fire season to the historical role of fire for the Bob Marshall-Great Bear-Scapegoat wilderness complex. A report on file at the USDA For. Serv., Intermountain Fire Sciences Lab., Missoula, Montana.

Lotan, James E.; Perry, David A. 1983. Ecology and regeneration of lodgepole pine. Agric. Hdbk. No. 606. Washington, DC: U.S. Department of Agriculture, Forest Service. 51 p.

Lovett, Gary M.; Lindberg, Steven E. 1993. Atmospheric deposition and canopy interactions of nitrogen in forests. Can. J. For. Res. 23:1603-1616.

Lynch, Donald W. 1959. Effects of wildfire on mortality and growth of young ponderosa pine trees. Res. Note INT-66. Ogden, UT: U.S. Department of Agriculture, Forest Service, Intermountain Forest and Range Experiment Station. 8 p.

Maclean, D. A.; Wien, R. W. 1978. Weight loss and nutrient changes in decomposing litter and forest floor material in New Brunswick forest stands. Canadian Journal of Botany. 56:2730-2749.

Maier, C.A.; Teskey, R.O. 1992. Internal and external control of net photosynthesis and stomatal conductance of mature eastern white pine (*Pinus strobus*). Can. J. For. Res. 22:1387-1394.

Mäkelä, Annikki; Hari, Pertti. 1986. Stand growth model based on carbon uptake and allocation in individual trees. Ecological Modeling. 33:205-229.

Marks, P.L. 1975. On the relation between extension growth and successional status of deciduous trees of the Northeastern United States. Bull. Torrey Bot. Club. 102:172-177.

Marsden, Michael A. 1983. Modeling the effect of wildfire frequency on forest structure and succession in the Northern Rocky Mountains. Journal of Environmental Managment. 16(1):45-62.

Marshall, J.D.; Waring, R.H. 1985. Predicting fine root production and turnover by monitoring root starch and soil temperature. Can. J. For. Res. 15:791-800.

Martin, Robert E. 1982. Shrub control by burning before timber harvest. In: Baumgartner, David M., ed. Site Preparation and Fuels Management on Steep Terrain, Proceedings of a symposium, 1982 February 15-17, Spokane, WA. Pullman, WA: Cooperative Extension, Washington State University: 35-40.

Massman, W.J.; Kaufmann, M.R. 1991. Stomatal response to certain environmental factors: a comparison of models for subalpine trees in the Rocky Mountains. Agric. For. Meteorol. 54:155-167.

Mathews, Edward E. 1972. The accretion of fuel in lodgepole pine forests of southwest Montana. Missoula, MT: University of Montana. 39 p. Thesis.

Matthes-Sears, U.; Larson, D.W. 1990. Environmental controls of carbon uptake in two woody species with contrasting distributions at the edge of cliffs. Can. J. Bot. 68: 2371-2380.

Matyssek, R. 1986. Carbon, water and nitrogen relations in evergreen and deciduous conifers. Tree Physiology. 2:177-187.

McCaughey, Ward W.; Schmidt, Wyman C.; Shearer, Raymond C. 1985. Seed dispersal characteristics of conifers of the Inland Mountain West. In: R.C. Shearer (compiler). Proc. Symp. Conifer Seed in Inland Mountain West, 5-6 April 1985, Missoula, MT, pp. 50-61.

McDonald, Philip M. 1992. Estimating seed crops of conifer and hardwood species. Can. J. For. Res. 22:832-838.

McMurtrie, R.; Wolf, L. 1983. Above-and below-ground growth of forest stands: a carbon budget model. Annals of Botany. 52:437-448.

McMurtrie, R.; Wolf, L. 1983. A model of competition between trees and grass for radiation, water and nutrients. Annals of Botany. 52:449-458.

McMurtrie, R.E.; Landsberg, J.J. 1992. Using a simulation model to evaluate the effects of water and nutrients on the growth and carbon partitioning of *Pinus radiata*. Forest Ecology and Management. 52:243-260.

McMurtrie, R.E.; Leuning, R.; Thompson, W.A.; Wheeler, A.M. 1992. A model of canopy photosynthesis and water use incorporating a mechanistic formulation of leaf CO_2 exchange. For. Ecol. Manage. 52:261-278.

Means, J. E.; Cromack, K; Macmillan, P. C. 1985. Comparison of decomposition models using wood density of Douglas-fir logs. Canadian Journal of Forest Research. 15: 1092-1098.

Means, Joseph, E.; Hansen, Heather A.; Koerper, Greg J.; Alaback, Paul B.; Klopsch, Mark W. 1994. Software for computing plant biommass—Biopak users guide. General Technical Report PNW-GTR-340. 123 p.

Meetenmeyer, V. 1978. Macroclimate and lignin control of decomposition rates. Ecology. 59:465-472.

Milner, Kelsey S. 1992. Site index and height growth curves for ponderosa pine, western larch, lodgepole pine and Douglas-fir in western Montana. Western Journal of Applied Forestry. 7(1):9-14.

Minore, D. 1979. Comparative autecological charateristics of northwestern tree species: a literature review. Gen. Tech. Rep. PNW-87. Portland, OR: U.S. Department of Agriculture, Forest Service, Pacific Northwest Forest and Range Experiment Station. 28 p.

Moeur, Melinda. 1985. COVER: A user's guide to the CANOPY and SHRUBS extension of the stand prognosis model. Gen. Tech. Rep. INT-190. Ogden, UT: U.S. Department of Agriculture, Forest Service, Intermountain Research Station. 49 p.

Moeur, Melinda. 1981. Crown width and foliage weight of Northern Rocky Mountain conifers. Res. Pap. INT-283. Ogden, UT: U.S. Department of Agriculture, Forest Service, Intermountain Forest and Range Experiment Station. 14 p.

Mohren, G.M.J.; Bartelink, H.H. 1989. Modeling the effects of needle mortality rate and needle area distribution on dry matter production of Douglas fir. Netherlands Journal of Agricultural Science. 38:53-66.

Mohren, G.M.J.; Van Gerwen, C.P.; Spitters, C.J.T. 1984. Simulation of primary production in even-aged stands of Douglas fir. For. Ecol. Manage. 9:27-49.

Myers, Clifford A.; Alexander, Robert A. 1972. Bark thickness and past diameters of Engelmann spruce in Colorado and Wyoming. Res. Note RM-217. Fort Collins, CO: U.S. Department of Agriculture, Forest Service, Rocky Mountain Forest and Range Experiment Station. 2 p.

Nadelhoffer, Knute J.; Aber, John D.; Melillo, Jerry M. 1985. Fine roots, net primary production, and soil nitrogen availability: a new hypothesis. Ecology. 66:1377-1390.

Nadelhoffer, Knute J.; Raich, James W. 1992. Fine root production estimates and belowground carbon allocation in forest ecosystems. Ecology. 73(4):1139-1147.
Nambiar, E.K.S. 1987. Do nutrients retranslocate from fine roots? Can. J. For. Res. 17:913-918.
Nambiar, E.K.S.; Fife, D.N. 1991. Nutrient retranslocation in temperate conifers. Tree Physiology. 9:185-207.
Neilson, Ronald P. 1992. A model for predicting continental-scale vegetation distribution and water balance. Corvallis, OR: U.S. EPA, Environmental Research Laboratory. 96 p.
Norman, J.J.; Jarvis, P.G. 1974. Photosynthesis in Sitka spruce (*Picea sitchensis* (bong.) carr.). J. of Applied Ecology. 11:375-398.
Norum, Rodney A. 1974. Fire intensity-fuel reduction relationships associated with understory burning in larch/Douglas-fir stands. In: Proceedings of a symposium, Tall Timbers Fire Ecology Conference Number 14 and Intermountain Fire Council and Land Management; 1974 October 8-10, Missoula, MT. Tallahassee, FL: Tall Timbers Research Station: 559-572.
Pastor, J.; Post, W.M. 1985. Development of a linked forest productivity-soil process model. Environmental Sciences Division Publication No. 2455. Oak Ridge, TN: Martin Marietta Energy Systems, Inc. for the U.S. Department of Energy, Environmental Sciences Division. 162 p.
Pastor, John; Post, W.M. 1986. Influence of climate, soil moisture, and succession on forest carbon and nitrogen cycles. Biogeochemistry. 2:3-27.
Pearson, J.A.; Fahey, T.J.; Knight, D.H. 1984. Biomass and leaf area in contrasting Lodgepole Pine forests. Can. J. For. Res. 17:259-265.
Pehl, Charles E.; Red, Jane T.; Shelnutt, Henry E. 1986. Controlled burning and land treatment influences on chemical properties of a forest soil. For. Ecol. Manage. 17: 119-128.
Persson, Hans 1979. Fine-root production, mortality and decomposition in forest ecosystems. Vegetation. 41(2):101-109.
Peterson, D.L. 1985. Crown scorch volume and scorch height: estimates of post-fire tree condition. Canadian Journal of Forest Research. 15:596-598.
Pfister, R.D.; Shearer, R.C. 1977. Potential vegetation as an indicator of reforestation opportunity. In: National Silviculture workshop, 1977 September 26-30, Flagstaff, AZ: 1-21.
Pfister, Robert D.; Kovalchik, Bernard L.; Arno, Stephen F.; Presby, Richard C. 1977. Forest habitat types of Montana. Gen. Tech. Rep. INT-34. Ogden, UT: U.S. Department of Agriculture, Forest Service, Intermountain Forest and Range Experiment Station. 174 p.
Piene, H.; Van Cleve, K. 1978. Weight loss of litter in cellulose bags in a thinned white spruce forest in interior Alaska. Canadian Journal of Forest Research. 8:42-46.
Pinty, Jean-Pierre; Mascart, Patrick; Bechtold, Peter; Rosset, Robert. 1992. An application of the vegetation-atmosphere coupling concept to the HAPEX-MOBILHY experiment. Agricultural and Forest Meteorology. 61:253-279.
Prescott, C.E.; Taylor, B.R.; Parons, W.F.J. 1993. Nutrient releases from decomposing litter in Rocky Mountain coniferous forests: influence of nutrient availability. Can. J. For. Res. 23:1576-1586.
Press, William H.; Teukolsky, Saul A.; Vetterling, William T.; Flannery, Brian P. 1992. Numerical recipes in C—The art of scientific computing. Second Edition. Cambridge University Press. 994 p.
Pukkala, Timo. 1987. Simulation model for natural regeneration of *Pinus sylvestris*, *Picea abies*, *Betula pendula* and *Betula pubescens*. Silva Fennica. 21(1):37-53.
Raison, R.J.; Myers, B.J.; Benson, M.L. 1992. Dynamics of Pinus radiata foliage in relation to water and nitrogen stress: I. Needle production and properties. Forest Ecology and Management. 52:139-158.
Reed, K.L. 1980. An ecological approach to modeling growth of forest trees. Forest Science. 26:33-50.
Reed, K.L.; Clark, S.G. 1979. SUCcession SIMulator: a coniferous forest simulator. Model documentation. Bull. No. 11. Seattle: University of Washington, Coniferous Biome Ecosystem Analysis. 96 p.
Reed, William J. 1994. Estimating the historic probability of stand-replacement fire using age-class distribution of undisturbed forest. Forest Science. 40(1):104-119.
Reich, P.B.; Walters, M.B.; Ellsworth, D.S. 1992. Leaf life-span in relation to leaf, plant, and stand characteristics among diverse ecosystems. Ecological Monographs, 62(3): 365-392.

Reinhardt, Elizabeth D.; Brown, James K.; Fischer, William C.; Graham, Russell T. 1991. Woody fuel consumption by prescribed fire in Northern Idaho mixed conifer slash. Research Paper INT 443. Ogden, UT: U.S. Department of Agriculture, Forest Service, Intermountain Forest and Range Experiment Station. 174 p.

Ribbens, Eric; Silander, John A.; Pacala, Stephen, W. 1994. Seedling recruitment in forests: Calibrating models to predict patterns of tree seedling dispersion. Ecology. 75(6):1794-1806.

Rothermel, Richard C. 1972. A mathematical model for predicting fire spread in wildland fuels. Res. Pap. INT-115. Ogden, UT: U.S. Department of Agriculture, Forest Service, Intermountain Forest and Range Experiment Station. 40 p.

Running, Steven W. 1984. Documentation and preliminary validation of H2OTRANS and DAYTRANS, two models for predicting transpiration and water stress in western coniferous forests. Research Paper RM-252. Fort Collins, CO: U.S. Department of Agriculture, Forest Service, Rocky Mountain Forest and Range Experiment Station. 45 p.

Running, S.W.; Coughlan, Joseph C. 1988. A general model of forest ecosystem processes for regional applications. I. Hydrologic balance, canopy gas exchange and primary production processes. Ecological Modeling. 42:125-154.

Running, S.W.; Gower, Stith T. 1991. FOREST-BGC, a general model of forest ecosystem processes for regional applications. II. Dynamic carbon allocation and nitrogen budgets. Tree Physiology. 9:147-160.

Running, S.W.; Nemani, R.R.; Peterson, D.L.; Band, L.E.; Potts, D.F.; Pierce, L.L.; Spanner, M.A. 1989. Mapping regional forest evapotranspiration and photosynthesis by coupling satellite data with ecosystem simulation. Ecology. 70(4):1090-1101.

Running, S.W.; Nemani, R.R. 1991. Regional hydrologic and carbon balance responses of forests resulting from potential climate change. Climatic Change. 19:349-368.

Running, Steven W.; E. Raymond Hunt. 1993. Generalization of a forest ecosystem process model for other biomes, BIOME-BGC, and an application for global-scale models. In: Scaling physiological processes: leaf to globe. Academic Press, Inc. Pages 141-157.

Ryan, Kevin C.; Peterson, David L.; Reinhardt, Elizabeth D. 1987. Modeling long-term fire-caused mortality of Douglas-fir. Forest Science. 34(1):190-199.

Ryan, Kevin C.; Reinhardt, Elizabeth D. 1988. Predicting postfire mortality of seven western conifers. Canadian Journal of Forest Research. 18:1291-1297.

Ryan, Michael G. 1991. Effects of climate change on plant respiration. Ecological Applications 1(2):157-167.

Ryan, Michael G.; Covington, W. Wallace 1986. Effect of a prescribed burn in ponderosa pine on inorganic nitrogen concentrations of mineral soil. Research Note RM-464. Fort Collins, CO: U.S. Department of Agriculture, Forest Service, Rocky Mountain Forest and Range Experiment Station. 5 p.

Ryan, Michael G.; Waring, Richard H. 1992. Maintenance respiration and stand development in a subalpine lodgepole pine forest. Ecology. 73(6):2100-2108.

Sampson, A. W. 1944. Plant succession on burned chaparral lands in Northern California. Bull. 685. Berkeley, CA: University of California, Agricultural Experiment Station. 144 p.

Sandberg, David V. 1980. Duff reduction by prescribed underburning in Douglas-fir. Res. Pap. PNW-272. Portland, OR: U.S. Department of Agriculture, Forest Service, Pacific Northwest Forest and Range Experiment Station. 18 p.

Sandford, A.P.; Jarvis, P.G. 1986. Stomatal responses to humidity in selected conifers. Tree Physiology. 2:89-103.

Santantonio, D.; Hermann, R.K. 1985. Standing crop, production, and turnover of fine roots on dry, moderate, and wet sites of mature Douglas-fir in western Oregon. Ann. Sci. For. 42(2):113-142.

Schmidt, Wyman C.; Shearer, Raymond C.; Rowe, Arthur L. 1976. The ecology and silviculture on western larch forests. Res. Pap. INT-167. Ogden, UT: U.S. Department of Agriculture, Forest Service, Intermountain Forest and Range Experiment Station. 96 p.

Schoch, Peter; Binkley, Dan. 1986. Prescribed burning increased nitrogen availability in a mature loblolly pine stand. For. Ecol. Manage. 14:13-22.

Seidel, K.W. 1975. Response of western larch to changes in stand density and structure. Res. Note PNW-258. Portland, OR: U.S. Department of Agriculture, Forest Service, Pacific Northwest Forest and Range Experiment Station. 4 p.

Sharpe, Peter J.H.; Walker, Joe; Penridge, Les. K.; Wu, Hsin-I; Rykiel, Edward J., Jr. 1986. Spatial considerations in physiological models of tree growth. Tree Physiology. 2:403-421.

Shearer, Raymond C., compiler. 1985. Cone production on Douglas-fir and westernlarch in Montana. In: Conifer Tree Seed in Inland Mountain West, Symposium, 1985 August 5-6; Missoula, MT: University of Montana. Ogden, UT: U.S. Department of Agriculture, Forest Service, Intermountain Research Station: 63-68.

Shearer, Raymond C. 1974. Early establishment of conifers following prescribed broadcast burning in western larch/Douglas-fir forests. In: Proceedings of a symposium, Tall Timbers Fire Ecology Conference Number 14 and Intermountain Fire Council and Land Management; 1974 October 8-10, Missoula, MT. Tallahassee, FL: Tall Timbers Research Station: 481-500.

Shearer, Raymond C. 1975. Seedbed characteristics in western larch forests after prescribed burning. Res. Pap. INT-167. Ogden, UT: U.S. Department of Agriculture, Forest Service, Intermountain Forest and Range Experiment Station. 26 p.

Shearer, Raymond C.; Schmidt, Wyman C. 1970. Natural regeneration in ponderosa pine forests in western Montana. Res. Pap. INT-86. Ogden, UT: U.S. Department of Agriculture, Forest Service, Intermountain Forest and Range Experiment Station. 20 p.

Sheriff, D.W.; Nambiar, E.K.S.; Fife, D.N. 1986. Relationships between nutrient status, carbon assimilation and water use efficiency in *Pinus radiata* (D.Don) needles. Tree Physiology. 2:73-88.

Shugart, H.H.; Nobel, I.R. 1981. A computer model of succession and fire response of the high-altitude Eucalyptus forest of the Brindabella Range, Australian Capital Territory. Australian Journal of Ecology. 6:149-164.

Shugart H.H.; Seagle, S.W. 1985. Modeling forest landscapes and the role of disturbance in ecosystems and communities. In: The Ecology of Natural Disturbance and Patch Dynamics, San Diego, CA: Academic Press: 353-368.

Shugart, H.H.; West, D.C. 1980. Forest succession models. Bioscience. 30(5):308-313.

Sievänen, Risto. 1993. A process-based model for the dimensional growth of even-aged stands. Scand. J. For. Res. 8:28-48.

Sievänen, R.; Burk, T.E. 1993. Adjusting a process-based growth model for varying site conditions through parameter estimation. Can. J. For. Res. 23:1837-1851.

Sievänen, R.; Burk, T.E.; Ek, A.R. 1988. Construction of a stand growth model utilizing photosynthesis and respiration relationships in individual trees. Can. J. For. Res. 18:1029-1035.

Simpson, William T. 1993. Specific gravity, moisture content, and density relationship for wood. Gen. Tech. Rep. FPL-GTR-76. Madison, WI: U.S. Department of Agriculture, Forest Service, Forest Products Laboratory. 13 p.

Smith, J. H. G. 1972. Persistence, size, and weight of needles on Douglas-fir and western hemlock branches. Canadian Journal of Forest Research. 2:173-178.

Soil Conservation Service. 1981. Average annual precipitation, Montana, based on 1941-1970 base period. USDA Soil Conservation Service, Portland, OR. 16 p.

Sollins, P.; Brown, A.T.; Swartzman, G.L. 1979. CONIFER: a model of carbon and water flow throught a coniferous forest. Revised documentation, US IBP, Univ. of Washington, Seattle, Conif. For. Biome Null. 152 pp.

Sprugel, Douglas G. 1990. Components of woody-tissue respiration in young *Abies amabilis* (Dougl.) Forbes trees. Trees. 4:88-98.

Standish, J.T.; Manning, G.H.; Demaerschalk, J.P. 1985. Development of biomass equations for British Columbia tree species. Information Report BC-X-264. Victoria, B.C.: Canadian Forestry Service, Pacific Forest Research Centre. 47 p.

Stanek, W.; State, D. 1978. Equations predicting primary productivity (biomass) of trees, shrubs and lesser vegetation based on current literature. Information Report BC-X-183. Canadian Forestry Service. 14 p.

Steele, R.W. 1960. The role of forest fire in the Bob Marshall Wilderness Area. Montana Forest and Range Experiment Station Report. On file at Intermountain Fire Sciences Laboratory. Missoula, Montana.

Swartzman, Gordon L. 1979. Simulation modeling of material and energy flow through an ecosystem: methods and documentation. Ecological Modeling. 7:55-81.

Tomback, D.F. 1982. Dispersal of whitebark pine seeds by Clark's nutcracker: a mutualism hypothesis. J. of Animal Ecol. 51:451-467.

Tomback, D.F.; Hoffmann, L.A.; Sund, S.K. 1990. Coevolution of whitebark pine and nutcrackers: Implications of forest regeneration. In: Proceedings of whitebark pine ecosystems: ecology and management of a high mountain resource. March 29-31, 1989, Bozeman, Montana. USDA Forest Service Gen. Tech. Report INT-270:118-130.

Trost, N. 1990. An approximate formula for the daily photoproduction of forest tree canopies. Ecological Modeling. 49:297-309.
Turner, J.; Long, J.N. 1975. Accumulation of organic matter in a series of Douglas-fir stands. Canadian Journal of Forest Research. 5:681-690.
Urban, Dean L. 1990. A versatile model to simulate forest pattern. Charlottesville, Virginia: Environmental Sciences Department, The University of Virginia. Dissertation. 108 p.
Urban, D.L.; Bonan, G.B.; Smith, T.M.; Shugart, H.H. 1991. Spatial applications of GAP models. For. Ecol. Manage. 42:95-110.
Urban, Dean L.; Shugart, Herman H. 1992. Individual-based models of forest succession. In: Glenn-Lewin, David C.; Peet, Robert K.; Veblen, Thomas T., eds. Plant succession theory and prediction, London: Chapman and Hall:249-292.
USA CERL. 1990. GRASS 4.0 Reference Manual. United States Army Corps of Engineers, Construction Engineering Research Laboratory, Champaign, Illinois. 208 p.
Van Gerwen, C.P.; Spitters, C.J.T.; Mohren, G.M.J. 1987. Simulation of competition for light in even-aged stands of Douglas fir. For. Ecol. Manage. 18:135-152.
Van Hulst, Robert. 1978. On the dynamics of vegetation: patterns of environmental and vegetational change. Vegetation. 38:2:65-75.
Van Wagner, C.E. 1973. Height of crown scorch in forest fires. Canadian Journal of Forest Research. 3:373-378.
Van Wagner, C.E. 1978. Age-class distribution and the forest fire cycle. Can. J. For. Res. 8:220-227.
Versfeld, D.B.; Donald, D.G.M. 1991. Litterfall and nutrient release in *Pinus radiata* in the South-western cape. South African Forestry Journal. 156:61-69.
Wallace, L.L. 1991. Comparative physiology of successional forest trees. In: W.T. Swank and D.A. Crossley, editors, Forest Hydrology and Ecology at Coweeta. Springer-Verlag, New York:181-189.
Wang, Y.P.; Jarvis, P.G. 1990. Description and validation of an array model-MAESTRO. Agric. For. Meteorol. 51:257-280.
Waring, R.H. 1989. Resource allocation in trees and ecosystems. In: Biologic markers of air-pollution stress and damage in forests. Washington, DC: National Academy Press. 363 p.
Waring, Richard H.; Schlesinger, William H. 1985. Forest Ecosystems Concepts and Management. San Diego, CA: Academic Press, Inc. 340 p.
Webb, Warren L. 1977. Seasonal allocation of photoassimilated carbon in Douglas Fir seedlings. Plant Physiol. 60:320-322.
Webb, Warren L. 1975. The distribution of photoassimilated carbon and the growth of Douglas-fir seedlings. Can J. For. Res. 5:68-72.
Weinstein, D.A.; Shugart, H.H.; West, D.C. 1982. The long-term nutrient retention properties of forest ecosystems: a simulation investigation. ORNL/TM-8472. Oak Ridge, TN: Oak Ridge National Laboratory, Environmental Sciences Divison. 145 p.
Weishampel, John F.; Urban, Dean L.; Shugart, Herman H.; Smith, Jackson B. Jr. 1992. Semivariograms from a forest transect gap model compared with remotely sensed data. Journal of Vegetation Science 3:521-526.
Whitehead, D.; Kelliher, F.M. 1991. Modeling the water balance of a small *Pinus radiata* catchment. Tree Physiology. 9:17-33.
Yue, De; Margolis, Hank A. 1993. Photosynthesis and dark respiration of black spruce cuttings during rooting in response to light and temperature. Can. J. For. Res. 23: 1150-1155.

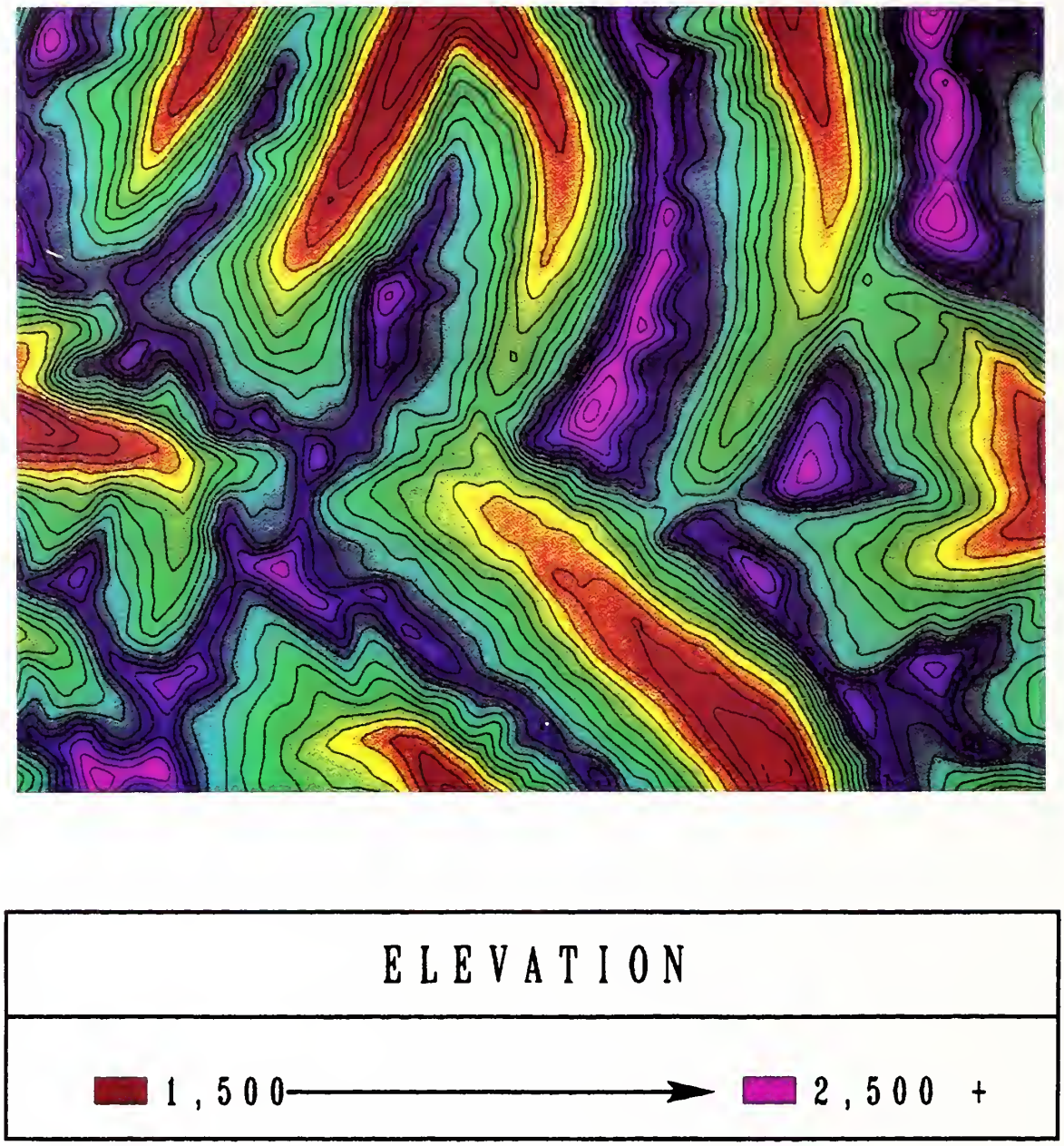

Color Plate 1—Generalized topography of the Monture Simulation Area created from a Digital Elevation Model.

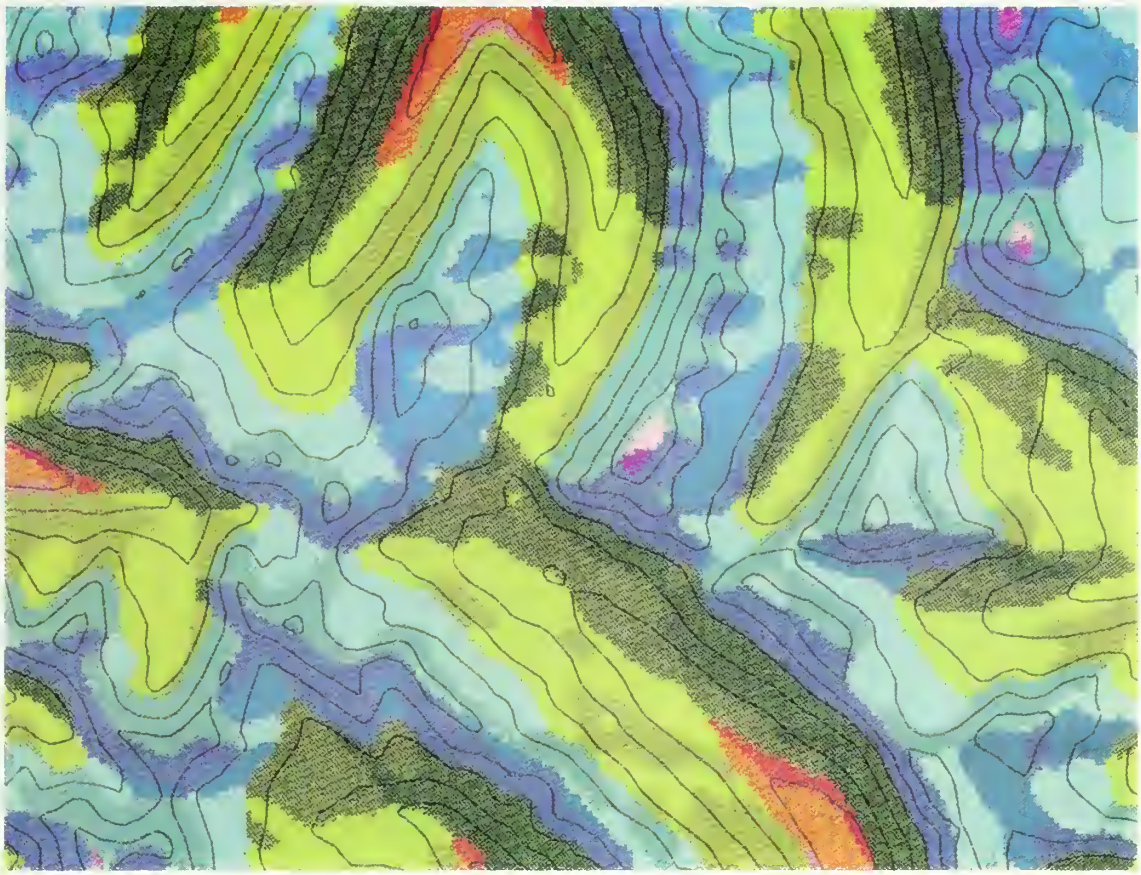

SITE CLASSES

Elevation	Aspect	Slope	Elevation	Aspect	Slope
1,528 to 1,830	N	Flat	2,135 to 2,440	N	Flat
1,528 to 1,830	N	Steep	2,135 to 2,440	N	Steep
1,528 to 1,830	S	Flat	2,135 to 2,440	S	Flat
1,528 to 1,830	S	Steep	2,135 to 2,440	S	Steep
1,830 to 2,135	N	Flat	2,440 +	N	Flat
1,830 to 2,135	N	Steep	2,440 +	N	Steep
1,830 to 2,135	S	Flat	2,440 +	S	Flat
1,830 to 2,135	S	Steep	2,440 +	S	Steep

Color Plate 2—Delineation of site classes on the Simulation Area using topographic criteria.

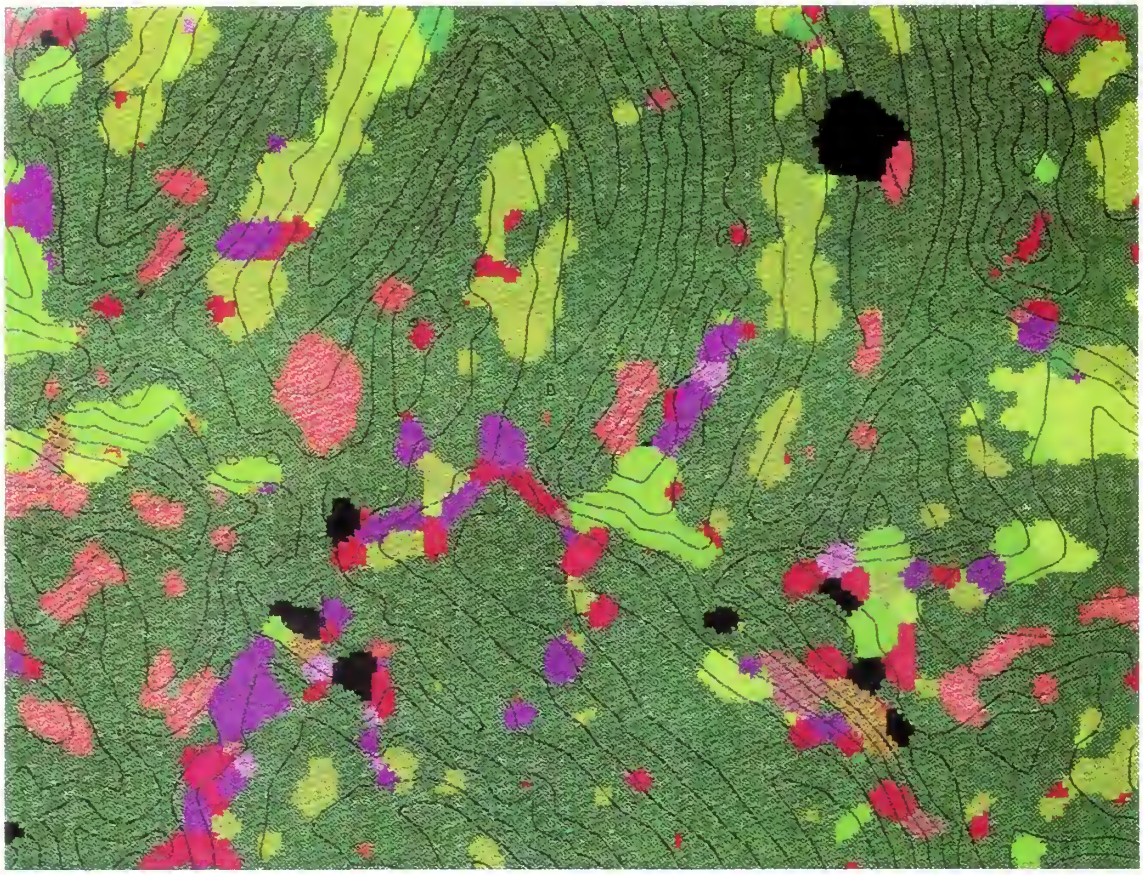

COVER TYPES	
PIAL ABLA PIEN	PICO ABLA
ABLA PIEN PIAL	ABLA PIEN
PIAL PICO ABLA	PICO
ABLA PIAL PICO	SHRUBS
PIAL PICO	HERBS
PIAL LALY ABLA	ROCK, TALUS
ABLA PIAL LALY	BARE SOIL

Color Plate 3—Spatial delineation of cover types in the Simulation Study Area. Species codes: PIPO-*Pinus ponderosa*, ABGR-*Abies grandis*, PSME-*Pseudotsuga menziesii*, PICO-*Pinus contorta*, LAOC-*Larix occidentalis*, ABLA-*Abies lasiocarpa*, PIEN-*Picea engelmannii*, PIAL-*Pinus albicaulis*, LALY-*Larix lyallii*, PIMO-*Pinus monticola*, THPL-*Thuja plicata*, TSHE-*Tsuga heterophylla*.

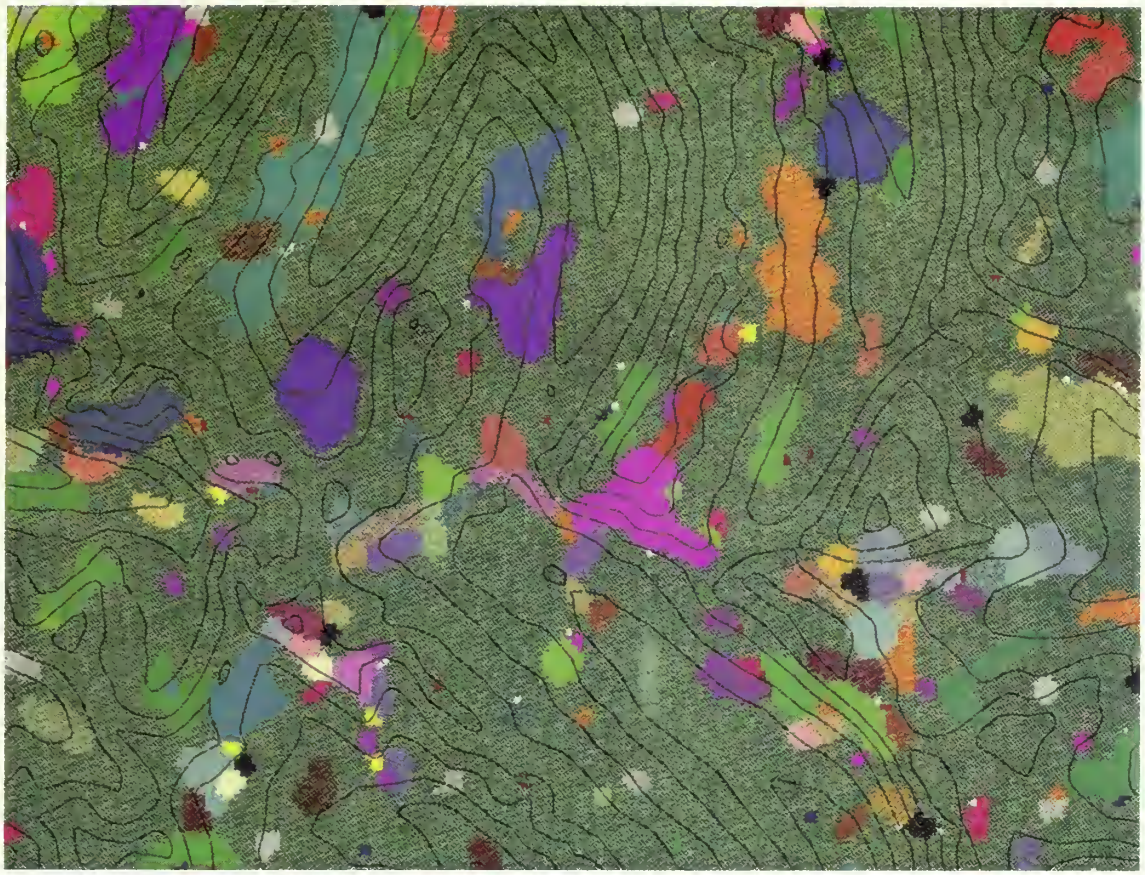

STANDS

Color Plate 4—Final map of stands within the Simulation Area. Stand delineations are based on the cover type classification.

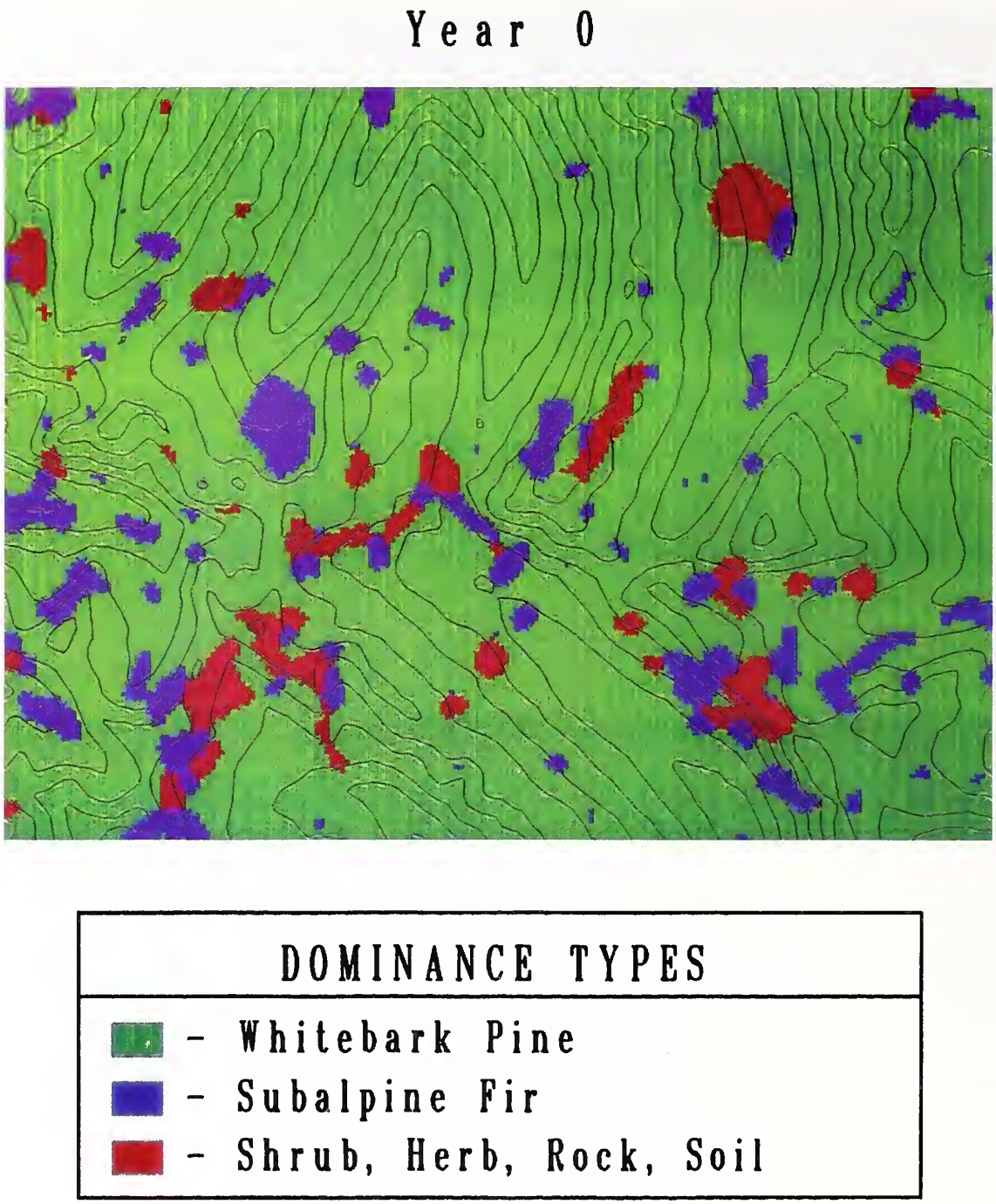

Color Plate 5—Reclassification of the cover type layer to three dominance types for comparison to landscapes created by FIREBGC simulations.

Year 50

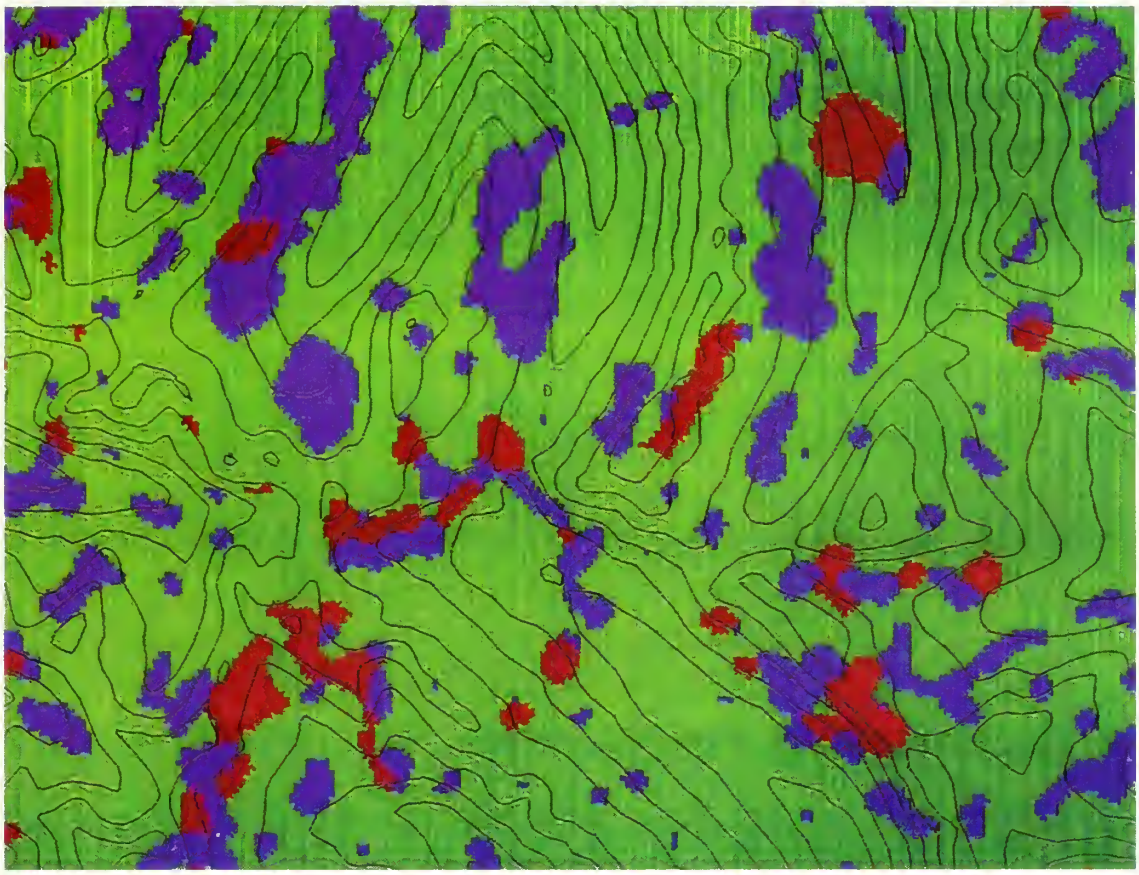

DOMINANCE TYPES

- Whitebark Pine
- Subalpine Fir
- Shrub, Herb, Rock, Soil

Color Plate 6—The predicted MSSA simulation landscape at simulation year 50 for the NOFIRE scenario using FIREBGC.

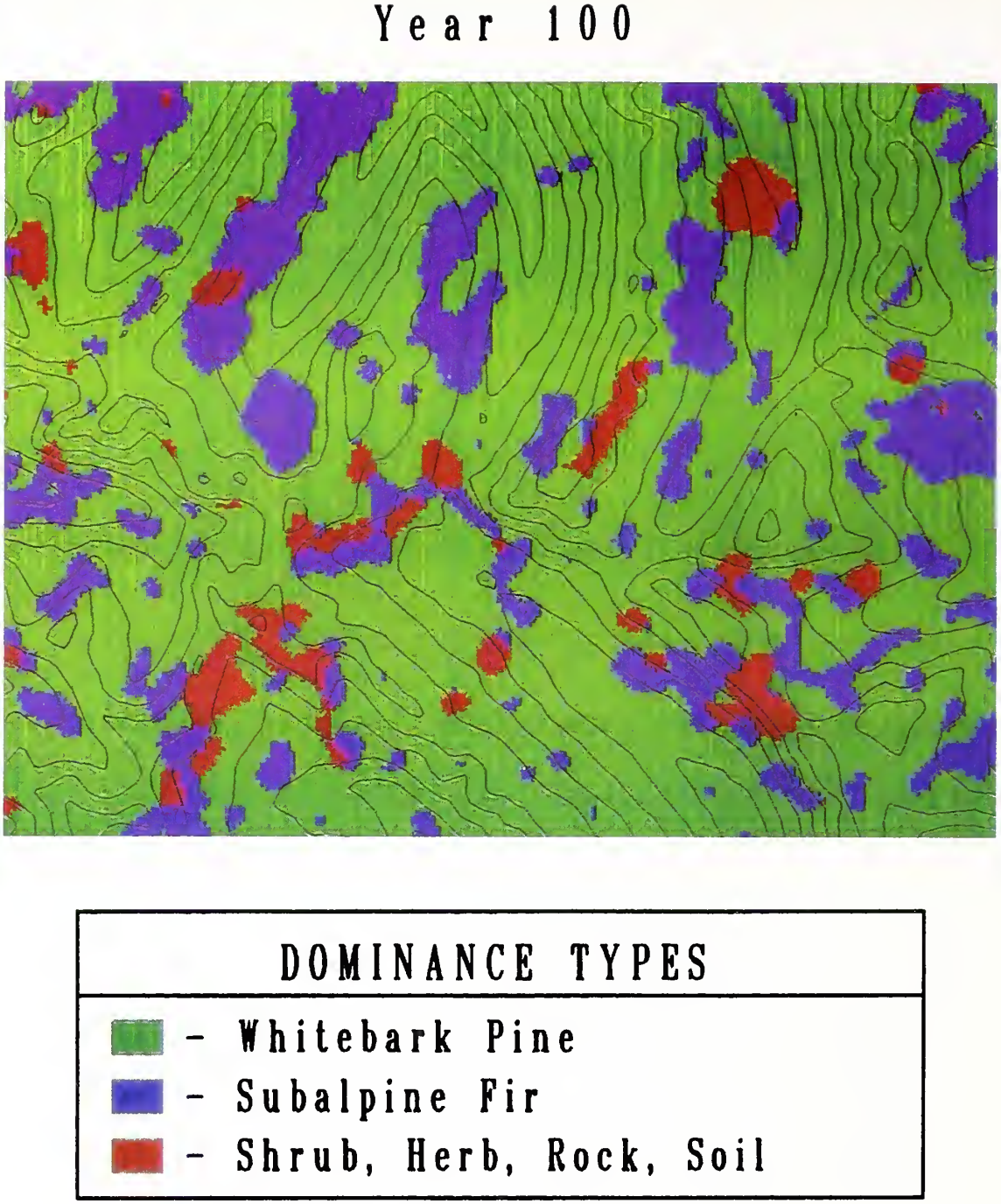

Color Plate 7—The predicted MSSA simulation landscape at simulation year 100 for the NOFIRE scenario using FIREBGC.

Year 150

DOMINANCE TYPES

- Whitebark Pine
- Subalpine Fir
- Shrub, Herb, Rock, Soil

Color Plate 8—The predicted MSSA simulation landscape at simulation year 150 for the NOFIRE scenario using FIREBGC.

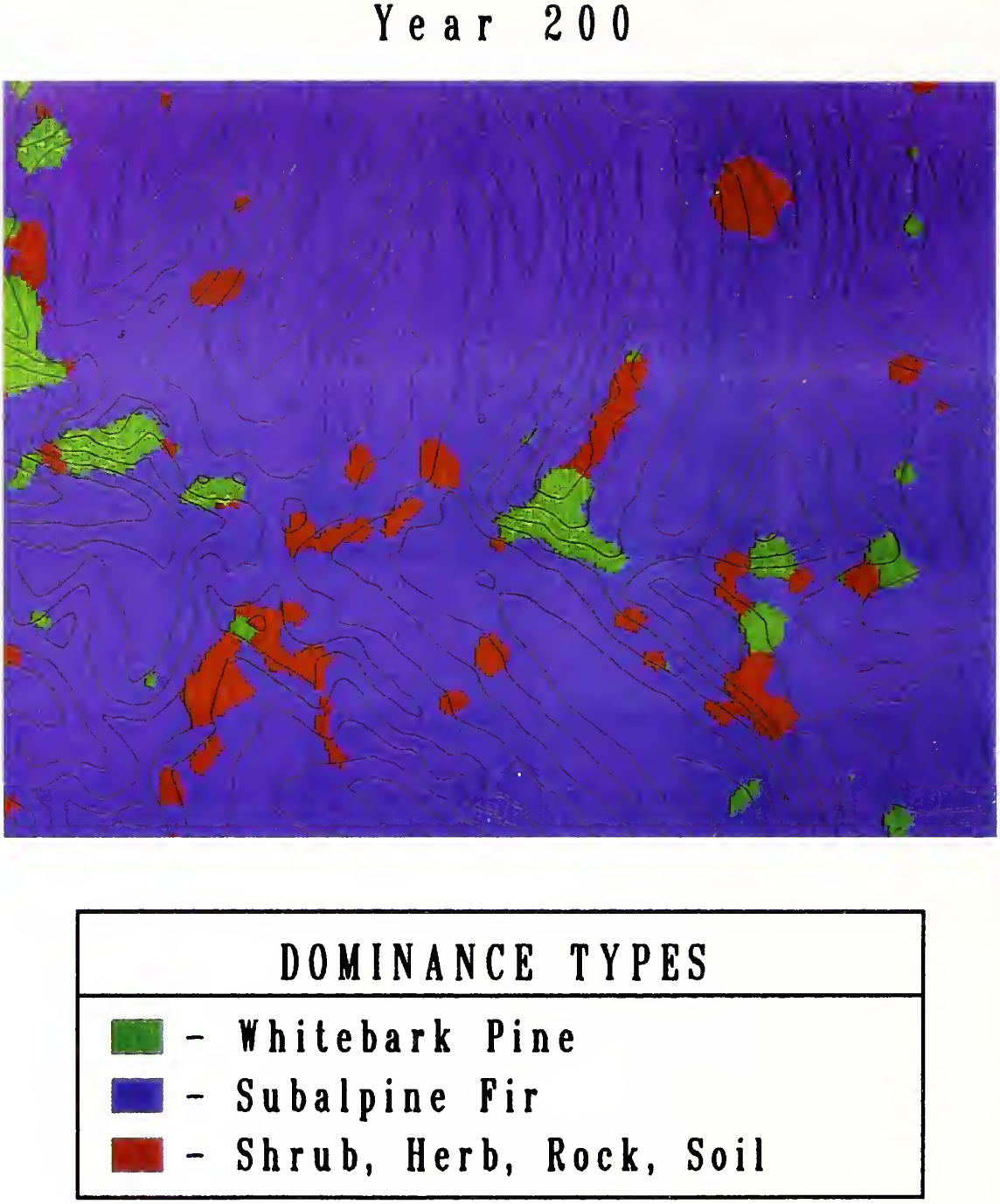

Color Plate 9—The predicted MSSA simulation landscape at simulation year 200 for the NOFIRE scenario using FIREBGC.

Appendix A: Description of Variables Used in FIRE-BGC

General Equation Variables

Variable	Description	Units
γ	Psychometric constant	mbar $°C^{-1}$
λ	Latent heat of water vaporization	J kg^{-1}
Δ	Slope of the saturation vapor pressure curve	mbar $°C^{-1}$
ϵ	Tree random mortality coefficient	year
AGE	Tree age	year
AL	Proportion of available light	proportion
BA	Basal area of stand	m^2 ha^{-1}
BINFEST	Simulation year that identifies start of beetle infestation	years
BULK	Bulk density of the litter and duff layers	kg m^{-3}
C_i	Weibull probability density function shape factor for site i	dimensionless
CF_i	Consumption fraction of i fuel component	kg C burned kg C^{-1}
CK	Percent of tree crown killed by fire (scorched)	%
CL	Crown length	m
CLA	Cumulative leaf area for a canopy layer	m^2
CM_i	Biomass of crown material i (twigs, foliage, and so forth)	kg
$CONSUME_i$	Consumption of shrub and herb biomass (i = 1 live, i = 2 dead)	kg biomass
c_p	Specific heat of air	J kg^{-1} $°C^{-1}$
CS	Length of crown that is scorched by fire	m
CW	Crown width	m
$CROOT_m$	Coarse root biomass	kg
$CROWN_m$	Crown biomass	m
DBH	Tree diameter at breast height	cm
DBH_{min}	Minimum diameter growth in a year	cm
dCO_2	Carbon dioxide diffusion gradient	kg m^{-2}
$DEPTH_{d,l}$	Depth of the litter and duff components combined	cm
DIST	Distance from stand to seed source	m
DMOIST	Duff moisture content	% dry weight
$FFREQ_i$	Fire-free interval for site i	years
FI	Fire intensity	kW m^{-1}
FL	Flame length	m
$FROOT_m$	Fine root biomass	kg
$FSIZE_i$	Average fire size for site i	m^2
$FREBURN_i$	Average time before fire can reburn site i	years
GS_{mid}	Midpoint of the growing season for a species	yearday
HBC	Height to bottom of tree crown	m
$HINC_{max}$	Maximum possible annual height increment	m
HSIZE	Thickness of the vertical canopy layer	m
HT	Tree height	m
HT_{max}	Maximum computed tree height	m
ID	Identification number–pertains to site, stand and fuels	dimensionless
k	Extinction coefficient	dimensionless
L_n	Leaf nitrogen concentration	kg N kg C^{-1}
LA	Stand all-sided leaf area	m^2
LAG	Number lag years to delay tree regeneration after stand-replacement fire	years
LAI	Stand projected leaf area index	m^2 m^{-2}
LAI_{max}	Maximum possible stand leaf area index	m^2 m^{-2}
LAT	Latitude of site	decimal degrees
LWP	Leaf water potential	–Mpa

Variable	Description	Units
LWP_{max}	Maximum leaf water potential experienced in a year	–Mpa
$MASS_i$	The current biomass in undergrowth compartment i	kg biomass m^{-2}
MXHGT	Maximum number of vertical canopy layers	number
MXSPP	Maximum number of species in the simulation	number
NSPAN	Number of years in simulation	years
n_{pixel}	Number of pixels on the simulation landscape	number
p_a	Air density	kg m^{-2}
P_d	Probability of a species' seed being dispersed to a stand	probability
P_{beetle}	Probability of tree death from mountain pine beetles	probability
P_f	Probability of a fire occurring in a stand	probability
P_{fp}	Probability of a fire starting in a pixel	probability
P_{fire}	Probability of tree death from fire	probability
P_{infec}	Probability of infection from white pine blister rust	probability
P_{path}	Probability of tree death from pathogens	probability
P_{random}	Probability of tree death from random events	probability
P_{rust}	Probability of tree death from white pine blister rust	probability
P_{stress}	Probability of tree death from environmental stress	probability
PAREA	Area of the simulation plot	m^2
PIXEL	Width of the square pixel comprising the landscape	m
PLA_i	Projected leaf area conversion factor for species i	m^2
PSN	Net annual photosynthesis for stand	kg C
PSN_{max}	Maximum possible carbon gain for a species in a stand	kg C
r_a	Aerodynamic canopy resistance	sec m^{-1}
r_{al}	Growth allocation scalar for available light	scalar
r_c	Canopy resistance to water vapor transfer	sec m^{-1}
r_{dens}	Regeneration scalar for stand crowding	scalar
r_{disp}	Regeneration scalar for seed dispersal	scalar
r_{ht}	Height reduction scalar for available light	scalar
r_{shade}	Regeneration scalar for degree of shading	scalar
r_{st}	Seed dispersal scalar for limited seed tree density	scalar
r_{sur}	Regeneration scalar for seedling survival in duff	scalar
$rPSN_i$	Species carbon allocation factor for photosynthetic capacity	scalar
RNUM	Random number between 0.0 and 1.0 inclusive	scalar
$ROOT_m$	Root biomass (coarse and fine roots)	kg
SEED	Number seedlings established on simulation plot for a species	number
$SEED_{max}$	Maximum number seedlings annually established on simulation plot	number
SH	Scorch height	m
SHADE	Species shade tolerance category {1-5}	ordinal
$SPPPSN_i$	Species carbon allocation factor for species	kg C
STEMC	Stem carbon without branchwood carbon	kg C
$STEM_m$	Stem biomass	kg
T_{kill}	Lethal temperature for tree foliage	°C
$TREE_{seed}$	Number of seed producing trees on simulation plot	number
V	Power parameter for temperature effect on mesophyll conductance	dimensionless
WIND	Wind speed	km hr^{-1}
X_j	Time since last fire disturbance for stand j	years
XRUST	Proportion of a species resistant to white pine blister rust	proportion
Y_{stress}	Years of stress experienced by a tree	year
YBEETLE	Initial year of a mountain pine beetle infestation	year
YRUST	Initial year of a white pine blister rust epidemic	year
YD	Yearday or Julian date	yearday

Simulation Plot Intermediate Variables

Variable	Description	Units
GP_0	Rainfall reaching the forest floor	m^3 H_2O day^{-1}
GP_1	Snowfall	m^3 H_2O day^{-1}
GP_2	Snowmelt	m^3 H_2O day^{-1}
GP_3	Potential evaporation of precipitation	m^3 H_2O day^{-1}
GP_4	Radiation-limited evaporation	m^3 H_2O day^{-1}
GP_5	Energy-limited potential evaporation	m^3 H_2O day^{-1}
GP_6	Soil water fraction	scalar 0–1
GP_7	Soil water lost to runoff and ground water	m^3 H_2O day^{-1}
GP_8	EMPTY	
GP_9	Predawn leaf water potential (that is, soil water potential)	–Mpa
GP_{10}	Maximum canopy conductance with leaf water potential reduction	m sec^{-1}
GP_{11}	Canopy conductance with night temperature reduction	m sec^{-1}
GP_{12}	Canopy conductance humidity deficit reduction	scalar 0–1
GP_{13}	Canopy conductance radiation reduction	scalar 0–1
GP_{14}	Canopy leaf conductance	m sec^{-1}
GP_{15}	Penman-Monteith transpiration estimate	m^3 H_2O LAI^{-1} sec^{-1}
GP_{16}	Canopy transpiration	m^3 H_2O day^{-1}
GP_{17}	Ground water outflow	m^3 H_2O day^{-1}
GP_{18}	Canopy nitrogen concentration effect on mesophyll conductance	scalar 0–1
GP_{19}	Light effect on mesophyll conductance	scalar 0–1
GP_{20}	Temperature effect on mesophyll conductance	scalar 0–1
GP_{21}	Final mesophyll conductance	m sec^{-1}
GP_{22}	Gross photosynthesis	kg C LAI^{-1} day^{-1}
GP_{23}	Daily canopy gross photosynthesis	kg CO_2 day^{-1}
GP_{24}	Night respiration of leaves	kg C day^{-1}
GP_{25}	Net 24-hour carbon gain	kg C day^{-1}
GP_{26}	EMPTY	
GP_{27}	EMPTY	
GP_{28}	EMPTY	
GP_{29}	Stem respiration	kg C day^{-1}
GP_{30}	Root respiration	kg C day^{-1}
GP_{31}	Twigwood turnover (1-hour fuelwood)	kg C
GP_{32}	Branchwood turnover (10-hour fuelwood)	kg C
GP_{33}	Large branchwood turnover (100-hour fuelwood)	kg C
GP_{34}	EMPTY	
GP_{35}	Leaffall contribution to litter nitrogen	kg N
GP_{36}	Leaffall contribution to duff nitrogen	kg N
GP_{37}	Root turnover contribution to fine roots nitrogen	kg N
GP_{38}	Root turnover contribution to coarse roots nitrogen	kg N
GP_{39}	Maximum Leaf Area Index (LAI) possible for stand	m^2 m^{-2}
GP_{40}	Canopy nitrogen as a percent of maximum canopy N	proportion
GP_{41}	Canopy leaf N concentration	kg N kg C^{-1}
GP_{42}	Canopy leaf N retranslocation fraction	scalar 0–1
GP_{43}	Leaf retention time	years
GP_{44}	Leaffall contribution to litter carbon compartment	kg C
GP_{45}	Leaffall contribution to duff carbon compartment	kg C
GP_{46}	Fine root turnover contribution to soil carbon compartment	kg C
GP_{47}	Coarse root turnover contribution to soil carbon compartment	kg C
GP_{48}	EMPTY	

Variable	Description	Units
GP_{49}	Annual average of daily soil water fraction	proportion
GP_{50}	Nitrogen availability index	scalar 0–1
GP_{51}	Leaf/root ratio (max = 0.5)	dimensionless
GP_{52}	C-limited leaf carbon allocation to leaves	kg C
GP_{53}	N-limited leaf carbon allocation to leaves	kg C
GP_{54}	H_2O-limited leaf carbon allocation to leaves	kg C
GP_{55}	Final carbon allocation to leaves, MIN(GP_{52-54})	kg C
GP_{56}	Leaf carbon allocation as fraction of net photosynthesis	proportion
GP_{57}	Root carbon allocation as fraction of net photosynthesis	proportion
GP_{58}	Stem carbon allocation as fraction of net photosynthesis	proportion
GP_{59}	Gross Leaf carbon growth	kg C
GP_{60}	Gross Stem carbon growth	kg C
GP_{61}	Gross Root carbon growth	kg C
GP_{62}	Leaf growth respiration	kg C
GP_{63}	Stem growth respiration	kg C
GP_{64}	Root growth respiration	kg C
GP_{65}	Total growth respiration	kg C
GP_{66}	Net leaf carbon allocation	kg C
GP_{67}	Net stem carbon allocation	kg C
GP_{68}	Net root carbon allocation	kg C
GP_{69}	Leaf nitrogen allocation	kg N
GP_{70}	Stem nitrogen allocation	kg N
GP_{71}	Root nitrogen allocation	kg N
GP_{72}	Leaf nitrogen retranslocated to available nitrogen pool	kg N
GP_{73}	Nitrogen loss from available nitrogen pool from growth allocation	kg N
GP_{74}	EMPTY	
GP_{75}	Fine root fraction of total root carbon	kg C kg C^{-1}
GP_{76}	Nitrogen proportion of 1-hour twigwood	kg N kg C^{-1}
GP_{77}	Nitrogen proportion of 10-hour branchwood	kg N kg C^{-1}
GP_{78}	Nitrogen proportion of 100-hour large branchwood	kg N kg C^{-1}
GP_{79}	Leaf/Root litter nitrogen decomposition factor	proportion
GP_{80}	Soil nitrogen decomposition factor	proportion
GP_{81}	EMPTY	
GP_{82}	Litter nitrogen decompositon factor	kg N kg C^{-1}
GP_{83}	Duff nitrogen decomposition factor	kg N kg C^{-1}
GP_{84}	Mineral soil decompositon factor	kg N kg C^{-1}
GP_{85}	Litter nitrogen mineralization	kg N $year^{-1}$
GP_{86}	Duff nitrogen mineralization	kg N $year^{-1}$
GP_{87}	Mineral soil mineralization	kg N $year^{-1}$
GP_{88}	Woody fuel nitrogen mineralization	kg N $year^{-1}$
GP_{89}	Average annual soil water fraction	proportion
GP_{90}	Maximum annual leaf water potential	–MPa
GP_{91}	Annual sum of temperature degree days	degree–days
GP_{92}	Average annual leaf water potential	–MPa
GP_{93}	Nitrogen mineralized from leaf/root litter	kg N
GP_{94}	Nitrogen mineralized from soil	kg N
GP_{95}	Annual sum of night respiration	kg $year^{-1}$
GP_{96}	Annual sum of stem maintenance respiration	kg $year^{-1}$
GP_{97}	Annual sum of root maintenance respiration	kg $year^{-1}$
GP_{98}	EMPTY	
GP_{99}	Annual sum of maintenance respiration	kg $year^{-1}$

Variable	Description	Units
GP_{100}	Leaf/root litter carbon decomposition factor	kg decomp kg C^{-1}
GP_{101}	Leaf/Root litter carbon decomposed	kg C $year^{-1}$
GP_{102}	Soil carbon decomposition factor	kg decomp kg C^{-1}
GP_{103}	Soil carbon decomposed	kg $year^{-1}$
GP_{104}	Annual sum of leaf/root litter carbon decompositon	kg $year^{-1}$
GP_{105}	Annual sum of soil carbon decomposition	kg $year^{-1}$
GP_{106}	EMPTY	
GP_{107}	EMPTY	
GP_{108}	EMPTY	
GP_{109}	Annual sum of litter + soil carbon decomposition	kg $year^{-1}$
GP_{110}	Litter carbon decay rate	kg decomp kg C^{-1}
GP_{111}	Litter carbon decomposed	kg C day^{-1}
GP_{112}	Litter carbon decomposition annual sum	kg C $year^{-1}$
GP_{113}	Duff carbon decay rate	kg decomp kg C^{-1}
GP_{114}	Duff carbon decomposed	kg C day^{-1}
GP_{115}	Duff carbon decomposition annual sum	kg C $year^{-1}$
GP_{116}	Mineral soil carbon decay rate	kg decomp kg C^{-1}
GP_{117}	Mineral soil carbon decomposed	kg C day^{-1}
GP_{118}	Mineral soil carbon decomposition annual sum	kg C $year^{-1}$
GP_{119}	Woody fuel decay rate	kg decomp kg C^{-1}
GP_{120}	Twigwood (1-hour) carbon decomposed	kg C day^{-1}
GP_{121}	Twigwood (1-hour) carbon decomposition annual sum	kg C $year^{-1}$
GP_{122}	Branchwood (10-hour) carbon decomposed	kg C day^{-1}
GP_{123}	Branchwood (10-hour) carbon decomposition ann sum	kg C $year^{-1}$
GP_{124}	Large branchwood (100-hour) carbon decomposed	kg C day^{-1}
GP_{125}	Large branchwood (100-hour) carbon annual sum	kg C $year^{-1}$
GP_{126}	Logwood (1,000-hour) carbon decomposed	kg C day^{-1}
GP_{127}	Logwood (1,000-hour) carbon decomposition ann sum	kg C $year^{-1}$
GP_{128}	EMPTY	
GP_{129}	EMPTY	
GP_{130}	Twigwood (1-hour) nitrogen annual sum	kg N $year^{-1}$
GP_{131}	Branchwood (10-hour) nitrogen annual sum	kg N $year^{-1}$
GP_{132}	Large branchwood (100-hour) nitrogen annual sum	kg N $year^{-1}$
GP_{133}	Logwood (1,000-hour) nitrogen annual sum	kg N $year^{-1}$
GP_{134}	EMPTY	
GP_{135}	EMPTY	
GP_{136}	EMPTY	
GP_{137}	EMPTY	
GP_{138}	EMPTY	
GP_{139}	Available nitrogen pool	kg N
GP_{140}	Litter carbon pool	kg C
GP_{141}	Duff carbon pool	kg C
GP_{142}	Soil carbon pool	kg C
GP_{143}	Twigwood and branchwood (1 + 10-hour) carbon pool	kg C
GP_{144}	Large branchwood and logwood (100 + 1,000-hour) carbon pool	kg C
GP_{145}	Litter nitrogen pool	kg N
GP_{146}	Duff nitrogen pool	kg N
GP_{147}	Soil nitrogen pool	kg N
GP_{148}	Twigwood and branchwood (1 + 10-hour) nitrogen pool	kg N
GP_{149}	Large branchwood and logwood (100 + 1,000-hour) nitrogen	kg N

Simulation Plot State Variables

Variable	Description	Units
XP_0	Snowpack	m^3 H_2O
XP_1	Soil water content	m^3 H_2O
XP_2	Water outflow or loss	m^3 H_2O
XP_3	Canopy transpiration	m^3 H_2O
XP_4	Evaporation	m^3 H_2O
XP_5	Photosynthesis	kg C
XP_6	Autotrophic respiration	kg C
XP_7	Leaf carbon	kg C
XP_8	Stem carbon	kg C
XP_9	Coarse root carbon	kg C
XP_{10}	Fine root carbon	kg C
XP_{11}	Decomposition respiration carbon	kg C
XP_{12}	Soil carbon	kg C
XP_{13}	Available nitrogen	kg N
XP_{14}	Leaf nitrogen	kg N
XP_{15}	Stem nitrogen	kg N
XP_{16}	Coarse root nitrogen	kg N
XP_{17}	Fine root nitrogen	kg N
XP_{18}	Soil nitrogen	kg N
XP_{19}	Nitrogen loss	kg N
XP_{20}	Leaf/litter carbon	kg C
XP_{21}	Leaf/litter nitrogen	kg N

Forest Floor State Variables

Variable	Description	Units
$AVAIL_n$	Available nitrogen pool	kg N
$DUFF_c$	Duff carbon	kg C
$LITTER_c$	Litter carbon	kg C
$SOIL_c$	Mineral soil carbon	kg C
${}_1WOOD_c$	Twigwood carbon (1-hour timelag fuel component)	kg C
${}_2WOOD_c$	Branchwood carbon (10-hour timelag fuel)	kg C
${}_3WOOD_c$	Large branchwood carbon (100-hour timelag fuel component)	kg C
${}_4WOOD_c$	Logwood carbon (1,000-hour timelag fuel component)	kg C
$DUFF_n$	Duff nitrogen	kg N
$LITTER_n$	Litter nitrogen	kg N
$SOIL_n$	Mineral soil nitrogen	kg N
${}_1WOOD_n$	Twigwood nitrogen (1-hour timelag fuel component)	kg N
${}_2WOOD_n$	Branchwood nitrogen (10-hour timelag fuel)	kg N
${}_3WOOD_n$	Large branchwood nitrogen (100-hour timelag fuel component)	kg N
${}_4WOOD_n$	Logwood nitrogen (1,000-hour timelag fuel component)	kg N

Fuel Component Variables

Variable	Description	Units
CF_i	Consumption fraction for fuel component i	kg burned kg C^{-1}
$BULK_j$	Bulk density of litter and duff	kg biomass m^{-3}
$HERB_{dead}$	Dead herbaceous fuel loading	kg biomass m^{-2}
$HERB_{live}$	Live herbaceous fuel loading	kg biomass m^{-2}
LHV_i	Heat content of fuel component i	kJ kg $biomass^{-1}$
$LOAD_i$	Loading of fuel component i	kg biomass m^{-2}
$MEXT_k$	Moisture of extinction for live and dead fuels	%
$MOIST_i$	Moisture content of fuel component i	proportion
$RHOP_i$	Ovendry particle density of fuel component i	kg biomass m^{-3}
$SHRUB_{dead}$	Dead shrubby loading	kg biomass m^{-2}
$SHRUB_{live}$	Live shrubby loading	kg biomass m^{-2}
SVR_i	Surface area-to-volume ratio for fuel component i	m^2 m^{-3}
WIND	Windspeed at time of fire	m sec^{-1}

Undergrowth Parameters and State Variables

Variable	Description	Units
$CFRAC_j$	Fraction of undergrowth compartment j biomass that is carbon	kg C kg $biomass^{-1}$
$FDEAD_j$	Fraction of compartment j biomass that is dead at fire	proportion
$FLEAF_j$	Fraction of compartment j biomass that is foliage	proportion
$FLIG_j$	Fraction of compartment j biomass that is lignin	proportion
$GROWTH_j$	Growth of undergrowth compartment j	kg biomass
$HERB_i$	Biomass contained in the shade intolerant herb compartment	kg
$HERB_{la}$	Leaf area for both herb compartments in undergrowth	m^2
$HERB_t$	Biomass contained in the shade tolerant herb compartment	kg
$MASS_j$	Current year's biomass of undergrowth compartment j	kg
$MASS_{max,j}$	Maximum biomass for undergrowth compartment	kg m^{-2}
$NFRAC_j$	Fraction of compartment j biomass that is nitrogen	kg biomass kg N^{-1}
n_j	Growth equation constant for undergrowth compartment j	$year^{-1}$
$SHRUB_i$	Biomass contained in the shade intolerant shrub compartment	kg
$SHRUB_{la}$	Leaf area for both shrub compartments in undergrowth	m^2
$SHRUB_t$	Biomass contained in the shade tolerant shrub compartment	kg
$TURNB_j$	Fraction biomass turnover in undergrowth compartment j	prop
$TURNW_j$	Fraction woody turnover in undergrowth compartment j	prop
$UHGT_j$	Height of undergrowth compartment j	m
$USLA_j$	Specific leaf area of undergrowth compartment j	m^2 kg^{-1}

Simulation Plot Parameters

Variable	Description	Units
BP_0	Specific leaf area	m^2 kg C^{-1}
BP_1	Canopy light extinction coefficient	dimensionless
BP_2	Soil water holding capacity	m^3 H_2O
BP_3	Canopy interception coefficient	m LAI^{-1} day^{-1}
BP_4	Optimum temperature for photosynthesis	°C
BP_5	Snowmelt coefficient	m $°C^{-1}$ day^{-1}
BP_6	Fraction leaf biomass that is carbon	kg C kg $biomass^{-1}$
BP_7	1—surface albedo	dimensionless
BP_8	Minimum springtime leaf water potential	–MPa

Variable	Description	Units
BP_9	Maximum radiation threshold for canopy conductance	kJ m^{-1} day^{-1}
BP_{10}	Maximum canopy conductance	m sec^{-1}
BP_{11}	Leaf water potential at stomatal closure	–MPa
BP_{12}	Slope of the absolute humidity reduction	m sec^{-1} μg^{-1} m^{-3}
BP_{13}	Photosynthetic light compensation point	kJ m^{-2} day^{-1}
BP_{14}	Radiation at 0.5 maximum photosynthesis	kJ m^{-2} day^{-1}
BP_{15}	Maximum mesophyll conductance	m sec^{-1}
BP_{16}	Minimum temperature threshold for photosynthesis	°C
BP_{17}	Maximum temperature threshold for photosynthesis	°C
BP_{18}	Leaf respiration coefficient	kg C kg C^{-1}
BP_{19}	Stem respiration coefficient	kg C kg C^{-1}
BP_{20}	Root respiration coefficient	kg C kg C^{-1}
BP_{21}	Fraction of stem biomass that is carbon	kg C kg $biomass^{-1}$
BP_{22}	Temperature adjustment for mesophyll conductance	scalar 0-1
BP_{23}	Fraction of root biomass that is carbon	kg C kg $biomass^{-1}$
BP_{24}	Coefficient Q_{10} = 2.3 for exponential respiration	dimensionless
BP_{25}	Maximum canopy leaf nitrogen concentration	kg N dry $weight^{-1}$
BP_{26}	Minimum canopy leaf nitrogen concentration	kg N dry $weight^{-1}$
BP_{27}	Maximum leaf nitrogen retranslocation factor	scalar 0-1
BP_{28}	Soil water loss factor	scalar 0-1
BP_{29}	Decomposition release fraction for N:C ratio	scalar 0-1
BP_{30}	Maximum projected leaf area index	m^2 m^{-2}
BP_{31}	Leaf retention time	years
BP_{32}	Leaf lignin fraction	kg lignin kg C^{-1}
BP_{33}	EMPTY	
BP_{34}	Available nitrogen litter allocation factor	dimensionless
BP_{35}	Date of the beginning of spring leaf growth	julian day
BP_{36}	Date of fall leaf drop	julian day
BP_{37}	Mobile nitrogen retention time	year
BP_{38}	Atmospheric nitrogen deposition	kg $year^{-1}$
BP_{39}	Biological nitrogen fixation	kg $year^{-1}$
BP_{40}	Stem turnover coefficient	kg C kg C^{-1}
BP_{41}	Root turnover coefficient	kg C kg C^{-1}
BP_{42}	Leaf growth respiration coefficient	kg C kg C^{-1}
BP_{43}	Stem growth respiration coefficient	kg C kg C^{-1}
BP_{44}	Root growth respiration coefficient	kg C kg C^{-1}
BP_{45}	Optimum temperature for decomposition	°C
BP_{46}	Litter to soil decomposition fraction	kg C kg C^{-1}
BP_{47}	Decompositon rate	kg C kg C^{-1}
BP_{48}	Wood to litter decomposition fraction	scalar {0-1}
BP_{49}	Leaf area conversion factor - all sided to projected	m^2 m^{-2}
BP_{50}	Proportion nitrogen volatilized by fire	kg N kg C^{-1}
BP_{51}	Nitrogen fraction of leaf carbon	proportion
BP_{52}	Nitrogen fraction of stem carbon	proportion
BP_{53}	Nitrogen fraction of coarse root carbon	proportion
BP_{54}	Nitrogen fraction of fine root carbon	proportion
BP_{55}	Maximum basal area	m^2 ha^{-1}

Tree State Variables

Variable	Description	Units
XT_0	Leaf area	m^2
XT_1	Soil water available to tree	m^3 H_2O
XT_2	Snowpack available to tree	m^3 H_2O
XT_3	Last year's stem carbon	kg C
XT_4	Effective tree area	m^2
XT_5	Photosynthesis (PSN)	kg C
XT_6	Maintenance respiration of stem and roots	kg C
XT_7	Leaf carbon	kg C
XT_8	Stem carbon	kg C
XT_9	Coarse root carbon	kg C
XT_{10}	Fine root carbon	kg C
XT_{11}	Leaf nitrogen	kg N
XT_{12}	Stem nitrogen	kg N
XT_{13}	Coarse root nitrogen	kg N
XT_{14}	Fine root nitrogen	kg N
XT_{15}	Nitrogen available to tree	kg N
XT_{16}	Resource allocation factor	dimensionless

Species Parameters

Variable	Description	Units
BS_0	Specific leaf area	m^2 kg C^{-1}
BS_1	Canopy light extinction coefficient	dimensionless
BS_2	Canopy interception coefficient	m LAI^{-1} day^{-1}
BS_3	1—surface albedo	dimensionless
BS_4	Minimum springtime leaf water potential	–MPa
BS_5	Maximum radiation threshold for canopy conductance	kJ m^{-2} day^{-1}
BS_6	Maximum canopy conductance	m sec^{-1}
BS_7	Leaf water potential at stomatal closure	-MPa
BS_8	Slope of the absolute humidity reduction	m sec^{-1} $ABSHD^{-1}$
BS_9	Photosynthetic light compensation point	kJ m^{-2} day^{-1}
BS_{10}	Radiation at 0.5 maximum photosynthesis	kJ m^{-2} day^{-1}
BS_{11}	Maximum mesophyll conductance	m sec^{-1}
BS_{12}	Minimum temperature threshold for photosynthesis	°C
BS_{13}	Maximum temperature threshold for photosynthesis	°C
BS_{14}	Leaf respiration coefficient	kg C kg C^{-1}
BS_{15}	Stem respiration coefficient	kg C kg C^{-1}
BS_{16}	Root respiration coefficient	kg C kg C^{-1}
BS_{17}	Temperature adjustment for mesophyll conductance	scalar 0-1
BS_{18}	Coefficient Q_{10} = 2.3 for respiration	dimensionless
BS_{19}	Maximum canopy leaf nitrogen concentration	kg N kg C^{-1}
BS_{20}	Minimum canopy leaf nitrogen concentration	kg N kg C^{-1}
BS_{21}	Maximum leaf nitrogen retranslocation factor	scalar 0-1
BS_{22}	Maximum leaf area index, all sides	m^2 m^{-2}
BS_{23}	Leaf retention time	year
BS_{24}	Leaf lignin fraction	kg lignin C kg C^{-1}
BS_{25}	Available nitrogen litter allocation factor	dimensionless
BS_{26}	Date of the beginning of spring leaf growth	julian day
BS_{27}	Date of fall leaf drop	julian day

Variable	Description	Units
BS_{28}	Stem turnover coefficient	kg C kg C^{-1}
BS_{29}	Coarse root turnover coefficient	kg C kg C^{-1}
BS_{30}	Leaf growth respiration coefficient	kg C kg C^{-1}
BS_{31}	Stem growth respiration coefficient	kg C kg C^{-1}
BS_{32}	Root growth respiration coefficient	kg C kg C^{-1}
BS_{33}	Fine root turnover coefficient	kg C kg C^{-1}
BS_{34}	Maximum attainable age	years
BS_{35}	Site index at 50 years	m
BS_{36}	Probability of good cone crop	probability
BS_{37}	Years after cone crop when there is no crop	years
BS_{38}	Reproductive age	years
BS_{39}	Minimum diameter growth increment	cm
BS_{40}	Regeneration survival by duff depth - alpha coefficient	probability
BS_{41}	Regeneration survival by duff depth - beta coefficient	probability cm^{-1}
BS_{42}	Seed dispersal curve—alpha coefficient	probability
BS_{43}	Seed dispersal curve—beta coefficient	probability cm^{-1}
BS_{44}	Factor to convert from all-sided to projected leaf area	m^2 m^{-2}
BS_{45}	Bark thickness coefficient	cm bark cm DBH^{-1}
BS_{46}	Crown twigwood (0-1 cm) turnover fraction	kg C kg C^{-1}
BS_{47}	Crown branchwood (1-3 cm) turnover fraction	kg C kg C^{-1}
BS_{48}	Crown large branchwood (3-7 cm) turnover fraction	kg C kg C^{-1}
BS_{49}	Density of stem wood	kg m^{-2}
BS_{50}	Density of bark wood	kg m^{-2}
BS_{51}	Initial live crown ratio for mature trees	m m^{-1}
BS_{52}	Optimal temperature for photosynthesis	°C
BS_{53}	Minimum annual soil water fraction threshold	m^3 H_2O m^{-2} soil
BS_{54}	Tree establishment age	years
BS_{55}	Tree establishment live crown ratio	m^2 m^{-2}
BS_{56}	Tree establishment height	m
BS_{57}	EMPTY	
BS_{58}	EMPTY	
BS_{59}	Needle fraction consumed by surface fire	proportion
BS_{60}	Twigwood fraction consumed by surface fire	proportion
BS_{61}	Branchwood fraction consumed by surface fire	proportion
BS_{62}	Large branchwood fraction consumed by surface fire	proportion
BS_{63}	Logwood fraction consumed by surface fire	proportion
BS_{64}	Beginning growing season	yearday
BS_{65}	End of growing season	yearday
BS_{66}	Latest tolerable spring frost	yearday
BS_{67}	Earliest tolerable autumn frost	yearday

Weather Variables

Variable	Description	Units
α	Amplitude of the diurnal day length sin function	dimensionless
γ	Psychometric constant	mbar $°C^{-1}$
λ	Latent heat of water vaporization	J kg^{-1}
Δ	Slope of the saturation vapor pressure curve	mbar $°C^{-1}$
D_l	Daylength	sec
H_a	Absolute humidity deficit	$\mu g\ m^{-3}$
H_r	Relative humidity	%
PPT	Precipitation	m
R_c	Average canopy radiation of the stand	kJ m^{-2} day^{-1}
R_n	Net radiation to the site above the canopy	kJ m^{-2} day^{-1}
R_s	Shortwave radiation to site above the canopy	kJ m^{-2} day^{-1}
SVP	Saturation vapor pressure	mbar
T_{ave}	Average daily temperature	°C
T_{day}	Daytime average air temperature	°C
T_{dew}	Dew point temperature	°C
T_{max}	Maximum air temperature	°C
T_{min}	Minimum air temperature	°C
T_{night}	Average nighttime air temperature	°C
T_{soil}	Soil temperature	°C
VPD	Vapor pressure deficit	mbar

Appendix B: Examples of Input Data Files Used in the FIRE-BGC Program

Driver File -- DRIVER.DAT

```
This is the title line
echo.out                                This is the output file name for echo of model input
sim1.dat                                This is the input file for simulation specifics
species.dat                             File containing species-specific parms for tree equations
fuel.dat                                File containing parameters for decomposition equations
site1.dat                               File containing general site descriptors for input stand
pial.dat                                File containing whitebark pine parameters for simulation
plant1.dat                              File containing understory plant parameters for input
stand1.dat                              File containing initial stand conditions for vegetation
tree1.dat                               File containing initial stand densities and ages for trees
stand.day                               File used to store daily STAND int results
tree.list                               File used to tree list from TREE
stand.yr                                File used to store yearly STAND results from model
tree.yr                                 File used to store yearly TREE intermediate model results
firebgc.out                             File used to store yearly output
Print specifications for various variables
gp  18  19  20  23  24  66  67  68   0   0
gy   0   0   0   0   0   0   0   0   0   0
xp   1   5   6   7   8   9   0   0   0   0
gt  52  53  54  55  56  57  58   0   0   0
xt   3   4   6   7   8   9   0   0   0   0
map  1   2   3   0   0   0   0   0   0   0
Beg.Day            1
End.Day          365
Tree.num          20
```

Simulation File -- SIM.DAT

```
Here are the general simulation input parameters
       100 Number of years to simulate succession
      1800  Starting year date of simulation
         1  Number of sites on the modeled landscape
         1  Number of stands on the modeled landscape
        12  Number of tree species to account for in the succession
         1  Number of fire behavior fuel models to use in the simulation
         8  Number of dead biomass (fuel) types that are used in fire behave
         2  Number of live biomass (fuel) types that are used in fire behave
        38  Number of full years in the weather file record for all sites
        10  Starting year of Moutain Pine beetle epidemic
        10  Starting year of blister rust epidemic
      0.50  Probability of rust infection
     400.0  Size of simulation plot(s) in square meters
       2.0  Size of height increment used in model
```

Fuel File -- FUEL.DAT

```
Fuel characteristics/ Dead Biomass accumulation/decomposition file - Bob Keane
Fuel Comp        Duff     Litter     1 hour    10 hour    100 hr    1000 hr     Shrub      Herb
         1 Fuel Model Number
rhop-dead       0.550      0.510      0.390      0.390     0.390      0.390     0.510     0.510
lhv-dead      18586.7    18586.7    18586.7    18586.7   18586.7    18586.7   18586.7   18586.7
mps-dead        111.0     57.410     11.760      2.880     0.980      3.156   91.8560    3.0000
moistdead        0.60      0.080      0.060      0.080     0.100      0.200    0.1000    0.0500
consumptn        0.90      0.900      0.890      0.845     0.845      0.790    0.9000    0.9900
rhop-live       0.513      0.513
lhv-live      18595.0    18595.0
mps-live       49.200     91.860
moistlive       0.900      0.750
consumptn       0.500      0.900
st-l/d           .055       .055
se               .010       .010
mext             .250       .250
bulk-d/l       0.0115      0.001
duflitbulk       76.9       44.1
fdepth            0.3
         2 Fuel Model Number
rhop-dead       0.550      0.510      0.390      0.390     0.390      0.390     0.510     0.510
lhv-dead      18586.7    18586.7    18586.7    18586.7   18586.7    18586.7   18586.7   18586.7
mps-dead        111.0     57.410     11.760      2.880     0.980      3.156   91.8560    3.0000
moistdead        0.60      0.080      0.060      0.080     0.100      0.200    0.1000    0.0500
consumptn        0.90      0.900      0.890      0.845     0.845      0.790    0.9000    0.9900
rhop-live       0.513      0.513
lhv-live      18595.0    18595.0
mps-live       49.200     91.860
moistlive       0.900      0.750
consumptn       0.500      0.900
st-l/d           .055       .055
se               .010       .010
mext             .250       .250
bulk-d/l       0.0115      0.001
duflitbulk       76.9       44.1
fdepth            0.3
```

```
Site data input file for FIRE-BGC
SITE NUMBER 1
         1  Site number one (Well drained valley bottom)
         1  Number of initial stands on this site at simulation start
         1  Fuel Model ID number for this site
bgc.clm             Weather record file for the site
         6  Fire group of the site --  See fischer and others
     45.35  Latitude of site in decimal degrees
       125  Beginning of the growing season julian date
       280  End of growing season julian date
       5.0  Maximum number of seedlings per sq meter of plotspace -- spm
        25  Number of lag years for seedling establishment after fire
     144.0  Average fire free interval (years)
 1000000.0  Average fire size (m2)
       2.0  Weibull prob density function shape factor
      25.0  Distance from seed wall for all species after fire (m)
       5.0  Average windspeed at site during a fire (m/s)
      30.0  Ambient temperature at time of fire (deg C)
       5.0  Average slope of site (degrees)
      25.0  BP(0)    Specific leaf area (m2/kg-C)
      -0.5  BP(1)    Canopy light extinction coefficient
    0.1330  BP(2)    Soil water capacity (m3 soil water/m2 plot area)
    0.0005  BP(3)    Interception coefficient (M LAI-1 day-1)
      20.0  BP(4)    Optimum temp PSN                  (Deg C)
    0.0007  BP(5)    Snowmelt coefficient (M C-1 day-1)
      0.48  BP(6)    Proportion of leaf mass that is Carbon
      0.80  BP(7)    1-surface albedo (dimensionless)
       0.5  BP(8)    Spring minimum plant moisture stress (-MPa)
    3000.0  BP(9)    Rad. red CC threshold             (Kj/m**2/day)
    0.0016  BP(10)   Max canopy average CC             (m/sec)
      2.00  BP(11)   LWP at stomatal closure           (-MPa)
      0.05  BP(12)   Slope abs hd reduction            (m/sec/abshd)
     432.0  BP(13)   PSN light comp point             (Kj/m**2/day)
    9720.0  BP(14)   Light at 1/2 PSN max             (Kj/m**2/day)
    0.0008  BP(15)   Max CC CO2                       (m/sec)
       0.0  BP(16)   Min temp. PSN                    (Deg C)
      40.0  BP(17)   Max temp. PSN                    (Deg C)
   0.00015  BP(18)   Leaf respiration Coefficient
    0.0020  BP(19)   Stem respiration Coefficient
    0.0002  BP(20)   Root respiration Coefficient
      0.55  BP(21)   Proportion of stem wood that is carbon
       4.0  BP(22)   Mesophyll cond adjustment Coefficient
      0.55  BP(23)   Fraction of root biomass that is carbon
     0.085  BP(24)   Q10=2.3 constant for exponential respiration surface
     0.044  BP(25)   Maximum can ave Leaf Nitrogen conc  (%x 2.2 C/CH2O)
    0.0132  BP(26)   Minimum can ave Leaf Nitrogen conc
      0.50  BP(27)   Max Leaf Nitrogen retranslocation fraction  (dim)
       1.0  BP(28)   Soil water decomp rate factor (0-1) (dim)
       0.5  BP(29)   N/C decomp release fraction (dim)
      12.0  BP(30)   Maximum Leaf Area Index--all sides  (dim)
       3.0  BP(31)   Leaf turnover rate (YR)
      0.25  BP(32)   Leaf lignin fraction  (%/100)
     0.075  BP(33)   Proportion of wood Carbon that is nitrogen
       1.0  BP(34)   Nitrogen Avail Leaf/Root ALLOCATION factor (dim)
       0.0  BP(35)   Date of spring Leaf growth (yearday)
     365.0  BP(36)   Date of fall Leaf drop (yearday)
      20.0  BP(37)   Mobile N retention time  (YR)
    0.0005  BP(38)   Atmospheric deposition N  (kg/m2/yr)
    0.0001  BP(39)   Biological fixation N  (kg/m2/yr)
      0.02  BP(40)   Stem turnover Coefficient
      0.80  BP(41)   Root turnover Coefficient
      0.35  BP(42)   Leaf growth respiration
      0.30  BP(43)   Stem growth respiration
      0.35  BP(44)   Root growth respiration
      50.0  BP(45)   Decomposition temperature optimum (deg C)
      0.03  BP(46)   Duff/Litter C decomp fraction (dim)
      0.30  BP(47)   Decomposition rate scalar (dim)
```

```
  0.01  BP(48)   Wood/litter C decomp fraction (dim)
   2.2  BP(49)   Leaf projection conversion factor
  0.80  BP(50)   Proportion nitrogen loss that is volitalized
  0.04  BP(51)   Nitrogen fraction of leaf C
  0.01  BP(52)   Nitrogen fraction of stem C
  0.01  BP(53)   Nitrogen fraction of course root C
  0.04  BP(54)   Nitrogen fraction of fine root C
 60.00  BP(55)   Maximum stand basal area (m2/ha)
```

Plant File -- PLANT.DAT

```
Understory plant parameter Input for Model Execution
INTshrub  TOLshrub  INTherb   TOLherb <-- Column Headings
         1  Site id number
 10.000    10.000     3.000     4.000     Specific leaf area - m2/kg
  2.000     1.000     0.100     0.100     Average Height - m
  0.014     0.010     0.011     0.020     Max biomass(kg/m2)
  0.400     0.450     1.000     1.000     Proportion biomass leaf
  0.050     0.050     0.000     0.000     Twig turnover prop
  0.900     0.900     0.950     0.950     Leaf turnover prop
  0.550     0.550     0.550     0.550     Leaf fraction carbon
  0.008     0.008     0.015     0.015     Leaf fraction nitrogen
  0.258     0.250     0.250     0.250     Leaf lignin content
  0.250     0.250     1.000     1.000     Proportion dead at fire
```

Species File -- SPECIES.DAT

This is the file containing all tree species parameters for model
12 Number of species in this simulation

SppCode---------->	PIPO	ABGR	PSME	PICO	LAOC	ABLA	PIEN	PIAL	LALY	PIMO	THPL	TSHE
shadetolerance	1	4	3	1	1	4	4	2	1	2	5	5
bs(0)-spec-leaf-area	20.0	40.0	22.8	21.9	14.0	35.0	30.0	22.0	14.0	25.0	20.0	30.0
bs(1)-ext-coeff--k	-0.35	-0.45	-0.45	-0.30	-0.312	-0.45	-0.45	-0.30	-0.312	-0.40	-0.50	-0.50
bs(2)-intercept-cof	0.0005	0.0005	0.0005	0.0005	0.0005	0.0005	0.0005	0.0005	0.0005	0.0005	0.0005	0.0005
bs(3)-surface-albedo	0.9	0.88	0.90	0.90	0.90	0.86	0.90	0.90	0.90	0.90	0.86	0.86
bs(4)-spring-min-LWP	0.5	0.5	0.5	0.5	0.5	0.5	0.5	0.5	0.5	0.5	0.5	0.5
bs(5)-rad-CC-thres	4000.0	3000.0	3000.0	3000.0	5000.0	4000.0	4000.0	4000.0	5000.0	3000.0	3000.0	3000.0
bs(6)-Max-canopy-con	0.0025	0.003	0.0016	0.0020	0.0020	0.0030	0.0025	0.0020	0.0020	0.0025	0.0022	0.0022
bs(7)-LWP-@-stomate	1.65	1.4	1.90	1.46	1.50	1.30	1.60	1.65	1.00	1.50	1.40	1.30
bs(8)-slope-CC-humid	0.05	0.05	0.05	0.05	0.05	0.05	0.05	0.05	0.05	0.05	0.05	0.05
bs(9)-light-comp-pt	560.0	370.0	300.0	550.0	550.0	400.0	400.0	440.0	600.0	450.0	300.0	300.0
bs(10)-1/2-photomax	11000.0	8208.0	9700.0	10000.0	9730.0	8200.0	7128.0	9000.0	10000.0	9740.0	9000.0	5400.0
bs(11)-max-meso-k	0.0008	0.0008	0.0008	0.0008	0.0008	0.0008	0.0008	0.0008	0.0008	0.0008	0.0008	0.0008
bs(12)-min-temp-PSN	-1.0	-1.0	-2.0	-5.0	-3.0	-7.0	-4.0	-9.0	-10.0	-1.0	0.0	0.0
bs(13)-max-temp-PSN	45.0	41.0	41.0	40.0	38.0	38.0	37.0	37.0	35.0	40.0	40.0	40.0
bs(14)-leaf-resp-cof	0.00015	0.00015	0.00015	0.00015	0.00015	0.00015	0.00015	0.00015	0.00015	0.00015	0.00015	
bs(15)-stem-resp-cof	0.00200	0.00200	0.00200	0.00200	0.00200	0.00200	0.00200	0.00200	0.00200	0.00200	0.00200	
bs(16)-root-resp-cof	0.00020	0.00020	0.00020	0.00020	0.00020	0.00020	0.00020	0.00020	0.00020	0.00020	0.00020	
bs(17)-temp-meso-k	4.0	4.0	4.0	4.0	4.0	4.0	4.0	4.0	4.0	4.0	4.0	4.0
bs(18)-Q10-resp	0.085	0.085	0.085	0.085	0.085	0.085	0.085	0.085	0.085	0.085	0.085	0.085
bs(19)-Max-Leaf-N	0.045	0.0480	0.0440	0.0460	0.0390	0.0220	0.0220	0.0420	0.0370	0.0450	0.040	0.040
bs(20)-Min-Leaf-N	0.010	0.0150	0.0132	0.0120	0.0100	0.0110	0.0110	0.0120	0.0100	0.0100	0.0100	0.0100
bs(21)-Max-N-trans	0.50	0.50	0.50	0.50	0.90	0.50	0.40	0.50	0.90	0.50	0.50	0.50
bs(22)-Max-LAI-all	8.00	12.00	10.00	7.00	6.00	12.00	12.00	6.00	5.00	8.00	13.00	15.00
bs(23)-Leaf-turnover	3.0	6.0	5.0	5.0	1.0	6.0	6.0	6.0	1.0	3.0	6.0	4.0
bs(24)-Leaf-Lignin	0.25	0.28	0.28	0.23	0.20	0.28	0.22	0.22	0.20	0.22	0.21	0.206
bs(25)-N-l/r-alloca	1.0	1.0	1.0	1.0	1.0	1.0	1.0	1.0	1.0	1.0	1.0	1.0
bs(26)-Spring-date	120.0	110.0	120.0	180.0	115.0	140.0	140.0	150.0	150.0	120.0	150.0	150.0
bs(27)-Fall-date	200.0	280.0	280.0	280.0	280.0	280.0	250.0	250.0	210.0	250.0	250.0	250.0
bs(28)-Stem-turnover	0.04	0.09	0.01	0.05	0.05	0.10	0.10	0.05	0.05	0.10	0.10	0.10
bs(29)-CRoot-turnov	0.08	0.01	0.03	0.05	0.10	0.10	0.10	0.10	0.10	0.10	0.10	0.10
bs(30)-Leaf-grow-Res	0.35	0.40	0.30	0.35	0.40	0.40	0.40	0.35	0.40	0.35	0.35	0.35
bs(31)-Stem-grow-Res	0.30	0.30	0.30	0.30	0.30	0.30	0.30	0.30	0.30	0.30	0.30	0.30
bs(32)-Root-grow-Res	0.30	0.35	0.30	0.35	0.35	0.35	0.35	0.35	0.35	0.30	0.35	0.35
bs(33)-Froot-turnov	0.80	0.80	0.80	0.80	0.80	0.80	0.70	0.80	0.80	0.80	0.80	0.80
bs(34)-agemx	650.000	350.000	400.000	220.000	450.000	230.000	350.000	1000.000	800.000	600.000	750.000	500.000
bs(35)-Site-Index	21.0	20.0	15.0	22.0	30.0	18.0	23.0	17.0	15.0	25.0	22.0	21.0
bs(36)-conecrop-p	0.5	0.3330	0.1700	0.3180	0.3680	0.3330	0.1670	0.4000	0.3680	0.3180	0.2500	0.2500
bs(37)-coneblock	2	2	2	2	2	2	2	1	2	2	2	2
bs(38)-yeartocone	20.0	15.0	20.0	15.0	15.0	25.0	25.0	60.0	50.0	15.0	20.0	20.0
bs(39)-MinDiaGrow	0.01	0.020	0.050	0.005	0.016	0.008	0.008	0.006	0.007	0.016	0.006	0.006
bs(40)-sura	10.5900	40.0100	38.6900	14.1200	20.1700	40.0100	40.0100	40.0100	40.0100	40.0100	40.0100	40.01
bs(41)-surb	2.7400	5.1150	4.2400	2.2800	5.5900	6.1150	6.1150	6.1150	6.1150	6.1150	6.1150	6.1150

bs(42)-distequ-a	13.1251	13.4099	14.1251	12.6760	14.3257	13.4099	12.7470	12.7470	12.7470	12.7470	12.7470	12.7470
bs(43)-distequ-b	0.0255	0.0183	0.0222	0.0376	0.0148	0.0183	0.0251	0.0251	0.0251	0.0251	0.0251	0.0251
bs(44)-leafprojside	3.54	2.35	2.85	3.54	2.25	2.04	2.80	3.54	2.25	3.50	2.80	2.80
bs(45)-bark-conv	0.070	0.033	0.065	0.014	0.071	0.015	0.022	0.022	0.022	0.014	0.050	0.033
bs(46)-1hr-loss	0.02	0.0400	0.0400	0.0300	0.0300	0.0500	0.0500	0.0300	0.0300	0.0500	0.0500	0.0500
bs(47)-10hr-loss	0.01	0.030	0.0200	0.0100	0.0100	0.0300	0.0300	0.0100	0.0100	0.0300	0.0300	0.0300
bs(48)-100hr-loss	0.01	0.0200	0.0200	0.0100	0.0100	0.0200	0.0200	0.0100	0.0100	0.0200	0.0200	0.0200
bs(49)-wood-density	400.460	320.367	480.550	410.070	512.588	320.367	349.200	410.070	518.995	379.635	320.367	320.367
bs(50)-bark-density	349.200	599.087	438.903	424.487	389.246	438.903	490.162	424.487	389.246	419.681	599.870	599.870
bs(51)-Mature.LCR	0.4	0.8	0.8	0.5	0.4	0.8	0.8	0.4	0.4	0.5	0.8	0.8
bs(52)-OptPSNtemp	26.0	21.0	20.0	21.0	20.0	17.0	18.0	13.0	17.0	20.0	18.0	18.0
bs(53)-avesoilmoist	0.10	0.30	0.20	0.20	0.20	0.30	0.30	0.20	0.20	0.30	0.3	0.3
bs(54)-seedling-age	15.0	10.0	15.0	10.0	7.0	25.0	25.0	30.0	27.0	15.0	30.0	30.0
bs(55)-LiveCrownRat	0.50	0.80	0.60	0.50	0.40	0.80	0.60	0.40	0.40	0.40	0.80	0.80
bs(56)-seedling-hgt	1.4	1.5	1.4	1.4	1.8	1.5	1.5	1.5	1.4	1.8	1.5	1.5
bs(57)-EMPTY	0.0	0.0	0.0	0.0	0.0	0.0	0.0	0.0	0.0	0.0	0.0	0.0
bs(58)-EMPTY	0.0	0.0	0.0	0.0	0.0	0.0	0.0	0.0	0.0	0.0	0.0	0.0
bs(59)-needle.comb%	0.95	1.00	0.95	0.90	1.00	1.00	1.00	1.00	1.00	1.00	1.00	1.00
bs(60)-1hr.comb%	0.90	0.90	0.90	0.80	0.90	0.90	0.90	0.90	0.90	0.90	0.90	0.90
bs(61)-10hr.comb%	0.80	0.80	0.80	0.10	0.80	0.80	0.80	0.80	0.80	0.80	0.80	0.80
bs(62)-100hr.comb%	0.10	0.20	0.10	0.10	0.20	0.20	0.20	0.20	0.20	0.20	0.20	0.20
bs(63)-1000hr.comb	0.0	0.0	0.0	0.0	0.0	0.0	0.0	0.0	0.0	0.0	0.0	0.0
bs(64)-BegGrowSeas	120.00	90.00	90.00	90.00	90.00	90.00	90.00	90.00	90.00	90.00	90.00	90.00
bs(65)-EndGrowSeas	280.00	280.00	280.00	280.00	280.00	280.00	280.00	280.00	280.00	280.00	280.00	280.00
bs(66)-latefrost	120.0	110.0	180.0	200.0	150.0	210.0	210.0	220.0	220.0	110.0	110.0	110.0
bs(67)-earlyfrost	260.00	260.00	260.00	260.00	260.00	260.00	260.00	240.00	240.00	280.00	280.00	280.00
bs(68)-EMPTY	0.00	0.00	0.00	0.00	0.00	0.00	0.00	0.00	0.00	0.00	0.0	0.0
bs(69)-EMPTY	0.00	0.00	0.00	0.00	0.00	0.00	0.00	0.00	0.00	0.00	0.0	0.0

Whitebark File -- PIAL.DAT

```
Input file containing all whitebark pine parameters
     600.0 Maximum number of cones per bird for a site
      60.0 Minimum age of cone production       (yrs)
      20.0 Minimum diameter for cone production (cm)
       3.0 Number Clarks Nutcrackers using site
      58.8 Number of seeds per cone
       3.7 Number of seeds per Nutcracker cache
     0.800 Proportion of caches found by nutcracker
    0.3521 Cumulative probability for a poor or bad cone year
    0.4673 Cumulative probability for a moderate or medium cone year
    0.7825 Cumulative probability for a good cone year
    1.0000 Cumulative probability for a bumper cone year
       7.0 Maximum leaf area allowable for nutcracker caching
      60.0 Average number of cones per tree
     0.120 Proportion of seeds consumed by nutcracker during caching
```

Stand File -- STAND.DAT

```
Stand Data Input for Model Execution
Default Stand Compartment Values for all Stands
    0.3344  XP(  0)   Snowpack                    ( m**3/m2)
    0.0800  XP(  1)   Soil water content          ( m**3/m2)
       0.0  XP(  2)   Water outflow               ( m**3/m2)
       0.0  XP(  3)   Transpiration               ( m**3/m2)
       0.0  XP(  4)   Evaporation                 ( m**3/m2)
    0.0005  XP(  5)   PSN                         ( kg/m2)
       0.0  XP(  6)   Autotrophic respiration     ( kg/m2)
    1.2200  XP(  7)   Leaf Carbon                 ( kg/m2 )
   10.0000  XP(  8)   Stem Carbon                 ( kg/m2 )
    2.5500  XP(  9)   Course Root Carbon          ( kg/m2 )
    1.5500  XP( 10)   Fine Root Carbon            ( kg/m2 )
       0.0  XP( 11)   Respiration Decomp, C       ( kg/m2 )
    3.0000  XP( 12)   Soil Carbon                 ( kg/m2 )
    0.0100  XP( 13)   Available Nitrogen          ( kg/m2 )
    0.0180  XP( 14)   Leaf Nitrogen (1.5% OF X8   ( kg/m2 )
    0.1000  XP( 15)   Stem Nitrogen               ( kg/m2 )
    0.0560  XP( 16)   Course Root Nit .75% of x10 ( kg/m2 )
    0.0560  XP( 17)   Fine Root Nit.75% OF X10    ( kg/m2 )
    0.0300  XP( 18)   Soil Nitrogen (1% XP13)     ( kg/m2 )
       0.0  XP( 19)   Nitrogen Loss               ( kg/m2 )
    3.0000  XP( 20)   L/R Litter Carbon           ( kg/m2 )
    0.0300  XP( 21)   L/R Litter Nitrogen 1%X20   ( kg/m2 )
Stand Inital loadings
site stand litterC DuffC soilC  1hr    10hr   100hr  1000hr Ishrub Tshrub Iherb  Therb
  1    1   0.047  0.047  0.100  0.012  0.073  0.184  3.659  0.001  0.002  0.001  0.002
```

Tree File -- TREE.DAT

This is the individual tree file
nbins 10
width 5
Site 1 Stand 1

Dia class	-1-	-2-	-3-	-4-	-5-	-6-	-7-	-8-	-9-	-10-
spp1-cnt	0	0	0	0	0	0	0	0	0	0
spp1-age	0	0	0	0	0	0	0	0	0	0
spp2-cnt	0	0	0	0	0	0	0	0	0	0
spp2-age	0	0	0	0	0	0	0	0	0	0
spp3-cnt	0	0	0	0	0	0	0	0	0	0
spp3-age	0	0	0	0	0	0	0	0	0	0
spp5-cnt	0	0	0	0	0	0	0	0	0	0
spp4-cnt	0	0	0	0	0	0	0	0	0	0
spp4-age	0	0	0	0	0	0	0	0	0	0
spp5-age	0	0	0	0	0	0	0	0	0	0
spp6-cnt	20	5	0	0	2	1	1	1	0	0
spp6-age	40	60	0	0	100	120	120	120	0	0
spp7-cnt	0	0	0	0	0	0	0	0	0	0
spp7-age	0	0	0	0	0	0	0	0	0	0
spp8-cnt	16	4	1	0	4	0	3	4	2	0
spp8-age	40	50	70	0	90	0	160	180	200	0
spp9-cnt	0	0	0	0	0	0	0	0	0	0
spp9-age	0	0	0	0	0	0	0	0	0	0
spp10-cnt	0	0	0	0	0	0	0	0	0	0
spp10-age	0	0	0	0	0	0	0	0	0	0
spp11-cnt	0	0	0	0	0	0	0	0	0	0
spp11-age	0	0	0	0	0	0	0	0	0	0
spp12-cnt	0	0	0	0	0	0	0	0	0	0
spp12-age	0	0	0	0	0	0	0	0	0	0

Appendix C: Examples of Output Files Created by the FIRE-BGC Program

ECHO.OUT

```
****** Simulation Inputs ******
Sim nspan: 100
Sim date: 1800
Sim nsite: 1
Sim nstands: 1
Sim nspp: 12
Sim fuel mod: 1
Sim nd: 8
Sim nl: 2
Sim nl: 38
Sim fire int: 50
Sim fire type: 1
Sim beetle: 10
Sim rust: 10
Sim parea: 400.000000
Sim hsize: 2.000000


****** Printer Inputs ******
Print start day: 1
Print end day: 365
Print tree num: 20
Print gp(i) intermediate values
  gp(18)   gp(19)   gp(20)   gp(23)   gp(24)   gp(66)   gp(67)   gp(68)   gp(0)   gp(0)
Print gy(i) intermediate values
  gy(0)   gy(0)   gy(0)   gy(0)   gy(0)   gy(0)   gy(0)   gy(0)   gy(0)   gy(0)
Print gt(i) intermediate values
  gt(52)   gt(53)   gt(54)   gt(55)   gt(56)   gt(57)   gt(58)   gt(0)   gt(0)   gt(0)
Print xp(i) state values
  xp(1)   xp(5)   xp(6)   xp(7)   xp(8)   xp(9)   xp(0)   xp(0)   xp(0)   xp(0)
Print xt(i) state values
  xt(3)   xt(4)   xt(6)   xt(7)   xt(8)   xt(9)   xt(0)   xt(0)   xt(0)   xt(0)

****** Species Inputs ******
Species= PIPO  Shade: 0  Num: 0  bs(0) = 20.000000
Species= PIPO  Shade: 0  Num: 0  bs(1) = -0.350000
Species= PIPO  Shade: 0  Num: 0  bs(2) = 0.000500
Species= PIPO  Shade: 0  Num: 0  bs(3) = 0.900000
Species= PIPO  Shade: 0  Num: 0  bs(4) = 0.500000
Species= PIPO  Shade: 0  Num: 0  bs(5) = 4000.000000
Species= PIPO  Shade: 0  Num: 0  bs(6) = 0.002500
Species= PIPO  Shade: 0  Num: 0  bs(7) = 1.650000
Species= PIPO  Shade: 0  Num: 0  bs(8) = 0.050000
Species= PIPO  Shade: 0  Num: 0  bs(9) = 560.000000
Species= PIPO  Shade: 0  Num: 0  bs(10) = 11000.000000
Species= PIPO  Shade: 0  Num: 0  bs(11) = 0.000800
Species= PIPO  Shade: 0  Num: 0  bs(12) = -1.000000
Species= PIPO  Shade: 0  Num: 0  bs(13) = 45.000000
Species= PIPO  Shade: 0  Num: 0  bs(14) = 0.000150
Species= PIPO  Shade: 0  Num: 0  bs(15) = 0.002000
Species= PIPO  Shade: 0  Num: 0  bs(16) = 0.000200
Species= PIPO  Shade: 0  Num: 0  bs(17) = 4.000000
Species= PIPO  Shade: 0  Num: 0  bs(18) = 0.085000
Species= PIPO  Shade: 0  Num: 0  bs(19) = 0.045000
Species= PIPO  Shade: 0  Num: 0  bs(20) = 0.010000
Species= PIPO  Shade: 0  Num: 0  bs(21) = 0.500000
Species= PIPO  Shade: 0  Num: 0  bs(22) = 8.000000
Species= PIPO  Shade: 0  Num: 0  bs(23) = 3.000000
Species= PIPO  Shade: 0  Num: 0  bs(24) = 0.250000
Species= PIPO  Shade: 0  Num: 0  bs(25) = 1.000000
Species= PIPO  Shade: 0  Num: 0  bs(26) = 120.000000
Species= PIPO  Shade: 0  Num: 0  bs(27) = 200.000000
Species= PIPO  Shade: 0  Num: 0  bs(28) = 0.040000
```

```
Species= PIPO  Shade: 0  Num: 0  bs(29) = 0.080000
Species= PIPO  Shade: 0  Num: 0  bs(30) = 0.350000
Species= PIPO  Shade: 0  Num: 0  bs(31) = 0.300000
Species= PIPO  Shade: 0  Num: 0  bs(32) = 0.300000
Species= PIPO  Shade: 0  Num: 0  bs(33) = 0.800000
Species= PIPO  Shade: 0  Num: 0  bs(34) = 650.000000
Species= PIPO  Shade: 0  Num: 0  bs(35) = 21.000000
Species= PIPO  Shade: 0  Num: 0  bs(36) = 0.500000
Species= PIPO  Shade: 0  Num: 0  bs(37) = 2.000000
Species= PIPO  Shade: 0  Num: 0  bs(38) = 20.000000
Species= PIPO  Shade: 0  Num: 0  bs(39) = 0.010000
Species= PIPO  Shade: 0  Num: 0  bs(40) = 10.590000
Species= PIPO  Shade: 0  Num: 0  bs(41) = 2.740000
Species= PIPO  Shade: 0  Num: 0  bs(42) = 13.125100
Species= PIPO  Shade: 0  Num: 0  bs(43) = 0.025500
Species= PIPO  Shade: 0  Num: 0  bs(44) = 3.540000
Species= PIPO  Shade: 0  Num: 0  bs(45) = 0.070000
Species= PIPO  Shade: 0  Num: 0  bs(46) = 0.020000
Species= PIPO  Shade: 0  Num: 0  bs(47) = 0.010000
Species= PIPO  Shade: 0  Num: 0  bs(48) = 0.010000
Species= PIPO  Shade: 0  Num: 0  bs(49) = 400.460000
Species= PIPO  Shade: 0  Num: 0  bs(50) = 349.200000
Species= PIPO  Shade: 0  Num: 0  bs(51) = 0.400000
Species= PIPO  Shade: 0  Num: 0  bs(52) = 26.000000
Species= PIPO  Shade: 0  Num: 0  bs(53) = 0.100000
Species= PIPO  Shade: 0  Num: 0  bs(54) = 15.000000
Species= PIPO  Shade: 0  Num: 0  bs(55) = 0.500000
Species= PIPO  Shade: 0  Num: 0  bs(56) = 1.400000
Species= PIPO  Shade: 0  Num: 0  bs(57) = 0.000000
Species= PIPO  Shade: 0  Num: 0  bs(58) = 0.000000
Species= PIPO  Shade: 0  Num: 0  bs(59) = 0.950000
Species= PIPO  Shade: 0  Num: 0  bs(60) = 0.900000
Species= PIPO  Shade: 0  Num: 0  bs(61) = 0.800000
Species= PIPO  Shade: 0  Num: 0  bs(62) = 0.100000
Species= PIPO  Shade: 0  Num: 0  bs(63) = 0.000000
Species= PIPO  Shade: 0  Num: 0  bs(64) = 120.000000
Species= PIPO  Shade: 0  Num: 0  bs(65) = 280.000000
Species= PIPO  Shade: 0  Num: 0  bs(66) = 120.000000
Species= PIPO  Shade: 0  Num: 0  bs(67) = 260.000000
Species= PIPO  Shade: 0  Num: 0  bs(68) = 0.000000
Species= PIPO  Shade: 0  Num: 0  bs(69) = 0.000000
.
. [All species and parameters are presented from species.dat file]
.

****** Whitebark Inputs ******
PIAL cmax:  600.000000
PIAL mage: 60.000000
PIAL mdbh:  20.000000
PIAL birds:  3.000000
PIAL spc:  58.800000
PIAL spcache: 3.700000
PIAL pfind: 0.800000
PIAL fmax: 7.000000
PIAL cpt: 60.000000
PIAL eatseeds: 0.120000
PIAL cyr(7): 0.352100
PIAL cyr(7): 0.467300
PIAL cyr(7): 0.782500
PIAL cyr(7): 1.000000


****** Fuel Model Inputs ******
DEAD  fmod= 0  rp: 0.550000  lh: 18586.700000  svr = 111.000000  m= 0.600000  c: 0.900000
DEAD  fmod= 0  rp: 0.510000  lh: 18586.700000  svr = 57.410000  m= 0.080000  c: 0.900000
DEAD  fmod= 0  rp: 0.390000  lh: 18586.700000  svr = 61.166000  m= 0.060000  c: 0.890000
DEAD  fmod= 0  rp: 0.390000  lh: 18586.700000  svr = 11.760000  m= 0.080000  c: 0.845000
DEAD  fmod= 0  rp: 0.390000  lh: 18586.700000  svr = 2.880000  m= 0.100000  c: 0.845000
DEAD  fmod= 0  rp: 0.390000  lh: 18586.700000  svr = 0.980000  m= 0.200000  c: 0.790000
DEAD  fmod= 0  rp: 0.510000  lh: 18586.700000  svr = 3.156000  m= 0.100000  c: 0.900000
DEAD  fmod= 0  rp: 0.510000  lh: 18586.700000  svr = 91.856000  m= 0.050000  c: 0.990000
```

```
LIVE fmod= 0  rp: 0.513000  lh: 18595.000000  svr = 49.200000  m= 0.900000  c= 0.500000
LIVE fmod= 0  rp: 0.513000  lh: 18595.000000  svr = 91.860000  m= 0.750000  c= 0.900000
DO/L1= 0  se: 0.055000  si: 0.010000  mext = 0.250000  bulk= 0.011500 bulkom = 76.900000
DO/L1= 0  se: 0.055000  si: 0.010000  mext = 0.250000  bulk= 0.001000 bulkom = 44.100000


****** Site Inputs ******
Site num stands: 1
Site fuel model: 0
Weather file: bgc.clm
Site fire group: 6
Site beg grow season: 125
Site end grow season: 280
Site seedlings/m2: 5.000000
Site seed lag: 25
Site seed dist: 25.000000
Site fire wind: 5.000000
Site fire temp: 30.000000
Site fire slope: 5.000000
Site: 0   bd(0) = 25.000000
Site: 0   bd(1) = -0.500000
Site: 0   bd(2) = 53.200000
Site: 0   bd(3) = 0.000500
Site: 0   bd(4) = 20.000000
Site: 0   bd(5) = 0.000700
Site: 0   bd(6) = 0.480000
Site: 0   bd(7) = 0.800000
Site: 0   bd(8) = 0.500000
Site: 0   bd(9) = 3000.000000
Site: 0   bd(10) = 0.001600
Site: 0   bd(11) = 2.000000
Site: 0   bd(12) = 0.050000
Site: 0   bd(13) = 432.000000
Site: 0   bd(14) = 9720.000000
Site: 0   bd(15) = 0.000800
Site: 0   bd(16) = 0.000000
Site: 0   bd(17) = 40.000000
Site: 0   bd(18) = 0.000150
Site: 0   bd(19) = 0.002000
Site: 0   bd(20) = 0.000200
Site: 0   bd(21) = 0.550000
Site: 0   bd(22) = 4.000000
Site: 0   bd(23) = 0.550000
Site: 0   bd(24) = 0.085000
Site: 0   bd(25) = 0.044000
Site: 0   bd(26) = 0.013200
Site: 0   bd(27) = 0.500000
Site: 0   bd(28) = 1.000000
Site: 0   bd(29) = 0.500000
Site: 0   bd(30) = 12.000000
Site: 0   bd(31) = 3.000000
Site: 0   bd(32) = 0.250000
Site: 0   bd(33) = 0.075000
Site: 0   bd(34) = 1.000000
Site: 0   bd(35) = 0.000000
Site: 0   bd(36) = 365.000000
Site: 0   bd(37) = 20.000000
Site: 0   bd(38) = 0.200000
Site: 0   bd(39) = 0.040000
Site: 0   bd(40) = 0.020000
Site: 0   bd(41) = 0.800000
Site: 0   bd(42) = 0.350000
Site: 0   bd(43) = 0.300000
Site: 0   bd(44) = 0.350000
Site: 0   bd(45) = 50.000000
Site: 0   bd(46) = 0.030000
Site: 0   bd(47) = 0.300000
Site: 0   bd(48) = 0.010000
Site: 0   bd(49) = 2.200000
Site: 0   bd(50) = 0.800000
Site: 0   bd(51) = 0.040000
```

```
Site: 0   bd(52) = 0.010000
Site: 0   bd(53) = 0.010000
Site: 0   bd(54) = 0.040000
Site: 0   bd(55) = 60.000000


****** Understory Plant Parm Inputs ******
Plant SLA: IS: 10.000000  TS: 10.000000  IH: 3.000000  TH: 4.000000
Plant Hgt: IS: 2.000000  TS: 1.000000  IH: 0.100000  TH: 0.100000
Plant Mxbio: IS: 0.014000  TS: 0.010000  IH: 0.011000  TH: 0.020000
Plant Leaf: IS: 0.400000  TS: 0.450000  IH: 1.000000  TH: 1.000000
Plant Twgturn: IS: 0.050000  TS: 0.050000  IH: 0.000000  TH: 0.000000
Plant leafturn: IS: 0.900000  TS: 0.900000  IH: 0.950000  TH: 0.950000
Plant LeafC: IS: 0.550000  TS: 0.550000  IH: 0.550000  TH: 0.550000
Plant leafN: IS: 0.008000  TS: 0.008000  IH: 0.015000  TH: 0.015000
Plant Lignin: IS: 0.258000  TS: 0.250000  IH: 0.250000  TH: 0.250000
Plant Dead: IS: 0.250000  TS: 0.250000  IH: 1.000000  TH: 1.000000


****** Stand Inputs for this site ******
Site ID: 0
Stand ID: 1
Number trees: 64
Crown close: 1
Leaf area: 2522.030286
Basal area: 39.132103
xp(0) = 133.760000
xp(1) = 32.000000
xp(2) = 0.000000
xp(3) = 0.000000
xp(4) = 0.000000
xp(5) = 0.200000
xp(6) = 0.000000
xp(7) = 90.988947
xp(8) = 2926.900831
xp(9) = 60.001121
xp(10) = 208.516337
xp(11) = 0.000000
xp(12) = 40.000000
xp(13) = 4.000000
xp(14) = 3.639558
xp(15) = 29.269008
xp(16) = 0.600011
xp(17) = 8.340653
xp(18) = 3.000000
xp(19) = 0.000000
Shrub(0) = 0.040000
Shrub(1) = 0.798800
Herb(0) = 0.040000
Herb(1) = 0.880000
Litter carbon: 18.931200
Duff carbon: 18.931200
Soil carbon: 40.000000
Woody carbon(0) = 4.928000
Woody carbon(1) = 29.568000
Woody carbon(2) = 73.920000
Woody carbon(3) = 1463.616000
Litter nitrogen: 1.419840
Duff nitrogen: 1.419840
Soil nitrogen: 3.000000
Woody N (0) = 0.369600
Woody N (1) = 2.217600
Woody N (2) = 5.544000
Woody N (3) = 109.771200
Avail nitrogen: 4.000000


****** Tree Inputs for stand in site ******
Tree ID: 1    Stand ID: 1    Species ID: 5    Species name: ABLA
DBH: 4.083110   Height: 9.460431   Height to Crown: 1.892086
Age: 40.000000   Burn: 0   Rust: 0   Stress: 0
```

```
xt( 0) =  16.133682  xt( 1) =   0.551198  xt( 2) =   2.304009  xt( 3) =   1.047694
xt( 4) =   6.889980  xt( 5) =   0.004610  xt( 6) =   0.000000  xt( 7) =   0.460962
xt( 8) =   1.047694  xt( 9) =   0.059042  xt(10) =   1.056372  xt(11) =   0.018438
xt(12) =   0.010477  xt(13) =   0.000590  xt(14) =   0.042255  xt(15) =   0.025711
xt(16) =   0.006428
Tree ID: 2    Stand ID: 1    Species ID: 5    Species name: ABLA
DBH: 2.204065   Height: 9.460431   Height to Crown: 1.892086
Age: 40.000000   Burn: 0   Rust: 0   Stress: 0
xt( 0) =  12.631942  xt( 1) =   0.551198  xt( 2) =   2.304009  xt( 3) =   0.305282
xt( 4) =   6.889980  xt( 5) =   0.003609  xt( 6) =   0.000000  xt( 7) =   0.360913
xt( 8) =   0.305282  xt( 9) =   0.023829  xt(10) =   0.827091  xt(11) =   0.014437
xt(12) =   0.003053  xt(13) =   0.000238  xt(14) =   0.033084  xt(15) =   0.020131
xt(16) =   0.005033
Tree ID: 3    Stand ID: 1    Species ID: 5    Species name: ABLA
DBH: 2.362050   Height: 9.460431   Height to Crown: 1.892086
Age: 40.000000   Burn: 0   Rust: 0   Stress: 0
xt( 0) =  12.845765  xt( 1) =   0.551198  xt( 2) =   2.304009  xt( 3) =   0.350615
xt( 4) =   6.889980  xt( 5) =   0.003670  xt( 6) =   0.000000  xt( 7) =   0.367022
xt( 8) =   0.350615  xt( 9) =   0.025980  xt(10) =   0.841092  xt(11) =   0.014681
xt(12) =   0.003506  xt(13) =   0.000260  xt(14) =   0.033644  xt(15) =   0.020471
xt(16) =   0.005118
Tree ID: 4    Stand ID: 1    Species ID: 5    Species name: ABLA
DBH: 2.204065   Height: 9.460431   Height to Crown: 1.892086
Age: 40.000000   Burn: 0   Rust: 0   Stress: 0
xt( 0) =  12.631942  xt( 1) =   0.551198  xt( 2) =   2.304009  xt( 3) =   0.305282
xt( 4) =   6.889980  xt( 5) =   0.003609  xt( 6) =   0.000000  xt( 7) =   0.360913
xt( 8) =   0.305282  xt( 9) =   0.023829  xt(10) =   0.827091  xt(11) =   0.014437
xt(12) =   0.003053  xt(13) =   0.000238  xt(14) =   0.033084  xt(15) =   0.020131
xt(16) =   0.005033
.
. [All trees are presented as entered in the Tree file]
.
```

STAND.DAY

Stand	Day	GP(23)	GP(24)	XP(1)	XP(5)	XP(6)	XP(7)
1	1	0.000000	0.009738	31.999548	0.906968	0.068097	90.988947
1	2	0.000000	0.025345	31.998576	0.899365	0.164862	90.988947
1	3	0.000000	0.019635	31.997986	0.893474	0.244568	90.988947
1	4	0.000000	0.032913	31.997165	0.883600	0.345482	90.988947
1	5	0.000000	0.014442	31.996019	0.879267	0.411346	90.988947
1	6	0.000000	0.016467	31.994863	0.874327	0.478176	90.988947
1	7	0.000000	0.014689	31.993761	0.869921	0.538576	90.988947
1	8	0.000000	0.016980	31.992498	0.864827	0.601888	90.988947
1	9	0.000000	0.020688	31.992013	0.858620	0.670482	90.988947
1	10	0.000000	0.042933	31.991968	0.845740	0.779358	90.988947
1	11	0.000000	0.093775	31.991910	0.817608	0.982752	90.988947
1	12	0.000000	0.080923	31.991632	0.793331	1.165613	90.988947
1	13	0.000000	0.076026	31.991440	0.770523	1.337355	90.988947
1	14	0.000000	0.072416	31.991309	0.748798	1.502058	90.988947
1	15	0.000000	0.073983	31.991227	0.726603	1.663320	90.988947
1	16	0.000000	0.038232	31.988440	0.715134	1.778800	90.988947
1	17	0.000000	0.035103	31.985598	0.704603	1.889319	90.988947
1	18	0.000000	0.059332	31.983349	0.686803	2.042670	90.988947
1	19	0.000000	0.045343	31.983061	0.673201	2.164860	90.988947
1	20	0.000000	0.109316	31.982968	0.640406	2.411938	90.988947
1	21	0.000000	0.163514	31.979368	0.591352	2.749476	90.988947
1	22	0.000000	0.067031	31.975403	0.571242	2.936624	90.988947
1	23	0.000000	0.062609	31.973259	0.552460	3.101678	90.988947
1	24	0.000000	0.072298	31.970300	0.530770	3.285137	90.988947
1	25	0.000000	0.051199	31.966601	0.515410	3.430775	90.988947
1	26	0.000000	0.036401	31.963293	0.504490	3.544535	90.988947
1	27	0.000000	0.046127	31.963055	0.490652	3.660321	90.988947
1	28	0.000000	0.062189	31.961878	0.471995	3.807872	90.988947
1	29	0.000000	0.028167	31.959135	0.463545	3.898441	90.988947
1	30	0.000000	0.020022	31.956729	0.457539	3.969808	90.988947
1	31	0.000000	0.023562	31.954613	0.450470	4.047401	90.988947
1	32	0.000000	0.050381	31.951876	0.435356	4.177848	90.988947
1	33	0.000000	0.022838	31.949675	0.428504	4.257865	90.988947
1	34	0.000000	0.073527	31.949549	0.406446	4.422635	90.988947
1	35	0.000000	0.064107	31.948028	0.387214	4.591190	90.988947
1	36	0.000000	0.150007	31.946192	0.342212	4.926324	90.988947
1	37	0.000000	0.101287	31.944276	0.311826	5.178006	90.988947
1	38	0.000000	0.150567	31.941660	0.266656	5.500208	90.988947
1	39	0.000000	0.047375	31.938994	0.252444	5.639044	90.988947
1	40	0.000000	0.129179	31.937490	0.213690	5.962340	90.988947
1	41	0.000000	0.199379	31.937362	0.153876	6.377470	90.988947
1	42	0.000000	0.186200	31.936240	0.098016	6.775693	90.988947
1	43	0.000000	0.177118	31.935294	0.044881	7.157754	90.988947
1	44	0.007512	0.206431	32.024168	-0.014795	7.605704	90.988947
1	45	0.000000	0.130302	32.019244	-0.053886	7.927576	90.988947
1	46	0.000000	0.052252	32.018244	-0.069561	8.069985	90.988947
1	47	0.000000	0.068560	32.016535	-0.090129	8.258492	90.988947
1	48	0.000000	0.130449	32.015615	-0.129264	8.566792	90.988947
1	49	0.000000	0.144980	32.014276	-0.172758	8.911453	90.988947
1	50	0.000000	0.152168	32.007657	-0.218408	9.264581	90.988947
1	51	0.000000	0.111146	32.003105	-0.251752	9.549140	90.988947
1	52	0.000000	0.084319	31.998376	-0.277047	9.779479	90.988947
1	53	0.000000	0.080502	31.994435	-0.301198	9.995600	90.988947
1	54	0.000000	0.044978	31.990688	-0.314691	10.136597	90.988947
1	55	0.000000	0.087212	31.986098	-0.340855	10.380809	90.988947
1	56	0.000000	0.148110	31.983050	-0.385288	10.749988	90.988947
1	57	0.010190	0.179119	31.988046	-0.435966	11.182042	90.988947
1	58	0.000000	0.167847	31.965293	-0.486320	11.587512	90.988947
1	59	0.000000	0.140470	31.961387	-0.528461	11.936195	90.988947
1	60	0.000000	0.079546	31.956184	-0.552325	12.164420	90.988947
1	61	0.000000	0.063861	31.949946	-0.571483	12.365735	90.988947
1	62	0.000000	0.057723	31.941394	-0.588800	12.570633	90.988947
1	63	0.000000	0.099334	31.935445	-0.618600	12.857248	90.988947
1	64	0.275376	0.201619	32.407283	-0.596473	13.353184	90.988947
1	65	0.517924	0.213727	38.434946	-0.505214	13.885043	90.988947
1	66	1.150663	0.224206	40.583747	-0.227277	14.430409	90.988947

STAND.YR

Stand	Year	GP(23)	GP(24)	XP(1)	XP(7)	XP(8)
1	0	0.000000	0.077697	26.480141	90.988947	2926.900831
1	1	0.000000	0.105814	35.707037	105.581934	2926.251535
1	2	0.000000	0.046805	36.544305	87.040246	2915.304912
1	3	0.000000	0.011971	39.803064	97.535971	2912.221802
1	4	0.000000	0.141184	24.001221	101.752184	2910.129062
1	5	0.000000	0.012162	37.300849	99.090074	2793.603914
1	6	0.000000	0.103026	32.709794	102.800562	2792.107049
1	7	0.000000	0.047982	31.011580	89.230265	2790.975219
1	8	0.000000	0.027388	35.546488	94.106106	2788.508350
1	9	0.000000	0.075563	30.809190	99.640346	2787.966335
1	10	0.000000	0.049001	29.636536	91.124150	409.785064
1	11	0.000000	0.129352	12.749777	102.400549	292.692912
1	12	0.000000	0.110187	25.405210	129.036566	292.006153
1	13	0.000000	0.130157	53.165080	120.987030	293.040570
1	14	0.000000	0.258624	53.192535	116.757879	298.574332
1	15	0.000000	0.117983	53.165569	109.671079	297.264043
1	16	0.000000	0.031886	32.367671	109.559405	303.584662
1	17	0.000000	0.244886	53.192599	110.555718	306.284191
1	18	0.000000	0.101592	33.722663	106.221382	303.994314
1	19	0.000000	0.042089	21.005651	103.438167	302.021601
1	20	0.000000	0.089540	25.649066	104.858349	307.473313
1	21	0.000000	0.134217	29.989009	99.935189	309.031593
1	22	0.004840	0.157688	14.550844	93.031941	314.331924
1	23	0.000000	0.151312	25.437267	72.311721	305.464356
1	24	0.000000	0.172952	53.193029	78.080456	313.579318
1	25	0.000000	0.023800	34.510140	81.776051	313.673854
1	26	0.000000	0.045472	29.338141	84.562628	322.144413
1	27	0.000000	0.122423	22.975356	88.230962	328.738514
1	28	0.000000	0.050532	28.873951	93.972340	333.600656
1	29	0.000000	0.068781	30.415614	90.697692	337.392878
1	30	0.000000	0.045471	29.185882	84.559930	349.012499
1	31	0.000000	0.076052	14.523157	89.062506	357.666505
1	32	0.000000	0.093322	30.799701	93.117906	128.326837
1	33	0.000000	0.047215	28.958922	87.803251	149.318198
1	34	0.000000	0.179679	20.685063	85.868431	153.989486
1	35	0.000000	0.080138	25.637800	93.847871	158.042317
1	36	0.000000	0.036740	20.955447	90.292756	165.212341
1	37	0.000000	0.120909	16.140989	89.525432	175.213302
1	38	0.000000	0.092047	33.410433	96.241268	176.095166

TREE.LIST

Year	Stand	TreeID	Spec	dbh	ht	age
0	1	1	ABLA	4.08311	9.46043	41.00000
0	1	2	ABLA	2.20406	9.46043	41.00000
0	1	3	ABLA	2.36205	9.46043	41.00000
0	1	4	ABLA	2.20406	9.46043	41.00000
0	1	6	ABLA	2.20406	9.46043	41.00000
0	1	7	ABLA	2.20406	9.46043	41.00000
0	1	8	ABLA	1.73564	9.46043	41.00000
0	1	9	ABLA	4.62784	9.46043	41.00000
0	1	10	ABLA	2.20406	9.46043	41.00000
0	1	11	ABLA	4.62784	9.46043	41.00000
0	1	12	ABLA	3.53301	9.46043	41.00000
0	1	13	ABLA	3.69100	9.46043	41.00000
0	1	14	ABLA	2.20406	9.46043	41.00000
0	1	15	ABLA	1.89363	9.46043	41.00000
0	1	16	ABLA	2.20406	9.46043	41.00000
0	1	17	ABLA	4.62784	9.46043	41.00000
0	1	18	ABLA	1.73564	9.46043	41.00000
0	1	19	ABLA	1.89363	9.46043	41.00000
0	1	20	ABLA	1.00000	9.46043	41.00000
0	1	21	ABLA	5.95679	13.96638	61.00000
0	1	22	ABLA	7.20406	13.96638	61.00000
0	1	23	ABLA	8.69100	13.96638	61.00000
0	1	24	ABLA	8.06460	13.96638	61.00000
0	1	25	ABLA	7.20406	13.96638	61.00000
0	1	26	ABLA	24.39354	21.57579	101.00000
0	1	27	ABLA	21.73564	21.57579	101.00000
0	1	28	ABLA	29.39354	24.03843	121.00000
0	1	29	ABLA	30.95679	24.03843	121.00000
0	1	30	ABLA	37.20406	24.03843	121.00000
0	1	31	PIAL	1.00100	11.30362	41.00000
0	1	32	PIAL	4.86683	11.18160	41.00000
0	1	33	PIAL	4.39794	11.18160	41.00000
0	1	34	PIAL	2.20627	11.20672	41.00000
0	1	35	PIAL	1.00100	11.30362	41.00000
0	1	36	PIAL	4.86683	11.18160	41.00000
0	1	37	PIAL	4.08719	11.18160	41.00000
0	1	38	PIAL	4.39794	11.18160	41.00000
0	1	39	PIAL	1.00100	11.30362	41.00000
0	1	40	PIAL	4.39794	11.18160	41.00000
0	1	41	PIAL	1.00100	11.30362	41.00000
0	1	42	PIAL	1.00100	11.30362	41.00000
0	1	43	PIAL	3.69469	11.18160	41.00000
0	1	44	PIAL	1.00100	11.30362	41.00000
0	1	45	PIAL	2.75691	11.19769	41.00000
0	1	46	PIAL	2.20627	11.20672	41.00000
0	1	47	PIAL	6.90035	13.68519	51.00000
0	1	48	PIAL	5.72822	13.68519	51.00000
0	1	49	PIAL	6.90052	13.68519	51.00000
0	1	50	PIAL	7.52738	13.68519	51.00000
0	1	51	PIAL	11.59461	18.54305	71.00000
0	1	52	PIAL	22.22627	21.72868	91.00000
0	1	53	PIAL	20.74322	21.72868	91.00000
0	1	54	PIAL	24.41794	21.72868	91.00000
0	1	55	PIAL	20.11619	21.72868	91.00000
0	1	56	PIAL	31.76738	26.72169	161.00000
0	1	57	PIAL	33.72452	26.72169	161.00000
0	1	58	PIAL	34.42794	26.72169	161.00000
0	1	59	PIAL	39.35655	27.36658	181.00000
0	1	60	PIAL	39.82544	27.36658	181.00000
0	1	61	PIAL	36.93035	27.36658	181.00000
0	1	62	PIAL	38.49516	27.36658	181.00000
0	1	63	PIAL	43.10766	27.68644	201.00000
0	1	64	PIAL	40.83960	27.68644	201.00000
0	1	65	PICO	1.92992	1.40000	10.00000
0	1	66	PICO	1.55518	1.40000	10.00000
0	1	67	PICO	2.27420	1.40000	10.00000

TREE.YR

Year	stand	Spec	dbh	ht	age	GT(52)	GT(53)	XT(7)	XT(8)
0	1	ABLA	1.000000	9.46	40.0	0.829030	0.043775	0.074933	0.273684
1	1	ABLA	1.000000	9.46	41.0	0.856196	0.009757	0.017913	0.228187
2	1	ABLA	1.000000	9.46	42.0	0.842213	0.161084	0.012868	0.193094
3	1	ABLA	1.000000	9.46	43.0	0.862258	0.085908	0.019693	0.168339
4	1	ABLA	1.262603	9.66	44.0	0.874422	0.000000	0.024556	0.148818
5	1	ABLA	1.262603	9.66	45.0	0.873693	0.077237	0.023934	0.131977
6	1	ABLA	1.852085	9.87	46.0	0.883264	0.001865	0.027756	0.117655
7	1	ABLA	1.852085	9.87	47.0	0.869746	0.132637	0.028467	0.105536
8	1	ABLA	1.852085	9.87	48.0	0.877407	0.061731	0.033731	0.099190
9	1	ABLA	2.470314	10.07	49.0	0.884938	0.000000	0.029473	0.088639
10	1	ABLA	2.470314	10.07	50.0	0.855324	0.114819	0.038800	0.081425
11	1	ABLA	2.470314	10.07	51.0	0.865792	0.021662	0.034473	0.071538
12	1	ABLA	3.186934	10.28	52.0	0.903753	0.003318	0.028578	0.060995
13	1	ABLA	3.186934	10.28	53.0	0.899673	0.000000	0.027732	0.054359
14	1	ABLA	3.186934	10.28	54.0	0.897032	0.000000	0.027509	0.050176
15	1	ABLA	3.842146	10.47	55.0	0.888535	0.000000	0.027362	0.046193
40	1	PSME	1.742548	1.40	15.0	1.084679	0.000000	0.031690	0.149524
41	1	PSME	1.742548	1.40	16.0	1.047624	0.016935	0.016816	0.119751
42	1	PSME	1.742548	1.40	17.0	1.020385	0.000000	0.014474	0.096043
43	1	PSME	1.742548	1.40	18.0	1.003688	0.000000	0.011634	0.077745
44	1	PSME	1.742548	1.40	19.0	0.989414	0.000000	0.010630	0.063586
45	1	PSME	1.742548	1.40	20.0	0.981694	0.000000	0.008292	0.052051
47	1	PSME	0.648864	1.40	15.0	1.228974	0.000000	0.006929	0.031382
48	1	PSME	0.648864	1.40	16.0	1.175174	0.000000	0.004351	0.025106
49	1	PSME	0.648864	1.40	17.0	1.125651	0.000000	0.004049	0.020086
50	1	PSME	0.648864	1.40	18.0	1.083282	0.000000	0.004068	0.016226
51	1	PSME	0.648864	1.40	19.0	1.050079	0.000000	0.003308	0.013150
52	1	PSME	0.648864	1.40	20.0	1.023431	0.000000	0.002764	0.010758
53	1	PSME	0.648864	1.40	21.0	1.004124	0.000000	0.002641	0.008849
54	1	PSME	0.648864	1.40	22.0	0.992337	0.092716	0.002258	0.007289
55	1	PSME	0.648864	1.40	23.0	0.982687	0.027296	0.002155	0.006022
56	1	PSME	0.649513	1.40	24.0	0.973408	0.011240	0.002268	0.004969
57	1	PSME	0.658951	1.61	25.0	0.965405	0.000000	0.002306	0.004140
58	1	PSME	0.659610	1.61	26.0	0.959571	0.030618	0.002090	0.003489
59	1	PSME	0.660270	1.61	27.0	0.953982	0.048430	0.002017	0.002971
60	1	PSME	0.660930	1.61	28.0	0.951874	0.047442	0.002019	0.002568
61	1	PSME	0.661591	1.62	29.0	0.950637	0.000000	0.002233	0.002240
62	1	PSME	0.662252	1.62	30.0	0.948522	0.000000	0.002118	0.001986
63	1	PSME	0.662915	1.62	31.0	0.943153	0.011656	0.002202	0.001732
64	1	PSME	0.665055	1.82	32.0	0.935720	0.107548	0.002150	0.001485

Keane, Robert E.; Morgan, Penelope; Running, Steven W. 1996. FIRE-BGC—A mechanistic ecological process model for simulating fire succession on coniferous forest landscapes of the Northern Rocky Mountains. Res. Pap. INT-RP-484. Ogden, UT: U.S. Department of Agriculture, Forest Service, Intermountain Research Station. 122 p.

An ecological process model of vegetation dynamics mechanistically simulates long-term stand dynamics on coniferous landscapes of the Northern Rocky Mountains. This model is used to investigate and evaluate cumulative effects of various fire regimes, including prescribed burning and fire exclusion, on the vegetation and fuel complex of a simulation landscape composed of many stands. Detailed documentation of the model FIRE-BGC (a FIRE BioGeoChemical succession model) with complete discussion of all model parameters is followed with results of an application of the FIRE-BGC to a whitebark pine landscape in the Bob Marshall Wilderness Complex. Simulation results of several management scenarios are contrasted to predict the fate of whitebark pine over 200 years. Model testing reveals predictions within 10 to 30 percent of observed values.

Keywords: mechanistic model, simulation model, landscape modeling, fire, fire effects, fire regime, forest succession, vegetation dynamics, whitebark pine

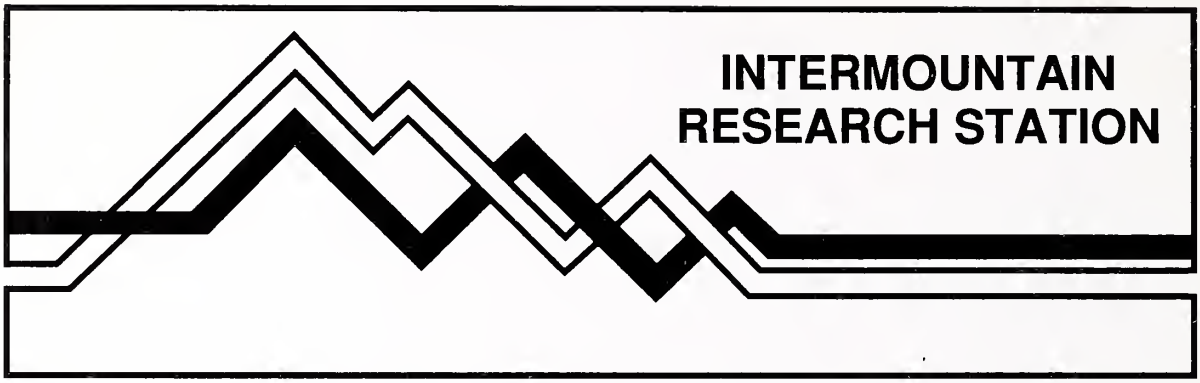

The Intermountain Research Station provides scientific knowledge and technology to improve management, protection, and use of the forests and rangelands of the Intermountain West. Research is designed to meet the needs of National Forest managers, Federal and State agencies, industry, academic institutions, public and private organizations, and individuals. Results of research are made available through publications, symposia, workshops, training sessions, and personal contacts.

The Intermountain Research Station territory includes Montana, Idaho, Utah, Nevada, and western Wyoming. Eighty-five percent of the lands in the Station area, about 231 million acres, are classified as forest or rangeland. They include grasslands, deserts, shrublands, alpine areas, and forests. They provide fiber for forest industries, minerals and fossil fuels for energy and industrial development, water for domestic and industrial consumption, forage for livestock and wildlife, and recreation opportunities for millions of visitors.

Several Station units conduct research in additional western States, or have missions that are national or international in scope.

Station laboratories are located in:

Boise, Idaho

Bozeman, Montana (in cooperation with Montana State University)

Logan, Utah (in cooperation with Utah State University)

Missoula, Montana (in cooperation with the University of Montana)

Moscow, Idaho (in cooperation with the University of Idaho)

Ogden, Utah

Provo, Utah (in cooperation with Brigham Young University)

Reno, Nevada (in cooperation with the University of Nevada)